Eurasian Journal of Soil Science

Federation of Eurasian Soil Science Societies

FEDERATION OF EURASIAN SOIL SCIENCE SOCIETIES

2011

F.E.S.S.S

Editor(s)-in-chief

Dr.Rıdvan KIZILKAYA
Dr.Evgeny SHEIN
Dr.Coskun GULSER

http://ejss.fesss.org

ABOUT THIS JOURNAL: Eurasian Journal of Soil Science is the official English language journal of the Federation of Eurasian Soil Science Societies. Eurasian Journal of Soil Science peer-reviewed open access journal that publishes research articles, critical reviews of basic and applied soil science in all related to soil and plant studies and general environmental soil science.

ABSTRACTING AND INDEXING: SCOPUS, CABI, FAO-Agris, EBSCOhost, ProQuest, DOAJ, OAJI, TR Dizin, TURKISH Journalpark, CrossRef, CiteFactor, CAS, etc.

CONTENTS

Eurasian Journal of Soil Science

Journal homepage : http://ejss.fesss.org

Synchrotron-based techniques for elemental analysis in soil-plant system under polluted environment

Mikhail Kirichkov [a,*]**, Marina Burachevskaya** [a]**, Saglara Mandzhieva** [a]**,
Tatiana Minkina** [a]**, Vishnu Rajput** [a]**, Dina Nevidomskaya** [a]**, Sudhir Shende** [a]**,
Victoria Tsitsuashvili** [a]**, Aleksey Maksimov** [b]**, Svetlana Sushkova** [a]**,
Coşkun Gülser** [c]**, Rıdvan Kızılkaya** [c]

[a] Southern Federal University, Bolshaya Sadovaya str., no. 105/42, Rostov-on-Don, 344006, Russia
[b] National Medical Research Centre for Oncology, 14th Line str., no. 63, Rostov-on-Don, 344006, Russia
[c] Ondokuz Mayıs University, Faculty of Agriculture, Department of Soil Science and Plant Nutrition, Samsun, Türkiye

Abstract

Author(s)

M.Kirichkov *
M.Burachevskaya
S.Mandzhieva
T.Minkina
V.Rajput
D.Nevidomskaya
S.Shende
V.Tsitsuashvili
A.Maksimov
S.Sushkova
C.Gülser
R.Kızılkaya

* Corresponding author

Analytical techniques for elemental analysis in the soil-plant system have significance importance, especially emerging techniques such as synchrotron radiation (SR). Improved techniques allow samples to be examined in a non-invasive manner at high speed and resolution, resulting in better sample data. By applying various analytical techniques based on SR, it is possible to gather different information about the structure of the studied samples. In mining ecology, such techniques are widely used in assessing heavy metal-polluted sites, i.e., overburden dumps and areas around operating and mothballed mines. The present review elaborated insights into different analytical techniques for applying SR in plant-soil samples. The review also compared traditional research techniques with SR-based emerging and improved techniques. The need to use SR techniques for the complex diagnostics of sample structures to study their elemental and phase composition is substantiated. Using an integrated approach with SR, we can study the dynamics and speciation of HMs with carrier phases and uncover the mechanisms underlying the interactions between the adsorption centers of minerals, organic components, and heavy metals. It also improves the efficiency and accuracy of analysis and broadens the range of information obtained, which could lead to a more precise analysis of samples.

Keywords: Synchrotron radiation (SR), heavy metals, ore, spectroscopy, XRD, XAFS, FTIR, SRμCT.

Introduction

One of Earth Science's top concerns is understanding how human activity affects soil and plant health (Hazarika et al., 2022). Heavy metal (HM) pollution is one of the primary effects of human activity (Singh et al., 2015; Khasanova et al., 2023; Shi et al., 2023). Heavy metals (HMs) have the potential to enter the biosphere through various human interferences, including motor vehicles, mineral and organic fertilizers, and wastewater and industrial pollution sources (Masindi et al., 2021; Jamali et al., 2022; Konstantinova et al., 2023; Liu et al., 2023).

The HM content is among the most significant evaluation indices of soil quality. High-pH soil can and may encourage the adsorption of metal cations to soil particles as well as the precipitation of HMs, which may then influence the uptake of HMs by plants since high-pH soils are electronegative (Wang et al., 2017b). Many physiological processes in living things are inhibited when HMs accumulate in soils, leading to their

degradation (Kulikov and Galiullina, 2006; Su et al., 2014). Excess HM exposure in living things poses major health hazards (Seth, 2012; Roy and McDonald, 2015). In humans, HMs cause the inactivation of enzymes by attaching themselves to their sulfhydryl groups. Furthermore, they can harm the central nervous system (Roy and McDonald, 2013). A variety of physical, chemical, and biological treatments (such as phytoremediation, microbial cleaning, etc.) can be used to clean up areas contaminated with HMs (Seth, 2012; Chandel et al., 2023; Schommer et al., 2023).

Considering this, the novel methods based on SR are crucial for examining the structure of soil and plant materials. Traditional methods of analyzing plant samples frequently result in their loss or damage, which reduces the accuracy of the data gathered during the analyses (Karunakaran et al., 2015). The researcher can identify the trace concentrations of elements using SR, which has higher parameters than standard X-ray tubes (Stańczyk et al., 2023). This reduces the sample exposure time significantly and prevents sample damages reported by Wang et al. (2017a). Synchrotron techniques in ore geology and mining have great potential for monitoring the biogeochemical behavior of ores, assessing contaminating impurities in ores, determining the presence of liquid fractions and inclusions, and conducting elemental and phase analyses of ores (Von der Heyden 2020; Loron et al., 2022).

Synchrotron Radiation (SR)-based Techniques

Radiation from electrons travelling at a high centripetal acceleration is known as Synchrotron Radiation (SR). Strong directivity and excellent brightness- orders of magnitude higher than in X-ray tubes- are its defining characteristics (Hofmann, 2007; Ternov, 2007). This study explains several SR-based techniques in detail in later sections.

Synchrotron Radiation X-ray Tomographic Microscopy (SRXTM or SRμCT) is a frequently used technique for SR. Since it enables the internal structures of fossils to be scanned with a resolution and accuracy not possible with other non-destructive techniques (Tafforeau et al., 2006), this technique is well-established in the study of plant parts and fossils (Smith et al., 2009). Synchrotron Phase-Contrast Imaging (SRPCI or SRPμCT) is a different sort of X-ray tomography where the sample is positioned at a variable distance from the detector, producing diffraction fringes (Brar et al., 2018). Low-density media interfaces in the sample can be seen thanks to this technique (Lauridsen et al., 2014). Thus far, SRPμCT has proven to be the least intrusive method for examining the internal structure of both soil and mineral samples. The method is also frequently used to analyze plant parts. Using this technology for spatial analysis, such as 3D tomograms and layer-by-layer sample scanning, is also usual practice.

For a thorough examination of chemical composition, spectromicroscopy using SR-based Fourier Transform Infrared (SR-FTIR) is a relatively recent method (Wetzel and LeVine, 1999). Using the ability of their functional groups to absorb specific infrared wavelengths, these molecules can be identified in large numbers inside the sample being studied (Holman et al., 2003). Furthermore, the absorption intensity is directly correlated with the concentration of each individual group of atoms, and its value is also specific to those groups. Thus, it is possible to find the concentration of a particular component in the sample by measuring the absorption intensity. Only employing the FTIR approach is uncommon (Xiao et al., 2018). Typically, FTIR is used in conjugation with methods like XRF or XRD that reveal the sample's elemental composition (Xiao et al., 2022; Hou et al., 2023). FTIR spectroscopy is used to analyze the organic component of soils, as opposed to XRD and XANES spectroscopy techniques, which study the mineral composition. FTIR approach allows the tracking of the primary mechanisms of immobilization, transformation, and movement of HMs in soils and plants.

The near-edge structure of the X-ray absorption spectrum (X-ray absorption near-edge structure method, or XANES) or the far-edge structure (EXAFS technique: Extended X-ray absorption fine structure) of samples can be investigated using X-ray Absorption Fine Structure (XAFS) spectroscopy. According to Tsitsuashvili et al. (2021), XAFS is the fluctuations close to a structureless step curve that should be monitored for an isolated atom. XANES provides information on atom charge states and the symmetry of the local atomic environment. Coordination numbers, some angles between chemical bonds, and the radii of coordination spheres are among the details of the absorbing atom's local geometry contained in EXAFS. Using XAFS, scientific teams can monitor the samples' redox potential, evaluate the oxidation state of metal pollutants, and examine the local atomic structure of soil and ore components.

Similar to the other methods mentioned, XAFS functions best when used in conjugation with other methods of physicochemical analysis (Manceau et al., 2004; Bauer et al., 2022). However, the technique's applicability is restricted by the heterogeneity and polydispersity of soil samples. It is challenging to extrapolate, using only the XAFS technique, the spectra of heavily contaminated soils that contain a wide variety of HM mineral forms from the spectra of regular samples.

Large (> 100 μm) single crystals are not necessary to ascertain the atomic structure of crystalline materials through X-ray diffraction (XRD) analysis. The atomic structure of a crystalline sample, unit cell parameters, spatial symmetry, position, and atom type can all be ascertained using this technique. It is feasible to ascertain properties like valence and interatomic distances using the unit cell parameters. Without prior knowledge of the structure or elemental composition of the microcrystals under study, XRD allows for determining their structure. It is an effective analytical tool for examining how atoms are arranged in crystalline materials (Tsitsuashvili et al., 2021). For XRD analyses, laboratory radiation sources are most frequently utilized. Simultaneously, SR is increasingly used because of its enhanced parameters, which primarily relate to high resolution (Nevidomskaya et al., 2021; Kumari et al., 2023). Analyses of soils and soil-like environments, including sediments, dust from the side of the road, and individual soil components, such as ores and their components, are conducted (Brown, 2002; Fan and Gerson, 2011).

Applications of Synchrotron Radiation-based Techniques

A significant number of works (Lauridsen et al., 2014; Meneses et al., 2018; Ma et al., 2020) use SRμCT. SRμCT for instance, has been applied to detect gas deposits on hydrophobic surfaces visually. The 3D tomograms that showed the spatial distribution of gas in the tissue and on the leaf's surface when submerged in water were made public by Lauridsen et al. (2014). On the superhydrophobic adaxial side of the leaf, the gas film formed elongated triangular gas volumes by filling the surface tissue furrows at the base and the tip of the leaf segment. The entire observed exterior gas volume was gas-phase coupled as a result of the comparatively high volume of gas layers within each furrow being connected by a thin network of gas film covering the tissue ridges between each furrow. On the other hand, no gas films were observed on the leaf's abaxial side (Lauridsen et al., 2014).

In the field of earth sciences, SRμCT is effectively utilized for the morphological examination of rocks and soil as well as the evaluation of their internal structures. Meneses et al. (2018) employed layer-by-layer SRμCT scanning of pumice to ascertain the porosity and friability- two key characteristics of this igneous rock. Artificial neural networks were trained on the acquired images using a variety of segmentation techniques. The statistical analysis of the Krasker-Wallace test revealed significant differences between the segmentation techniques. In the study by Ma et al. (2020), SRμCT was used to evaluate the influence of pore characteristics on the stability of black soil in freeze-thaw cycles. Porosity rose with the number of freeze-thaw cycles, leading to the development of macropores, linked channels, blocks, and fracture structures. Additionally, there was a shift in the shape of pores: there were more oblong pores and less regularly and irregularly formed pores. The increase in the number of pores was related to volumetric changes in ice during freezing, which caused soil particles to separate from each other. Furthermore, the capacity to recover from deformation brought on by ice crystal extrusion progressively diminished with an increase in the frequency of freeze-thaw cycles. In another study, Scheckel et al. (2007) examined the features of the distribution and compartmentalization of thallium (Tl) in Iberis intermedia using synchrotron X-ray differential absorption-edge computed microtomography (CMT). CMT studies were conducted at the GeoSoilEnviroCARS (GSECARS) bending magnet beamline 13-BM-Dat at the Advanced Photon Source (APS) at the Argonne National Laboratory, USA. According to the authors, CMT is the only method that can identify the compartmentalization of Tl in the vascular system of cotyledons and leaves of Iberis intermedia.

According to research conducted by Von der Heyden (2020) and Lahlali et al. (2015), SRPμCT is currently the least invasive method for investigating the internal structure of samples. In order to optimize data quality in wheat and rapeseed, Karunakaran et al. (2015) demonstrated the advantages of SRPμCT for visualization and quantification of internal plant and root structures over a wide range of imaging parameters. The linear profiles of the samples clearly showed the details of the sample's internal structure and the presence of cavitations in the stem vessels and their connecting structures. The authors state that the relatively low dose of radiation absorbed by the samples will enable future longitudinal studies in which the same living plant can be photographed in a series of time-separated exposures. In another study, Lahlali et al. (2015) applied the SRPμCT technique to wheat varieties infected with Fusarium root rot and confirmed the structural differences between resistant and susceptible varieties. The artificially infected and uninfected rachis and ears scanned showed different resistance in Sumai3, FL62R1, and Muchmore varieties. Differences in mass density and phase contrast signals between healthy and infected sections were observed and proved most pronounced in the Muchmore variety. Healthy ones appeared in white and were filled with internal structures, while infected ones were mostly empty and transparent due to water and tissue loss.

The Synchrotron radiation-Fourier transform infrared (SR-FTIR) spectroscopy can be used to reveal and demonstrate the composition and distribution of components in humus fractions. In their study, Solomon et

al. (2005) used SR-FTIR to observe the effect of land use change on the content, composition, and stability in the soil of various organic forms of carbon occurrence in the extracted humic compounds. Easily degradable components of soil organic matter (polysaccharides, labile components of aliphatic fragments) were more prominent in the humic matter of forest soils, while aromatic and recalcitrate aliphatic forms prevailed in the humic deposits of the permanently cultivated fields. In another study, Lehmann et al. (2007) employed the SR-FTIR technique for the spatial description of carbon forms in soil organic matter, revealing the distribution of total carbon and spatial patterns in the distribution of some of its forms. The correlation analysis confirmed these empirical data. Observations on carbon distribution in soil microaggregates allowed a new look at the mechanisms of their formation and stabilization of organic carbon.

The authors suggested that in the studied soils, microaggregate formation is initiated mainly by the accumulation of organic matter on the surfaces of clay particles rather than by the occlusion of organic debris by clay particles. Clay cluster and biopolymer distribution exhibited spatial heterogeneity, as demonstrated by Xiao et al. (2019) using SR-FTIR. According to the authors, all soil microaggregates in clay soil samples were dominated by the OH, C-H, C=C, Si-O, and Al-O functional groups, and there was a significant association between these functional groups. The absorptions of Si–O (1030 cm^{-1}, silicates) and Al–O (915 cm^{-1}, kaolinite, and smectite) functional groups were stronger than others. These findings demonstrated that the biopolymers and clay clusters had a diverse spatial distribution. The correlation suggested that mineral clusters could bind various biopolymers.

Holman et al. (2002) investigated the catalysis of polycyclic aromatic hydrocarbons (pyrene) by humic acid using the SR-FTIR spectroscopy method. SR-FTIR spectra were recorded during pyrene degradation on magnetite surfaces by Mycobacterium sp. JLS bacteria, both in the presence and absence of Elliott Soil Humic Acid. Based on the collected data, SR-FTIR mapping of the samples revealed the spatial distribution of the infrared absorption peaks related to pyrene, Elliott Soil Humic Acid, and Mycobacterium sp. JLS bacteria.

In another report, Wan et al. (2019) used the SR-FTIR spectroscopy method to study the concentration and characteristics of Fe-linked carbon in twelve agricultural soil samples obtained from different areas of central and eastern China, which demonstrated a direct correlation between the spatial distribution of aliphatic compounds, carboxylic acids, peptides, lignin derivatives, and polysaccharides and the Fe-O distribution. The correlation coefficients of Fe-O with organic compounds had the following order: polysaccharides or aliphatic compounds > peptides > carboxylic acids > lignin derivatives. Stronger associations occurred between Fe-O and polysaccharides, aliphatic compounds, or peptides than between carboxylic acids or lignin derivatives. In addition, the correlation coefficients between Fe-O and organic compounds showed that these three compounds were closely related to iron oxides. Therefore, assuming that more polysaccharides, aliphatic compounds, and peptides are associated with Fe oxides than carboxylic acids and lignin derivatives, it can be concluded that iron oxides preferentially stabilize polysaccharides and aliphatic compounds in arable soils.

The distribution of HMs in soil has been examined using SR-FTIR. The study by Yu et al. (2017) demonstrated the association of Cu with mineral elements and functional groups within soil particles. Through SR-FTIR, the non-uniform distribution of Cu in soil particles was shown. The areas of high and low Cu concentrations represented the newly added and original Cu, respectively. Information about the distribution pattern of functional groups in the soil particles was also obtained. All functional groups had a distribution similar to Cu, which may indicate their ability to bind Cu.

The XAFS technique is not as commonly used in earth sciences as XRF or XRD, for example, but the frequency of its application has expanded considerably in recent years. Most studies with this technique use SR, as laboratory facilities are very scarce. In geology, XAFS can be used to probe crystalline and weakly crystalline materials. Based on the chemical composition of weakly crystalline materials, conclusions can be drawn about the contaminants in the mined rock (McNear et al., 2010). Analysis of XANES spectra provides information on the redox properties and coordination numbers of metals in mineral and metal-ligand compositions (Cook et al., 2011). In-situ XANES spectral imaging has been used to study the dynamics of the oxidation degree of a particular HM in a particular ore (Etschmann et al., 2017).

Prietzel et al. (2007) identified various Fe (II) and Fe (III) compounds in soil samples using the XANES method. The contribution of various organic and inorganic Fe-containing compounds was evaluated using the linear combination fitting method. In another study, Strawn and Baker (2009) analyzed five soil samples using the XAFS method, in which they determined the molecular structure of Cu compounds and the energy transitions of electrons by the peaks splitting and their intensity. Using these data together with statistical analysis and theoretical modeling allowed the authors to suggest that Cu-SOM (soil organic material) complexes are the

predominant species in soils. Based on these results, it was hypothesized that more than 90% of Cu in soil samples is present in the form of Cu-SOM complexes.

Using XAFS to analyze the dynamics of toxic heavy metals, such as cadmium (Cd), allows determining the ability of soils and plants to accumulate them and studying the speciation of pollutants and their extractability. A study conducted on six soil samples from different regions of Brazil showed a progressive natural attenuation of soil contamination by Cd-containing phases. Cd (II) entering these soils was mainly immobilized by organic matter and oxide minerals binding to the soil. The degree of Cd extractability dynamics was evaluated four months after contamination using chemical fractionation. By analyzing the XANES spectra of the samples, a high content of Cd bound to soil organic matter was determined (Colzato et al., 2017). In another study, Kim et al. (2002) investigated Cr speciation and dynamics. By analyzing XANES spectra, the authors obtained information on soil and plants' sorption and extraction capacities concerning Cr-containing compounds. Cr (III) and Cr (VI) were found in the samples. It is emphasized that Cr (VI) is a strong oxidant and poses a danger to plants, even in small amounts. The conversion of Cr (III) to Cr (VI) was initiated by manganese, a strong oxidant present in the samples.

The lower Cr (VI) content in the near-surface soil horizons compared to the deeper soil horizons was due to different kinetics of Cr (III) oxidation to Cr (VI). The content and dynamics of Cr (VI) in soil were also controlled by the anion-exchange capacity of Fe oxides (Garnier et al., 2013). In addition to Cr, its compounds are also toxic, particularly Cr_2O_3, which is most dangerous in the form of nanoparticles (NPs). Using EXAFS in the study, Kumari et al. (2023) determined the functional groups of Cr oxide, which had phytotoxic effects such as stunting the germination of plant samples. Another illustrative example of work centered around the analysis of a single HM is the paper by Prietzel et al. (2023). The study examined the speciation of aluminum (Al) in soils, which is important for Al cycling and toxicity in terrestrial ecosystems. Three forest soil profiles were analyzed using synchrotron-based XANES and XRD techniques (Synchrotron Light Research Institute, Thailand). Al K-edge XANES allowed us to estimate the relative contribution of different Al species to the total Al in soil samples. The authors claimed that XANES, in combination with XRD and elemental analysis, is a promising methodological complex for the speciation of Al in soils with a great potential to promote the understanding of Al biogeochemistry in terrestrial ecosystems.

The XANES spectroscopy was used to investigate the structure of various soil samples and soil phases saturated with Cu^{2+} and Zn^{2+} ions (Minkina et al., 2014). Soil samples of ordinary black soil were saturated with $Cu(NO_3)_2$ and CuO. Samples of individual soil components (calcite, kaolinite, bentonite, and humic acid preparations isolated from ordinary black soil) were saturated with Zn^{2+} and Cu^{2+} ions. The analysis of XANES spectra of the K-edge of the zinc absorbed by the carbonate phase (Figure 1) showed that Zn ions substitute Ca ions in octahedral positions and demonstrate the 1s → 4p electronic transition. When comparing the intensity of maximum A and the energy position of spectral features B and C in the XANES spectra of the K-edge for Zn in humic acid, it was observed that metal ions, regardless of what minerals they consist of, have similar mechanisms of interaction with soil organic matter.
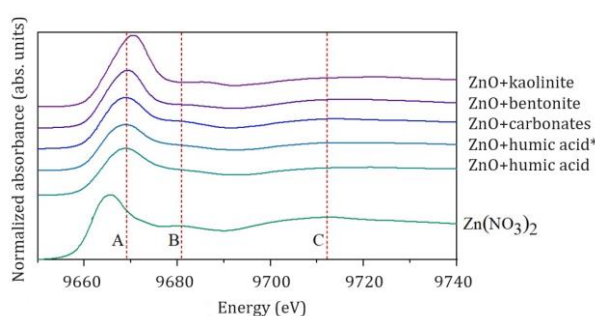
Figure 1. XANES absorption spectra of the Zn K-line (Minkina et al., 2014)

An urgent interdisciplinary goal is to study soil and plant contamination in order to gather comprehensive information on the dynamics and speciation of HMs. Adding various metal NP concentrations to the soil sample under investigation while maintaining other experimental conditions is one of the most effective approaches for studying the accumulation and transformation of HM NPs. In order to determine the phases of copper-containing compounds under various circumstances, a sample of black soil was examined (Burachevskaya et al., 2021). Based on a comparison with model compounds, XANES measurements demonstrated a high sensitivity to the geometry of bonds produced by Cu atoms, which characterizes the near surroundings of Cu atoms in soil samples (Figure 2). After the soil was incubated with the tested compounds,

XANES analysis was carried out. When comparing the soil sample saturated with CuONPs to the control sample, there were no noticeable changes to the X-ray absorption spectra.
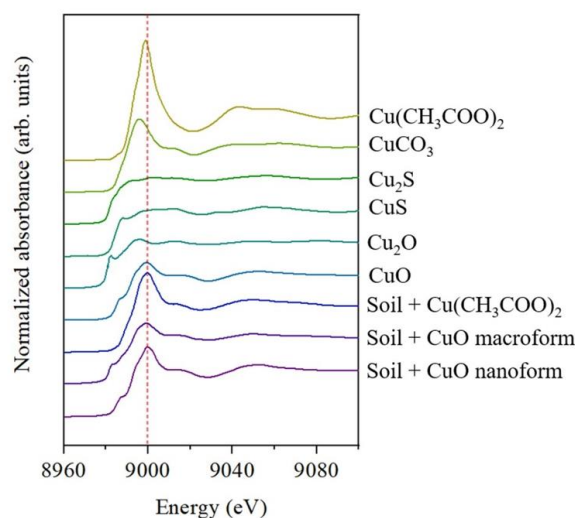
Figure 2. XANES spectra of Cu compounds in the Hordeum sativum (Burachevskaya et al., 2021)

The presence of heavy metals (Pb and Sb) in the soils of military ranges causes pollution of surface and ground waters, a decrease in biological activity, and an increase in the uptake of metals by biota. The evaluation of the immobilization capacity of soil organic matter by the EXAFS technique carried out by Ahmad et al. (2013) made it possible to develop remediation measures for Pb-polluted soils. EXAFS spectra of soil samples in which organic sorbents (mussel shells, cattle bone meal, and biochar) were added showed a significant presence of organically bound Pb compounds, and introducing additives led to an increase in pH. EXAFS spectra, in combination with SEM and XRD, revealed stable Pb compounds in samples containing organic additives, which, according to the authors, suggests a mechanism of Pb immobilization. In another example of Pb research (Nevidomskaya et al., 2015), analyses of the connection between metal ions and different soil components using XANES (Figure 3a) and EXAFS (Figure 3b) showed that the local atomic environment of Pb can vary greatly depending on the structure of the mineral phase. Lead (Pb^{2+}) ions in bentonite, kaolinite, hydromuscovite, gibbsite, and calcite are included in the positions of the intra-muscovite complex, replacing some aluminum ions in the octahedral sites. This results in a change in the Pb-O distances in the Pb-bearing octahedrons. Pb^{2+} is also sorbed by dimeric (Pb-Pb) silicate and aluminum groups. The adsorbent surface structure plays a key role in the sorption of Pb^{2+} across mineral phases.
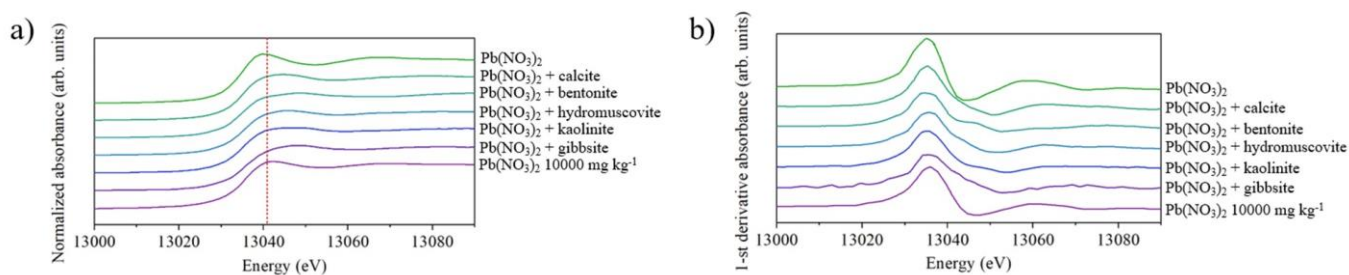
Figure 3. XANES spectra of L-lines (a) and their derivatives (b) for $Pb(NO_3)_2$, different soil samples, and a soil sample at 10000 mg Pb kg^{-1} (Nevidomskaya et al., 2015)

During mining and subsequently processing minerals, coastal floodplains, which play a key role in transporting nutrients and HMs between surface water and groundwater, are heavily polluted. This type of pollution often involves arsenic (As), which is present in coastal soils as As (V) and the more toxic As (III). Using the EXAFS technique, it was found that most of the As is represented by As (V). As was mostly bound to Fe hydroxyl compounds in the studied samples and concentrated around the roots. The As bound to Fe proportion reached up to half or more of the total arsenic content. This was explained by the highest adsorption affinity of As with Fe (Voegelin et al., 2007).

The EXAFS technique is used to study adsorption properties and forms of radionuclides in soils. As a result of intensive nuclear and thermonuclear weapons testing, as well as the Chornobyl and Fukushima accidents, a large amount of Caesium (^{137}Cs) was released into the soil through atmospheric precipitation. Fan et al. (2014) revealed that the species of adsorbed Cs depend mainly on the clay minerals contained in the soil. The authors observed a strong affinity for Cs binding on illite $(K_{0.75}(H_3O)_{0.25})Al_2(Si_3Al)O_{10}((H_2O)_{0.75}(OH)_{0.25})_2$ and vermiculite $(Mg^{+2},Fe^{+2}, Fe^{+3})3 [(Al,Si)_4O_{10}]\cdot(OH)_2\cdot4H_2O$. The Cs was also well sorbed on the zeolite. In the study of ores, Newville (2004) used the XANES and EXAFS spectroscopy methods to determine the information on coordination numbers, degrees of disorder in the local coordination environment, bond lengths, and the chemical identity of HM atoms. Most of the works related to the application of EXAFS spectroscopy in ore research are related to the study of the formation of metal-ligand complexes in the hydrothermal fluid model in a wide elemental range, e.g., gold (Liu et al., 2014) or platinum group elements (Mei et al., 2015).

XAFS is actively used for other purposes besides analyzing the content of heavy metals in soil samples. An example is the study by Lombi et al. (2006), where phosphorus (P) speciation and distribution in fertilized soil were investigated. Studies have shown that P is highly heterogeneously distributed in soil samples. Evidence also showed that P is invariably associated with Ca rather than Fe on the nanoscale. It was also shown that near fertilizer granules, P precipitation in the form of octacalcium phosphate or apatite-like compounds is the dominant mechanism responsible for decreases in P lability. In another study, Alotaibi et al. (2018) used a combination of synchrotron-based XANES and sequential chemical extraction to study phosphorus speciation in a prairie soil after growing Canola plants with the addition of meat and bone meal ash (MBMA) and dried distiller's grains ash (DDGA). The phosphorus sequential extraction protocol used is based on the Hedley et al. (1982) procedure. According to the research results, P transformed from the initial ash sources into a much less crystalline form when it was added to the soil, and Canola plants were grown on the soil for five weeks. The authors argue that the lack of differences in XANES spectra of MBMA and DDGA after adding them to soil may indicate that some transformations of P-form ash have occurred.

The advantage of using XRD with SR is the possibility of obtaining an extremely thin, high-intensity, parallel beam of X-rays, which reduces the heterogeneity of elemental composition in the investigated area of the soil sample. The XRD method is often combined with other methods of analysis: XRF, FTIR, and XAFS. The most common analyses are performed on agricultural soils. Another intensively studied area is technogenic soils polluted with HMs, i.e., soils around factories, industries, and various active and abandoned mines.

The analysis of the elemental composition of soil NPs by XRD using SR was considered in the study conducted by Tsao et al. (2013) on the example of clay minerals of different fractions. In the 2000 nm fraction, quartz was the dominant mineral phase. In the 450-2000 nm fraction, intense diffraction peaks of illite, kaolinite, goethite, and haematite were detected. The NPs of illite, kaolinite, goethite, and haematite were also identified in the 1-100 nm fraction. The analysis of diffraction peaks showed an increase in kaolinite content with decreasing particle size in red soils. The proportion of illite, on the contrary, decreased with decreasing fractions. When interacting with Pb, the phosphorus contained in bones forms the pyromorphite $Pb_5(PO_4)3Cl$. This was demonstrated by Landrot et al. (2020), who examined soil samples at three locations in a residential area of Klithi village (Kanchanaburi, Thailand) near a landfill and a house and in a garden. Analyses of the soil sample near the landfill revealed diffraction peaks of hydroxyapatite, a component of fish bones. On the contrary, analyses of the soil samples near the house and in the garden did not show the presence of pyromorphite mineral phases. Huynh et al. (2003) used synchrotron-based XRD to study the partial substitution of Cd for Fe in goethites. The authors claimed that Cd could be incorporated by isomorphous substitution of up to ~9.5% of the Fe3+ ions in the octahedra of goethite. XRD and TEM revealed that incorporating Cd increased all unit-cell parameters but an overall decrease in crystallite size.

XRD mapping using SR can provide new insights into the mineralogy and orientation of clay particles during the formation of soil crusts. Only the general morphological state of such processes on the soil surface was investigated for a long time, but the mineral composition was uncertain due to the clay particles being too small. A quantitative description of such processes is also lacking. XRD mapping is an efficient way to establish the composition and texture of soil crusts at a depth of a few centimetres with high resolution. This is well illustrated by the XRD mapping of clay layers in soil crust samples studied by Geoffroy et al. (2022). Fitzpatrick et al. (2019) presented an exemplary work that used both laboratory- and synchrotron-based XRD methods. Soil samples on the surface of the fabric (pyjamas) were examined. Synchrotron-based investigations were conducted on the powder diffraction beamline at the Australian Synchrotron Facility. Laboratory XRD results showed that all samples contain similar amounts of quartz (dominant), layer silicate clays (minor and trace amounts of chlorite, smectite, kaolin, and illite), feldspars (minor amounts of albite and orthoclase), and rutile

(traces). Synchrotron-based XRD data showed the mineralogy of very small amounts of the soil samples, which comprises tiny soil particles and fragments on the fabric in the in-situ mode using the high-throughput stage.

The XRD method was found to have an application in studying exchange processes in the rhizosphere. Fancello et al. (2019) stated that quartz, phyllosilicates, feldspars, and ore metal sulphides are probably inherited from the bedrock, while other phases are the product of biological or geochemical secondary processes. HM sulphates, and carbonates are the result of alteration and oxidation of Pb-Zn-Fe, and kaolinite is the result of feldspar weathering.

XRD performs best when combined with other techniques. A clear example is the study by Fischel et al. (2023). The combination of µXRD and µXRF mapping allowed the authors to determine the phase and elemental composition of the Graskop manganiferous soil samples and nodules of concentric bands of Mn and Fe that form during redox cycles. Moreover, the study showed the correlation between Si and Ca in stabilizing these metal oxides in the soil matrix and nodules. The authors claimed that using SR makes it possible to analyze Mn at the micron scale and determine its species and distribution in diverse geochemical systems, including soils with trace Mn concentrations. In another study, Kumari et al. (2023) used a combination of synchrotron-based XRD and XAFS to study the total content, mobility, and factor toxicity index of the Cr macro- and NPs in contaminated barley (*Hordeum vulgare* L.). For this study, Cr_2O_3 macro- and NPs were injected into the Haplic Chernozem samples, where barley plants were subsequently grown. All studies were performed using ash-fertilized plants. The presence of the Cr crystalline phase in plants from both sets was indicated and confirmed by the narrow and intense diffraction peaks in the respective spectra (Figure 4). The most intense peaks in the patterns correspond to crystalline Cr_2O_3 (eskolaite). The sample contaminated with NPs also contained a noticeable amount of KCl (sylvite). The accumulation and translocation of Cr in barley plants were confirmed by synchrotron XAFS analysis.
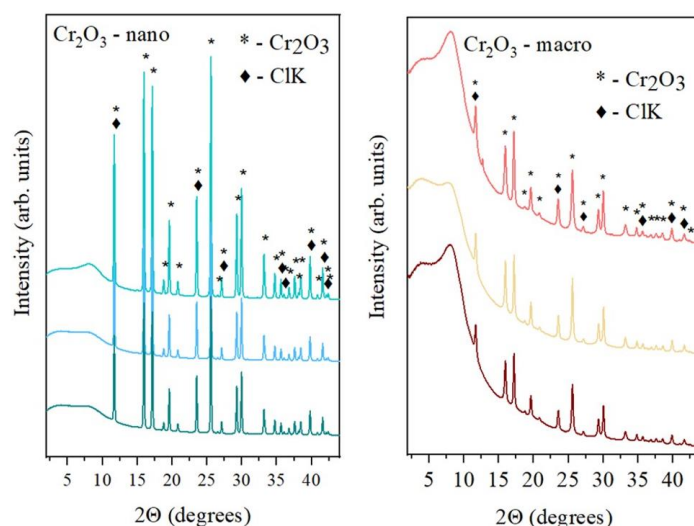
Figure 4. X-ray diffraction pattern of ash fertilized Hordeum vulgare L. plants grown on soils polluted with Cr_2O_3 nanoparticles (left) and Cr_2O_3 macroparticles (right) compounds

XRD is a technique used in geology and ore studies to determine details about the unit cell characteristics of mineral phases and the geometry and orientation of a mineral's crystal lattice (Lavina et al., 2014). Working with small samples is made possible by the X-ray spot's small size, high brightness, low noise, and intensity (Reynolds et al., 2010), for instance, to research the properties of the manganese nodule's surface crystallites (Manceau et al., 2014).

Conclusion

The review showcases the advancements of contemporary techniques for studying metalloid forms and heavy metals. Although XAS is a powerful analytical tool, it is best applied as one of several analytical techniques to obtain the clearest picture of the processes controlling HM mobility in soil environments. This is based on the generalization of the literature and our data obtained using synchrotron analysis. Other sophisticated spectroscopic methods are frequently employed in addition to the conventional analytical methods in soil chemistry to supplement the elementally specific data acquired from XAS. Based on the analysis of the reviewed works, it can be concluded that using SR-based methods is preferable when analyzing polydisperse samples. This is because these methods allow one to study the distribution of metalloids and HMs in soil and plant samples without destroying them, as well as the oxidation degree of elements of variable valence and

solid-phase sample elemental and phase compositions in micro volumes. Using an integrated approach, we can study the dynamics and speciation of HMs with carrier phases and uncover the mechanisms underlying the interactions between the adsorption centres of minerals, organic components, and heavy metals. It also improves the efficiency and accuracy of analysis and broadens the range of information obtained.

Acknowledgments

References

Ahmad, M., Lee, S.S., Lim, J.E., Lee, S.-E., Cho, J.-S., Moon, D.H., Hashimoto, Y., Ok, Y.-S., 2013. Speciation and phytoavailability of lead and antimony in a small arms range soil amended with mussel shell, cow bone and biochar: EXAFS spectroscopy and chemical extractions. *Chemosphere* 95: 433–441.

Alotaibi, K., Schoenau, J., Kar, G., Peak, D., Fonstad, T., 2018. Phosphorus speciation in a prairie soil amended with MBM and DDG ash: Sequential chemical extraction and synchrotron-based XANES spectroscopy investigations. *Scientific Reports* 8(1): 3617.

Bauer, T.V., Pinskii, D.L., Minkina, T.M., Shuvaeva, V.A., Soldatov, A.V., Mandzhieva, S.S., Tsitsuashvili, V.S., Nevidomskaya, D.G., Semenkov, I.N., 2022. Application of XAFS and XRD methods for describing the copper and zinc adsorption characteristics in hydromorphic soils. *Environmental Geochemistry and Health* 44(2): 335–347.

Brar, G.S., Karunakaran, C., Bond, T., Stobbs, J., Liu, N., Hucl, P., Kutcher, H., 2018. Showcasing the application of synchrotron-based X-ray computed tomography in host-pathogen interactions: The role of wheat rachilla and rachis nodes in Type-II resistance to Fusarium graminearum: Type-II resistance to Fusarium spread in wheat. *Plant, Cell and Environment* 42(2): 509–526.

Brown, G. 2002. An overview of synchrotron radiation applications to low temperature geochemistry and environmental science. *Reviews in Mineralogy and Geochemistry* 49 (1): 1–115.

Burachevskaya, M., Minkina, T., Mandzhieva, S., Bauer, T., Nevidomskaya, D., Shuvaeva, V., Sushkova, S., Kizilkaya R., Gülser, C., Rajput, V., 2021. Transformation of copper oxide and copper oxide nanoparticles in the soil and their accumulation by Hordeum sativum. *Environmental Geochemistry and Health* 43(4): 1655-1672.

Chandel S., Dar R., Singh D., Thakur S., Kaur R., Singh, K., 2023. Plant assisted bioremediation of heavy metal polluted soils. In: Bio-Inspired Land Remediation, Pandey, V.C., (Ed.). Springer-Verlag Berlin, Heidelberg, pp. 85–114.

Colzato, M., Kamogawa, M., P. de Carvalho, H.W., Alleoni, L., Hesterberg, D., 2017. Temporal changes in cadmium speciation in Brazilian soils evaluated using Cd L –Edge XANES and chemical fractionation. *Journal of Environment Quality* 46(6): 1206-1214.

Cook, N., Ciobanu, C., Brugger, J., Howard, D., de Jonge, M., Ryan, C., Paterson, D., 2011. Determination of the oxidation state of Cu in substituted Cu-In-Fe-bearing sphalerite via -XANES spectroscopy. *American Mineralogist* 97(2-3): 476-479.

Etschmann, B., Liu, W., Li, K., Dai, S., Reith, F., Falconer, D., Kerr, G., Paterson, D., Howard, D.L., Kappen, P., Wykes, J., Brugger, J.L., 2017. Enrichment of germanium and associated arsenic and tungsten in coal and roll-front U deposits. *Chemical Geology* 463: 29-49.

Fan, Q., Yamaguchi, N., Tanaka, M., Tsukada, H., Takahashi, Y., 2014. Relationship between the adsorption species of cesium and radiocesium interception potential in soils and minerals: An EXAFS study. *Journal of Environmental Radioactivity* 138: 92–100.

Fan, R., Gerson, A., 2011. Nickel geochemistry of a Philippine laterite examined by bulk and microprobe synchrotron analyses. *Geochimica Et Cosmochimica Acta* 75(21): 6400-6415.

Fancello, D., Scalco, J., Medas, D., Rodeghero, E., Martucci, A., Meneghini, C., Giudici, G., 2019. XRD-thermal combined analyses: An approach to evaluate the potential of phytoremediation, phytomining, and biochar production. *International Journal of Environmental Research and Public Health* 16(11): 1976.

Fischel, M., Clarke, C., Sparks, D., 2023. Synchrotron resolved microscale and bulk mineralogy in manganese-rich soils and associated pedogenic concretions. *Geoderma* 430(9): 116305.

Fitzpatrick, R., Raven, M., 2019. The forensic comparison of trace amounts of soil on a pyjama top with hypersulfidic subaqueous soil from a river as evidence in a homicide cold case. *Forensic Soil Science and Geology* 492(1).

Garnier, J., Quantin, C., Guimarães, E., Vantelon, D., Montarges-Pelletier, E., Becquer, T., 2013. Cr(VI) genesis and dynamics in Ferralsols developed from ultramafic rocks: The case of Niquelândia, Brazil. *Geoderma* 193–194: 256–264.

Geoffroy, V., Dazas, B., Ferrage, E., Berenguer, F., Boissard, C., Michot, L., van Oort, F., Tertre, E., Hubert, F., 2022. Soil crusting: New insight from synchrotron 2D micro X-ray diffraction mapping of clay-particle orientation and mineralogy. *Geoderma* 428(3): 116096.

Hazarika P., Medhi B., Swami S., 2022. Implications of toxic heavy metals on plant, soil, aquatic environment and human health: A review. In: Advances in Hill Agriculture. Swami, S. (Ed.). AkiNik Books, New Delhi, India. 5: 13-32.

Hedley, M.J., Stewart, J.W.B., Chauhan, B.S., 1982. Changes in inorganic and organic soil phosphorus fractions induced by cultivation practices and by laboratory incubations. *Soil Science Society of America Journal* 46(5): 970-976.

Hofmann, A., 2007. The physics of synchrotron radiation. Cambridge University Press, Cambridge, 323p.

Holman, H.-yn., Martin, M.C., McKinney, W., 2003. Synchrotron-based FTIR spectromicroscopy: Cytotoxicity and heating considerations. *Journal of Biological Physics* 29(2–3): 275–286.

Holman, H.-y., Nieman, K., Sorensen, D., Miller, C., Martin, M., McKinney, W., Sims, R., 2002. Catalysis of PAH biodegradation by humic acid shown in synchrotron ınfrared studies. *Environmental Science and Technology* 36(6): 1276-1280.

Hou, Z.-W., Li, J.-H., Li, C.-S., Zhang, J.-M., Lin, Q.-H., Zhao, Q.-J., Wu, Z.-P., Wang, Y., 2023. Effect of coconut fiber biochar and its nitrate modification on Pb passivation in Paddy soils. *Huan Jing Ke Xue* 44(8): 4497-4506.

Huynh, T., Tong, A.R., Singh, B., Kennedy, B.J., 2003. Cd-substituted goethites — A structural investigation by synchrotron X-ray diffraction. *Clays and Clay Minerals* 51: 397–402.

Jamali, M., Bayat, J., Hashemi, S.H., Talakesh, S., 2022. Investigation of heavy metals and petroleum hydrocarbons pollution source in agricultural lands in the south of Tehran. *Environmental Sciences* 20(3): 251–264.

Karunakaran, C., Lahlali, R., Zhu, N., Webb, M., Schmidt, M., Fransishyn, K., Belev, G., Wysokinski, T.W., Olson, J., Cooper, D.M.L., Hallin, E.L., 2015. Factors influencing real time internal structural visualization and dynamic process monitoring in plants using synchrotron-based phase contrast X-ray imaging. *Scientific Reports* 5: 12119.

Khasanova, R., Semenova, I., Suyundukov, Y., Ilbulova, G., 2023. Assessment of urban soil pollution by heavy metals (Russian Federation, Republic of Bashkortostan). In: Smart and Sustainable Urban Ecosystems: Challenges and Solutions. Korneykova, M., Vasenev, V., Dovletyarova, E., Valentini, R., Gorbov, S., Vinnikov, D., Dushkova, D. (Eds.). Springer Geography. Springer, Cham. pp. 67–75.

Kim, J.-G., Dixon, J., Chusuei, C., Deng, Y., 2002. Oxidation of chromium(III) to (VI) by manganese oxides. *Soil Science Society of America Journal* 66(1): 306–315.

Konstantinova, E., Minkina, T., Mandzhieva, S., Nevidomskaya, D., Bauer, T., Zamulina, I., Sushkova, S., Lychagin, M., Rajput, V.D., Wong, M.H., 2023. Ecological and human health risks of metal–PAH combined pollution in riverine and coastal soils of Southern Russia. *Water* 15(2): 234.

Kulikov, Yu.A., Galiullina, A.S., 2006. Heavy metals - migration into the soil system - plants and the impact on the loss of basic nutrients from soddy-podzolic soil and amaranth crop. Scientific Notes of Kazan Federal University, Environmental Science 148(4): 90–99. [in Russian].

Kumari, A., Mandzhieva, S.S., Minkina, T.M., Rajput, V.D., Shuvaeva, V.A., Nevidomskaya, D.G., Kirichkov, M.V., Veligzhanin, A.A., Svetogorov, R., Khramov, E.V., Ahmed, B., Singh, J., 2023. Speciation of macro- and nanoparticles of Cr_2O_3 in Hordeum vulgare L. and subsequent toxicity: A comparative study. *Environmental Research* 223: 115485.

Lahlali R., Karunakaran C., Wang L., Willick I., Schmidt M., Liu X., Borondics, F., Forseille, L., Robert, P.R., Tanino, K.K., et al., 2015. Synchrotron based phase contrast X-ray imaging combined with FTIR spectroscopy reveals structural and biomolecular differences in spikelets play a significant role in resistance to Fusarium in wheat. *BMC Plant Biology* 15: 24.

Landrot, G., Khaokaew, S., 2020. Determining the Fate of Lead (Pb) & Phosphorus (P) in Alkaline Pb-polluted soils amended with P and acidified using multiple synchrotron-based techniques. *Journal of Hazardous Materials* 399: 123037.

Lauridsen, T., Glavina, K., Colmer, T., Winkel, A., Irvine, S., Lefmann, K., Feidenhans'l, R., Pedersen, O., 2014. Visualisation by high resolution synchrotron X-ray phase contrast micro-tomography of gas films on submerged superhydrophobic leaves. *Journal of Structural Biology* 188(1): 66–70.

Lavina, B., Dera, P., Downs, R., 2014. Modern X-ray diffraction methods in mineralogy and geosciences. *Reviews in Mineralogy and Geochemistry* 78: 1-31.

Lehmann, J., Kinyangi, J., Solomon, D., 2007. Organic matter stabilization in soil microaggregates: Implications from spatial heterogeneity of organic carbon contents and carbon forms. *Biogeochemistry* 85(1): 45-57.

Liu, W., Etschmann, B., Testemale, D., Hazemann, J.L., Rempel, K., Müller, H., Brugger, J., 2014. Gold transport in hydrothermal fluids: Competition among the Cl−, Br−, HS− and $NH_{3(aq)}$ ligands. *Chemical Geology* 376: 11–19.

Liu, W., Xing, X., Li, M., Yu, Y., Hu, T.P., Mao, Y., Liang, L., Zhang, Y., Zhang, J., Qi, S., 2023. New insight into the geochemical mechanism and behavior of heavy metals in soil and dust fall of a typical copper smelter. *Environmental Research* 225: 115638.

Lombi, E., Scheckel, K., Armstrong, R., Forrester, S., Cutler, J., Paterson, D., 2006. Speciation and distribution of phosphorus in a fertilized soil: A synchrotron-based ınvestigation. *Soil Science Society of America Journal* 70(6): 2038-2048.

Loron, C.C., Sforna, M.C., Borondics, F., Sandt, C., Javaux, E.J., 2022. Synchrotron FTIR investigations of kerogen from Proterozoic organic-walled eukaryotic microfossils. *Vibrational Spectroscopy* 123(9): 103476.

Ma, R., Jiang, Y., Liu, B., Fan, H., 2020. Effects of pore structure characterized by synchrotron-based micro-computed tomography on aggregate stability of black soil under freeze-thaw cycles. *Soil and Tillage Research* 207(3): 104855.

Manceau, A., Lanson, M., Takahashi, Y., 2014. Mineralogy and crystal chemistry of Mn, Fe, Co, Ni, and Cu in a deep-sea Pacific polymetallic nodule. *American Mineralogist* 99(10): 2068-2083.

Manceau, A., Marcus, M.A., Tamura, N., Proux, O., Geoffroy, N., Lanson, B., 2004. Natural speciation of Zn at the micrometer scale in a clayey soil using X-ray fluorescence, absorption, and diffraction. *Geochimica et Cosmochimica Acta* 68(11): 2467-2483.

Masindi, V., Mkhonza, P., Tekere, M., 2021. Sources of heavy metals pollution. In: Remediation of heavy metals. Environmental chemistry for a sustainable world. Innamudin, Ahamed, M.I., Lichtfouse, E., Altalhi, T., (Eds.). Springer, Cham, pp. 419–454.

McNear, D., Tappero, R., Sparks, D., 2010. Shining Light on metals in the environment. *Elements* 1(4): 211–216.

Mei, Y., Etschmann, B., Liu, W., Sherman, D., Barnes, S., Fiorentini, M., Seward, T.M., Testemale, D., Brugger, J., 2015. Palladium complexation in chloride- and bisulfide-rich fluids: Insights from ab initio molecular dynamics simulations and X-ray absorption spectroscopy. *Geochimica et Cosmochimica Acta* 161: 128–145.

Meneses, A.A.M., Palheta, D.B., Pinheiro, C.J.G., Barroso, R.C.R., 2018. Graph cuts and neural networks for segmentation and porosity quantification in Synchrotron Radiation X-ray μCT of an igneous rock sample. *Applied Radiation and Isotopes* 133: 121–132.

Minkina, T., Soldatov, A., Motuzova, G.V., Podkovyrina, Y., Nevidomskaya, D., 2014. Speciation of copper and zinc compounds in artificially contaminated chernozem by X-ray absorption spectroscopy and extractive fractionation. *Journal of Geochemical Exploration* 144(9): 306-311.

Nevidomskaya, D., Minkina, T., Soldatov, A., Bauer, T., Shuvaeva, V., Zubavichus, Y., Trigub A., Mandzhieva, S.S., Dorovatovskii, P.V., Popov, Yu.V., 2021. Speciation of Zn and Cu in Technosol and evaluation of a sequential extraction procedure using XAS, XRD and SEM–EDX analyses. *Environmental Geochemistry and Health* 43(6): 2301–2315.

Nevidomskaya, D., Minkina, T., Soldatov, A., Shuvaeva, V., Zubavichus, Y., Podkovyrina, Y., 2015. Comprehensive study of Pb (II) speciation in soil by X-ray absorption spectroscopy (XANES and EXAFS) and sequential fractionation. *Journal of Soils and Sediments* 16(4): 1183-1192.

Newville, M., 2004. Fundamentals of XAFS. *Reviews in Mineralogy and Geochemistry* 78 (1): 33–74.

Prietzel, J., Ayala, G., Häusler, W., Eusterhues, K., Mahakot, S., Klysubun, W., 2023. Aluminum speciation in forest soils and forest floor density fractions using synchrotron-based XANES spectroscopy. *Geoderma* 431: 116373.

Prietzel, J., Thieme, J., Eusterhues, K., Eichert, D., 2007. Iron speciation in soils and soil aggregates by synchrotron-based X-ray microspectroscopy (XANES,?-XANES). *European Journal of Soil Science* 58(5): 1027-1041.

Reynolds, H., Ram, R., Charalambous, F., Antolasic, F., Tardio, J., Bhargava, S., 2010. Characterisation of a uranium ore using multiple X-ray diffraction based methods. *Minerals Engineering* 23(9): 739–745.

Roy, M., McDonald, L., 2013. Metal uptake in plants and health risk assessments in metal-contaminated smelter soils. *Land Degradation and Development* 26(8): 785-792.

Roy, M., McDonald, L.M., 2015. Metal uptake in plants and health risk assessments in metal-contaminated smelter soils. *Land Degradation and Development* 26: 785-792.

Scheckel, K., Hamon, R., Jassogne, L., Rivers, M., Lombi, E., 2007. Synchrotron X-ray absorption-edge computed microtomography imaging of thallium compartmentalization in Iberis intermedia. *Plant and Soil* 290(1–2): 51-60.

Schommer, V., Vanin, A., Torres, N.M., Ferrari, V., Dettmer, A., Colla, L., Piccin, J., 2023. Biochar-immobilized Bacillus spp. for heavy metals bioremediation: A review on immobilization techniques, bioremediation mechanisms and effects on soil. *Science of The Total Environment* 881(1): 163385.

Seth, C., 2012a. A review on mechanisms of plant tolerance and role of transgenic plants in environmental clean-up. *The Botanical Review* 78: 32–62.

Shi, J., Zhao, D., Ren, F., Huang, L., 2023. Spatiotemporal variation of soil heavy metals in China: The pollution status and risk assessment. *Science of The Total Environment* 871: 161768.

Singh, S., Raju, N., Nazneen, S., 2015. Environmental risk of heavy metal pollution and contamination sources using multivariate analysis in the soils of Varanasi environs, India. *Environmental Monitoring and Assessment* 187(6): 345.

Smith, S., Collinson, M., Rudall, P., Simpson, D., Marone, F., Stampanoni, M., 2009. Virtual taphonomy using synchrotron tomographic microscopy reveals cryptic features and internal structure of modern and fossil plants. *Proceedings of the National Academy of Sciences of the United States of America* 106(29): 12013-12018.

Solomon, D., Lehmann, J., Kinyangi, J., Liang, B., Schäfer, T., 2005. Carbon K-edge NEXAFS and FTIR-ATR spectroscopic investigation of organic carbon speciation in soils. *Soil Science Society of America Journal* 69(1): 107-119.

Stańczyk, W., Czapla-Masztafiak, J., Błachucki, W., Kwiatek, W., 2023. Comparison between laboratory and synchrotron X-ray absorption spectroscopy setup examination of Cu (II) complexes with prospective anticancer properties. *Nuclear Instruments and Methods in Physics Research Section B: Beam Interactions with Materials and Atoms* 543: 165100.

Strawn, D., Baker, L., 2009. Molecular characterization of copper in soils using X-ray absorption spectroscopy. *Environmental Pollution* 157(10): 2813-2821.

Su, C., Jiang, L., Zhang, W., 2014. A review on heavy metal contamination in the soil worldwide: Situation, impact and remediation techniques. *Environmental Skeptics and Critics* 3(2): 24-38.

Tafforeau, P., Boistel, R., Boller, E., Bravin, A., Brunet, M., Chaimanee, Y., Cloetens, P., Feist, M., Hoszowska, J., aeger, J.J., Kay, R.F., Lazzari, V., Marivaux, L., Nel, A., Nemoz, C., Thibault, X., Vignaud, P., Zabler, S., 2006. Applications of X-ray Synchrotron microtomography for non-destructive 3D studies of paleontological specimens. *Applied Physics A* 83: 195–202.

Ternov, I.M., 1967. Synchrotron radiation. *Physics-Uspekhi* 38: 409–434.

Tsao, T., Chen, Y., Sheu, H., Tzou, Y., Chou, Y., Wang, M., 2013. Separation and identification of soil nanoparticles by conventional and synchrotron X-ray diffraction. *Applied Clay Science* 85: 1–7.

Tsitsuashvili, V., Minkina, T., Soldatov, A., Nevidomskaya, D., 2021. On synchrotron radiation for studying the transformation of toxic elements in the soil–plant system: A review. *Journal of Surface Investigation: X-ray, Synchrotron and Neutron Techniques* 15: 814-822.

Voegelin, A., Weber, F.-A., Kretzschmar, R., 2007. Distribution and speciation of arsenic around roots in a contaminated riparian floodplain soil: Micro-XRF element mapping and EXAFS spectroscopy. *Geochimica et Cosmochimica Acta* 71: 5804-5820.

Von der Heyden, B., 2020. Shedding light on ore deposits: A review of synchrotron X-ray radiation use in ore geology research. *Ore Geology Reviews* 117: 103328.

Wan, D., Ye, T., Lu, Y., Chen, W., Cai, P., Huang, Q., 2019. Iron oxides selectively stabilize plant-derived polysaccharides and aliphatic compounds in agricultural soils. *European Journal of Soil Science* 70(6): 1153-1163.

Wang, P., Lombi, E., Donner, E., 2017a. Synchrotron-based X-Ray approaches for examining toxic trace metal(loid)s in soil–plant systems. *Journal of Environment Quality* 46(6): 1175-1189.

Wang, S., Wu, W., Liu, F., Liao, R., Hu, Y., 2017b. Accumulation of heavy metals in soil-crop systems: a review for wheat and corn. *Environmental Science and Pollution Research* 24: 15209–15225.

Wetzel, D.L., LeVine, S.M., 1999. Imaging molecular chemistry with infrared microscopy. *Science* 285(5431): 1224-1225.

Xiao, J., Chen, W., Wang, L., Zhang, X., Wen, Y., Bostick, B., Wen, Y., He, X., Zhang, L., Zhuo, X., Huang, K., Wang, N., Ji, J., Liu, Y., 2022. New strategy for exploring the accumulation of heavy metals in soils derived from different parent materials in the karst region of southwestern China. *Geoderma* 417(1): 115806.

Xiao, J., Wen, Y.-L., Dou, S., Bostick, B., Ran, W., Yu, G.H., Shen, Q.R., 2019. A new strategy for assessing the binding microenvironments in intact soil microaggregates. *Soil and Tillage Research* 189: 123-130.

Xiao, J., Wen, Y., Yu, G.H., Dou, S., 2018. Strategy for microscale characterization of soil mineral-organic associations by synchrotron-radiation-based FTIR Technology. *Soil Science Society of America Journal* 82(6): 1583-1591.

Yu, G.H., Fusheng, S., 2017. Using new hetero-spectral two-dimensional correlation analyses and synchrotron-radiation-based spectromicroscopy to characterize binding of Cu to soil dissolved organic matter. *Environmental Pollution* 223: 457–465.

Eurasian Journal of Soil Science

Journal homepage : http://ejss.fesss.org
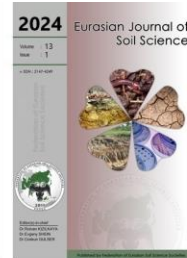
Determination of change in the land use and land cover of the Samsun Bafra Delta Plain from 1990 to 2020 using GIS and Remote Sensing Techniques

İnci Demirağ Turan [a,*], Orhan Dengiz [b], Sena Pacci [b], David Tavi Agbor [c]

[a] Samsun University, Faculty of Human and Social Sciences, Department of Geography, Samsun, Türkiye
[b] Ondokuz Mayıs University, Faculty of Agriculture, Department of Soil Science and Plant Nutrition, Samsun, Türkiye
[c] Department of Agronomic and Applied Molecular Sciences, Faculty of Agriculture and Veterinary Medicine, University of Buea, Cameroon

Abstract

Land use and land cover changes can have detrimental effects on the ecology, if they are not properly aligned with the characteristics of the land. This study aims to evaluate the temporal changes in land use and land cover of Bafra Delta plain, situated in the east of Samsun province. The region is one of the most significant plains within the Black Sea area. Remote sensing technique was utilized in this research which made use of Landsat images from 1990, 2000, 2010, and 2020. Supervised classification was applied in ENVI 5.3v software to perform calculations, resulting in six main classes. Field work was applied to classify the unclassified classes. The resulting six land use-land cover classes were agriculture lands, forest, dune, marshy, water surface, and artificial areas. To determine land use efficiency, analogue data was digitised and transferred to a GIS database. The agricultural areas occupy the largest portion of the plain, followed by hazelnut and artificial areas. The changes over the last decade, notably the growth of artificial areas and water surfaces, and the reduction of arable lands, highlight significant variations in size across the areas. Furthermore, the study indicated that remote sensing and geographic information system techniques play a crucial role in identifying and monitoring land cover and land use trends on a large-scale to produce accurate and timely data. Poorly adapted land use changes can cause major ecological damage. The aim of this study is to identify the changes over time in land use and land cover of Bafra Delta plain, located to the east of Samsun city and one of the most significant plains in the Black Sea region, using remote sensing techniques. To this end, Landsat images from 1990, 2000, 2010 and 2020 are utilized. To perform the calculations, ENVI 5.3v software was employed, applying a supervised classification technique that resulted in forming six main classes. Fieldwork was conducted to classify the unclassified classes. The resulting land-use and land-cover classes were agricultural land, forest, dunes, marshland, water surface, and artificial areas. To evaluate land-use efficiency, analogue data were digitalised and imported into a GIS database. The plain's most extensive land-use areas consist of agricultural lands, followed by hazelnut and artificial areas. In the last decade, the rise in artificial and water surfaces and the decline in agricultural areas highlights significant changes in the region's size. This study also emphasises the crucial role of remote sensing and geographic information system techniques in generating fast and consistent data for monitoring large-scale land cover and land use trends.

Keywords: Land use-land cover, change analysis, Bafra Plain

Introduction

Life on Earth, human progress, as well as scientific findings that elaborate the interactions between ecosystems and humans are highly dependent on land, making land the most valuable human asset on Earth necessary for development (Pflugmacher al., 2019). Despite the indispensability of land to humans, land is undergoing a series of changes due to natural or anthropogenic activities called land use/land cover change (Liu et al., 2014). These changes have recently experienced massive investment in the form of research to provide checks and balances in global ecological fields (Samie et al., 2017). This can be seen in the publication of a catalogue of plans by the International Geosphere-Biosphere Programme (IGBP) and the International Human Dimensions Programme on Global Environmental Change (IHDP) to stimulate research in the field of land use/land cover (Wu, 2019; Song et al., 2020). Land use/land cover remains a topic of serious concern in recent times as it greatly affects global human progress as a critical component of climate change that alters ecosystem functions and services (Roy et al., 2022; Xu and Xiao, 2022). Hence, to furnish scientific evidence for natural resource management and global development, it is imperative to conduct investigations and assessments on the factors that drive land use and land cover changes. This is crucial for proper utilisation, allocation, and planning of land resources. (Cui et al., 2022). In this regard, remote sensing and GIS are critical tools for the study and analysis of land use/land cover (Hussain et al., 2020; MohanRajan, et al., 2020).

Remote sensing and GIS are effective methods for studying changes in land use and land cover, thanks to their ability to efficiently and technically cover a wide range of observations and provide a large amount of information over a small period. They are also valuable tools for monitoring the environmental impact of global human development. (Bansod and Dandekar, 2018; Nguyen et al., 2020). Remote sensing and GIS have the potential to deliver timely, precise, and dependable insights on changes in land use and land coverage over specific time intervals in a cost-effective and efficient way. (Chen et al., 2017; Govender et al., 2022). The study of land use/land cover change has brought remote sensing and GIS tools into focus for researchers. It is apparent that the IGBP and the United States Geological Survey (USGS) collaborated to create a global LULC data product with 1 km resolution, utilizing Advanced Very High Resolution Radiometer (AVHRR) data (Loveland et al., 2000). LULC change in the Yellow River Basin of Shandong Province was studied by Cui et al. (2022) using remote sensing and GIS from 2000 to 2020. Similar work was done by Stefanski et al. (2014), where they studied LULC change in western Ukraine from 1986 to 2010 using Landsat and ERS SAR data. The trend has been continued by other researchers such as Souza et al. (2020) in Brazil, Abdullah et al. (2019) in Bangladesh, and many others. In order to detect the changes associated with LULC attributes using the different satellite datasets, change detection involves using RS information to investigate the previous quantitative consequences of an event (Arora and Wolter 2018; Yasir et al., 2020). In order to perform supervised classifications, it is necessary to have prior knowledge of the scene areas, the area where a material of interest is located, the training sites, and the data to be retained and delimited for use in the algorithm (Orimoloye et al., 2018; Pushpanjali et al., 2022).

Climate change is an undeniable reality, with adverse effects on every country worldwide, including Turkey, and posing a significant threat to the livelihoods of small landowners and farmers. This is primarily because small-scale farmers heavily rely on agriculture for their survival, and the agricultural sector is the most vulnerable to climate change's impacts in contemporary times. Bafra is a district in Turkey's Samsun province, known for its rich soils and high quality tobacco growing conditions, making Bafra prominent in tobacco production. However, tobacco production in Bafra has recently declined drastically due to the adverse effects of climate change on the district, resulting in significant LULC changes in the area. Despite the evidence of land degradation in Bafra district, there has been no previous study of LULC changes over time, despite Bafra district's vulnerability status to climate change. Bafra district is facing hazardous situations due to traffic congestion, urbanisation leading to congestion, accidents and pollution as a result of the ever increasing population which is not keeping pace with the available resources. Therefore, there is a need for LULC change studies over a long period of time using GIS and remote sensing in Bafra district to provide information on the dynamics of LULC. Therefore, this paper investigates LULC change over a long time period of 30 years using GIS and remote sensing to identify different LULC change drivers, perform NDVI analysis, generate maps and detect change using satellite data.

Material and Methods

The study area description

This research was done in Samsun-Bafra delta plain district. The Bafra Plain is located in the central Black Sea region of Turkey (Figure 1). The research area is located 30 km to the west of the province of Samsun (4620-4600 km N- 230-260 km E UTM).
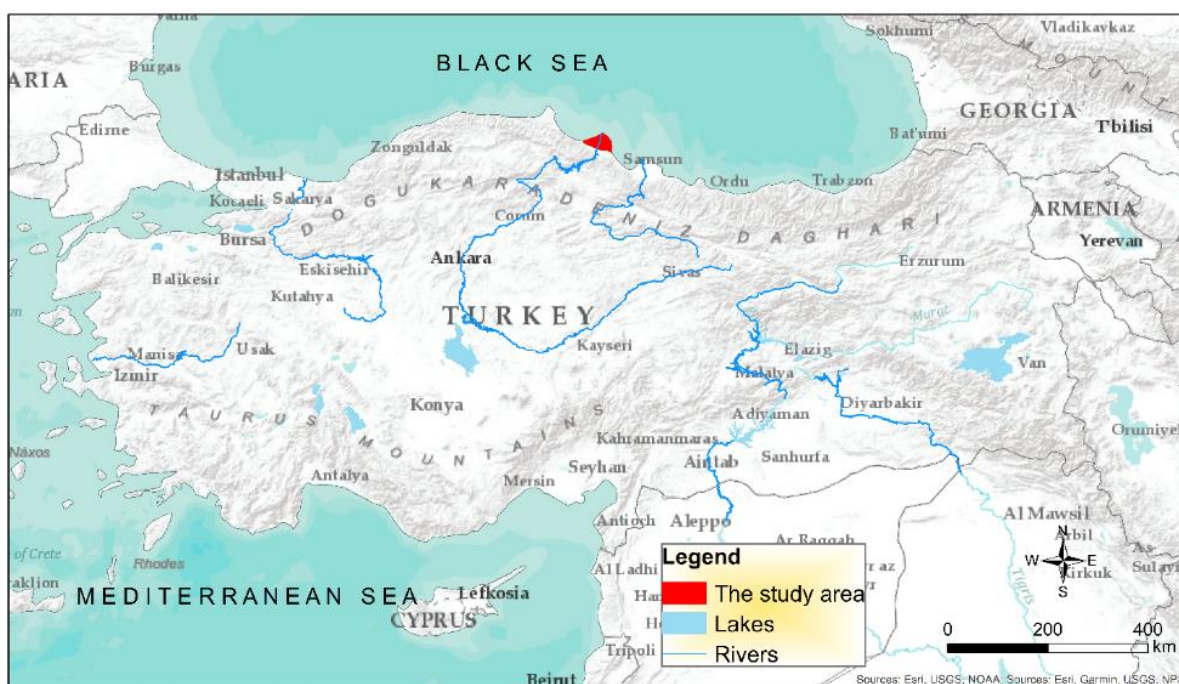
Figure 1. Location of the study area.

The area has a surface area of 72052 ha and lies at an elevation of 0-204 m above sea level with a semi-humid climate (Figure 2). Most of the study area has a slope of less than 2 percent (Figure 2). The area has four seasons; summers, autumn, warmer and spring with an average temperature of 6.9 ºC in summer and 22.2 ºC in summer. The area has mean temperature, rainfall and evaporation per annum of are 13.6 ºC, 764.3 mm and 726.7 mm respectively. Mesic soil temperature and ustic moisture regimes are present at the study site (Soil Survey Staff, 1999) dominated by alluvial lands; Vertisol, Inceptisol and Entisol. The range of organic matter in soils is 1.70% to 5.92%, while soil EC and pH values are varying at 7.28 to 8.01 and 0.61-2.79 dSm^{-1}, respectively. The study area is mostly dominated by agriculture as economic activity with crops like maize, rice, maize, watermelon, pepper, cucumber, tomato and tobacco.
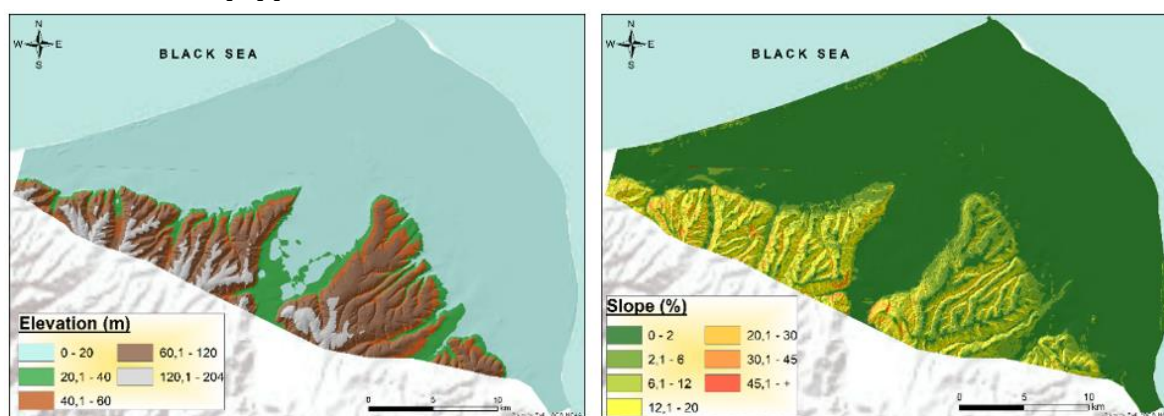
Figure 2. Elevation and slope map of the study area

Data collection

Land use and land cover changes, as well as alterations in NDVI and NDBI, were identified by using satellite images from Landsat 8, Thematic Mapper (TM) and Enhanced TM Plus (ETM+). For this study, Landsat satellite images were obtained for the years 1990, 2000, 2010 and 2020 (Figure 3). The images were downloaded easily and at no cost from the United States Geological Survey (USGS) through the earth explorer website (USGS, 2020), as displayed in Table 1.

Table 1. Landsat satellite image specifications

Data type	Date of Production	Sensor	Path/Row
Landsat image	25.05.1990	LANDSAT 5 /TM	175/31
Landsat image	20.05.2000	LANDSAT 5 /TM	175/31
Landsat image	30.04.2010	LANDSAT 5 /TM	175/31
Landsat image	26.05.2020	LANDSAT 8/ OLI_TIRS	175/31
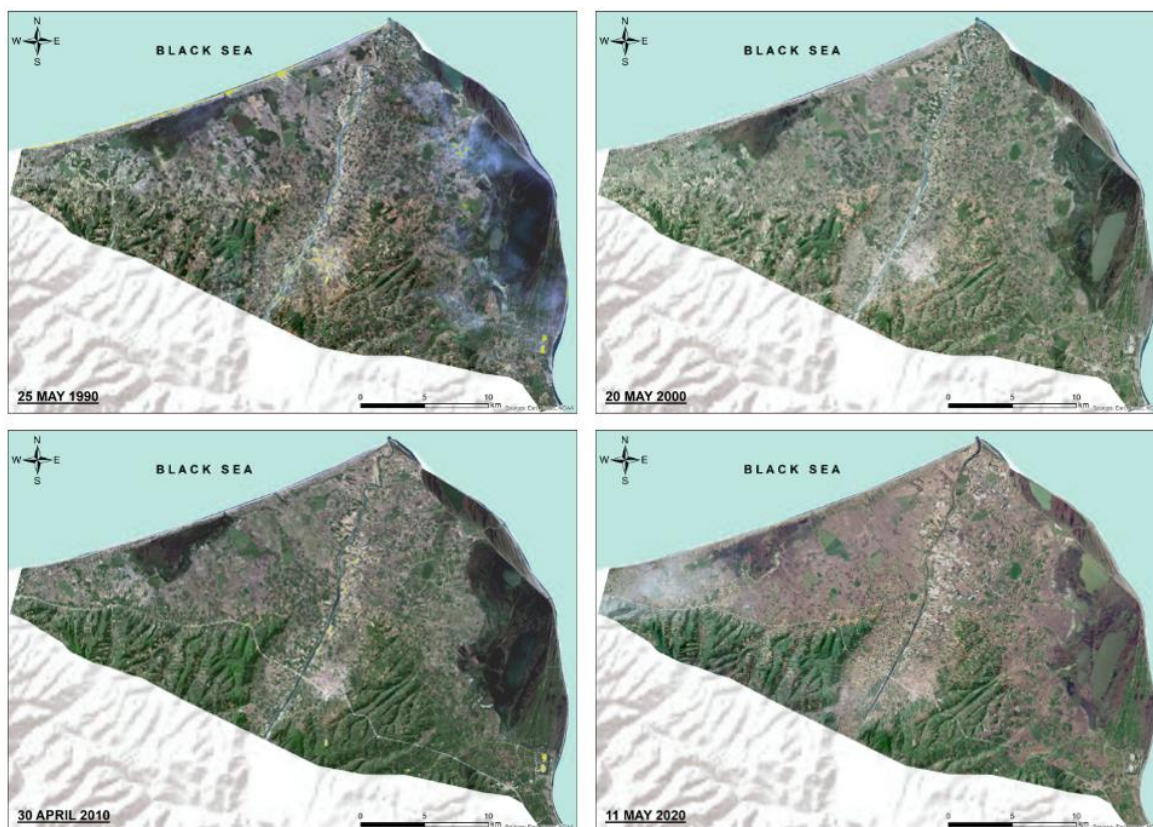
Figure 3. Satellite images for each year

Image classification

The Landsat images were created by combining bands 4, 3 and 1, achieved through layer stacking. Subsequently, using the extraction by mask tools and an image based on the study area, the subsetting procedure was executed in Arc GIS 10.1 software (Iqbal and Khan, 2014). The supervised classification method was used to classify the digital LULC data using field knowledge for the captured images. Supervised classification was utilised to produce LULC maps, while taking into consideration the study area. These LULC images were reclassified utilizing ArcGIS 10.7.1 which enabled us to compare the changes detected over time. The classification approach is graphically demonstrated in Figure 4. The LULC categories comprised farming, human-made (encompassing all facilities, business and housing units, roads and communities), sandbank zones (areas covered in sand), woodland areas, marshlands and bodies of water (rivers, lakes, ponds, canals, low-lying regions and marshes) (Aboelnour and Engel, 2018).
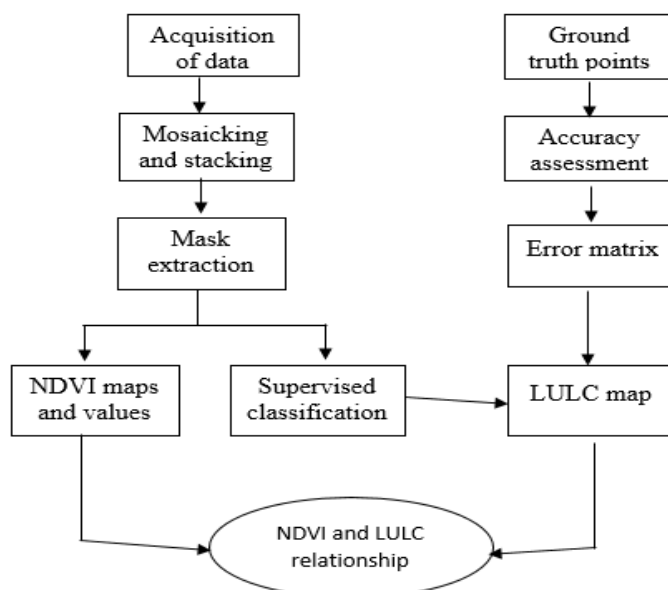
Figure 4. Classification approach

Accuracy assessment

A significant component in various processing procedures leading to image classification is accuracy (Lin et al., 2015; Ibharim et al., 2015). This gives the degree to which images classified are accurate to the natural reality termed error matrix (Lu et al., 2013). Accuracy gives the percentage to which the image classified using different statistical processes of image assessment is true (Zhang et al., 2016).

Overall accuracy = number of sampled classes correctly classified / number of reference   (1)
sampled classes number of reference sampled classes

The KHAT is the measure the magnitude to which RS classification falls in line with the reference data (Usman et al., 2015). KHAT is mathematical represented as follows:

K = observed accuracy - chance assessment / 1 - chance agreement   (2)

Change of land use-land cover (LULC)

The current study aimed to evaluate multi-temporal land use/cover changes (LULC) by integrating GIS and remote sensing data. To this end, satellite imagery from Landsat 4 TM, Landsat 7 ETM, Landsat 5 TM, and Landsat 8 OLI-TIRS was used, spanning from May 1990 to May 2020 at an approximate 30 m resolution. The images were registered in Universal Transverse Mercator (UTM-m), zones 36N and WGS 84. The study included supervised classification and accuracy assessment stages. Six land use and land cover (LULC) classes were utilised: dune area, wetland, artificial area, agriculture area, water surface, and forest land. The maximum likelihood function of ENVI 5.1v was used for supervised classification. Furthermore, to validate the status of each LULC, ground control with GPS was conducted at specified coordinates during supervised classification.

Results and Discussion

Temporal change in land use and land cover

The present study utilised image processing to determine changes in land use/land cover from 1990 to 2020. Among all types of land, agricultural land had the highest coverage in the study area (Table 2). Figure 5 presents the land use/land cover distribution maps for different years. In 1990, agricultural land constituted 75.1% of the land use/land cover, but this has declined to 73.3% in 2020 (Table 2 and Figure 5). Forest land is present in regions where the gradient and elevation rise towards the south in the study area. In addition, the areas covered by water increased from 3.7% in 1990 to 5.0% in 2020. In this change, some places in the study area are changing as marsh areas and water areas. Artificial (all infrastructure, commercial and residential; road networks; and settlements distributed on the plain increased from about 3.8% in 1990 to 5.2% in 2000, and the distribution increased slightly in 2010 and reached 5.5%. in 2020, this rate has increased to 5.9%. This increase has been realized especially with the change from agricultural lands to artificial areas. With the increase of urbanization in different regions, land use land cover studies are increasing. Bağcı and Bahadır (2019) determined in their study that the proportion of water areas in the Kızılırmak Delta increased between 1987 and 2018, while agricultural areas from 359.1 km² to 347 km². In addition, similar results were obtained in the same study and they found that human activities increased from 45 km² to 63 km². Bağcı and Bahadır (2019) determined in their study that the proportion of water areas in the Kızılırmak Delta increased between 1987 and 2018, while agricultural areas from 359.1 km² to 347 km². In addition, similar results were obtained in the same study and it was determined that human activities increased from 45 km² to 63 km². Devkota et al. (2023) conducted their study in 12 rapidly urbanising cities of Nepal. Among these cities, Kathmandu city is experiencing a significant change. In this city, there is an increase of 65.61% in artificial areas between 2010 and 2020. In the same city, there is a decrease of -42.73% in agricultural areas.

Table 2. The changes in the area and proportional distributions of the land use land cover in the Bafra Plain for the years 1990, 2000, 2010 and 2020

LU/LC	1990		2000		2010		2020	
	ha	%	ha	%	ha	%	ha	%
Artificial area	2764	3.8	3719	5.2	3939	5.5	4276	5.9
Water bodies	2691	3.7	2895	4.0	3265	4.5	3596	5.0
Dune area	1572	2.2	1526	2.1	1502	2.1	1504	2.1
Marshy land	8859	12.3	8020	11.1	7960	11.0	7810	10.8
Forest area	2053	2.8	2205	3.1	2134	3.0	2074	2.9
Agriculture area	54113	75.1	53687	74.5	53252	73.9	52792	73.3
Total	72052	100.0	72052	100.0	72052	100.0	72052	100.0
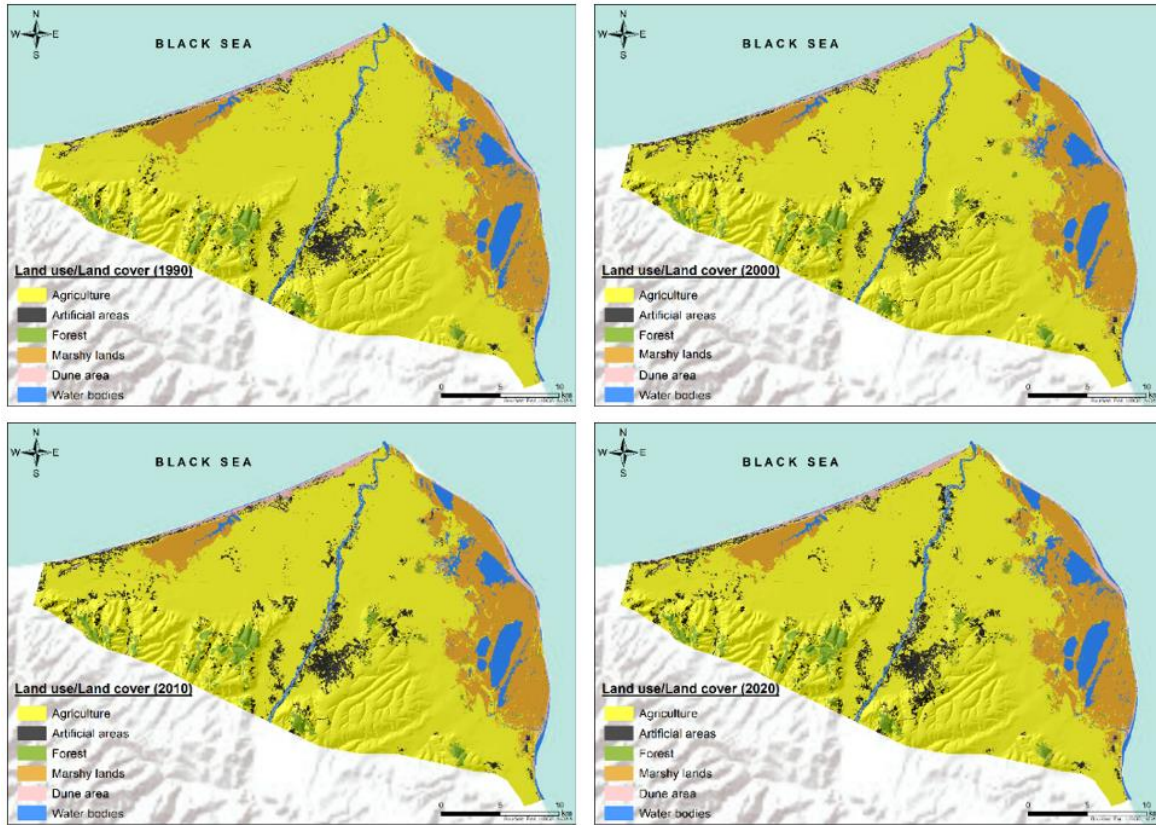
Figure 5. Land use/Land cover distribution maps for each year for the Bafra plain

Figure 6 depicts the percentage differences in total equivalent pixels within paired images classified during 1990 to 2020, with inter-period intervals of 1990-2000, 1990-2010, 2000-2010, 2000-2020, 2010-2020, and 1990-2020. These results obtained by the subtraction of total initial class count from total final count unveil the differences in land use and land coverage classes represented in the images. The most significant changes were observed between 1990 and 2020, followed by the changes from 1990 to 2010.
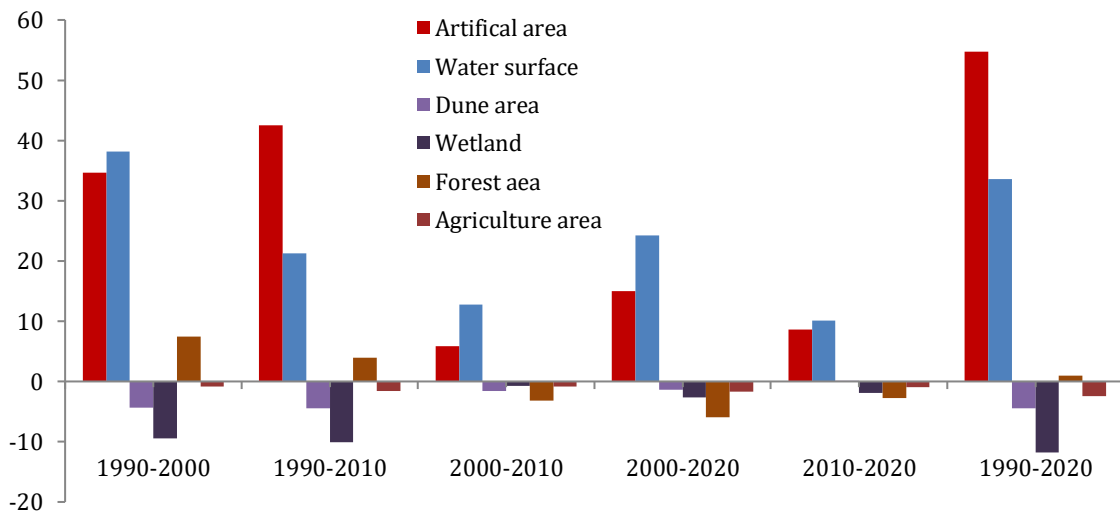
Figure 6. Land cover and land use differences for six time periods of the study area

The accuracy analysis results

Landsat (TM) satellite imagery of the study site taken on 20th May 1990, 20th May 2000, and 30th April 2010, as well as a Landsat-8 OLI satellite image captured on 26th May 2020, were analysed against 300 ground control points established during field investigations. The accuracy analysis results obtained after classification of each satellite image were given in Table 3. According to the results obtained, 90.66% accuracy was reached in the satellite image dated 20.05.1990. According to this value, the classification is considered to be accurate and reliable (Koç and Yener, 2001; Özdemir and Özkan, 2003). In addition, the kappa value of 0.88 indicates that the agreement between the observers is complete. The highest user accuracy in the image

was obtained from dune areas with 100 % (Table 3). In the satellite image dated 20.05.2000, 86.12 % accuracy was achieved for the classification results and it was determined that the agreement between the observers was complete with a kappa value of 0.84. The highest user accuracy was obtained from dune areas with 94.07%. The overall classification accuracy was 92.66% for artificial areas (92.66%), followed by marsh areas (91.20%), forest (82.15%), water areas (80.19%) and agricultural areas (80.02%). In the satellite image dated 26.05.2020, 92.65% accuracy was achieved for the classification results and the kappa value was 0.90, indicating that the agreement between the observers was complete. The highest user accuracy in the image was obtained from marshy lands with 98.65%.

Table 3. Accuracy analysis results obtained after classification of each satellite image

Class	Agriculture	Forest	Marshy lands	Dune areas	Artificial areas	Water bodies	Producer Accuracy	User Accuracy
20.05.1990 (%) Overall Accuracy = % 90.66 Kappa Value = 0.88								
Agriculture	44	0	4	1	1	0	88.26	92.2
Forest	2	49	4	0	0	0	84.53	78.13
Marshy lands	1	1	40	0	0	0	98.59	98.24
Dune areas	1	0	0	45	1	0	97.03	100
Artificial areas	1	0	0	4	48	0	94.19	91.44
Water bodies	1	0	2	0	0	50	85.19	89.1
Total	50	50	50	50	50	50		
20.05.2000 (%) Overall Accuracy = % 86.12 Kappa Value = 0.84								
Agriculture	44	0	4	1	1	0	81.15	84.64
Forest	2	49	4	0	0	0	84.46	90.34
Marshy lands	1	1	40	0	0	0	93.27	88.16
Dune areas	1	0	0	45	1	0	94.07	84.34
Artificial areas	1	0	0	4	48	0	93.76	83.94
Water bodies	1	0	2	0	0	50	79.89	89.63
Total	50	50	50	50	50	50		
30.04.2010 (%) Overall Accuracy = % 86.13 Kappa Value = 0.83								
Agriculture	45	0	4	1	1	0	80.02	85.14
Forest	1	48	4	0	0	0	82.15	89.20
Marshy lands	1	1	40	0	1	0	91.20	87.06
Dune areas	1	1	0	46	1	0	95.12	85.15
Artificial areas	1	0	0	3	47	2	92.66	82.98
Water bodies	1	0	2	0	0	48	80.19	90.23
Total	50	50	50	50	50	50		
11.05.2020 (%) Overall Accuracy = % 92.65, Kappa Value = 0.90								
Agriculture	45	0	2	2	1	0	89.32	93.22
Forest	1	49	3	0	0	0	85.13	88.18
Marshy lands	1	1	44	0	1	0	98.65	99.12
Dune areas	1	0	0	46	1	0	97.23	99.18
Artificial areas	2	0	0	2	47	0	93.11	90.20
Water bodies	0	0	2	0	0	50	95.19	95.10
Total	50	50	50	50	50	50		

In this study, the spatial arrangement of vegetation cover was mapped using NDVI data from annual images. The results are displayed in Figure 7.

Table 4 presents the areas and proportions of vegetation density classes within the NDVI maps. For 1990 NDVI images, the majority of the study area fell under the very weak and weak density classes, accounting for 52.5% of the total area. These were trailed by intensive (24.7%) and moderate density classes (22.7%). The 2000 NDVI mapping showed almost the same outcome. Table 4 also provides information regarding positive and negative trends in land productivity dynamics (LPD) between 1990 and 2020. Conversely, there is a decrease in the area exhibiting high plant density, indicating a negative trend. The data shows an increase in the area with low plant density. However, a small portion of the study area reflects an increase in high plant density, indicating a positive trend.

Furthermore, Figure 8 illustrates discrepancies in vegetation cover density over six time periods, with the least fluctuations occurring in 1990-2000, 1990-2010, 2000-2010, 2000-2020, 2010-2020 and 1990-2020.
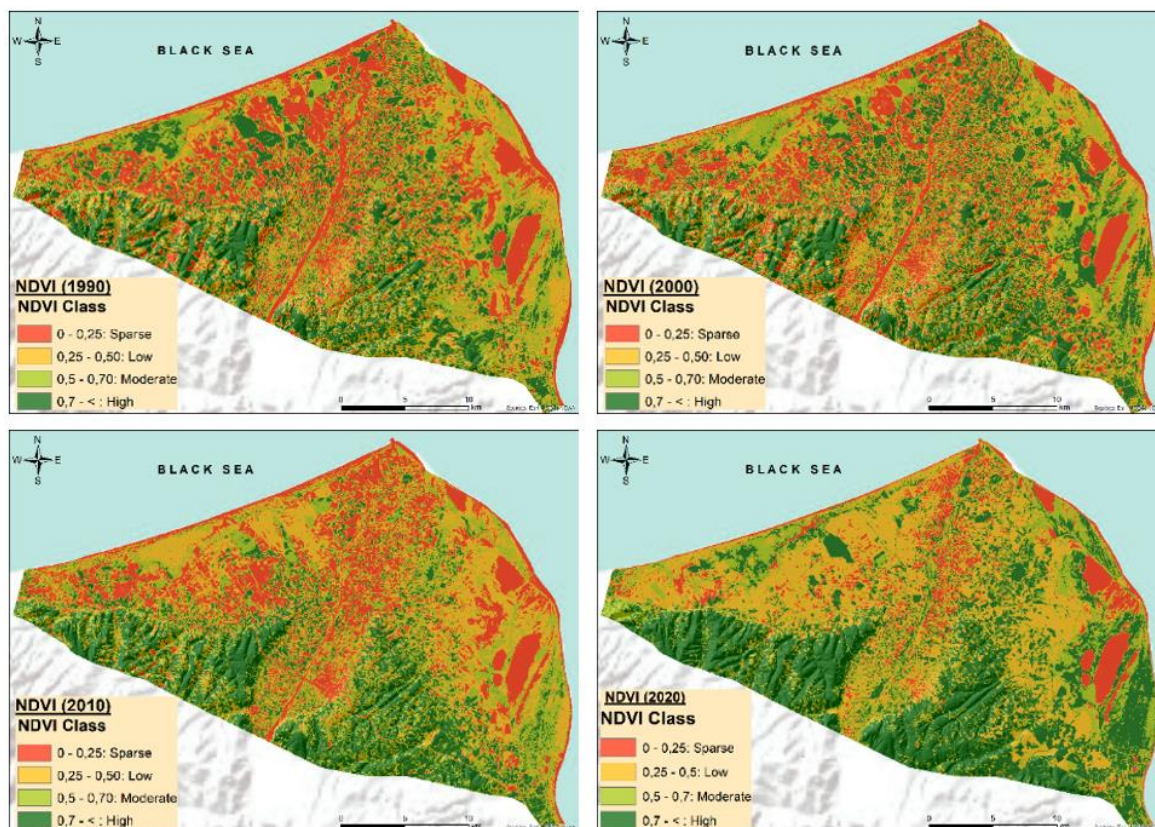
Figure 7. Maps of spatial distribution of plant density classes in 1990, 2000, 2010 and 2020 for the Bafra Delta Plain, Turkey

Table 4. Distribution of NDVI classes (area and %) for each year in the Bafra Delta Plain, Turkey

NDVI	1990		2000		2010		2020		Relative Change, % 1990-2020	Effect on LPD (-/+)
	ha	%	ha	%	ha	%	ha	%		
Very Weak 0-0.25	18548	25.74	16676	23.47	15991	22.19	7110	9.87	61.67	-
Weak 0.25-0.50	19289	26.77	17538	24.68	21714	30.14	24054	33.38	24.70	+
Moderate 0.50-0.70	16385	22.74	16898	23.78	16652	23.11	13867	19.25	22.23	-
Intensive > 70	17830	24.75	19940	28.06	17695	24.56	27021	37.50	51.55	+
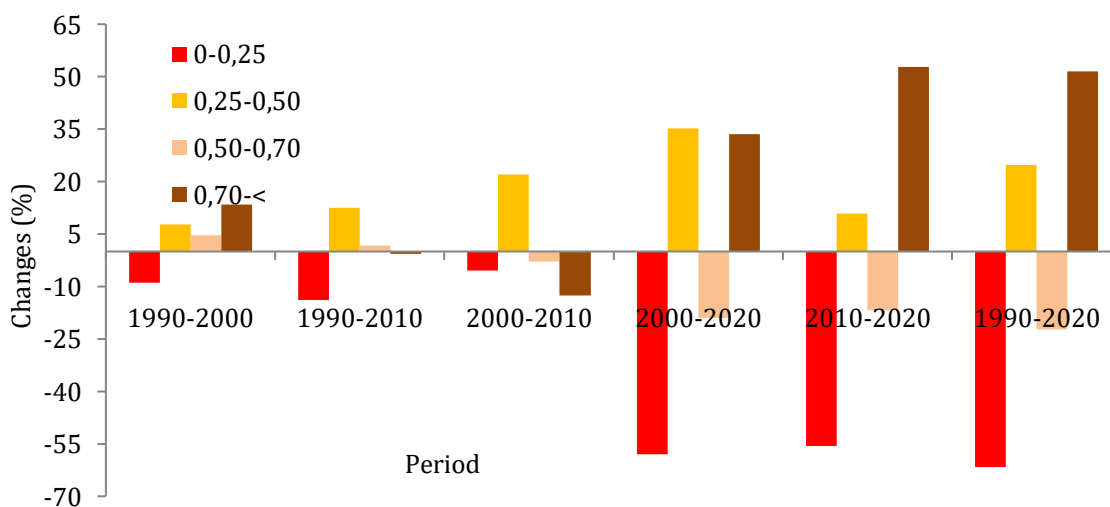
Figure 8. Vegetation density covers differences for six time periods Turkey

Conclusion

The review showcases the advancements of contemporary techniques for studying metalloid forms and heavy In this present study, six different land use and land cover changes in the last thirty years (1990-2020) were analysed by using Landsat satellite images of Bafra Plain, the second largest plain of Turkey, from four different dates with 10-year intervals. An accuracy rate of more than 85% was obtained in the classification of satellite images. The areas with the highest distribution in the plain are arable agricultural lands, while the areas with the least distribution are dune areas. While agricultural lands were 75.1% in 1990, this rate decreased to 73.3% in 2020. In the study area, while artificial (all infrastructure, commercial and residential; road networks; and settlements) was around 3.8% in 1990, it increased to 5.2% in 2000, and the distribution increased slightly in 2010 and reached 5.5%. In 2020, this rate increased to 5.9 per cent.

The results of the study reveal that the pressure on agricultural lands in Samsun Bafra Plain has been increasing day by day in the last thirty years. It is thought that the findings of the study and the applied approach can be a source for periodically providing spatial data that can be used as the most important basis in the management activities of authorities and decision makers in order to determine time-dependent changes reliably and accurately in a short period of time. In the future, the study will be carried out with higher spatial, temporal and spectral resolutions.

References

Abdullah, A.Y.M., Masrur, A., Adnan, M.S.G., Baky, M.A.A., Hassan, Q.K., Dewan, A., 2019. Spatio-temporal patterns of land use/land cover change in the heterogeneous coastal region of Bangladesh between 1990 and 2017. *Remote Sensing* 11(7): 790.

Aboelnour, M., Engel, B.A., 2018. Application of remote sensing techniques and geographic information systems to analyze land surface temperature in response to land use/land cover change in Greater Cairo Region, Egypt. Journal of Geographic Information System 10(1): 57-88.

Arora, G., Wolter, P.T., 2018. Tracking land cover change along the western edge of the US Corn Belt from 1984 through 2016 using satellite sensor data: Observed trends and contributing factors. *Journal of Land Use Science* 13(1-2): 59-80.

Bağcı, H.R., Bahadır, M., 2019. Land use and temporal change in Kızılırmak Delta (Samsun) (1987-2019). *The Journal of Academic Social Science Studies* 78: 295-312. [in Turkish]

Bansod, R.D., Dandekar, U.M., 2018. Evaluation of Morna river catchment with RS and GIS techniques. *Journal of Pharmacognosy and Phytochemistry* 7(1): 1945-1948.

Chen, J., Theller, L., Gitau, M.W., Engel, B.A., Harbor, J.M., 2017. Urbanization impacts on surface runoff of the contiguous United States. *Journal of Environmental Management* 187: 470-481.

Cui, J., Zhu, M., Liang, Y., Qin, G., Li, J., Liu, Y., 2022. Land use/land cover change and their driving factors in the Yellow River Basin of Shandong Province based on google earth Engine from 2000 to 2020. *ISPRS International Journal of Geo-Information* 11(3): 163.

Devkota, P., Dhakal, S., Shrestha, S., Shrestha, U.B., 2023. Land use land cover changes in the major cities of Nepal from 1990 to 2020. *Environmental and Sustainability Indicators* 13: 100227.

Govender, T., Dube, T., Shoko, C., 2022. Remote sensing of land use-land cover change and climate variability on hydrological processes in Sub-Saharan Africa: key scientific strides and challenges. *Geocarto International* 37(25): 10925-10949.

Hussain, S., Mubeen, M., Ahmad, A., Akram, W., Hammad, H.M., Ali, M., Masood, N., Amin, A., Farid, H.U., Sultana, R.R., Fahad, S., Wang, D., Nasim, W.,2020. Using GIS tools to detect the land use/land cover changes during forty years in Lodhran District of Pakistan. *Environmental Science and Pollution Research* 27(32): 39676-39692.

Ibharim, N.A., Mustapha, M. A., Lihan, T., Mazlan, A.G., 2015. Mapping mangrove changes in the Matang Mangrove Forest using multi temporal satellite imageries. *Ocean & Coastal Management* 114: 64-76.

Iqbal, M.F., Khan, I.A., 2014. Spatiotemporal land use land cover change analysis and erosion risk mapping of Azad Jammu and Kashmir, Pakistan. *The Egyptian Journal of Remote Sensing and Space Science* 17(2): 209-229.

Koç, A., Yener, H., 2001. Uzaktan algılama verileriyle İstanbul çevresi ormanlarının alansal ve yapısal değişikliklerinin saptanması. *İstanbul Üniversitesi, Orman Fakültesi Dergisi* 51(2): 17-36. [in Turkish]

Lin, C., Wu, C.C., Tsogt, K., Ouyang, Y.C., Chang, C.I., 2015. Effects of atmospheric correction and pansharpening on LULC classification accuracy using WorldView-2 imagery. *Information Processing in Agriculture* 2(1): 25–36.

Liu, J., Kuang, W., Zhang, Z., Xu, X., Qin, Y., Ning, J., Zhou, W., Zhang, S., Li, R., Yan, C., Wu, S., Shi, X., Jiang, N., Yu, D., Pan, X., Chi, W., 2014. Spatiotemporal characteristics, patterns, and causes of land-use changes in China since the late 1980s. *Journal of Geographical Sciences* 24(2): 195-210.

Loveland, T.R., Reed, B.C., Brown, J.F., Ohlen, D.O., Zhu, Z., Yang, L.W., Merchant, J.W., 2000. Development of a global land cover characteristics database and IGBP DISCover from 1 km AVHRR data. *International Journal of Remote Sensing* 21(6-7): 1303-1330.

Lu, D., Li, G., Moran, E., Hetrick, S., 2013. Spatiotemporal analysis of land use and land cover change in the Brazilian Amazon. *International Journal of Remote Sensing* 34(16): 5953–5978.

MohanRajan, S.N., Loganathan, A., Manoharan, P., 2020. Survey on Land Use/Land Cover (LU/LC) change analysis in remote sensing and GIS environment: Techniques and Challenges. *Environmental Science and Pollution Research* 27(24): 29900-29926.

Nguyen, L.H., Joshi, D.R., Clay, D.E., Henebry, G.M., 2020. Characterizing land cover/land use from multiple years of Landsat and MODIS time series: A novel approach using land surface phenology modeling and random forest classifier. *Remote Sensing of Environment* 238: 111017.

Orimoloye, I.R., Mazinyo, S.P., Nel, W., Kalumba, A.M., 2018. Spatiotemporal monitoring of land surface temperature and estimated radiation using remote sensing: human health implications for East London, South Africa. *Environmental Earth Sciences* 77: 77.

Pushpanjali, Osman, M.D., Srinivas, R.K., Kumar, P.P., Josily, S., Karthikeyan, K., Sammi, R.K., 2022. Land-use change mapping and analysis using remote sensing and GIS for watershed evaluation-A case study. *Journal of Soil and Water Conservation* 21(1): 1-6.

Özdemir, İ., Özkan, Y.U., 2003. Monitoring the changes of forest areas using landsat satellite images in Armutlu forest district. *Süleyman Demirel Üniversitesi Orman Fakültesi Dergisi* 4(1): 55-66. [in Turkish]

Pflugmacher, D., Rabe, A., Peters, M., Hostert, P., 2019. Mapping pan-European land cover using Landsat spectral-temporal metrics and the European LUCAS survey. *Remote Sensing of Environment* 221: 583-595.

Roy, P.S., Ramachandran, R.M., Paul, O., Thakur, P.K., Ravan, S., Behera, M.D., Sarangi, C., Kanawade, V.P., 2022. Anthropogenic land use and land cover changes—A Review on its environmental consequences and climate change. *Journal of the Indian Society of Remote Sensing* 50: 1615–1640.

Samie, A., Deng, X., Jia, S., Chen, D., 2017. Scenario-based simulation on dynamics of land-use-land-cover change in Punjab Province, Pakistan. *Sustainability* 9(8): 1285.

Soil Survey Staff, 1999. Soil taxonomy: A basic of soil classification for making and ınterpreting soil survey. USDA Natural Resources Conservation Service, Agriculture Handbook No: 436. Washington DC, USA. Available at [Access date: 09.07.2023]: https://www.nrcs.usda.gov/sites/default/files/2022-06/Soil%20Taxonomy.pdf

Stefanski, J., Chaskovskyy, O., Waske, B., 2014. Mapping and monitoring of land use changes in post-Soviet western Ukraine using remote sensing data. *Applied Geography* 55: 155-164.

Song, W., Song, W., Gu, H., Li, F., 2020. Progress in the remote sensing monitoring of the ecological environment in mining areas. *International Journal of Environmental Research and Public Health* 17(6): 1846.

Souza, C.M., Jr., Z. Shimbo, J., Rosa, M.R., Parente, L.L., A. Alencar, A., Rudorff, B.F.T., Hasenack, H., Matsumoto, M.G., Ferreira, L., Souza-Filho, P.W.M., de Oliveira, S.W., Rocha, W.F., Fonseca, A.W., Marques, C.B., Diniz, C.G., Costa, D., Monteiro, D., Rosa, E.R., Vélez-Martin, E., Weber, E.J., Lenti, F.E.B., Paternost, F.F., Pareyn, F.G.C., Siqueira, J.A., Viera, J.L., Neto, L.C.F., Saraiva, M.M., Sales, M.H., Salgado, M.P.G., Vasconcelos, R., Galano, S., Mesquita, V.V., Azevedo, T., 2020. Reconstructing three decades of land use and land cover changes in brazilian biomes with landsat archive and earth engine. *Remote Sensing* 12(17): 2735.

USGS, 2020. USGS EarthExplorer. Available at [Access date: 15.05.2020]: https://earthexplorer.usgs.gov/

Usman, M., Liedl, R., Shahid, M. A., Abbas, A., 2015. Land use/land cover classification and its change detection using multi-temporal MODIS NDVI data. *Journal of Geographical Sciences* 25(12): 1479–1506.

Wu, J., 2019. Linking landscape, land system and design approaches to achieve sustainability. *Journal of Land Use Science* 14(2): 173-189.

Xu, J., Xiao, P., 2022. A bibliometric analysis on the effects of land use change on ecosystem services: Current status, progress, and future directions. *Sustainability* 14(5): 3079.

Yasir, M., Hui, S., Binghu, H., Rahman, S. U., 2020. Coastline extraction and land use change analysis using remote sensing (RS) and geographic information system (GIS) technology–A review of the literature. *Reviews on Environmental Health* 35(4): 453-460.

Zhang, Z., Liu, S., Wei, J., Xu, J., Guo, W., Bao, W., Jiang, Z., 2016. Mass change of glaciers in Muztag Ata–Kongur Tagh, Eastern Pamir, China from 1971/76 to 2013/14 as derived from remote sensing data. *PLoS One* 11(1): e0147327.

Eurasian Journal of Soil Science

Journal homepage : http://ejss.fesss.org

2024 Eurasian Journal of Soil Science
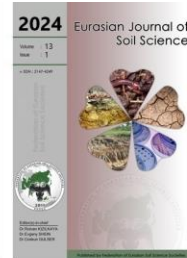
Profile distribution of polycyclic aromatic hydrocarbons in coastal soils of the Lower Don and Taganrog Bay, Russia

Tamara Dudnikova [a], Tatiana Minkina [a], Svetlana Sushkova [a,*],
Andrey Barbashev [a], Elena Antonenko [a], Evgenyi Shuvaev [a], Anastasia Nemtseva [a],
Aleksey Maksimov [b], Yuri Litvinov [a], Dina Nevidomskaya [a],
Saglara Mandzhieva [a], Coşkun Gülser [c], Rıdvan Kızılkaya [c]

[a] Southern Federal University, Rostov-on-Don, 344006, Russia
[b] National Medical Research Centre for Oncology, Rostov-on-Don, 344006, Russia
[c] Ondokuz Mayıs University, Faculty of Agriculture, Department of Soil Science and Plant Nutrition, Samsun, Türkiye

Abstract

The main regularities of pollutant distribution through the soil profile were established based on the analysis of the content of 15 priority PAHs in 29 soil sections of different soil types located in the coastal zone of the Lower Don and Taganrog Bay with different anthropogenic loads. It was shown that the total content of PAHs in the 0-20 cm layer of soils of coastal territories varies from 172 µg kg^{-1} to 16006 µg kg^{-1}. In addition, according to the total pollution indicator, (Zc) determines the level of soil pollution, which varies from "not polluted" to "extremely polluted". The influence of pollution sources falls on the 0-20 cm layer of soils of different types and is especially pronounced for subordinate landscapes. With increasing sampling depth, the total PAH content decreases with the redistribution of individual compounds of the PAH group towards the dominance of low molecular weight and 4-ring compounds in the composition of the sum of 15 PAHs and depends largely on the content of organic matter and soil pH. Based on the cluster analysis results, the main factor determining the profile distribution of PAHs is the type of pollutant origin source and its intensity.

Keywords: Landscape, Fluvisols, pollution, migration of pollutants, priority PAHs, organic carbon, coastal zone, transformation of pollutants.

Introduction

Regular flooding of soils of superaqual landscapes, the proximity of groundwater, the inflow of chemical elements with river runoff and from adjacent catchments, and intensive biological cycling have caused high activity and intensity of geochemical processes in floodplains. Such frequency of flooding creates special conditions for the formation of terrestrial landscapes of coastal territories, migration and concentration of chemical substances in them. The hierarchical ordering of the landscape organisation of coastal territories implies the accumulation of chemical substances in soils of subordinate positions of coastal territories landscape influenced by the unidirectional downward water current (Avessalomova et al., 2016). Natural-anthropogenic transsuperaqual and superaqual landscapes of coastal territories often experience a complex anthropogenic impact under conditions of urbanisation, developed agriculture, industry and transport infrastructure while performing the most important regulatory, resource-ecological and socio-ecological

functions. In this regard, the impact of industry, road and water transport, cities and agriculture leads to the accumulation of hazardous ecotoxicants in the soils of coastal territories.

Polycyclic aromatic hydrocarbons (PAHs) are among the most ecologically significant pollutants that enter the soil of coastal waters of various seas. This is a group of carcinogenic substances, the spread of which in the environment is primarily associated with fuel combustion and spills, as well as fires. 16 PAHs are listed as priority pollutants by the US Environmental Protection Agency (US Environmental Protection Agency, 2020), of which five compounds are highly likely to be carcinogenic, and benz(a)pyrene is a Class 1 carcinogen and mutagen (IARC, 2020). PAHs are not easily soluble in water, are stable in environmental objects, and can accumulate in soils and living organisms, causing various teratogenic and mutagenic effects (Chaplygin et al., 2022; Sun et al., 2021).

Contaminated soils of coastal territories are not subject to remediation. Methods of phytoremediation of such soils are ineffective due to the lack of information on PAH hyperaccumulator plants capable of vegetation under overwatering conditions, and common macrophytes growing near water bodies serve as indicators of environmental stress without significantly changing the concentration of PAHs in soils and sediments (Minkina et al., 2021; Chaplygin et al., 2022).

At the same time, coastal soils contaminated with PAHs can act as a secondary source of pollution by transporting PAH carrier soil particles with water mass (Zhao et al., 2021). Meanwhile, about 19% of the total annual PAH release enters water sources through soil erosion (Qiu et al., 2019). The intensification of coastal zone utilisation for economic purposes is increasing every year (Clark, 2008; Khan et al., 2015). The contradictions associated with the increased intensity of coastal use inevitably lead to acute conflicts between the desire to utilise coastal resources and the need to ensure their long-term reserve. Forecasting the transformation of coastal ecosystems is an urgent problem due to the general intensification of economic activity. Such a forecast requires knowledge of the regularities of coastal ecosystem development, including both general conditions and individual natural and anthropogenic factors.

Currently, an approach called Marine spatial planning is being actively developed, which involves making informed and coordinated decisions on the long-term, sustainable use of marine resources, including those adjacent to the coastal zone (Santos et al., 2019; Boretti and Rosa, 2019). A crucial tool for sustainable coastal management is modelling pollutant mass transfer processes in coastal soils, which is impossible without understanding the main patterns of migration and profile distribution of PAHs. A number of general regularities of pollutant behaviour in coastal soils and peculiarities of their lateral migration are described in the works of Dudnikova et al. (2023a,b), Dai et al. (2022), Shi et al. (2021) and Yang et al. (2015). It has been shown that the type and intensity of the source of PAH input, as well as soil properties, are key factors that determine the quantitative and qualitative content of pollutants in the soils of coastal areas. Peculiarities of the water regime of soils in coastal areas, including water level pulsation, upwelling, and recurrent flooding of soils, may contribute to PAHs leaching deep into the soil profile. In this regard, this study aimed to determine the main patterns of PAH profile distribution in soils of natural and natural-anthropogenic landscapes of the coastal zone.

Material and Methods

General characterisation of the study area

Under the influence of anthropogenic factors, the unstable balance of natural processes is rapidly disrupted, and the conditions for the formation of floodplain landscapes are significantly altered. The Lower Don Valley is characterised by a wide floodplain with an abundance of emergent and meadow vegetation. The Don Delta is represented by several sandy islands densely indented by shallow depressions of dried-up old river channels, arms and canals. The northern shore of the Taganrog Bay coastline is characterised by the predominance of abrasion and erosion processes, while the southern part is characterised by relatively more intensive accumulative processes. Floodplain and coastal landscapes of the Lower Don and Taganrog Bay are represented by alternating water bodies, willow thickets, floodplain meadows, sand dunes, beaches and spits, parks, gardens, and other tree plantations, some of which are shown in Figure 1.

The Lower Don River and the Taganrog Bay are key sections on the route of long-distance multi-tonnage tankers from the Sea of Azov and the Black Sea inland to the Gulf of Finland. Every day, dozens of water transport units pass through the Don Delta in the Volga-Don shipping channel (Kuzmichev et al., 2020), which forms a threat of accumulation of carcinogenic substances of the PAH group in soils and coastal sediments. In addition, the concentration of industrial, residential, agricultural, recreational and natural objects within the coastal zone of Taganrog Bay reflects the general trends of the intensity of the coastal territories' involvement for various human needs, a common feature of the entire southern coast of Russia.

(A)   (B)   (C)

Figure 1. General view of coastal-water communities of the Don delta (A), floodplain meadows (B), sandy loam-meadow community (C)

Soil cover characterisation and soil sampling

For the study, 29 full-profile transects were laid out in elluvial, trans-elluvial, and superaqual positions of the coastal zone landscape to assess the influence of topographic position on PAH accumulation in the soil. The trans-elluvial and superaqual positions contain predominantly Salic Fluvisols, Tidalic Fluvisols, Calcaric Fluvisols, Histic Fluvisols and Gleyic Solonchaks (Nachtergaele et al., 2023). Eluvial positions of landscapes are dominated by Calcic Chernozems, the most common soils occupied mainly for agricultural purposes (Kalinitchenko et al., 2022), but Rendzic Leptosols and Mollic Leptosols also occur (Figure 2) (World Reference Base for Soil Resources). In full-profile transects, soil sampling was conducted by soil horizon (Table 1). Often, when investigating the profile distribution of PAHs in soils, sampling is done layer by layer in 5, 10 or 20 cm increments. For the current study, a genetic approach was chosen in which the sampling depth corresponds to soil horizon boundaries. It was assumed that similar processes occur within the same horizon, with pollutants occurring regardless of the depth of the horizon. For horizon thicknesses above 40 cm, at least two samples were taken from different depths. The mass of the combined sample was 1 kg. To determine the level of soil contamination and to compare the content of PAHs in soils of the study area with background areas, a 0-20 cm soil layer was taken according to GOST 17.4.3.01-2017 (GOST 17.4.3.01-2017, 2018).
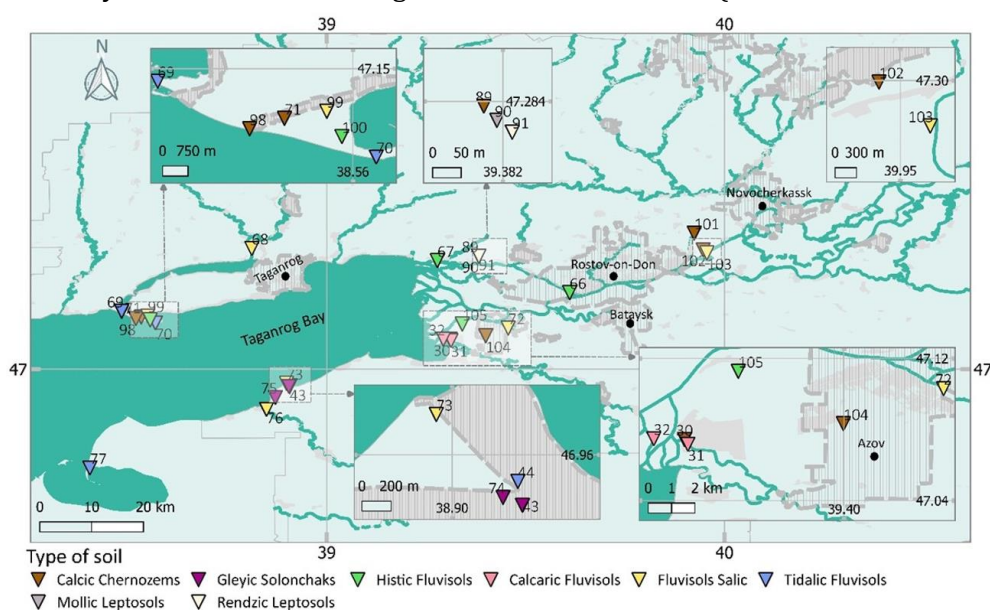
Figure 2. Location map of monitoring sites with soil type names indicated

Table 1. Correlation of PAH content with soil properties obtained by calculation of Spearman correlation coefficient

PAHs	Soil properties		PAHs	Soil properties	
	Organic carbon	pH		Organic carbon	pH
Naphthalene	0.40	-0.19	Chrysene	0.50	-0.22
Fluorene	0.58	-0.44	Benzo[a]anthracene	0.55	-0.23
Phenanthrene	0.55	-0.35	Benzo[b]fluoranthene	0.44	-0.12
Anthracene	0.36	-0.44	Benzo[k]fluoranthene	0.50	-0.25
Acenaphthene	0.52	-0.35	Benzo[a]pyrene	0.59	-0.36
Acenaphthylene	0.46	-0.20	Dibenzo[a,h]anthracene	0.39	-0.13
Fluoranthene	0.48	-0.15	Benzo[g,h,i]perylene	0.46	-0.15
Pyrene	0.54	-0.23			

Methods

Determining physical and chemical soil properties

The main physicochemical properties of soil samples were determined: organic carbon content – by bichromate oxidation method with titrimetry; content of granulometric fractions of physical clay (<0.01mm) and silt (<0.001mm) – by sedimentation method using Kachinsky pipette with pyrophosphate preparation (Korchagina and Vadyunina, 1986); pH of soil samples was determined by potentiometric method in the suspension of soil: water 1:2.5.

Identification and quantitative analysis of PAH content in soil samples

To determine the PAHs, 1 g of soil sample was weighed each. To remove the interfering lipid fraction, the soil sample was saponified by boiling for 3 h in 30 ml of 2% potassium hydroxide solution in a water bath with a reflux condenser. PAH extraction was carried out with 98% purity n-hexane (ISO 13877-2005, 2020). For this purpose, 15 ml of hexane was poured into the sample and placed on a shaker. After 10 min, the hexane supernatant was carefully poured into a separating funnel. The operation was repeated three times. After that, the hexane layers were separated from the residual fraction of the alcoholic alkali solution in the separating funnel. The extract was filtered through a paper filter with anhydrous sodium sulphate for mechanical purification and removal of residual liquid. The hexane extract was then evaporated at a rotary evaporator. After evaporation, the precipitate was dissolved in 1 mL of 99.9% acetonitrile.

Samples were analysed for the presence of PAHs using an Agilent 1260 Infinity high-performance liquid chromatography (HPLC) (Agilent Technologies, Santa Clara, CA, USA) equipped with fluorescence and UV detectors, in accordance with the requirements of ISO 13877-2005 (ISO 13877-2005). The HPLC system was equipped with a Hypersil BDS C18 reversed-phase column (Agilent Technologies) (125 × 4.6 mm, 5 μm). A mixture of 99.9% acetonitrile (Cryochrome, Moscow, Russia) (75%): bidistilled water (25%) at a flow rate of 0.5 ml min-1 was used as the mobile phase. The volume of extract injected was 20 μl. The present study determined the content of 15 priority PAHs from the US EPA priority pollutants list (US Environmental Protection Agency, 2020). Of these, the following are low molecular weight: 2-ringed (naphthalene) and 3-ringed (acenaphthylene, acenaphthene, fluorene, phenanthrene, anthracene), and high molecular weight: 4-ringed (fluoranthene, pyrene, benzo(a)anthracene, chrysene), 5-ringed (benzo(b)fluoranthene, benzo(k)fluoranthene, benzo(a)pyrene, dibenz(a,h)anthracene) and 6-ringed benz(g,h,i)perylene.

The extraction efficiency of target PAHs from soils was determined using the matrix method by constructing calibration curves. A fresh soil sample as well as an air-dry soil sample (1 g) were placed in a round bottom flask, and a standard solution of PAHs in acetonitrile was added to target PAH concentrations of 2, 4, 6, 8, 16 or 32 μg kg-1. After evaporating the solvent for 30 min under a fume hood, the PAH-added soil samples were incubated for 24 h at 4 °C. The samples were then analysed by the saponification method described above, followed by HPLC analysis.

Quality control of each detection by HPLC was performed according to Agilent Application Solution (Certificate 27-08). Individual standard solutions were purchased from Sigma-Aldrich (Merch) (Burlington, MA, USA). A calibration standard of the PAH mixture was injected after every six samples to correct for retention time drift during the analysis. After plotting the calibration curve, a detection coefficient was calculated for each detected PAH:

The PAH content in the tested samples was determined using the external standard method. The PAH content in soil was calculated using the equation (1):

$$Cs = k\ Si × Cst × V/(Sst × m) \tag{1}$$

where Cs is the PAH content in the soil sample (μg kg-1); Sst and Si are the areas of PAH peaks for standard solution and sample, respectively; Sst is the concentration of PAH standard solution (μg kg-1); k is the PAH extraction factor from the sample; V is the volume of acetonitrile extract (ml); m is the mass of the sample (g).

Certified reference materials and calibration curves were used to calculate the limits of detection and limits of quantification, which were 2-200 μg kg-1. For the developed methods for the isolation of target PAHs in soil, the random component of the measurement error was estimated, which was 3.5-14 % for the concentration range of 2-200 μg kg-1.

Solvents and reagents were of HPLC purity and included ethanol (96%, p.a.) (Aquatest, Rostov-on-Don, Russia), n-hexane (99%, p.a.) (Aquatest, Rostov-on-Don, Russia), potassium hydrate (98%, p.a.) (Aquatest), acetonitrile (99.9%, p.a.) (Kriochrome, St. Petersburg, Russia), NaOH (97%, p.a.) (Kriochrome, St. Petersburg, Russia). (Aquatest), acetonitrile (99.9%, b.w.a.) (Cryochrom, St. Petersburg, Russia), NaOH (97%, b.w.a.)

(Aquatest) and anhydrous Na2SO4 (Aquatest, Rostov-on-Don, Russia). A total of 15 priority PAH standards in acetonitrile with a concentration of 200 µg/cm³ manufactured by Merch Burlington, MA, USA (NIST® SRM® 1647f Priority PAH Contaminants (in acetonitrile)) were used to prepare standard solutions of total PAHs for HPLC analysis. Analytical standards were purchased from Sigma-Aldrich (Merch) and used as an internal analytical standard.

Determining the level of surface layer pollution and migration of PAHs along the profile

The degree of soil contamination was assessed using the total contamination index (Zc) according to the formula (2) (MU 2.1.7.7330-99, 1999; Kasimov and Vlasov, 2012; Fedorets et al., 2015):

$$Z_C = \sum Kc_i - (n-1) \tag{2}$$

where KCi is the concentration factor of individual compounds, n is the number of considered elements and compounds with KCi >1.

The concentration factor is calculated relative to background values (3):

$$Kc_i = Kb/K \tag{3}$$

Only soils with a profile depth of more than 40 cm were included in the calculation. Where Kb is the content of individual compounds in the background soil, K is the content of individual compounds in the studied soil. The background values determined in a study conducted earlier (Dudnikova et al., 2023a) were used for calculation.

The ratio of PAH content in the upper horizon to the lower horizon was calculated to study the migration capacity of PAHs in soils.

Statistical analysis and data visualisation

Statistical analysis of the obtained data and visualisation of the analysis results were performed using SigmaPlot 12.5, Origin 2018, STATISTICA 8 and QGIS 3.2 software. The relationship between the content of low and high molecular weight PAHs and depth was determined using regression analysis based on the exponential equation. Cluster analysis was performed using Ward's method with Euclidean distance as a proximity measure.

Results and Discussion

Profile characterisation of physical and chemical soil properties

The result of the analysis of the profile distribution of organic carbon showed that the thickness of organogenic horizons varies greatly. The highest thickness is Calcic Chernozems 41-52 cm, and the lowest is for alluvial meadow carbonate 10-11 cm. Organic carbon accumulation in soil profiles corresponds to the accumulative type, except for alluvial meadow-saturated layered soils of monitoring sites No. 68-70, 77. Redistribution of organic carbon in the soil profile is characteristic of the eluvial-illuvial type with maximum accumulation in the upper horizon (Figure 3).
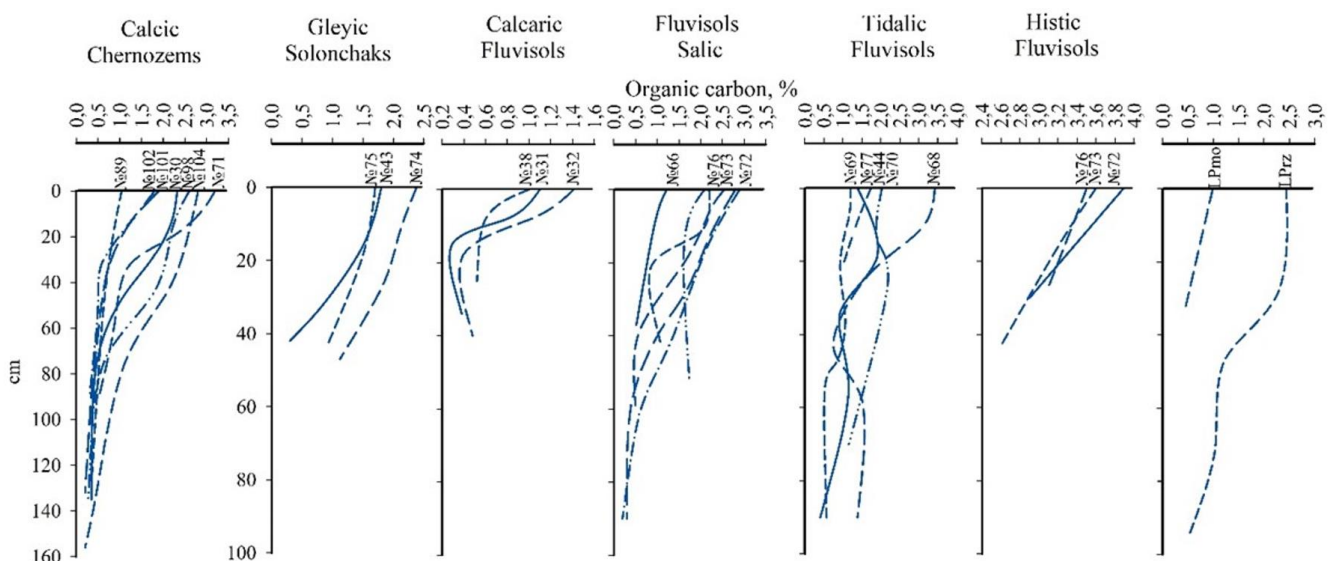
Figure 3. Profile distribution of organic carbon in soils of different types of the coastal zone of the Lower Don and Taganrog Bay (Note: LPmo - Mollic Leptosols, LPrz - Rendzic Leptosols)

The change of pH in soil profiles varies from neutral to slightly alkaline. Neutral reaction of the medium is typical for the upper horizons of Calcic Chernozems of monitoring site No. 71 and alluvial meadow carbonate soils of monitoring sites No. 31 and No. 32. In most of the soil profiles under consideration, the carbonate content increases with depth, which is caused by their occurrence in loess-like loams, alluvial, marine and alluvial-marine sediments. No significant changes in pH values were observed in the profile of the considered soils (Figure 4).
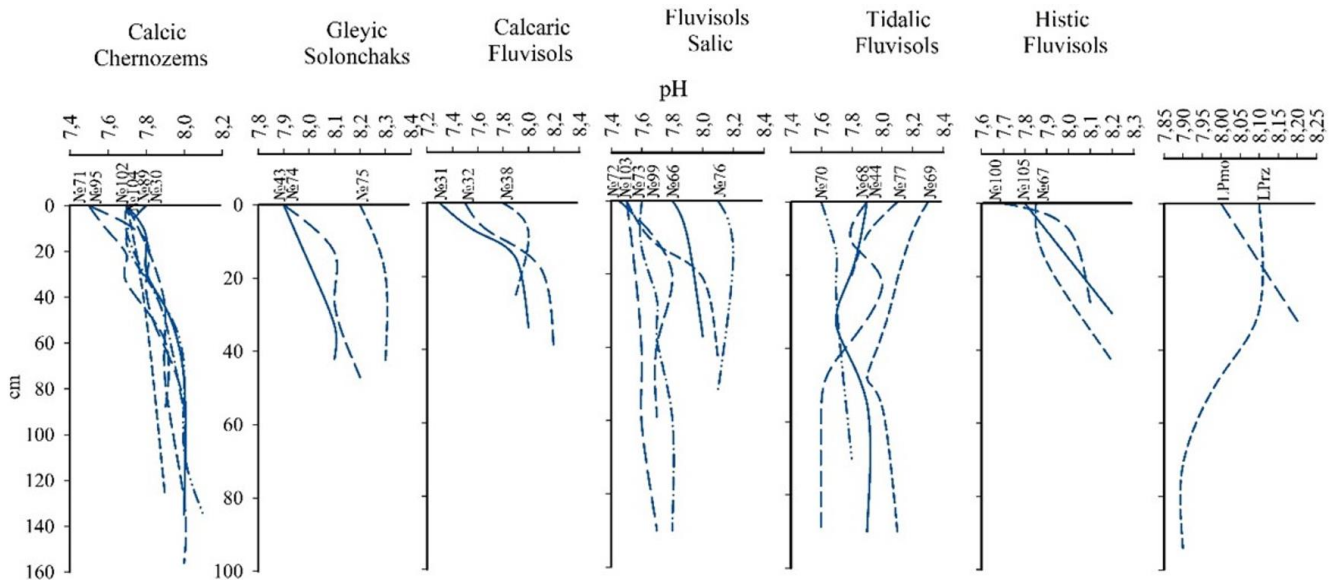
Figure 4. Profile distribution of pH in different types of soils of the coastal zone of the Lower Don and Taganrog Bay (Note: LPmo - Mollic Leptosols, LPrz - Rendzic Leptosols)

Profiles are predominantly undifferentiated in terms of the distribution of silt and physical clay fractions. In the presence of the gley process in the lower part of the profile, the content of fine-dispersed fraction of soils increases with depth, which is especially characteristic of Gleyic Solonchak and Calcaric Fluvisols. In alluvial sod carbonate, on the contrary, the content of physical clay and silt decreases with depth (Figure 5).
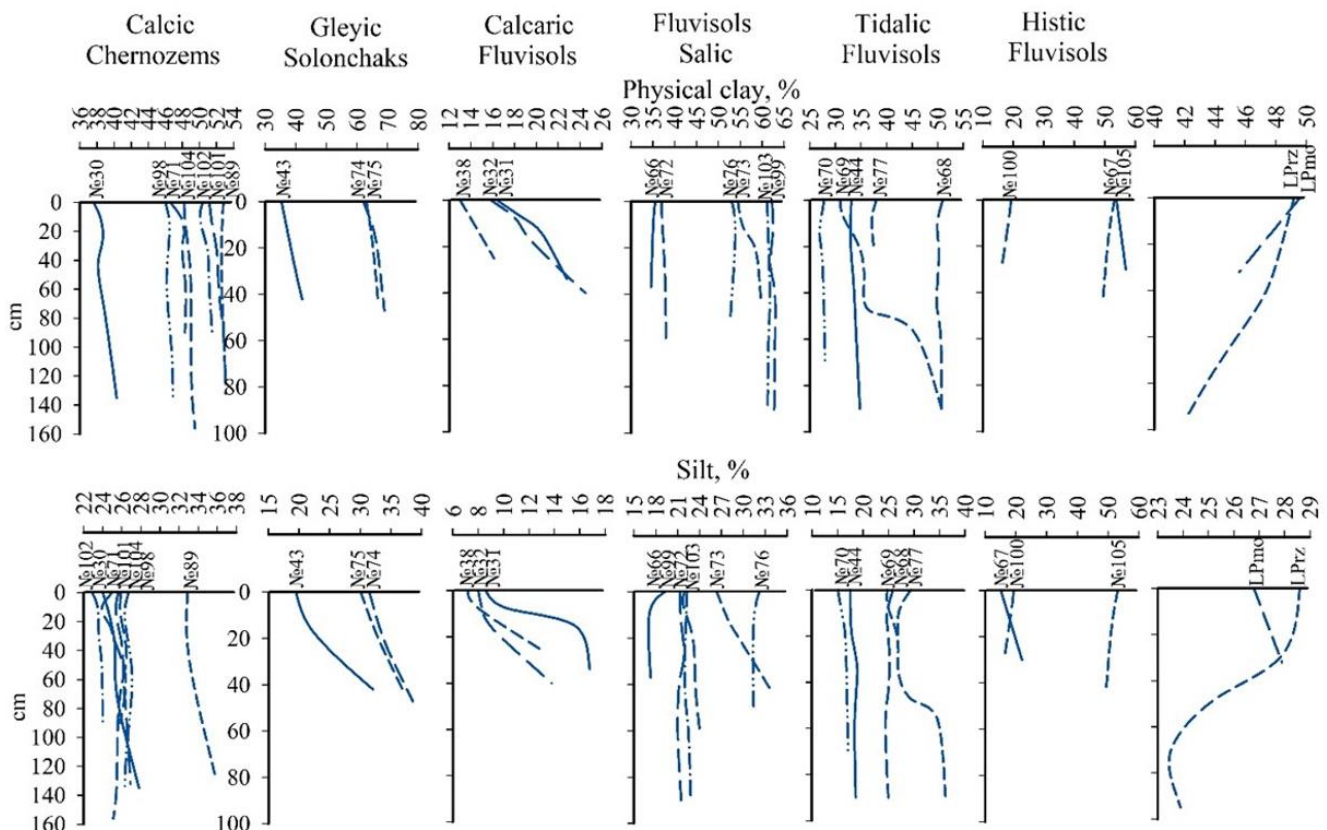

Figure 5. Profile distribution of physical clay and silt in different types of soils of the coastal zone of the Lower Don and Taganrog Bay (Note: LPmo - Mollic Leptosols, LPrz - Rendzic Leptosols)

PAH content in the upper 0-20 cm soil layer

In the surface horizon of soils (0-20 cm), the total PAH content varies widely from 172 µg kg^{-1} to 16006 µg kg^{-1} with a median value of 269 µg kg^{-1} (Figure 6). In the soils of subordinate landscapes, the median PAH content, as well as the variability of data, increases relative to eluvial landscapes. At the same time, the increase in the median value in the Autonomous (227 µg kg^{-1}) > Downslope (301 µg kg^{-1}) > Superaquatic (319 µg kg^{-1}) row indicates the migration of pollutants under gravitational and hydrological forces (Glazovskaya, 1998; Avessalomova et al., 2016). Increased variability of PAH values in a similar series may indicate greater vulnerability of superaquatic landscape soils to pollutants (Xu et al., 2021).
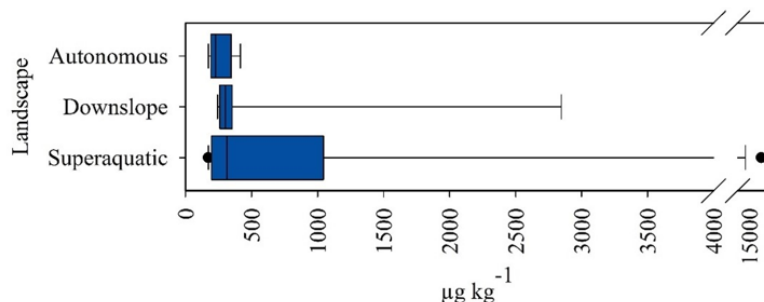
Figure 6. Total PAH content in 0-20 cm layer of soils of different landscapes of the Lower Don and Taganrog Bay

At low PAH content in soils relative to the global average, an increased number of individual compounds is observed compared to the regional background (Dudnikova et al., 2023a). The composition of individual PAHs by median values is dominated by pyrogenic-coal association of pollutants (Yunker et al., 2015; Tsibart et al., 2016; Sushkova et al., 2020; Dudnikova et al., 2023b), represented by phenanthrene, fluoranthene, pyrene, chrysene and benz(g,h,i)perylene, as well as benz(b)fluoranthene, the accumulation of which is characteristic of the soils of coastal areas influenced by liquid fuel spills (Figure 7).
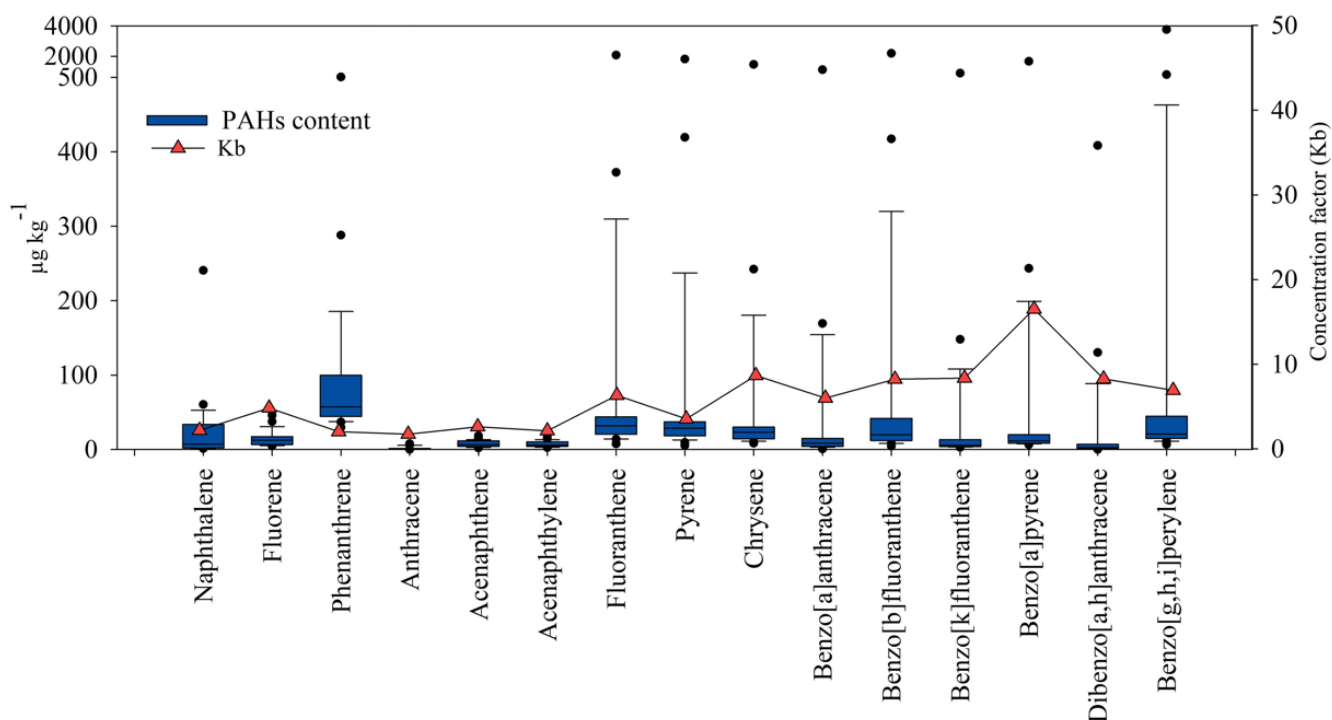
Figure 7. Content and median value of the concentration coefficient (Kb) of individual PAH compounds in the 0-20 cm layer of the Lower Don and Taganrog Bay soils

The results of the Kb calculation showed that with an increasing number of benzene rings in the PAH molecule, their accumulation in soil increases. High content of phenanthrene compared to other studied PAHs is noted both for soils of background areas and impact zones (Sushkova et al., 2020; Chaplygin et al., 2022; Dudnikova et al., 2023a,b). At the same time, its median Kb value is lower than the lowest phenanthrene concentration. Accordingly, about 50% of soils of the study area are characterised by pollutant dispersion. In this case, dispersion means not only its faster biodegradation compared to high molecular weight PAHs, but also more intensive mass transfer of phenanthrene in association with organic matter of coastal soils (Zhang and Fan, 2016; Benhabib et al., 2017).

Assessment of PAH contamination of the upper 0-20 cm soil layer

It has been established that the level of total PAH pollution in the soils of the monitoring sites varies from non-hazardous to extremely hazardous. The heterogeneity of pollutant sources causes wide limits of the variability of soil pollution in the study area, their proximity to monitoring sites and intensity, as well as soil properties (Dudnikova et al., 2023a). The higher degree of pollution is characteristic of the soils of the monitoring sites confined to the northern coast of Taganrog Bay, the territory of Beglitskaya Spit and the mouth of the Mius River. For the soils of the Don Delta, the highest degree of pollution is confined to the northern and southern parts of Taganrog Bay. Soils of the territories of periodically waterlogged gully No. 89- 91, located remotely from the Don River and Taganrog Bay, are characterised by low PAH content (Figure 8). It should be noted that the soils of the study area are contaminated with heavy metals to different degrees (Minkina et al., 2021). The presence of metal cations in clay minerals leads to an increase in pore size, causing aggregation and greater hydrophobicity of clay (Saeedi et al., 2018). Heavy metal ions can also accumulate on the clay surface, providing sites for π-bonding of the cation to PAHs (Saeedi et al., 2018; Duan et al., 2022).
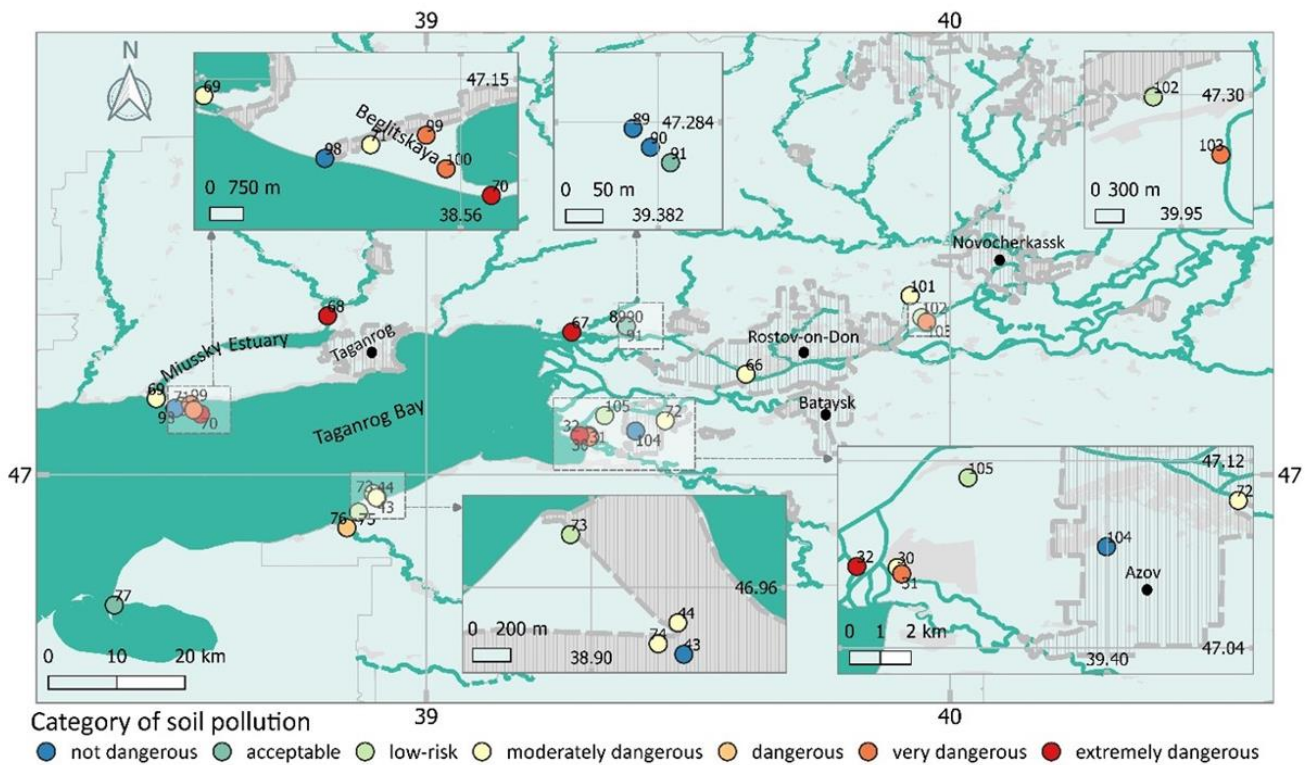
Figure 8. Soil pollution categories of the Lower Don and Taganrog Bay by total pollution indicator (Zc)

PAH distribution in the soil profile

The distribution analysis of the sum of 15 priority PAHs showed that the highest accumulation in the soils of the study area is in the upper horizons of 0-20 cm, in rare cases in the underlying horizons of 0-40 cm, which is more typical for Gleyic Solonchak and is caused by the distribution of organic matter in the soil profile (Figure 3, 9). The character of pollutant distribution corresponds to the accumulative type, which is consistent with studies of solonchaks in Portugal (Martins et al., 2008), the Niger Delta soils (Abbas and Brack, 2006), brown soils near Beijing (Cai et al., 2019), Albic Podzols of Siberia (Dymov and Gabov, 2015). The exception was Histic Fluvisoils type soils, for which the PAH distribution profile is either not differentiated or a slight increase in total PAH content with depth is present (Figure 9). In soils with standing water and reduction conditions, an increased PAH content compared to the upper horizon can be observed at depths below 70 cm (Atanassova and Brümmer, 2004), which is consistent with the results of studies of marsh soils of the Pearl River estuary (Xiao et al., 2014) and is due to the transformation of soil organic matter under the influence of reduction conditions (Thiele and Brummer, 2002). In this case, pedogenic PAHs are firmly bound to the highly aromatic soil organic matter (Aemig et al., 2016). In this regard, PAHs in the lower soil horizons become less labile, making them inaccessible to microbial degraders (Delegan et al., 2022; Ren et al., 2018). In addition, the activity of PAH-degrading microorganisms is predominantly observed in the most aerated 0-20 cm layer, which also does not favour the biodegradation of pollutants deep in the soil profile (Mazarji et al., 2022; Ren et al., 2018). Consequently, this group of pollutants is poorly degraded in the depth of the soil profile (Bu et al., 2009).
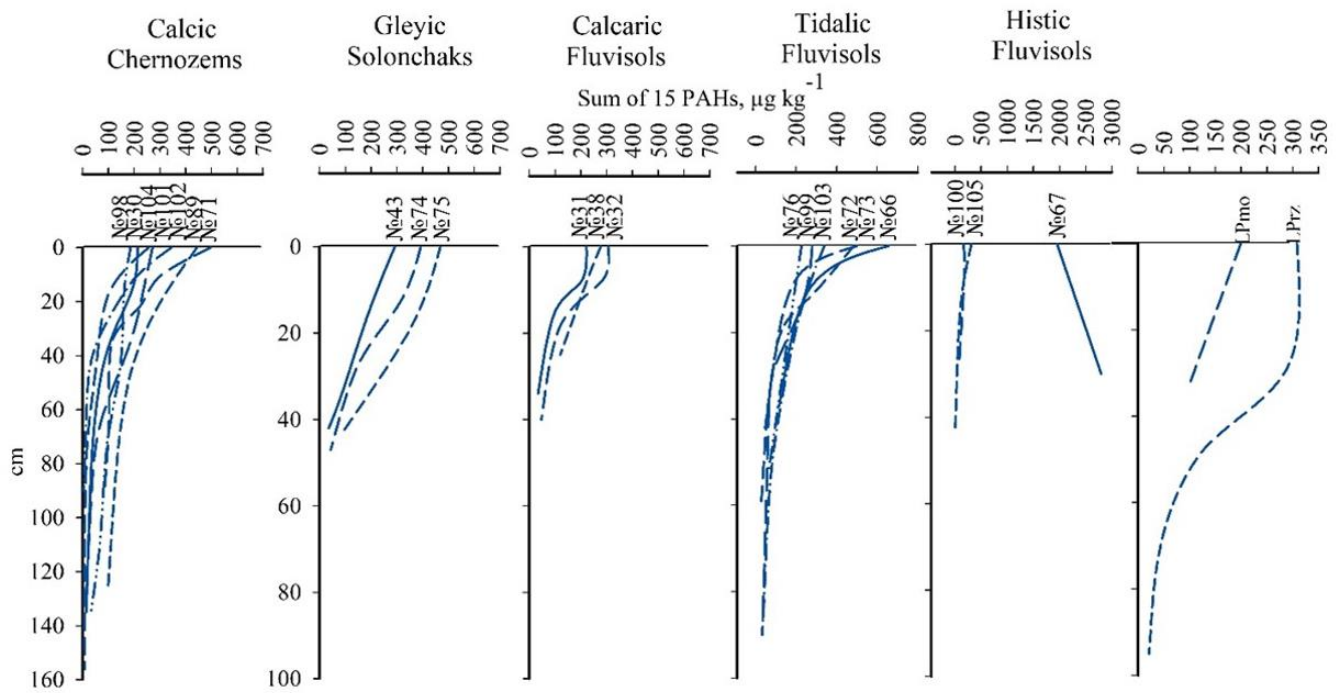
Figure 9. Profile distribution of the total content of 15 PAHs in different soil types of the Lower Don and Taganrog Bay soils

As the pollutant concentration decreases with depth, changes in the PAH composition are observed. For almost all soil types, there is an increase in low molecular weight compounds, especially phenanthrene, and 4-ring fluoranthene and pyrene (Figure 10). In general, low molecular-weight compounds are more capable of migration than high molecular-weight compounds (Cai et al., 2019). As noted by Ping et al. (2007), phenanthrene, due to its higher solubility, occurs in quantities of 50% of its content in the upper horizon, indicating its ability to migrate with groundwater as true solutes (Krauss et al., 2005). However, due to leaching, PAHs can be transported down the profile in concentrations that exceed their solubility (Benhabib et al., 2017). The accumulation and distribution of pollutants along the profile also depend on the degree of exposure to input sources (Mayer et al., 2019). The higher the PAH content in the surface horizon, the lower the percentage of migration across the profile (Cai et al., 2019).
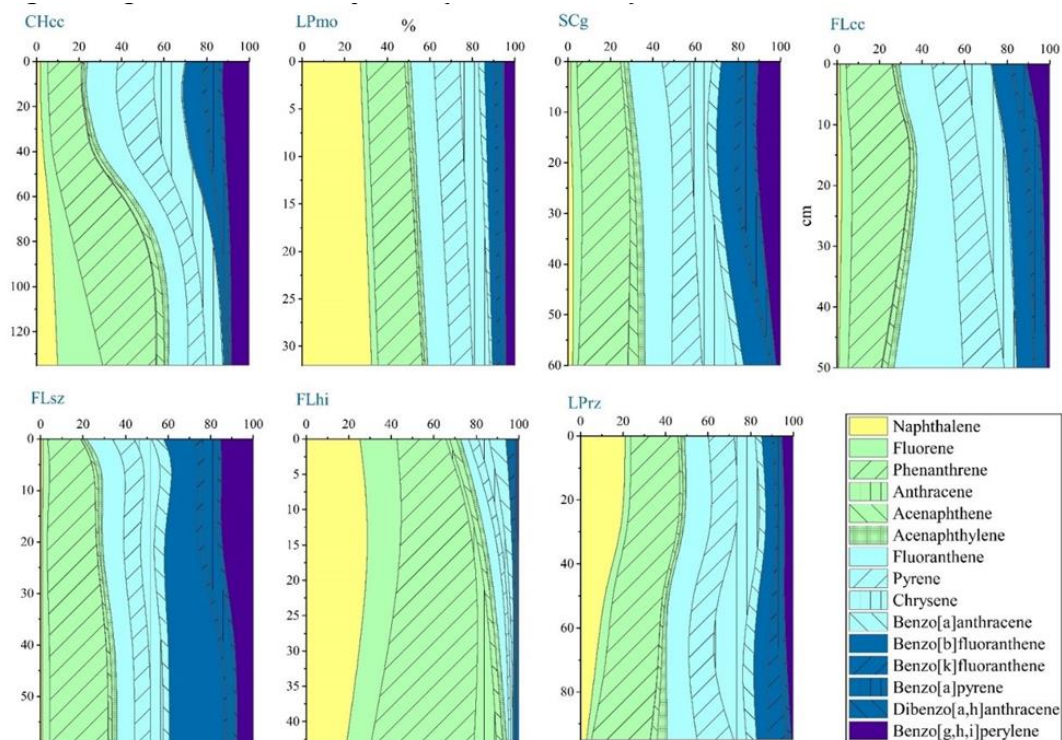
Figure 10. Profile distribution of individual compounds of 15 PAHs as a percentage of their total content in the soils of the Lower Don and Taganrog Bay soils

A distinctive feature of the profile distribution of PAHs in Tidalic Fluvisols is the presence of the second accumulation maximum in the middle of the profile. This effect is typical for less polluted soils of monitoring sites No. 69 and 77, where the total PAH content of upper horizons does not exceed 500 µg kg^{-1}. In case of higher pollution of the surface layer, the accumulation of pollutants in the middle of the profile is not pronounced.

When analysing individual PAH compounds, their differentiation along the soil profile is clearly traceable regardless of the pollution level (Figure 11). In general, changes in individual PAH compounds correspond to the distribution of organic carbon and pH in the profile of Tidalic Fluvisols (Figure 3, 4). This effect is due to the fact that the amount of low molecular weight compounds is almost unchanged across the soil profile, while the content of high molecular weight compounds decreases across the soil profile. Tidalic Fluvisol horizons with increased organic matter content prevent the movement of high molecular weight PAHs, primarily 4-ring compounds, acting as a natural "filter" on the way of pollutants migration from the soil profile surface deep into the parent rock. The most dangerous 5- and 6-ring compounds accumulate at a depth of up to 10 cm (Figure 11).
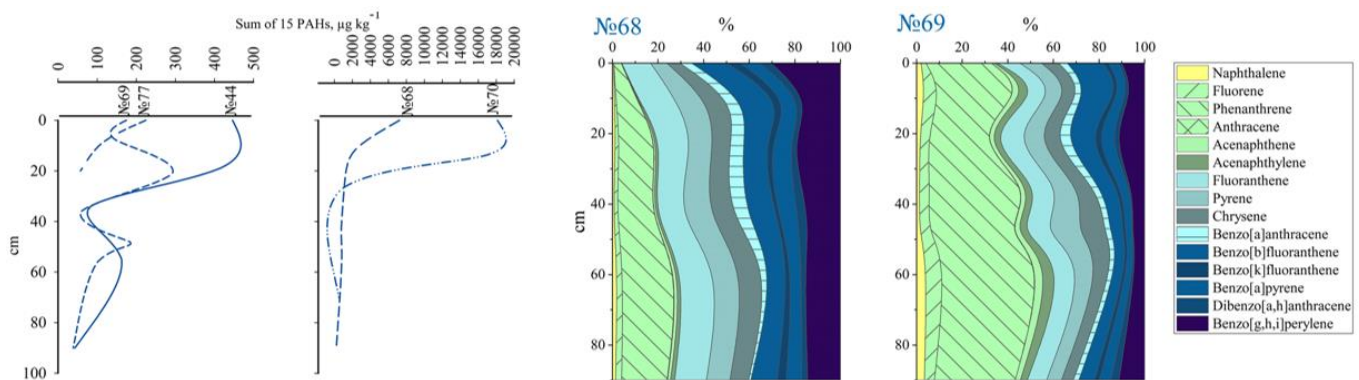
Figure 11. Profile distribution of total PAHs and individual compounds as a percentage of the total content in Tidalic Fluvisols of the Lower Don and Taganrog Bay

Transformation of PAH composition along the soil profile

It was found that with increasing molecular weight and size of the PAH molecule, the degree of PAH reduction with depth increases, as evidenced by the increase in the ratio of PAH content in the upper horizon to its content in the lower horizon (Figure 12).
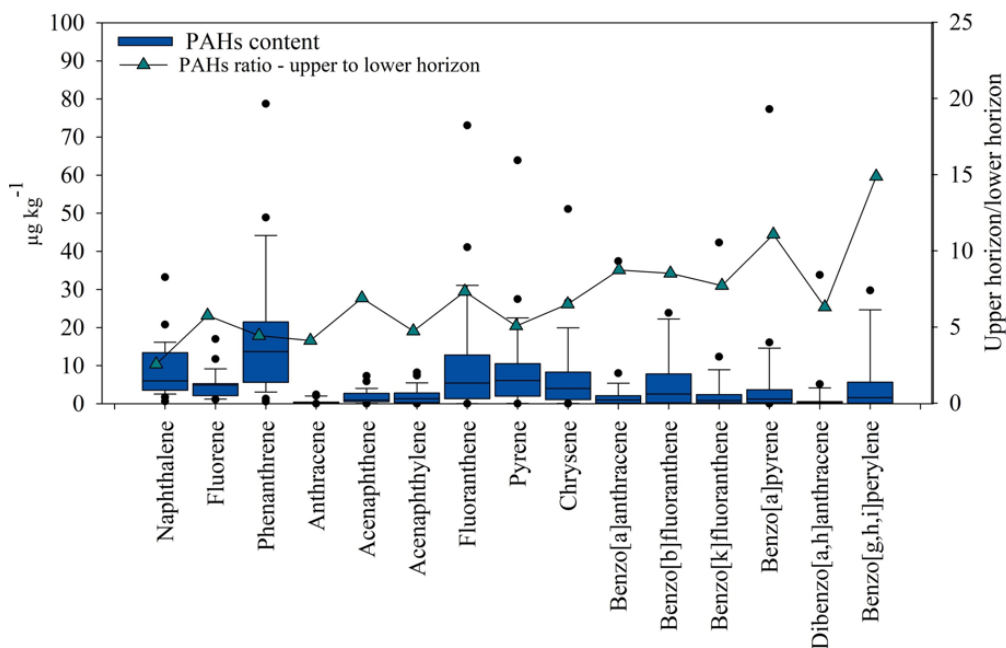
Figure 12. Content of individual PAH compounds in the lower soil horizons (below 40 cm), as well as the ratio of pollutant content in the upper (up to 20 cm) to lower (below 40 cm) soil horizons of the Lower Don and Taganrog Bay soils

The results were confirmed by regression analysis. The decrease in PAH content was approximated by an exponential equation, where the coefficient of determination R^2 =0,41 for low molecular weight compounds and R^2=0,50 for high molecular weight compounds (Figure 13). It was found that with increasing molecular

weight and size of the PAH molecule, the degree of PAH reduction with depth increases, as evidenced by the increase in the ratio of PAH content in the upper horizon to its content in the lower horizon (Figure 12). The results were confirmed by regression analysis. The decrease in PAH content was approximated by an exponential equation, where the coefficient of determination R^2 =0.41 for low molecular weight compounds and R^2=0.50 for high molecular weight compounds (Figure 13). Among all investigated compounds, phenanthrene and naphthalene clearly dominate due to their high migration ability in comparison with other PAHs and the increased content of relatively low molecular weight compounds. A noticeable contribution to the content of pollutants of the underlying soil horizons is made by 4-ring compounds, which are the dominant PAHs of the upper horizon and are the most soluble from the pool of pyrogenic-coal association (Figure 12).
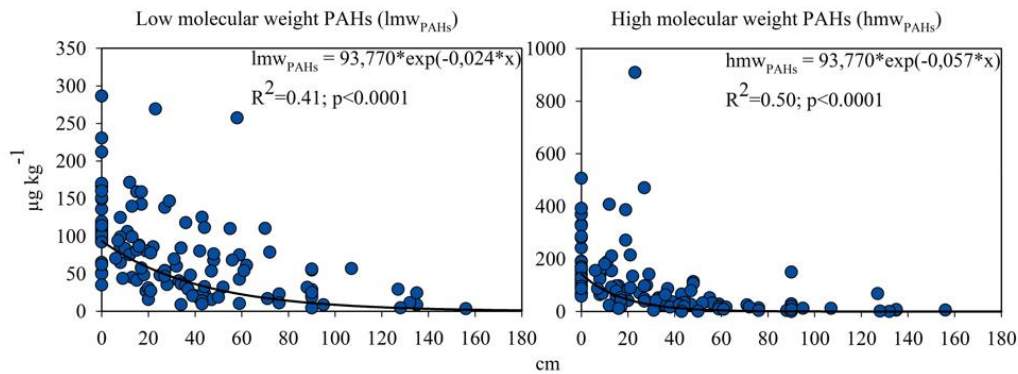
Figure 13. Correlation between the content of low-molecular and high-molecular PAHs and soil profile depth, obtained by regression analysis using the exponential equation

The results of the correlation analysis revealed the correlation between PAH content and soil properties. A significant positive correlation is observed between organic carbon and the total pool of PAHs considered, consistent with Fengpeng et al.'s studies (Fengpeng et al., 2009). The degree of correlation between soil organic matter and PAHs may vary depending on the type of land use (Xiao et al., 2014) and is due to the heterogeneity of soil organic matter and its amount (Ukalska-Jaruga et al., 2019). At the same time, less aromatic fractions of soil organic matter, such as fulvic acids, play a major role in the migration of PAHs through the soil profile (Dong et al., 2017). PH values mainly affect the redistribution of low molecular weight compounds in the soil profile (Table 1).

The clustering of PAHs in the upper (0-20 cm) layer of soils showed that pollutants constitute two distinct groups. The first one is represented by pyrogenic-coal association-benz(g,h,i)perylene, chrysene, pyrene, fluoranthene and phenanthrene, as well as benz(b)fluoranthene. These substances dominate the PAHs in the upper soil layer and are presumably introduced by the combustion of hydrocarbon materials from point and linear emission sources such as factories and motor vehicles, as well as from spills of hydrocarbon materials. Naphthalene, acenaphthylene, acenaphthene, fluorene, phenanthrene, anthracene, benzo(a)anthracene, chrysene, benzo(k)fluoranthene, benzo(a)pyrene, dibenz(a,h)anthracene benz(g,h,i)perylene constitute the second group of the PAHs less abundant in surface soil horizons (Figure 14). In the lower soil horizons, pollutants are grouped similarly to the upper 0-20 cm layer (Figure 14). This indicates the migration of PAHs through the soil profile. The composition of pollutants in the lower horizons depends primarily on the type of emission source and its intensity.
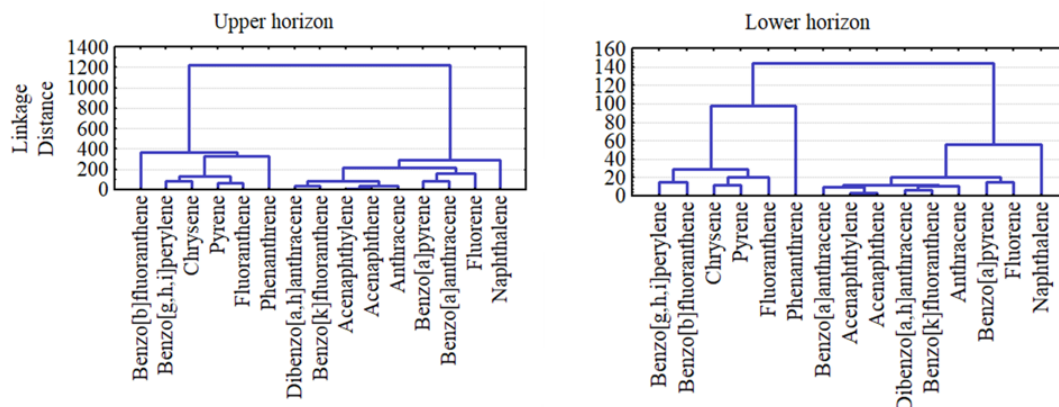
Figure 14. Grouping of individual PAH compounds in the upper and lower horizons according to the results of cluster analysis

Conclusion

In conclusion, it was found that the total PAH content in the 0-20 cm layer of the soils of the coastal territories of the Lower Don and Taganrog Bay varies from 172 µg kg^{-1} to 16006 µg kg^{-1}. The soils of subordinate landscapes are more susceptible to technogenic influence. The median value of the total PAH content increases in the Autonomous (227 µg kg^{-1}) > Downslope (301 µg kg^{-1}) > Superaquatic (319 µg kg^{-1}) row. The level of soil pollution varies from non-hazardous to extremely hazardous. It depends mainly on the content in the surface layer of pyrogenic coal association PAHs (phenanthrene, fluoranthene, pyrene, chrysene, benz(g,h,i)perylene) or benz(b)fluoranthene, the accumulation of which is associated with fuel spills. The distribution of PAHs in the soil profile of the studied soil types corresponds to the accumulative type, where the main influence of pollution sources falls on the 0-20 cm layer. The total PAH content decreases with increasing sampling depth. The decrease intensifies with increasing size and molecular weight of pollutant molecules, which leads to the redistribution of individual compounds of the PAH group in lower soil horizons. At the same time, 4-ringed PAHs and phenanthrene dominate in the lower soil horizons. Their migration depends on the organic matter content and pH in the soil profile. Using cluster analysis, it is shown that the main factor determining the profile distribution of PAHs is the type of pollutant origin source and its intensity.

Acknowledgments

References

Abbas, A.O., Brack, W., 2006. Polycyclic aromatic hydrocarbons in Niger Delta soil: contamination sources and profiles. *International Journal of Environmental Science and Technology* 2: 343–352.

Aemig, Q., Chéron, C., Delgenès, N., Jimenez, J., Houot, S., Steyer, J.P., Patureau, D., 2016. Distribution of Polycyclic Aromatic Hydrocarbons (PAHs) in sludge organic matter pools as a driving force of their fate during anaerobic digestion. *Waste Management* 48: 389–396.

Atanassova, I.D., Brümmer, G.W., 2004. Polycyclic aromatic hydrocarbons of anthropogenic and biopedogenic origin in a colluviated hydromorphic soil of Western Europe. *Geoderma* 120(1-2): 27–34.

Avessalomova I.A., Khoroshev A.V., Savenko A.V., 2016. Barrier function of floodplain and riparian landscapes in river runoff formation. In: Riparian zones. Characteristics, management practices, and ecological impacts, Pokrovsky, O.S., (Ed.). Nova Science Publishers, pp. 181-210.

Benhabib, K., Simonnot, M.O., Faure, P., Sardin, M., 2017. Evidence of colloidal transport of PAHs during column experiments run with contaminated soil samples. *Environmental Science and Pollution Research* 24: 9220–9228.

Boretti, A., Rosa, L., 2019. Reassessing the projections of the world water development report. *NPJ Clean Water* 2: 15.

Brümmer, G.W., Sören, T.B., 2002. Bioformation of polycyclic aromatic hydrocarbons in soil under oxygen deficit conditions. *Soil Biology and Biochemistry* 34(5): 733-735.

Bu, Q.W., Zhang, Z.H., Lu, S., He, F.P., 2009. Vertical distribution and environmental significance of PAHs in soil profiles in Beijing, China. *Environmental Geochemistry and Health* 31: 119-131.

Cai, T., Ding, Y., Zhang, Z., Wang, X., Wang, T., Ren, Y., Dong, Y., 2019. Effects of total organic carbon content and leaching water volume on migration behavior of polycyclic aromatic hydrocarbons in soils by column leaching tests. *Environmental Pollution* 254: 112981.

Certificate 27-08. Procedure of Measurements Benz(a)pyrene Content in Soils, Sediments and Sludges by Highly Effective Liquid Chromatography Method. State Register no. FR.1.31.2005.01725. 2008; 27p. Available at [Access date: 01.04.2008]: https://files.stroyinf.ru/Data2/1/4293809/4 293809324.htm?ysclid=ljg45vs6ub561614960

Chaplygin, V., Dudnikova, T., Chernikova, N., Fedorenko, A., Mandzhieva, S., Fedorenko, G., Sushkova, S., Nevidomskaya, D., Minkina, T., Sathishkumar, P., Rajput, V.D., 2022. Phragmites australis cav. As a bioindicator of hydromorphic soils pollution with heavy metals and polyaromatic hydrocarbons. *Chemosphere* 308: 136409.

Clark, J.R., 2008. Coastal Zone Management Handbook. First edition. CRC Press, Boca Raton, FL, USA.

Dai, C., Han, Y., Duan, Y., Lai, X., Fu, R., Liu, S., Leon, K.H., Tu, Y., Zhou, L., 2022. Review on the contamination and remediation of polycyclic aromatic hydrocarbons (PAHs) in coastal soil and sediments. *Environmental Research* 205: 112423.

Delegan, Y., Sushkova, S., Minkina, T., Filonov, A., Kocharovskaya, Y., Demin, K., Gorovtsov, A., Rajput, V.D., Zamulina, I., Grigoryeva, T., Dudnikova, T., Barbashev, A., Maksimov, A., 2022. Diversity and metabolic potential of a PAH-degrading bacterial consortium in technogenically contaminated haplic chernozem, Southern Russia. Processes 10: 2555.

Dong, W., Wan, J., Tokunaga, T.K., Gilbert, B., Williams, K.H., 2017. Transport and humification of dissolved organic matter within a semi-arid floodplain. *Journal of Environmental Sciences* 57: 24–32.

Dudnikova, T., Minkina, T., Sushkova, S., Barbashev, A., Antonenko, E., Konstantinova, E., Shuvaev, E., Nevidomskaya, D., Ivantsov, A., Bakoeva, G., Gorbunova, M., 2023. Background content of polycyclic aromatic hydrocarbons during monitoring of natural and anthropogenically transformed landscapes in the coastal area soils. *Water* 15(13): 2424.

Dudnikova, T., Sushkova, S., Minkina, T., Barbashev, A., Ferreira, C.S.S., Antonenko, E., Shuvaev, E., Bakoeva, G., 2023. Main factors in polycyclic aromatic hydrocarbons accumulations in the long-term technogenic contaminated soil. *Eurasian Journal of Soil Science* 12(3): 282–289.

Dymov, A.A., Gabov, D.N., 2015. Pyrogenic alterations of Podzols at the North-east European part of Russia: Morphology, carbon pools, PAH content. *Geoderma* 241-242: 230-237.

Fedorets, N.G., Bakhmet, O.N., Medvedeva, M.V., Akhmetova, G.V., Novikov, S.G., Tkachenko, Y.N., Solodovnikov, A.N., 2015. Heavy metals in the soils of Karelia. Akhmetova, G.V., (Ed.). Karelian Research Centre of the RAS, Petrozavodsk, Russia.

Fengpeng, H., Zhang, Z., Yunyang, W., Song, L., Liang, W., Qingwei, B., 2009. Polycyclic aromatic hydrocarbons in soils of Beijing and Tianjin region: Vertical distribution, correlation with TOC and transport mechanism. *Journal of Environmental Sciences* 21(5): 675–685.

Glazovskaya, M.A., 1998. Geochemistry of natural and technogenic landscapes of the USSR. High School, Moscow, Russia.

GOST 17.4.3.01-2017. Nature protection. Soils. General requirement for sampling. Standartinform, Moscow, Russia, 2018; p5. [in Russian]

Guidelines MU 2.1.7.730-99. Hygienic Evaluation of Soil in Residential Areas; Rospotrebnadzor: Moscow, Russia, 1999. [in Russian]

IARC, 2020. List of classifications, volumes 1-123.IARC Monographs on the Evaluation of Carcinogenic Risks to Humans. WHO International Agency for Research on Cancer. Lyon, France. Available at [Access date: 25.07.2020]: https://monographs.iarc.fr/list-of-classifications-volumes/

ISO 13877-2005. Soil Quality-Determination of Polynuclear Aromatic Hydrocarbons—Method Using High-performance Liquid Chromatography. ISO: Geneva, Switzerland.

Kalinitchenko, V.P., Glinushkin, A.P., Minkina, T.M., Mandzhieva, S.S., Sushkova, S.N., Sukovatov, V.A., Il'ina, L.P., Makarenov, D.A., Zavalin, A.A., Dudnikova, T.S., Barbashev, A.I., Bren, D.V., Rajput, P., Batukaev, A.A., 2022. Intra-soil waste recycling provides safety of environment. *Environmental Geochemistry and Health* 44: 1355-1376.

Kasimov, N.S., Vlasov, D.V., 2015. Technophilicity of chemical elements at the beginning of the XXI century. Moscow University Geology Bulletin 5: 15–22.

Khan, M.M.H., Bryceson, I., Kolivras, K.N., Faruque, F., Rahman, M.M., Haque, U., 2015. Natural disasters and land-use/land-cover change in the southwest coastal areas of Bangladesh. *Regional Environmental Change* 15: 241–250.

Korchagina, Z.A., Vadyunina, A.F., 1986. Methods of investigation of physical properties of soils. Third edition. Agropromizdat, Moscow, Russia. [in Russian]

Krauss, M., Wilcke, W., Martius, C., Bandeira, A.G., Garcia, M.V., Amelung, W., 2005. Atmospheric versus biological sources of polycyclic aromatic hydrocarbons (PAHs) in a tropical rain forest environment. *Environmental Pollution* 135(1): 143–154.

Kuzmichev, I.K., Kolotukhina, E.L., Kostrov, V.N., 2020. Technological and economic aspects of increasing the capacity of the shipping channel. In: Proceedings of the Great Rivers-2020. 27–29 May 2020. Nizhniy Novgorod, Russia.

Martins, M., Ferreira, A.M., Vale, C., 2008. The influence of Sarcocornia fruticosa on retention of PAHs in salt marsh sediments (Sado estuary, Portugal). *Chemosphere* 71: 1599–1606.

Mayer, S., Kölbl, A., Völkel, J., Kögel-Knabner, I., 2019. Organic matter in temperate cultivated floodplain soils: Light fractions highly contribute to subsoil organic carbon. *Geoderma* 337: 679–690.

Mazarji, M., Minkina, T., Sushkova, S., Mandzhieva, S., Barakhov, A., Barbashev, A., Dudnikova, T., Lobzenko, I., Giannakis, S., 2022. Decrypting the synergistic action of the Fenton process and biochar addition for sustainable remediation of real technogenic soil from PAHs and heavy metals. *Environmental Pollution* 303: 119096.

Minkina, T., Fedorenko, G., Nevidomskaya, D., Konstantinovna, E., Pol'shina, T., Fedorenko, A., Chaplygin, V., Mandzhieva, S., Dudnikova, T., Hassan, T., 2021. The Morphological and functional organization of cattails Typha laxmannii Lepech. and Typha australis Schum. and Thonn. under soil pollution by potentially toxic elements. *Water* 13: 227.

Nachtergaele, F., van Velthuizen, H., Verelst, L., Wiberg, D., Henry, M., Chiozza, F., Yigini, Y., 2023. Harmonized World Soil Database version 2.0. Food and Agriculture Organization of the United Nations and International Institute for Applied Systems Analysis, Rome, Laxenburg. 62p.

Ping, L.F., Luo, Y.M., Zhang, H.B., Li, Q.B., Wu, L.H., 2007. Distribution of polycyclic aromatic hydrocarbons in thirty typical soil profiles in the Yangtze River Delta region, east China. *Environmental Pollution* 147(2): 358–365.

Qiu, Y.Y., Gong, Y.X., Ni, H.G., 2019. Contribution of soil erosion to PAHs in surface water in China. *Science of the Total Environment* 686: 497–504.

Ren, X., Zeng, G., Tang, L., Wang, J., Wan, J., Liu, Y., Yu, J., Yi, H., Ye, S., Deng, R., 2018. Sorption, transport and biodegradation–an insight into bioavailability of persistent organic pollutants in soil. *Science of the Total Environment* 610-611: 1154–1163.

Saeedi, M., Li, L.Y., Grace, J.R., 2018. Effect of organic matter and selected heavy metals on sorption of acenaphthene, fluorene and fluoranthene onto various clays and clay minerals. *Environmental Earth Sciences* 77: 305.

Santos, S.F., Ehler, C.N., Agardy, T., Andrade, F., Orbach, M.K., Crowder, L.B., 2019. Marine spatial planning. In: World Seas: an environmental evaluation. Sheppard, C., (Ed.). Vol. 3, Academic Press, London, UK, pp. 571–592.

Shi, R., Li, X., Yang, Y., Fan, Y., Zhao, Z., 2023. Contamination and human health risks of polycyclic aromatic hydrocarbons in surface soils from Tianjin coastal new region, China. *Environmental Pollution* 268: 115938.

Sun, K., Song, Y., He, F., Jing, M., Tang, J., Liu, R., 2021. A review of human and animals exposure to polycyclic aromatic hydrocarbons: Health risk and adverse effects, photo-induced toxicity and regulating effect of microplastics. *Science of the Total Environments* 773: 145403.

Sushkova, S., Minkina, T., Tarigholizadeh, S., Antonenko, E., Konstantinova, E., Gülser, C., Dudnikova, T., Barbashev, A., Kizilkaya, R., 2020. PAHs accumulation in soil-plant system of Phragmites australis Cav. in soil under long-term chemical contamination. *Eurasian Journal of Soil Science* 9(3): 242–253.

Tsibart, A.S., Gennadiev, A.N., Koshovskii, T.S., Gamova, N.S., 2016 Polycyclic aromatic hydrocarbons in pyrogenic soils of swampy landscapes of the Meshchera lowland. *Eurasian Soil Science* 49: 285–293.

Ukalska-Jaruga, A., Smreczak, B., Klimkowicz-Pawlas, A., 2019. Soil organic matter composition as a factor affecting the accumulation of polycyclic aromatic hydrocarbons. *Journal of Soils and Sediments* 19: 1890-1900.

US Environmental Protection Agency, 2020. Integrated Risk Information System (IRIS). Office of Research and Development, Washington DC, USA. Available at [Access date: 13.06.2023]: https://cfpub.epa.gov/ncea/iris_drafts/AtoZ.cfm

Xu, Y., Shi, H., Fei, Y., Wang, C., Mo, L., Shu, M., 2021. Identification of soil heavy metal sources in a large-scale area affected by industry. *Sustainability* 13(2): 511.

Yang, W., Lang, Y.-H., Bai, J., Li, Z.-Y., 2015. Quantitative evaluation of carcinogenic and non-carcinogenic potential for PAHs in coastal wetland soils of China. *Ecological Engineering* 74: 117-124.

Yunker, M.B., Macdonald, R.W., Ross, P.S., Johannessen, S.C., Dangerfield, N., 2015. Alkane and PAH provenance and potential bioavailability in coastal marine sediments subject to a gradient of anthropogenic sources in British Columbia, Canada. *Organic Geochemistry* 89-90: 80–116.

Zhang, J., Fan, S.K., 2016. Influence of PAH speciation in soils on vegetative uptake of PAHs using successive extraction. *Journal of Hazardous Materials* 320: 114–122.

Zhao, Y., Li, J., Qi, Y., Guan, X., Zhao, C., Wang, H., Zhu, S., Fu, G., Zhu, J., He, J., 2021. Distribution, sources, and ecological risk assessment of polycyclic aromatic hydrocarbons (PAHs) in the tidal creek water of coastal tidal flats in the Yellow River Delta, China. *Marine Pollution Bulletin* 173: 113110.

Eurasian Journal of Soil Science

Journal homepage : http://ejss.fesss.org
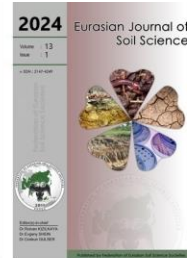
Unveiling the soil physicochemical dynamics of bare soils in Southeast Kazakhstan: A comprehensive study in the Akdala Massif

Ainur Doszhanova [a,*], Zhumagali Ospanbayev [b], Aizada Sembayeva [b], Akgul Kassipkhan [c], Aiman Nazarova [c], Mukhit Bekbauov [a], Dauren Kazkeyev [a]

[a] Kazakh National Agrarian Research University, Almaty, Kazakhstan
[b] Kazakh Research Institute of Agriculture and Plant Growing, Almalybak, Kazakhstan
[c] S.Seifullin Kazakh Agrotechnical Research University, Astana, Kazakhstan

Abstract

This study addresses desertification in Kazakhstan's Akdala region, aiming to propose sustainable solutions by examining the effects of various plants on soil properties and nutrient dynamics. Desertification poses a threat to land productivity in arid areas, and this research aims to determine its impact on soil and identify plants for mitigation. Field experiments over three years in the Akdala region utilized crops such as rice, corn, soybean, sudan grass, and sorghum to assess their influence on key soil parameters. Results revealed diverse effects on soil bulk density, agronomically valuable aggregates, water-stable aggregates, labile and total organic carbon, easily hydrolyzable nitrogen, nitrate, available phosphorus, and exchangeable potassium. While no significant differences in bulk density were observed among crops, variations in surface and subsurface soil layers emphasized the importance of depth-specific considerations. Sorghum stood out as a particularly influential crop, significantly increasing labile and total organic carbon levels, highlighting its potential role in enhancing soil quality. The experiments were conducted on the fields of "Birlik" LLP in the Balkhash district of the Almaty region from 2015 to 2017. The chosen crops, each with distinct characteristics, provided a comprehensive understanding of their impact on soil dynamics. Advanced techniques for soil sampling and analyses ensured accurate measurements of various soil parameters. The study site's sharply continental climate, marked by temperature variations, snowy winters, and hot, dry summers, added complexity to the investigation due to its influence on plant growth and soil interactions. In conclusion, this comprehensive study offers valuable insights into the intricate relationships between different crops and soil parameters for combating desertification. The findings contribute significantly to the development of sustainable soil management practices, providing a foundation for identifying suitable crops for soil improvement in arid regions. By understanding how different plants impact soil properties, this research supports informed decision-making in agricultural practices, promoting the long-term sustainability of farming in regions vulnerable to desertification.

Keywords: Desertification, Soil Management, Arid Regions, Phytomelioration, Sustainable Agriculture.

Introduction

Desertification, a complex phenomenon characterized by the decline or loss of land productivity and the transformation of landscapes into desert-like terrain, poses a significant environmental challenge globally. Arid, semiarid, and subhumid arid regions are particularly vulnerable to desertification, a process exacerbated by adverse climate changes and human activities (Geist and Lambin, 2004). This pervasive issue directly

impacts over 1 billion people and covers 40% of the world's total land surface (Reynolds et al., 2007; Verón et al., 2006). Kazakhstan, as the largest landlocked country, experiences this challenge acutely with its predominantly arid climate, manifesting in arid grasslands, deserts, and semideserts.

Historically, Kazakhstan has grappled with desertification, especially since the "Black Storm" in the 1960s, marking it as a country deeply affected by land degradation. The Soviet Union and Kazakhstan governments, recognizing the severity of the issue, invested significant efforts in combating and controlling desertification, achieving commendable success (Assanova, 2015). However, post the 1990s, the dynamics shifted with the country's independence and economic recovery. The reclamation of grasslands and the abandonment of croplands became prevalent, leading to an increased risk of land desertification (Hu et al., 2020).

Desertification is intrinsically linked to ecological vulnerability and sensitivity, with Kazakhstan primarily reflecting this through desertification sensitivity due to its arid to semiarid climate (Jiang et al., 2019; Kussainova et al., 2000). Ecological sensitivity becomes a critical factor in assessing the risk and possibility of ecological degradation, encompassing various forms such as desertification sensitivity, soil loss sensitivity, soil salinization sensitivity, and more. In Kazakhstan's context, where aridity prevails, desertification sensitivity takes center stage. The alleviation of saline lands' productivity, crucial in combatting desertification, hinges on the cultivation of crops resilient to soil salinity. Soil salt accumulation can lead to plant stress, posing a threat to agricultural productivity. The theory of the toxic effect of salts on plants highlights the significance of selecting crops that can resist and mitigate the harmful impacts of soil salts (Kvan et al., 2011; Bektayev et al., 2023).

Addressing this challenge, the study explores the influence of sweet clover on soils undergoing secondary salinization. The research investigates the impact of sweet clover on various soil parameters, including nitrogen forms, humus content, and salt-bearing biomass. The findings contribute to the understanding of phytomelioration, an effective and environmentally friendly approach to developing saline lands. The phytomeliorative effect, harnessing the natural potential of plants, offers a sustainable means to improve soil fertility and combat soil salinization, critical components in the broader efforts against desertification.

In light of the above considerations, this study conducts research on the agrobiological methods for the amelioration of degraded irrigated lands in the Akdala irrigation massif. The aim is to provide valuable insights into sustainable soil management practices, offering a potential solution to mitigate the impact of desertification in Kazakhstan's challenging climatic conditions. The primary objective of this study was to assess the impact of different crops on soil properties and nutrient dynamics in the Akdala massif, Kazakhstan, characterized by a sharply continental climate. The aim was to investigate variations in soil bulk density, agronomically valuable aggregates (AVA), water-stable aggregates (WSA), labile and total organic carbon (LOC and TOC), easily hydrolyzable nitrogen (EHN), nitrate (NO_3), available phosphorus (P_2O_5), and exchangeable potassium (K_2O) across various crops, soil depths, and sampling times. The study spanned three years (2015-2017) and utilized field experiments on the fields of "Birlik" LLP in the Balkhash district of the Almaty region, employing a diverse set of crops including rice, corn, soybean, sudan grass, and sorghum. The investigation aimed to enhance our understanding of the intricate relationships between different crops and soil parameters, contributing valuable insights for sustainable soil management practices in continental climates.

Material and Methods

Study site and climatic conditions

The research was conducted in the Akdala massif, Kazakhstan, characterized by a sharply continental climate. This region experiences substantial temperature variations between day and night, as well as between seasons. Winters are cold and snowy, with temperatures as low as -13 to -15°C in January. Conversely, summers are hot and dry, reaching a monthly average high of 23-25°C in July, with an absolute maximum of 40-45°C. Meteorological data from the Bakanas settlement indicate a positive average annual temperature ranging from +5.1 to 7.5°C. The cumulative temperatures above +5°C and +10°C are in the ranges of 3800-4000°C and 3400-3500°C, respectively, facilitating the cultivation of crops with a long growing season. The frost-free period spans approximately 150-160 days on average, with spring frosts ending around April 25 and fall frosts commencing in early October. Annual precipitation is 250 mm, with the majority (64%) falling in the spring-summer period. Summer precipitation, occasionally intense with 50-60 mm in a day, generally does not significantly impact vegetation. The region experiences hard soil freezing during winter (40-50 cm, up to 1 meter in severe winters), and snow cover, lasting 85-100 days, forms from late November to early December. Winter winds cause snow movement into natural depressions.

Experimental design

Field experiments were conducted on the fields of "Birlik" LLP in the Balkhash district of the Almaty region, Kazakhstan. The study focused on bare soils under various crops (rice, corn, soybean, sudan grass and sorghum) in the Akdala irrigation massif. The field trial lasted for three years, from 2015 to 2017.

Table 1. The plants used in the experiment and their planting and harvesting dates

Crops	Planting date	Harvesting date
Rice	April 26	October 15
Corn	April 25	October 5
Soybean	April 25	October 15
Sudan grass	April 25	August 12
Sorghum	April 25	August 12

The experimental layout covered 1 ha, with 5 different plant type, threefold repetition, and a plot area of 230 m^2. Sowing utilized a Vence Tudo direct seeder from Brazil, with ammophos fertilizer (46%N and 12%P$_2$O$_5$) applied at 100 kg/ha. Drip irrigation, with recommended rates for each crop, was employed.

Soil sampling and analyses

Soil samples were collected during June and September of each year, at depths of 0-20 cm and 20-40 cm, over the three-year field experimental period (2015-2017). The core method was employed for bulk density analyses. A core sampler, with a 5 cm height and 5 cm diameter metal cylinder, was pressed into the soil. The cylinder, maintaining its height, was removed to obtain a sample of 98.12 cm3 volume. Moist sample weight was recorded, followed by drying in an oven and subsequent weighing (Blake and Hartge, 1986).

Agronomically valuable aggregates (10-0.25 mm) were determined using the standard dry-sieving method, while water-stable aggregates (WSA) larger than 0.25 mm were determined by wet sieving (Kemper and Rosenau, 1986). Total organic carbon (TOC) and labile organic carbon (LOC), Easily Hydrolyzable Nitrogen (EHN) nitrate (NO$_3$), available phosphorus (P$_2$O$_5$), and exchangeable potassium (K$_2$O) content were determined through various methods, including titrimetric, Kjeldahl, potentiometric, and extraction methods as described by Tyurin (1965); Rowell (1996), Jones (2001), GOST 26213-2021 and GOST 26205-91. The analyses were conducted in the accredited analytical laboratory of the Kazakh Research Institute of Agriculture and Plant Growing.

Results and Discussion

The investigation into the impact of different crops on soil bulk density involved the collection of soil samples at varying time intervals. Figure 1 presents the bulk density values for different crops from 2015 to 2017, considering two soil depths (0-20 cm and 20-40 cm) and two sampling times (July and September). The results depict fluctuations in soil bulk density influenced by various crops. Bulk density is a crucial indicator affecting soil properties, including infiltration, rooting depth, water capacity, porosity, aeration, nutrient availability, and microbial activity (Abbott and Manning, 2015; Makovníková et al., 2017). Analyzing the data, no significant differences in bulk density emerged among crops sampled at different intervals. However, consistently higher bulk density in the 20-40 cm soil depth across all crops implies typical soil behavior, with subsoil layers experiencing greater compaction due to reduced organic matter, aggregation, and root penetration compared to surface soil. This aligns with findings from similar studies (Stirzaker et al., 1996; Duan et al., 2019), reflecting a general increase in bulk density with soil depth. While crop cultivation did not reveal significant differences in bulk density, the consistent increase at 20-40 cm depth emphasizes the importance of considering soil depth variations in understanding bulk density changes. These results contribute to our comprehension of the intricate relationship between different crops and soil bulk density, highlighting the need for comprehensive soil management practices accounting for depth-specific variations.

The investigation into the impact of different crops on Agronomically Valuable Aggregates (AVA) in soils involved soil samples collected at varying time intervals. Figure 2a illustrates the percentage of AVA for different crops from 2015 to 2017, considering two soil depths (0-20 cm and 20-40 cm) and two sampling times (July and September). The results exhibit variations in AVA values influenced by different crops, sampling times, and soil depths. In 2015, Corn demonstrated the highest AVA values in both soil depths, while in 2016, Sudan Grass exhibited the highest AVA values. In 2017, elevated AVA values were observed for both Corn and Sudan Grass. Interestingly, higher AVA values in 2015 were observed in the surface soil (0-20 cm), while in 2016, the 20-40 cm depth exhibited higher AVA values. Dry aggregate size distribution significantly impacts soil fertility, erosion resistance, and degradation, serving as an indicator of soil structure. The structural coefficient, commonly employed in Eastern European countries, highlights the proportion of agronomically valuable fractions (10-0.25 mm) in relation to other fractions (>10 and <0.25 mm) (Shein et al.,

2001; Ćirić et al., 2006). The content of these fractions is crucial for optimal porosity, water, and air capacity in the soil. The results emphasize the dynamic nature of AVA values influenced by different crops, sampling times, and soil depths. Shifts between surface and subsurface soils underscore the importance of considering soil depth variations. The relevance of dry aggregate size distribution, indicated by the structural coefficient, emphasizes the significance of agronomically valuable fractions for soil quality and optimal soil properties (Medvedev and Cybulko, 1995; Shein et al., 2001). These findings contribute to our understanding of the intricate relationship between crop cultivation and soil aggregate dynamics, urging further exploration for comprehensive soil management practices.
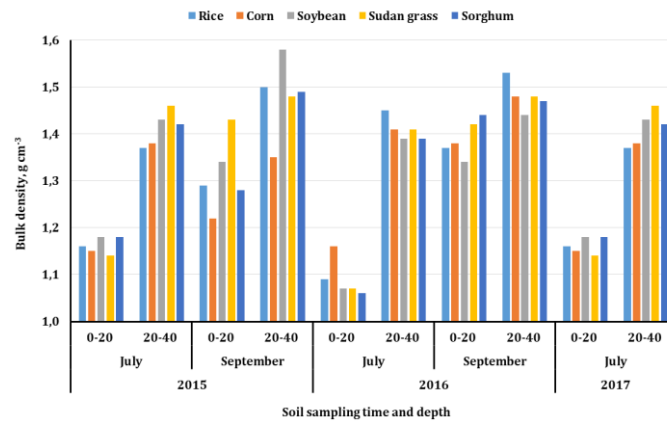
Figure 1. Bulk density variations across different crops, soil depths, and sampling times

The examination of different crops' influence on Water-Stable Aggregates (WSA) in soils involved collecting soil samples at varying time intervals. Figure 2b depicts the percentage of WSA for different crops from 2015 to 2017, considering two soil depths (0-20 cm and 20-40 cm) and two sampling times (July and September). The results illustrate variations in WSA values influenced by different crops, sampling times, and soil depths. Soil samples from the 20-40 cm depth consistently exhibited higher WSA values during all sampling periods. Significant differences were observed among sampling times and cultivated crops. In July 2015 and 2017, as well as September 2016, Rice recorded the highest WSA values in both soil depths. In September 2016, Sudan Grass demonstrated the highest WSA values. Soil aggregate stability, particularly water-stable aggregates, plays a crucial role in soil health by preserving organic matter, enhancing soil porosity, drainage, and water availability for plants, mitigating soil compaction, and supporting biological activity and nutrient cycling (Papadopoulos, 2011). WSA, especially those >1 mm in size, are indicative of soil structural stability (Tisdall and Oades, 1982). The decline in soil structure is considered a form of soil degradation associated with land use and soil/crop management practices. All sizes of water-stable aggregates contribute significantly to soil quality and serve as indicators of soil health (Sui et al., 2012). The consistently higher WSA values at the 20-40 cm depth highlight the importance of considering soil depth variations in assessing the effects of crop cultivation on soil aggregate stability. These findings contribute to our understanding of the intricate relationship between crop management and soil aggregate dynamics, emphasizing the importance of sustainable soil management practices for maintaining soil health.

(a)   (b)
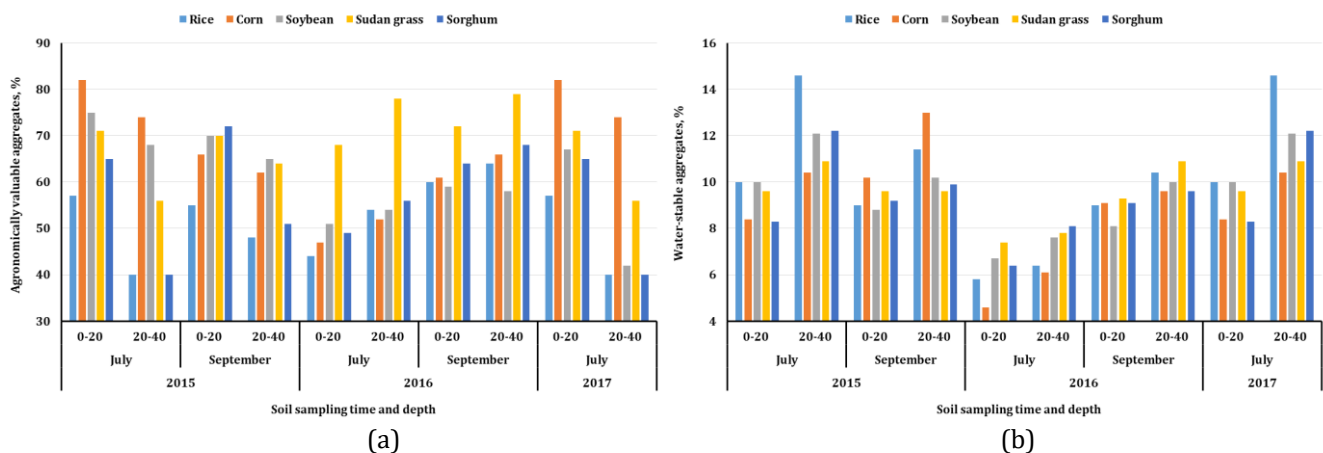
Figure 2. Agronomically Valuable Aggregates (AVA) percentages (a) and Water-Stable Aggregates (WSA) percentages (b) across different crops, soil depths, and sampling times

The investigation into the influence of different crops on Labile Organic Carbon (LOC) and Total Organic Carbon (TOC) in soils involved soil samples collected at varying time intervals. Figure 3a and 3b present the percentage of LOC and TOC, respectively, for different crops from 2015 to 2017, considering two soil depths (0-20 cm and 20-40 cm) and two sampling times (July and September). The results depict variations in LOC and TOC values influenced by different crops, sampling times, and soil depths. Regardless of the sampling time, Sorghum consistently had the highest impact on increasing both Labile Organic Carbon and Total Organic Carbon values in both surface soil (0-20 cm) and subsurface soil (20-40 cm). Notably, these increases were more pronounced in Labile Organic Carbon content. Soil Organic Carbon (SOC) comprises various organic carbon compounds derived from the gradual decomposition of plant residues, animals, and microbial materials (Tian et al., 2015). Labile organic carbon fractions act as transitional fractions between fresh plant residues and stabilized organic matter, with a temporary turnover time (Parton et al., 1987; Wang et al., 2017). These fractions, compared with total SOC, respond to multiple interactions within the soil system and serve as sensitive indicators reflecting shifts in soil quality (Dumale et al., 2009). The results highlight the significant influence of different crops on Labile Organic Carbon and Total Organic Carbon contents in both surface and subsurface soils. Sorghum, in particular, demonstrated a substantial impact on increasing organic carbon levels, emphasizing its potential role in enhancing soil quality. These findings contribute to our understanding of the intricate relationship between crop choices and soil organic carbon dynamics, emphasizing the importance of sustainable agricultural practices for maintaining soil health.

(a)   (b)
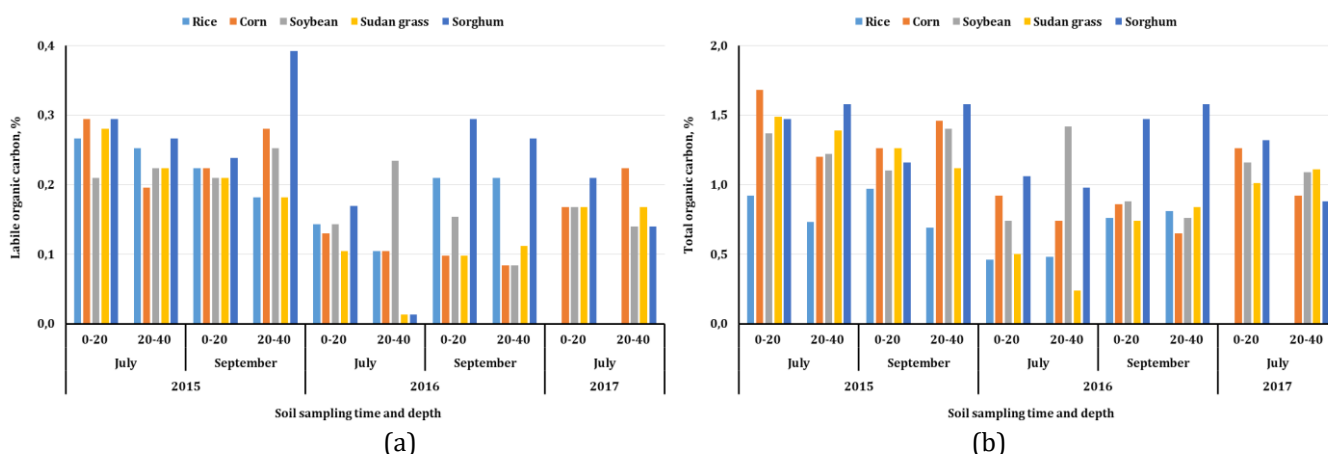
Figure 3. Labile Organic Carbon (LOC) (a) and Total Organic Carbon (TOC) (b) across different crops, soil depths, and sampling times

The examination of different crops' influence on Easily Hydrolyzable Nitrogen (EHN) and Nitrate (NO_3) in soils involved collecting soil samples at varying time intervals. Figure 4a and 4b present the concentrations of EHN and NO_3, respectively, for different crops from 2015 to 2017, considering two soil depths (0-20 cm and 20-40 cm) and two sampling times (July and September). The results illustrate variations in EHN and NO_3 values influenced by different crops, sampling times, and soil depths. No consistent trend of influence by different crops on EHN and NO_3 content in soil samples collected during all sampling periods was observed. However, in July 2015 and September 2016, the highest EHN values were observed for the Sorghum crop, while in September 2016, the highest NO_3 values were recorded for the Rice crop. Soil available nitrogen is a crucial indicator for evaluating soil nutrients and is directly absorbed by crop roots. Easily hydrolyzable nitrogen represents an alternative indicator of soil nitrogen-supplying capacity, as it is not readily leached and can be directly absorbed by crop roots (Kersebaum et al., 2005; Malhi et al., 2003; Roberts et al., 2011). On the other hand, nitrate (NO_3) is a form of nitrogen directly usable by plants and subject to leaching in soils (Meisinger, 1984). The study provides insights into the dynamic nature of soil nitrogen forms influenced by different crops. The observed variations in EHN and NO_3 content emphasize the importance of considering crop-specific effects on soil nitrogen dynamics. These findings contribute to a better understanding of nutrient cycling in agricultural systems, guiding sustainable practices for maintaining soil fertility and optimizing crop productivity.

The study aimed to investigate the impact of different crops on available P2O5 and Exchangeable K_2O content in soils, collecting samples at varying time intervals. Figure 5 presents the concentrations of P_2O5 and K_2O for different crops from 2015 to 2017, considering two soil depths (0-20 cm and 20-40 cm) and two sampling times (July and September). The results illustrate variations in available P2O5 and Exchangeable K_2O values influenced by different crops, sampling times, and soil depths.

(a)   (b)
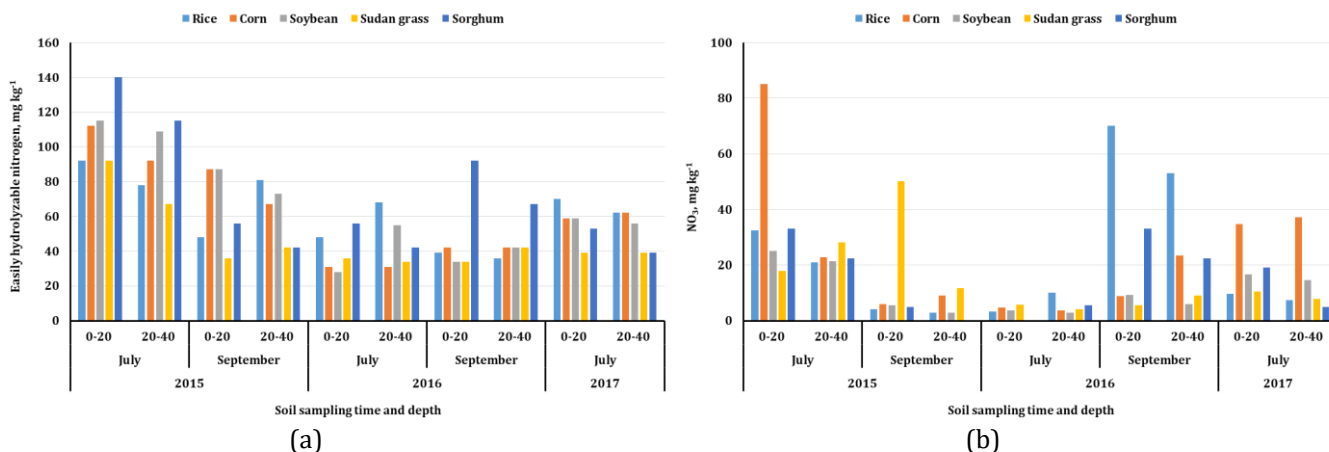
Figure 4. Easily Hydrolyzable Nitrogen (EHN) concentrations (a) and Nitrate (NO$_3$) concentrations (b) across different crops, soil depths, and sampling times

The findings suggest a lack of homogeneity in the influence of plant species on the content of available P$_2$O$_5$ and Exchangeable K$_2$O in soils collected during all sampling periods. This observation may be attributed to the relatively low mobility of phosphorus and potassium compared to nitrogen in the soil. Phosphorus tends to adsorb on calcareous surfaces (Anjos and Rowell, 1987; Eslamian et al., 2021; Zhaksybayeva et al., 2022), while potassium is adsorbed by clay minerals (Binner et al., 2017), resulting in reduced mobility. The study further revealed that the mobility of these two nutrients did not show significant variations between samples taken from the upper soil surface (0-20 cm) and those from the lower soil depth (20-40 cm). However, it is noteworthy that the highest available P$_2$O$_5$ content was recorded in the 0-20 cm depth of plots cultivating Corn in September 2016, while the highest Exchangeable K$_2$O was observed in the 0-20 cm depth of plots cultivating Sudan Grass in September 2016. The results highlight the complex dynamics of available P$_2$O$_5$ and Exchangeable K$_2$O in soils under different crops. The non-uniform effects across plant species emphasize the need for a nuanced approach to soil fertility management, considering the specific nutrient requirements of different crops. These findings contribute to the understanding of nutrient cycling in agricultural ecosystems, aiding in the development of sustainable soil management practices for optimized crop productivity.

(a)   (b)
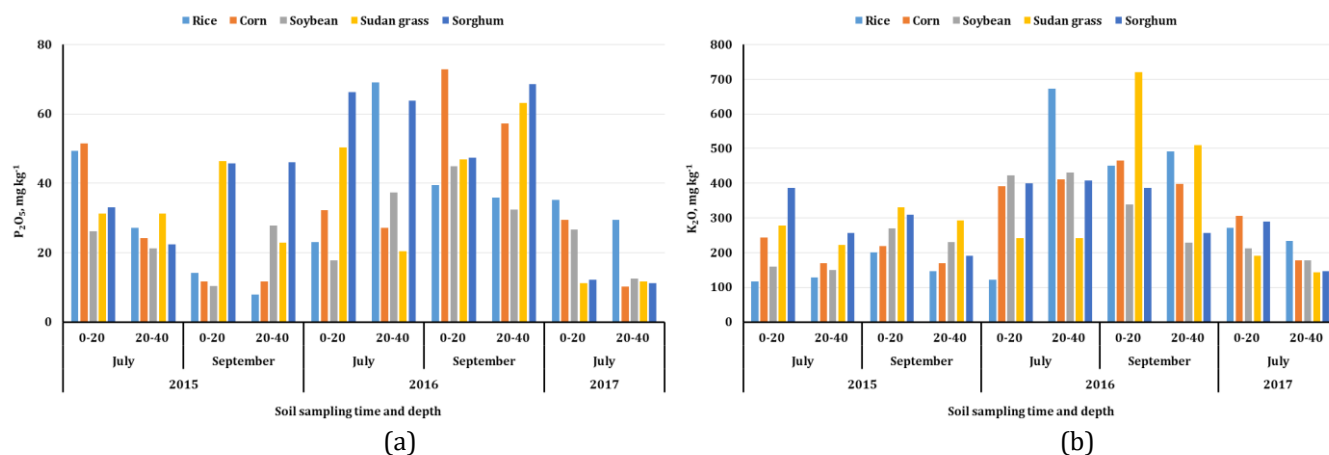
Figure 5. Available P$_2$O$_5$ and Exchangeable K$_2$O concentrations across different crops, soil depths, and sampling times

Conclusion

In conclusion, this study provides valuable insights into the intricate relationship between different crops and soil properties in the Akdala massif, Kazakhstan, characterized by a sharply continental climate. Desertification, a pressing global environmental challenge, particularly affects arid and semiarid regions, impacting over 1 billion people worldwide. Kazakhstan, as the largest landlocked country, faces significant challenges related to desertification, aggravated by adverse climate changes and human activities. Historically, Kazakhstan experienced desertification, marked by the "Black Storm" in the 1960s. Efforts by the Soviet Union and the Kazakhstan government successfully controlled desertification, but post-1990s dynamics, including grassland reclamation and cropland abandonment, increased the risk of land desertification. This study, rooted in the context of combating desertification, aimed to assess the impact of different crops on soil properties and nutrient dynamics in the Akdala massif. The research focused on the cultivation of rice, corn, soybean, sudan grass, and sorghum, employing a diverse set of crops to understand their influence on various

soil parameters. The study spanned three years (2015-2017), conducting field experiments on the fields of "Birlik" LLP in the Balkhash district of the Almaty region. The investigation aimed to enhance our understanding of soil bulk density, agronomically valuable aggregates (AVA), water-stable aggregates (WSA), labile and total organic carbon (LOC and TOC), easily hydrolyzable nitrogen (EHN), nitrate (NO_3), available phosphorus (P_2O_5), and exchangeable potassium (K_2O) across different crops, soil depths, and sampling times. The results revealed dynamic variations in soil parameters influenced by different crops, emphasizing the need for comprehensive soil management practices. While soil bulk density did not show significant differences among crops, the consistent increase at the 20-40 cm depth underscored the importance of considering soil depth variations. Agronomically valuable aggregates and water-stable aggregates exhibited fluctuations, showcasing the dynamic nature of soil structure influenced by different crops, sampling times, and depths. The influence of crops on Labile Organic Carbon and Total Organic Carbon demonstrated the significant impact of Sorghum on increasing organic carbon levels, contributing to enhanced soil quality.

The examination of different crops' influence on Easily Hydrolyzable Nitrogen and Nitrate emphasized the dynamic nature of soil nitrogen forms influenced by different crops, sampling times, and soil depths. The findings provide insights into nutrient cycling in agricultural systems, guiding sustainable practices for maintaining soil fertility and optimizing crop productivity. The study further investigated the impact of different crops on available P_2O_5 and Exchangeable K_2O, highlighting the non-uniform effects across plant species and the need for a nuanced approach to soil fertility management. In essence, this research contributes valuable knowledge for developing sustainable soil management practices in arid and semiarid regions. The findings underscore the importance of considering the specific impacts of different crops on soil properties and nutrient dynamics, offering guidance for optimizing soil health and combating desertification challenges. As global efforts intensify to address environmental degradation, studies like this play a crucial role in advancing our understanding and promoting practices that contribute to the sustainable management of ecosystems affected by desertification.

Acknowlegements

References

Abbott, L.K., Manning, D.A.C., 2015. Soil health and related ecosystem services in organic agriculture. *Sustainable Agriculture Research* 4(3): 116-125.

Anjos, J.T., Rowell, D.L., 1987. The effect of lime on phosphorus adsorption and barley growth in three acid soils. *Plant and Soil* 103: 75–82.

Assanova, M.A., 2015. Public policy and model of sustainable development in the republic of Kazakhstan. *Asian Social Science* 11(6): 237–243.

Bektayev, N., Mansurova, K., Kaldybayev, S., Pachikin, K., Erzhanova, K., Absatova, B., 2023. Comprehensive assessment and information database on saline and waterlogged soils in Kazakhstan: Insights from Remote Sensing Technology. *Eurasian Journal of Soil Science* 12(4): 290 - 299.

Binner, I., Dultz, S., Schellhorn, M., Schenk, M.K., 2017. Potassium adsorption and release properties of clays in peat-based horticultural substrates for increasing the cultivation safety of plants. *Applied Clay Science* 145: 28-36.

Blake, G.R., Hartge, K.H. 1986. Bulk Density. In: Methods of Soil Analysis: Part 1 Physical and Mineralogical Methods, 5.1, Second Edition. Klute, A. (Ed.). American Society of Agronomy, Soil Science Society of America, WI, Madison, USA. pp.363-375.

Ćirić, V., Manojlović, M., Nešić, L., Belić, M., 2012. Soil dry aggregate size distribution: effects of soil type and land use. *Journal of Soil Science and Plant Nutrition* 12 (4): 689-703.

Duan, A., Lei, J., Hu, X., Zhang, J., Du, H., Zhang, X., Guo, W., Sun, J., 2019. Effects of planting density on soil bulk density, ph and nutrients of unthinned Chinese Fir mature stands in south subtropical Region of China. *Forests* 10(4): 351.

Dumale, J.W.A., Miyazaki, T., Nishimura, T., Seki, K., 2009. CO2 evolution and short-term carbon turnover in stable soil organic carbon from soils applied with fresh organic matter. *Geophysical Researh Letters* 36(1): 1-6.

Eslamian, F., Qi, Z., Qian, C., 2021. Lime amendments to enhance soil phosphorus adsorption capacity and to reduce phosphate desorption. *Water, Air, & Soil Pollution* 232: 66.

Geist, H.J., Lambin, E.F., 2004. Dynamic causal patterns of desertification. *Bioscience* 54(9): 817–829.

GOST 26205-91. Soils. Determination of mobile compounds of phosphorus and potassium by Machigin method modified by CINAO. Available at [Access date: 11.11.2021]: https://gostperevod.com/gost-26205-91.html

GOST 26213-2021. Soils. Methods for determination of organic matter. Available at [Access date: 11.11.2021]: https://gostperevod.com/gost-26213-2021.html

Hu, Y., Han, Y., Zhang, Y., 2020. Land desertification and its influencing factors in Kazakhstan. *Journal of Arid Environments* 180: 104203.

Jiang, L., Bao, A., Jiapaer, G., Guo, H., Zheng, G., Gafforov, K., Kurban, A., De Maeyer, P., 2019. Monitoring land sensitivity to desertification in Central Asia: convergence or divergence? *Science of The Total Environment* 658: 669–683.

Jones, J.B., 2001. Laboratory guide for conducting soil tests and plant analyses. CRC Press, New York, USA. 363p.

Kemper, W.D. Rosenau, R.C., 1986. Aggregate Stability and Size Distribution. In: Methods of Soil Analysis: Part 1 Physical and Mineralogical Methods, 5.1, Second Edition. Klute, A. (Ed.). American Society of Agronomy, Soil Science Society of America, WI, Madison, USA. pp.425-442.

Kersebaum, K., Lorenz, K., Reuter, H., Schwarz, J., Wegehenkel, M., Wendroth, O., 2005. Operational use of agro-meteorological data and GIS to derive site specific nitrogen fertilizer recommendations based on the simulation of soil and crop growth processes. *Physics and Chemistry of the Earth, Parts A/B/C* 30(1-3): 59-67.

Kussainova, M., Spaeth, K., Zhaparkulova, E., 2020. Efficiency of using the rangeland hydrology and erosion model for assessing the degradation of pastures and forage lands in Aydarly, Kazakhstan. *Eurasian Journal of Soil Science* 9(2): 186 - 193.

Kvan, R.A., Kalashnikov, A.A., Paramonov, A.I., Kaldarova, S.M., 2011. Water resources and prospects for their use in irrigation of the Republic of Kazakhstan. *Vodnoe hozyajstvo Kazahstana* 3: 15-17. [in Russian]

Makovníková, J., Širáň M., Houšková B., Pálka B., Jones, A., 2017. Comparison of different models for predicting soil bulk density. Case study - Slovakian agricultural soils. *International Agrophysics* 31(4): 491–498.

Malhi, S., Gill, K., Harapiak, J., Nyborg, M., Gregorich, E., Monreal, C., 2003. Light fraction organic N, ammonium, nitrate and total N in a thin black Chernozemic soil under bromegrass after 27 annual applications of different N rates. *Nutrient Cycling in Agroecosystems* 65: 201-210.

Medvedev, V.V., Cybulko, W.G., 1995. Soil criteria for assessing the maximum permissible ground pressure of agricultural vehicles on Chernozem soils. *Soil and Tillage Research* 36(3-4): 153–164.

Meisinger, J., 1984. Evaluating plant-available nitrogen in soil–crop systems. In: Nitrogen in Crop Production. Hauck, R.D. (Ed.). American Sciety of Agronomy, Madison, WI, USA. pp. 391-416

Papadopoulos, A., 2011. Soil Aggregates, Structure, and Stability. In: Encyclopedia of Agrophysics. Gliński, J., Horabik, J., Lipiec, J. (Eds.). Encyclopedia of Earth Sciences Series. Springer, Dordrecht. pp 736–740.

Parton, W.J., Schimel, D.S., Cole, C.V., Ojima, D.S. 1987. Analysis of factors controlling soil organic matter levels in Great Plains grasslands. *Soil Science Society of America Journal* 51(5): 1173–1179.

Reynolds, J.F., Smith, D.M.S., Lambin, E.F., TurnerII, B.L., Mortimore, M., Batterbury, S.P.J., Downing, T.E., Dowlatabadi, H., Fernández, R.J., Herrick, J.E., Huber-Sannwald, E., Jiang, H., Leemans, R., Lynam, T., Maestre, F.T., Ayarza, M., Walker,B., 2007. Global desertification: building a science for dryland development. *Science* 316 (5826), 847–851.

Roberts, T., Ross, W., Norman, R., Slaton, N., Wilson, C., 2011. Predicting nitrogen fertilizer needs for rice in Arkansas using alkaline-hydrolyzable-nitrogen. *Soil Science Society of America Journal* 75 (3): 1161-1171.

Rowell, D.L., 1996. Soil Science: methods and applications. Longman, UK. 350p.

Shein, Y.V., Arhangel'skaya, T.A., Goncharov, V.M., Guber, A.K.,Pochatkova, T.N., Sidorova, M.A., Smagin, A.V., Umarova, A.B. 2001. Field and laboratory methods of physical properties and soil status investigations. The University of Moscow, Russia, 199 p. [in Russian].

Stirzaker, R.J., Passioura, J.B., Wilms, Y., 1996. Soil structure and plant growth: Impact of bulk density and biopores. *Plant and Soil* 185: 151-162.

Sui, Y.Y., Jiao, X.G., Liu, X.B., Zhang, X.Y., Ding, G.W., 2012. Water-stable aggregates and their organic carbon distribution after five years of chemical fertilizer and manure treatments on eroded farmland of Chinese Mollisols. *Canadian Journal of Soil Science* 92(3): 551–557.

Tian, H., Lu, C., Yang, J., Banger, K., Huntzinger, D.N., Schwalm, C.R., Michalak, A.M., Cook, R., Ciais, P., Hayes, D., Huang, M.Y., Lto, A., Jain, A.K., Lei, H., Mao, J.F., Pan, S.F., Post, W.M., Peng, S.S., Poulter, B., Ren, W., Ricciuto, D., Schaefer, K., Shi, X.Y., Tao, B., Wang, W., Wei, Y.X., Yang, Q.C., Zhang, B.W., Zheng, N., 2015. Global patterns and controls of soil organic carbon dynamics as simulated by multiple terrestrial biosphere models: current status and future directions. *Global Biogeochemical Cycles* 29(6): 775-792.

Tisdall, J.M., Oades, J.M., 1982. Organic matter and water-stable aggregate in soil *European Journal of Soil Science* 33(2): 141 -163.

Tyurin, I. V., 1965. Organic matter of soil and its role in fertility. Nauka, Moscow. 320p

Verón, S.R., Paruelo, J.M., Oesterheld, M., 2006. Assessing desertification. *Journal of Arid Environments* 66(4): 751–763.

Wang, X.Y., Yu, D.S., Xu, Z.C., Pan, Y., Pan, J.J., Shi, X.Z. 2017. Regional patterns and controls of soil organic carbon pools of croplands in China. *Plant and Soil* 421, 525–539.

Zhaksybayeva, G., Balgabayev, A., Vassilina, T., Shibikeyeva, A., Malimbayeva, A., 2022. Yield of sugar beet and changes in phosphorus fractions in relation to long term P fertilization in chestnut soil of Kazakhstan. *Eurasian Journal of Soil Science* 11(1): 25-32.

Eurasian Journal of Soil Science

Journal homepage : http://ejss.fesss.org
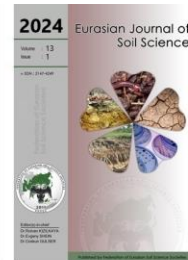
The impact of *Klebsiella quasipneumoniae* inoculation with nitrogen fertilization on baby corn yield and cob quality

Nguyen Van Chuong *

An Giang University, Faculty of Agriculture, Department of Crop Science, VNU-HCM City, Vietnam

Abstract

In response to the escalating costs and diminishing efficiency of nitrogen fertilizers, the agricultural community is actively seeking sustainable alternatives that leverage natural nitrogen sources derived from biological N-fixation processes to enhance crop yield. This study investigates the combined effects of *Klebsiella quasipneumoniae* inoculation and varying nitrogen fertilizer doses on soil fertility, nutrient availability, and the yield and quality parameters of baby corn (*Zea mays*. L). The study involved the application of five nitrogen levels (0, 75, 150, 225, and 300 kg N ha^{-1}) in conjunction with *Klebsiella quasipneumoniae* inoculum on HM-4 variety of baby corn, employing a comprehensive experimental design with five treatments and four replications. All treatments demonstrated increased ear count and weights of ear, silk, husk, edible cob, and biomass compared to the control. The study highlights the potential of *Klebsiella quasipneumoniae* inoculation in synergy with reduced nitrogen fertilizer to enhance total N contents in soil and positively impact baby corn yield and cob quality parameters. Optimal results were achieved with a 50% reduction in nitrogen fertilizer (150 kg N ha^{-1}), emphasizing the importance of integrated nutrient management. The findings contribute valuable insights to sustainable agriculture, offering a promising strategy for increased baby corn production, improved nutritional quality, and environmental conservation. This integrated approach, involving microbial inoculation and nitrogen management, emerges as a key element in modern agricultural practices, promoting both productivity and nutritional content in baby corn crops.

Keywords: *Klebsiella quasipneumoniae,* inoculation, fertilizer, plant yield, cob quality.

Introduction

Baby corn (*Zea mays*. L), renowned for its high nutritional value, undergoes inoculation with plant growth-promoting rhizobacteria (PGPR) to reduce the dependence on chemical fertilizers. The application of PGPR for plant growth promotion is crucial in enhancing various aspects of crop agronomy, yield traits, and overall yield, offering farmers a sustainable and profitable alternative (Kumar et al., 2014). With a short cultivation period of approximately 70 days from sowing to harvest, baby corn is predominantly utilized as a vegetable, particularly for its fresh ears in global culinary preparations. Its swift growth and minimal susceptibility to pests contribute significantly to the economic gains for farmers (Rani et al., 2015).

In Asian countries such as Vietnam, Thailand, and Taiwan, baby corn cultivation has gained popularity due to its high-income potential, short cultivation period, and robust export market, making it a valuable food source (Gondaliya et al., 2022). Nitrogen (N) nutrient plays a pivotal role in promoting the development of baby corn, enhancing leaf and height growth, reducing senescence, and optimizing essential components for ear formation. The positive impact of N nutrient on corn productivity, including seed number, weight, and seed size, has been well-documented in previous studies (Tolbert et al., 2011). The significance of N nutrient in the agronomy and productivity of baby corn has been emphasized in previous research (McCullough et al., 1994). Notably, the N requirement for baby corn varies based on factors such as farmland type, environmental conditions, and plant rotation practices (Blackmer et al., 1989; Bundy et al., 2011).

The intricate relationship between PGPR and crops within the farmland has been recognized as crucial for bio-exchange, particularly concerning farmland types (Bever et al., 2013). PGPR, encompassing a diverse range of genera, directly influences soil ecology and nutrient conditions (Liu et al., 2019). Recent studies, such as the work by Chuong et al. (2023), highlight the positive effects of fertilizing animal manures with PGPR on the maturity, productivity, and yield components of groundnuts. This underscores the potential of PGPR to enhance soil fertility and crop output across various plant types. The interaction between PGPR, soil, and crop roots on the root surface contributes significantly to crop growth by facilitating nutrient, salinity and moisture absorption (Riaz et al., 2019; Nguyen, 2023). Additionally, PGPR and legumes can form bio-interactions, with roots secreting compounds that promote vigorous plant growth. PGPR also plays a protective role by producing antibiotics to prevent root rot diseases and contribute to overall plant health (Qureshi et al. 2022). Moreover, PGPR's contribution extends to macronutrient provision, particularly nitrogen, influencing crop growth (Mendes et al., 2013; Lazcano et al., 2021). PGPR has the capacity to promote exudative metabolites and mediate signaling for soil regulation (Korenblum et al., 2020). The ability of PGPR to produce hormones further aids in enhancing nutrient absorption and reducing plant stress in challenging environmental conditions.

The taxonomy of the genus Klebsiella has been periodically revised. Currently, this genus includes K. pneumoniae subsp. Pneumoniae and some novel species: *Klebsiella quasipneumoniae*, Klebsiella variicola, and Klebsiella michiganensis (Martínez-Romero et al., 2018). Klebsiella species are ubiquitous in nature, found in water, soil, plants, insects, and other animals, including humans (Bagley, 1985). Although much is known about different free-living nitrogen-fixing organisms' impact on plant yield and soil fertility, very few studies have investigated *Klebsiella quasipneumoniae*'s effects on soil fertility and plant yield. Besides Klebsiella, the genetics of free-living, nitrogen-fixing bacteria remain largely unexplored. The primary objective of this study is to explore the effects of *Klebsiella quasipneumoniae* inoculation with varying nitrogen fertilizer doses on soil fertility, promoting soil nutrient availability, and influencing the yield and cob quality parameters of baby corn.

Material and Methods

Isolation and identification of *Klebsiella quasipneumoniae*: *Klebsiella quasipneumoniae* was isolated from baby corn roots using YEMA (Yeast Extract Mannitol Agar) medium and subsequently identified through the 16S rRNA sequencing method. The sequencing results revealed a 99.74% similarity to the known organisms. The isolation was carried out on the campus of An Giang University - VNU HCMC, utilizing colonies that were initially identified based on morphological and biochemical traits. Further confirmation was achieved through 16S rRNA gene sequencing on the NCBI database, confirming a 99.74% similarity to our target bacteria.

Experimental design and location: The experiment was conducted in an outdoor net house at the An Giang Research Center from August to October. To characterize the soil properties of the experimental site, soil samples were collected from the 0-20 cm depth prior to the experiment, and certain physicochemical attributes of the collected soil sample were determined according to the methodology reported by Carter and Gregoric (2007). The study comprised five treatments labeled BC0 (0 kg N ha^{-1}), BC1 (300 kg N ha^{-1}), BC2 (225 kg N ha^{-1}), BC3 (150 kg N ha^{-1}), and BC4 (75 kg N ha^{-1}), each replicated four times. In BC0, 0% of the required nitrogen for the plant was supplied, BC1 received 100% of the required nitrogen, BC2 received 75% of the required nitrogen, BC3 received 50% of the required nitrogen, and BC4 received 25% of the required nitrogen, all provided through chemical nitrogen fertilizer. In the experiment, alongside seed sowing, phosphorus (355 kg P_2O_5 ha^{-1}) and potassium fertilization (75 kg K_2O ha^{-1}) was applied to all plots. The planting layout consisted of holes spaced at 30 cm x 25 cm, with two seeds sown per hole. The "HM-4" baby corn variety has a growth period of approximately 60 days, ensuring rapid growth, health, and high output. The total research area covered 400 m2 (2 m x 10 m x 4 replicates x 5 plots).

Seed preparation and inoculation: The *Klebsiella quasipneumoniae* strain was cultivated to a quantity of 10^8 colony-forming units per milliliter (10^8 CFU mL^{-1}) on diluted YEMA medium. The "HM-4" variety of baby corn seeds, sourced from a breeding company in southern Vietnam, was utilized for the experiment. Two days prior to sowing in darkness, the baby corn seeds were inoculated with *Klebsiella quasipneumoniae* and subsequently sprayed. The spray inoculation of *Klebsiella quasipneumoniae* was applied to baby corn seeds intended for sowing in all plots, except for the control (BC0) treatment.

Measurement of agronomic and yield traits: The critical practice of tassel removal, performed at approximately 50 days after sowing (DAS), plays a pivotal role in stimulating the development of baby corn ears, thereby enhancing overall yield and nutrient concentration. Agronomic, yield, and edible cob output traits were systematically assessed from 15 DAS until harvest. The parameters monitored encompassed plant height, total chlorophyll content, biomass weight, fresh pod weight, silk weight, husk weight, and cob weight. Furthermore, for the determination of Baby corn cob quality, moisture, lipid, protein, phosphorus, and

potassium contents were quantified following the methodology outlined by Jones (2001). The total chlorophyll content of the plant was determined using a chlorophyll meter.

Soil analysis: At the end of the experiment, soil samples were collected from all plots to determine the effects induced by the implemented treatments on some soil properties. Soil pH was measured using a pH meter with a soil-to-water ratio of 1:2.5. Mineral nitrogen content was analyzed using the Kjeldahl method, while available phosphorus was determined employing the alkaline hydrolysis method (Carter and Gregoric, 2007).

Statistical data: The impact of treatments was assessed through ANOVA using Statgraphics software version XVIII. Means were compared, and all variance analyses were conducted at a significance level of 5% (P ≤ 0.05).

Results and Discussion

After analyzing the soil sample collected from the experimental site before the commencement of the trial, it was determined that the initial soil composition of the experimental area consisted of sandy loam texture (81% sand, 17.7% silt, and 1.3% clay), exhibited a neutral pH of 6.9, and possessed low levels of soil organic matter (0.790%), total nitrogen (0.075%) and moderate available phosphorus (591 mg kg^{-1}).

At the end of the experiment, changes in soil pH, mineral nitrogen, and available phosphorus content resulting from the applications were determined through soil analysis, as presented in Table 1. According to the obtained results, it was determined that the *Klebsiella quasipneumoniae* inoculation, applied in conjunction with inorganic nitrogen fertilizers, significantly influenced the examined soil properties. Despite the initial soil pH of 6.9, which ranged between 6.47 and 7.22 in all treatments, the highest pH was achieved in the BC1 treatment, where *Klebsiella quasipneumoniae* inoculation was not performed, and all required nitrogen for the plant was supplied through chemical means. Conversely, the lowest pH was observed in the BC4 treatment. However, while the total nitrogen and available phosphorus content of the soils were minimal in the BC1 treatment, the highest total nitrogen was found in the BC3 treatment, and the highest available phosphorus was observed in the control (BC0) treatment.

Table 1. Changes in soil pH, Mineral N, and Available P contents of soil samples collected from plots at the end of the experiment

Treatments	pH	Mineral N (mg kg^{-1})	Available P (mg kg^{-1})
BC0	6.692 ± 0.600	61.0b ± 0.007	573a ± 7.49
BC1	7.221 ± 0.648	41.0c ± 0.005	392b ± 5.12
BC2	6.683 ± 0.600	42.0c ± 0.005	510a ± 6.65
BC3	6.891 ± 0.619	91.0a ± 0.011	553a ± 7.22
BC4	6.471 ± 0.581	71.0b ± 0.009	510a ± 6.66

Sign (±) indicates the mean standard deviation of four repeats; The same letter denotes inadequately different means in a column for each trait.

At 15 and 30 days after sowing (DAS), changes in plant height, leaf count, and total chlorophyll content of baby corn plants due to the treatments are presented in Table 2. According to the obtained results, it was determined that all treatments increased plant height, leaf count, and total chlorophyll content compared to the control (BC0) at 15 DAS. However, by 30 DAS, it was observed that plant height and leaf count in the BC4 treatment were even lower than the control (BC0), indicating a decline in plant development over time. Specifically, plant height was lower in BC4 at 15 DAS, while at 30 DAS, it was lower in BC3. Leaf count was lower in BC4 at 15 DAS, while at 30 DAS, it was lower in BC2 and BC3. The total chlorophyll content was highest in BC1 at 15 DAS, whereas at 30 DAS, it was highest in BC2.

Table 2. Effects of treatments on plant height, leaf count, and total chlorophyll content of baby corn plants in measurements taken at 15 and 30 days after sowing (DAS)

Treatment	Crop height (cm)		Number of leaves (leaf plant^{-1})		Total chlorophyll (µg mL^{-1})	
	Days After Sowing (DAS)					
	15	30	15	30	15	30
BC0	33.53b ± 1.37	95.81 ± 4.51	6.51c ± 0.577	12.51ab ± 0.577	34.47c ± 1.00	34.92c ± 2.27
BC1	42.75a ± 5.35	97.70 ± 2.27	7.76ab ± 0.500	12.80a ± 0.957	43.31a ± 4.56	39.77b ± 2.58
BC2	40.38a ± 4.95	96.00 ± 9.22	7.01bc ± 0.816	13.31a ± 0.500	37.44bc ± 2.58	43.97a ± 2.16
BC3	38.75ab ± 4.13	102.00 ± 7.56	7.51ab ± 0.577	13.30a ± 0.500	39.40ab ± 2.88	39.80b ± 1.30
BC4	41.58a ± 3.25	90.92 ± 3.41	8.01a ± 0.001	11.81b ± 0.500	36.88bc ± 2.12	39.74b ± 2.22
F*test*	*	ns	*	*	**	**
CV (%)	12.42	16.70	10.1	16.31	10.6	18.86

ns: not significant; *: p ≤ 0.05; **: p ≤ 0.01; CV (%) expresses the coefficient of variation; Sign (±) indicates the mean standard deviation of four repeats; The same letter denotes inadequately different means in a column for each trait.

The effects of treatments on ear number, fresh weights of certain corn ear components (ear, silk, husk, and edible cob), and fresh plant biomass of baby corn plants are presented in Table 3. According to the obtained

results, it was observed that all nitrogen (N) fertilizer and N fertilizer with *Klebsiella quasipneumoniae* inoculation treatments (BC1, BC2, BC3, and BC4) significantly increased ear count, as well as the fresh weights of ear, silk, husk, edible cob, and biomass compared to the control (BC0). The highest ear count and silk weight were recorded in the BC1 treatment, while the highest weights for ear, husk, and plant biomass were observed in the BC2 treatment, and the highest edible cob weight was achieved in the BC3 treatment.

Table 3. Effects of treatments on ear number, fresh weight of ear, silk, husk, edible cob and biomass of baby corn plants

Treatments	Ear number (ears plant-1)	Fresh weingt (t ha-1)				
		Ear	Silk	Husk	Edible cob	Biomass
BC0	2.52d ± 0.016	6.32e±0.016	0.531d±0.001	3.50c±0.408	1.69d±0.008	26.8d±0.163
BC1	5.00a±0.817	14.8b±0.150	1.82a±0.007	9.80a±0.163	2.45b±0.041	34.8c±0.163
BC2	4.37b±0.057	15.3a±0.245	1.35b±0.040	10.1a±0.082	3.15a±0.041	42.2a±0.163
BC3	4.32b±0.016	10.8c±0.653	0.65c±0.041	6.23b±.025	3.30a±0.245	34.8c±0.163
BC4	3.48c±0.065	9.90d±0.082	0.65c±0.041	6.43b±0.025	2.23c±0.025	37.2b±0.163
Ftest	**	**	**	**	**	**
CV(%)	23.8	21.5	19.1	25.1	24.2	14.5

ns: not significant; *: p ≤ 0.05; **: p ≤ 0.01; CV (%) expresses the coefficient of variation; Sign (±) indicates the mean standard deviation of four repeats; The same letter denotes inadequately different means in a column for each trait.

The effects of treatments on baby corn cob quality parameters (moisture, lipid, protein, phosphorus, and potassium) are presented in Table 4. According to the obtained results, it was determined that the BC2 treatment predominantly increased the cob lipid and potassium content of the baby corn plant, while the BC3 treatment was found to enhance the cob protein and phosphorus content of baby corn plant.

Table 4. Effects of treatments on cob quality parameters of baby corn plants

Treatments	Cob quality parameters of baby corn plant				
	Moisture, %	Lipid, %	Protein, %	Phosphorous, %	Potassium, %
BC0	81.9d±0.082	0.165d±0.004	2.00b±0.817	0.040d±0.008	0.237c±0.002
BC1	86.6b±0.163	0.175c±0.004	2.32ab±0.016	0.061b±0.008	0.241b±0.003
BC2	85.6c±0.245	0,.215b±0.004	2.62a±0.016	0.049c±0.008	0.274a±0.004
BC3	87.9a±0.082	0.125e±0.004	2.74a±0.033	0.212a±0.002	0.245b±0.002
BC4	77.3e±0.245	0.245a±0.004	2.37ab±0.016	0.047c±0.067	0.237c±0.015
Ftest	**	**	*	**	**
CV(%)	4.70	23.1	17.4	12.2	5.86

*: p ≤ 0.05; **: p ≤ 0.01; CV (%) expresses the coefficient of variation; Sign (±) indicates the mean standard deviation of four repeats; The same letter denotes inadequately different means in a column for each trait.

Discussion

Sustainable agricultural practices are imperative for ensuring food security and environmental protection (McLaughlin and Kinzelbach, 2015). Chemical fertilizers have been extensively employed to boost food production. Conversely, the use of microbial inoculants presents a strategy to enhance soil quality and plant nutrition (Pylak et al., 2019). Microorganisms possess the ability to fix nitrogen from the atmosphere (Kızılkaya, 2008) and produce organic acids, enzymes, and hormones, thereby regulating the soil environment (Bai et al., 2021), fostering the proliferation and activities of soil microorganisms (Guo et al., 2023). These microorganisms can establish a symbiotic relationship with plant root systems, augmenting the nutrient uptake capacity of crops (Mi et al., 2022). *Klebsiella quasipneumoniae* is a bacterium with the ability to fix atmospheric nitrogen (Haahtel and Kari, 1986; Pishchik et al., 1998; Liu et al., 2018). In this study, it was observed that the application of *Klebsiella quasipneumoniae* to soils, in conjunction with chemical nitrogen fertilizers at varying doses, increased both the total nitrogen content of the soil and the yield and yield components of baby corn (Table 1-4), similar to previous findings (Yan et al., 2021; Brooks et al., 2022). This is primarily due to the superior release of organic acids in the combination of chemical fertilizer and microorganism inoculation (Morales-Santos et al., 2023), leading to increased microbial activity and a greater number of microorganisms. Consequently, the fertilizer and water become more readily available for uptake and utilization (Yusefi-Tanha et al., 2023). The combined approach proves more effective in meeting the nutritional needs of baby corn plants consistently, facilitating increased yields, while the microorganisms aid in organic matter decomposition and nitrogen release, thereby enhancing soil fertility.

Recent studies underscore the significant impact of jointly applying chemical fertilizers and microbial inoculants (Bargaz et al., 2018). A study conducted by Ye et al. (2020) demonstrated that an inoculant containing Trichoderma species, when combined with a reduced rate of chemical fertilizer, increased tomato yield and improved soil microbial activity. Additionally, Assainar et al. (2018) found that a well-balanced combination of microbial inoculants with rock-based fertilizer enhanced grain yield in maize under

greenhouse conditions. However, limited research exists on the effects of the simultaneous application of chemical fertilizer and microbial inoculant on soil quality and plant nutrition. Ortega (2015) referred to this strategy as integrated nutrient management, encompassing organic matter application, adjusted chemical fertilization, and microbial inoculants.

Furthermore, in this study, it was identified that the most effective application for increasing the yield and yield components of baby corn involved reducing the nitrogen fertilizer by 50% after inoculation with *Klebsiella quasipneumoniae* (BC3). Similarly, Ren et al. (2021) demonstrated that a 50% organic and 50% inorganic nitrogen management strategy resulted in the most significant yield and efficiency increase, aligning with the outcomes of this experiment. Fertilization with microbial inoculations varied across trials due to differences in crop species, types of microorganisms inoculated, trial locations, and climates (Kızılkaya, 2009; Imran and Amanullah, 2023). Nevertheless, field experiments in this study revealed that chemical fertilizer combined with *Klebsiella quasipneumoniae* inoculation significantly boosted yields, primarily due to increased plant fresh weight (Table 3) and improved baby corn cob quality parameters such as lipids, proteins, phosphorus, and potassium (Table 4). Therefore, maintaining or increasing plant weight and cob quality parameters is crucial for enhancing baby corn yield and yield parameters.

Conclusion

In conclusion, this study elucidates the synergistic impact of *Klebsiella quasipneumoniae* inoculation and a strategic reduction in nitrogen fertilizer application, showcasing remarkable outcomes in soil fertility, baby corn yield, and cob quality. The findings underscore the nitrogen-fixing capabilities and soil nutrient enhancement potential of the *Klebsiella quasipneumoniae* genus. Notably, the optimal efficacy was achieved with a 50% reduction in nitrogen fertilizer, revealing a substantial impact on both productivity and qualitative attributes. The study's significant contributions lie in revealing the positive effects of *Klebsiella quasipneumoniae* inoculation on productivity and qualitative attributes, including moisture content, lipid levels, raw protein content, as well as phosphorus (P) and potassium (K) concentrations in the edible cob. Moreover, the identification of the optimal nitrogen rate at 150 kg N per hectare, combined with *Klebsiella quasipneumoniae* inoculation, stands out for its ability to amplify edible cob weight. This signifies substantial potential for enhancing both the yield and nutritional content of baby corn cobs.

The pivotal role of an appropriate nitrogen fertilizer rate, when coupled with *Klebsiella quasipneumoniae* inoculation, is highlighted in elevating all nutritional traits and output parameters of baby corn. This combination emerges as a crucial component in sustainable agricultural practices, providing a pathway for enhanced food security and environmental protection. As a result, the study positions the integration of *Klebsiella quasipneumoniae* inoculation with nitrogen fertilizer reduction as a valuable strategy in modern agricultural landscapes, promising increased yields and improved nutritional quality for baby corn production.

References

Assainar, S.K., Abbott, L.K., Mickan, B.S., Whiteley, A.S., Siddique, K.H.M., Solaiman, Z.M., 2018. Response of wheat to a multiple species microbial inoculant compared to fertilizer application. *Frontiers in Plant Science* 9: 1601.

Bai, Y., Feng, P., Chen, W., Xu, S., Liang, J., Jia, J., 2021. Effect of three microbial fertilizer carriers on water ınfiltration and evaporation, microbial community and alfalfa growth in saline-alkaline soil. *Communications in Soil Science and Plant Analysis* 52(20): 2462–2470.

Bargaz, A., Lyamlouli, K., Chtouki, M., Zeroual, Y., Dhiba, D., 2018. Soil microbial resources for improving fertilizers efficiency in an integrated plant nutrient management system. *Frontiers in Microbiology* 9: 1606.

Bever, J.D., Broadhurst, L.M., Thrall, P.H., 2013. Microbial phylotype composition and diversity predicts plant productivity and plant–soil feedbacks. *Ecology Letters* 16(2): 167–174.

Blackmer, A.M., Pottker, D., Cerrato, M.E., Webb, J., 1989. Correlations between soil nitrate concentrations in late spring and corn yields in Iowa. *Journal of Production Agriculture* 2(2): 103-109.

Brooks, K., Mourtzinis, S., Conley, S.P., Reiter, M.S., Gaska, J., Holshouser, D.L., Irby, T., Kleinjan, J., Knott, C., Lee, C., Lindsey, L., Naeve, S., Ross, J.,Singh, M.P., Vann, R., Matcham, E., 2022. Soybean yield response to sulfur and nitrogen additions across diverse U.S. environments. *Agronomy Journal* 115(1): 370–383.

Bundy, L.G., Andraski, T.W., Ruark, M.D., Peterson, A.E., 2011. Long-term continuous corn and nitrogen fertilizer effects on productivity and soil properties. *Agronomy Journal* 103(5): 1346-1351.

Carter, M.R., Gregorich, E.G., 2007. Soil sampling and methods of analysis. Second Edition, CRC Press. 1264p.

Chuong, N.V., 2023. Response of peanut quality and yield to chicken manure combined with Rhizobium inoculation in sandy soil. *Communications in Science and Technology* 8(1): 31–37.

Gondaliya, B.R., Desai, K.D., Ahlawat, T.R., Mangroliya, R.M., Mandaliya, J.V., 2022. Effect of chemicals on growth and yield of baby corn (*Zea mays* L.). *The Pharma Innovation Journal* 11(9): 2761-2764.

Guo, K., Yang, J., Yu, N., Luo, L., Wang, E., 2023. Biological nitrogen fixation in cereal crops: Progress, strategies, and perspectives. *Plant Communications* 4: 100499.

Haahtel, K., Kari, K., 1986. The role of root-associated Klebsiella pneumoniae in the nitrogen nutrition of Poapratensis and Triticum aestivum as estimated by the method of ^{15}N isotope dilution. *Plant and Soil* 90(1-3): 245-254.

Imran, Amanullah, 2023. Soybean quality and profitability improved with peach (*Prunus persica* L;) remnants, phosphorus, and beneficial microbes. *Journal of Plant Nutrition* 46(3): 370–385.

Jones, J.B., 2001. Laboratory guide for conducting soil tests and plant analyses. CRC Press, New York, USA. 363p.

Kızılkaya, R., 2008. Yield response and nitrogen concentrations of spring wheat (*Triticum aestivum*) inoculated with *Azotobacter chroococcum* strains. *Ecological Engineering* 33(2): 150-156.

Kızılkaya, R., 2009. Nitrogen fixation capacity of Azotobacter spp. strains isolated from soils in different ecosystems and relationship between them and the microbiological properties of soils. *Journal of Environmental Biology* 30: 73-82.

Korenblum, E., Dong, Y., Szymanski, J., Panda, S., Jozwiak, A., Massalha, H., Meir, S., Rogachev, I., Aharoni, A., 2020. Rhizosphere microbiome mediates systemic root metabolite exudation by root-to-root signaling. *PNAS* 117(7): 3874–3883.

Kumar, A., Maurya, B.R., Raghuwanshi, R. 2014. Isolation and characterization of PGPR and their effect on growth, yield and nutrient content in wheat (Triticum aestivum L.). *Biocatalysis and Agricultural Biotechnology* 3(4): 121–128.

Lazcano, C., Boyd, E., Holme,s G., Hewavitharana, S., Pasulka, A., Ivors, K., 2021. The rhizosphere microbiome plays a role in the resistance to soil-borne pathogens and nutrient uptake of strawberry cultivars under field conditions. *Scientific Report* 11: 3188.

Liu, D., Chen, L., Zhu, X., Wang, Y., Xuan, Y., Liu, X., Chen, L., Duan, Y., 2018. Klebsiella pneumoniae SnebYK mediates resistance against Heterodera glycines and promotes soybean growth. *Frontiers in Microbiology* 9: 1134.

Liu, J., Cui, X., Liu, Z., Guo, Z., Yu, Z., Yao, Q., Siu, Y., Jin, J., Liu, X., Wang, G., 2019. The diversity and geographic distribution of cultivable bacillus-like bacteria across black soils of Northeast China. *Frontier Microbiology* 10: 1424.

McCullough, D.E., Mihajlovic. M., Aguilera, A., Tollenaar, M., Giradin, P., 1994. Influence of N supply on development and dry matter accumulation of an old and new maize hybrid. *Canadian Journal of Plant Science* 74(3): 471-477.

McLaughlin, D.; Kinzelbach, W. 2015. Food security and sustainable resource management. *Water Resourse Research* 51(7): 4966-4985.

Mendes, R., Garbeva, P., Raaijmakers, J.M., 2013. The rhizosphere microbiome: significance of plant beneficial, plant pathogenic, and human pathogenic microorganisms. *FEMS Microbiology Reviews* 37(5): 634–663.

Mi, S., Zhang, X., Wang, Y., Ma, Y., Sang, Y., Wang, X., 2022. Effect of different fertilizers on the physicochemical properties, chemical element and volatile composition of cucumbers. *Food Chemistry* 367: 130667.

Morales-Santos, A., García-Vila, M., Nolz, R., 2023. Assessment of the impact of irrigation management on soybean yield and water productivity in a subhumid environment. *Agricultural Water Management 284*: 108356.

Ortega, R., 2015. Integrated nutrient management in conventional intensive horticulture production systems. *Acta Horticulturae* 1076: 159-164.

Pishchik, V.N., Chernyaeva, I.I., Kozhemaykov, A.P., Vorobyov, N.I., Lazarev, A.M., Kozlov, L.P., 1998. Effect of inoculation with nitrogen-fixing *Klebsiella* on potato yield. In: Nitrogen Fixation with Non-Legumes. Malik, K.A., Mirza, M.S., Ladha, J.K. (Eds.). Developments in Plant and Soil Sciences, vol 79. Springer, Dordrecht. pp. 223–235.

Pylak, M.; Oszust, K.; Frac, M. 2019. Review report on the role of bioproducts, biopreparations, biostimulants and microbial inoculants in organic production of fruit. *Reviews in Environmental Science and Bio/Technology* 18(3): 597-616.

Qureshi, M.A., Iqbal, M.Z., Rahman, S., Anwar, J., Tanveer, M.H., Shehzad, A., Ali, M.A., Aftab, M., Saleem, U., Ehsan, S., 2022. Relative potential of Rhizobium sp for improving the rice-wheat crop in the semi-arid regions. *Eurasian Journal of Soil Science* 11(3): 216-224.

Rani, P.L, Sreenivas, G., Katti, G.S., 2015. Baby corn based inter cropping system as an alternative pathway for sustainable agriculture. *International Journal of Current Microbiology and Applied Sciences* 4(8):869-873.

Ren, T., Li, Z., Du, B., Zhang, X., Xu, Z., Gao, D., Zheng, B., Zhao, W., Li, G., Ning, T., 2021. Improvement of photosystem performance and seed yield of summer soybean in Huanghuaihai region by organic fertilizer application and rational planting. *Journal of Plant Nutrition and Fertilizers* 27: 1361–1375.

Riaz, A., Rafique, M., Aftab, M., Qureshi, M.A., Javed, H., Mujeeb, F., Akhtar, S., 2019. Mitigation of salinity in chickpea by Plant Growth Promoting Rhizobacteria and salicylic acid. *Eurasian Journal of Soil Science* 8(3): 221-228.

Torbert, H.A., Potter, K.N., Morrison, J.E., 2001. Tillage system, fertilizer nitrogen rate and timing effect on corn yield in the taxes black land prairie. *Agronomy Journal* 93(5): 1119-1124.

Yan, Z., Chunqiao, X., Sheng, Y., Yin, H., Yang, Z., Chi, R., 2021. Life cycle assessment and life cycle cost analysis of compound microbial fertilizer production in China. *Sustainable Production and Consumption* 28: 1622–1634.

Ye, L., Zhao, X., Bao, E., Li, J., Zou, Z., Cao, K., 2020. Bio-organic fertilizer with reduced rates of chemical fertilization improves soil fertility and enhances tomato yield and quality. *Scientific Reports* 10: 177.

Yusefi-Tanha, E., Fallah, S., Pokhrel, L.R., Rostamnejadi, A., 2023. Addressing global food insecurity: Soil-applied zinc oxide nanoparticles promote yield attributes and seed nutrient quality in Glycine max L. *Science of The Total Environment* 876: 162762.

Eurasian Journal of Soil Science

Journal homepage : http://ejss.fesss.org
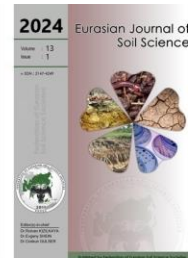
Alternate wetting and drying decreases arsenic content and increases yield of rice grown in organic matter amended soil

Khan Md Abrarur Rahman, Mohammad Golam Kibria, Md Hosenuzzaman, Mahmud Hossain, Md Anwarul Abedin *

Department of Soil Science, Bangladesh Agricultural University, Mymensingh 2202, Bangladesh

Abstract

Author(s)

K.M.A.Rahman
M.G.Kibria
M.Hosenuzzaman
M.Hossain
M.A.Abedin*

* Corresponding author

Organic matter (OM) shows a critical role in mobilization and uptake of arsenic (As) by rice, and water management practice can mitigate this problem. However, very few research highlighted the impact of management of water on rice as influenced by OM amendment. Therefore, this study has evaluated the changes in As mobilization in paddy soil under different OM amendment and water management practices. Here, rice was grown to maturity in a two-factorial pot experiment comprising two different water management practices [continuous flooding (CF) and alternate wetting drying (AWD)] and eight combinations of As and OM amendment [comprising two As treatments (0 and 20 ppm) and four OM amendments (0, 0.25%, 0.5% and 5.0% w/w)]. Application of OM in As contaminated soil caused a significant increase in As accumulation in rice, and exhibited decreased growth and yield of rice. However, the results showed that rice growth and yield was significantly higher under AWD practice compared to CF. Arsenic concentration in rice was the lowest in As and OM control pots (44.67 µg/kg in AWD and 62.13 µg/kg in CF), and higher in As treated pots. Moreover, As concentration in rice grain increased with increasing levels of OM amendment. The As concentration in rice grain (168.44 µg/kg in AWD and 183.85 µg/kg in CF) was significantly higher in As treated pots with 0.5% OM amendment compared to other treatment combinations. Application of 5% OM in As contaminated soil did not produce any grains due to extreme toxicity. Thus, As accumulation in rice can be decreased by AWD water management technique without compromising yield. The findings suggest that applying OM in paddy soils with high soil As content should be done with caution.

Keywords: Arsenic mobilization, water management, organic matter amendment, rice.

Introduction

Abiotic stresses such as extreme of salt, water logging and scarcity, and heavy metals (HM) are serious environmental treat to agriculture (Rhaman et al., 2022). Groundwater and sediment contamination by arsenic (As) is regarded as a significant environmental problem worldwide. In Bangladesh, however as in other parts of the Asian subcontinent soil As contamination is one of the most important problems (Mondal et al., 2020). Arsenic is particularly hazardous to most plant species at greater concentrations due to its interference with plant physiological processes, suppression of seedling growth, decrease in root development, and As induced phytotoxicity (Abbas et al., 2018; Zhang et al., 2021; Sharma et al., 2021). As a consequence, it is critical to examine the detrimental influence of As on plant growth, particularly in paddy soil, because it is a major issue in rice production using conventional water management approaches.

Rice is one of the dominant as well as staple food in many Asian countries, including Bangladesh (Rhaman et al., 2016; Mondal et al., 2020). However, rice production is severely affected by different environmental constrains. Especially, rice in particular is problem because rice is generally grown in submerged soil, and it causes a significant increase in As accumulation in rice grains due to the increasing bioavailability and mobility

of As in wetland soils (Upadhyay et al., 2019). Although the rice production under continuous flooded condition is productive, it is also associated with high water consumption, methane emission and As accumulation in rice (Zhao et al., 2010). Thus, development of sustainable agronomic practice to decrease the As accumulation in rice is crucial.

Arsenic accumulation in rice can be decreased by adopting efficient water management approaches, which can contribute to decrease the As mobility in soils (Harine et al., 2021). It has been reported that mobilization and bioavailability of As was increased by continuous flooding in the rice field and further enhances the accumulation of As in grain and straw. On the contrary, As accumulation was decreased by alternate wetting and drying (AWD) in rice field (Murugaiyan et al., 2021). The IRRI experts have promoted the idea of the AWD approach for water management to decrease water requirement for rice growing with some yield benefits as well (Mubeen et al., 2022). This technique keeps the soils oxygenated for a while and thus reduce the formation of greenhouse gases. Some reports have shown the potentials of water saving rice cultures like aerobic rice culture (Harine et al., 2021; Mubeen et al., 2022), and intermittent irrigation (Roberts et al., 2011) in reducing As mobilization in pore water and finally reduced As uptake by rice. However, anaerobic condition in paddy soil leads to As mobilization and, therefore, As uptake by rice could increase.

Applying organic matter (OM) to soil is considered as a beneficial practice, because it serves as a source of nitrogen, phosphorus, and other nutrients (Abbas et al., 2020). However, OM is important for the mobilization of soil As in paddy field and addition of OM in soil may increase the amount of As released into the paddy pore fluids and the amount of As assimilated by rice plants (Hossain et al., 2021). Furthermore, decreased water management techniques has been introduced in Bangladesh, such as Alternate Wetting and Drying (AWD), which may also alters As mobilization in paddy soil. Hence, it is important to test the mobilization of As under AWD system with OM amendment in paddy soil. Arsenic contamination of groundwater is a big issue everywhere, but direct interactions of As and OM under different water management practices requires further investigation. Therefore, this research was undertaken to assess the effectiveness of water management to alter As mobilization in paddy soil and increase yield of rice under OM amendment.

Material and Methods

Soil samples were collected from the Soil Science field laboratory of Bangladesh Agricultural University using an auger at 0–15 cm depth of soil. The unwanted materials such as plant debris were removed from the collected soil samples. Soils were air-dried, sieved (≤2 mm), and thoroughly blended with hand. The characteristics of the collected soil samples are presented in Table 1. The non-draining pots (405 mm in diameter and 385 mm in height) were filled with 10kg of soil. The most popular rice (*Oryza sativa*) variety of Bangladesh (BRRI dhan28) was grown to maturity in the plant growth facility of the department.

Table 1. Morphological, physical and chemical properties of the initial soil samples

Morphological characteristics			
AEZ (Agroecological zone)	Old Brahmaputra Floodplain (AEZ 9)		
General Soil Type	Non calcareous dark grey floodplain soil		
Parent Material	Old Brahmaputra river borne deposits		
Physical characteristics			
Textural class	Silty loam [sand (13.3 %), silt (64.7 %) and clay (22 %)]		
Chemical characteristics			
Organic Matter (%)	2.03	Available P (ppm)	11.58
pH	6.50	Available K (meq/100g soil)	0.10
EC (µS/cm)	51.50	Available S (ppm)	9.00
Available N (%)	0.13	Total As (ppm)	3.74

Mechanical analysis of soil was done by hydrometer method (Bouyoucos, 1926). Soil pH was measured with the help of a glass electrode pH meter, the soil-water ratio being maintained at 1: 2.5 (Jackson, 1962). Electrical conductivity of the soil was measured by the EC meter (soil: water= 1:5). Organic carbon in soil was determined volumetrically by wet oxidation method (Walkley and Black, 1934). Total N content of soil was estimated following the micro-Kjeldahl method (Bremner and Mulvaney, 1982). Available P was extracted from the soil with 0.5 M NaHCO$_3$ solutions (Olsen, 1954). Exchangeable potassium was determined on 1N NH$_4$OAc (pH 7.0) extract of the soil by using flame photometer (Najafi-Ghiri et al., 2021). Available S content of soil was determined by extracting the soil with CaCl$_2$ (0.15%) solution as described by Sarap et al. (2020).

Experimental design and approach

The two-factorial experiment consisted of two water managements (continuous flooding and AWD) and eight treatment combinations of As and OM amendments (As$_0$ OM$_0$, As$_0$ OM$_{0.25 \%}$, As$_0$ OM$_{0.5 \%}$, As$_0$ OM$_{5 \%}$, As$_{20 \text{ ppm}}$ OM$_0$, As$_{20 \text{ ppm}}$ OM$_{0.25 \%}$, As$_{20 \text{ ppm}}$ OM$_{0.5 \%}$ and As$_{20 \text{ ppm}}$ OM$_{5 \%}$) and was replicated three times using completely randomised design (CRD). Arsenic was added from analytical grade sodium arsenate @ 0 and 20 mg As/kg soil, while the OM (N: 1.07%, P: 0.57%, K:0.54%, S:0.32%) was added @ 0, 0.25, 0.5 and 5.0 % (w/w) during pot preparation. Each pot received 0.65 g N from urea, 0.375 g P from TSP, 0.24 g K from MoP and 0.42 g S

from gypsum, based on the fertilizer recommendation guide 2018. Except for N, all fertilizers were applied during final pot preparation. Urea was applied in three equal splits i.e., during pot preparation, 36 and 51 days after transplanting. Seventeen days healthy seedlings were transplanted in the pots. Three hills, each made up of two seedlings, were planted in each pot at an equal distance apart. All the pots were continuously submerged in water (4–6 cm) for 12 days following transplanting. Then, new water management techniques were introduced. In case of water management, 4–6 cm continuous standing water height was maintained in continuous flooding condition (CF). Under AWD condition, six cm water was added, and soil water was monitored using AWD pipes. Further irrigation was done when water level went 15 cm below the soil surface; this process was continued up to grain filling stage. Weeding and loosening of soils around the rice hills were done as and when necessary. The harvesting was conducted at maximum maturity stage on same day and time.

Data recorded

The data were collected from all the plants grown in each pot for all the yield contributing characteristic such as plant height, panicle length, number of filled and unfilled grains, number of effective and ineffective tillers pot[-1] and 100-grains weight. Following harvesting, both grain and straw yield of rice were recorded and stored for chemical analysis. The samples were dried at 60 °C in an oven for 48 hours, and then grinded homogenously for determining the As concentration in by rice grain and straw samples. About 0.5 g of sub sample was transferred in the digestion tube with 5 mL HNO3 and 2.5 mL H2O2, and allowed to stand overnight (Jahan et al., 2021). Then, the tubes containing the samples were subjected to digestion and heated slowly up to159°C for two hours, and allowed to cool. Again, the digestion tubes was heated up to 162°C, and continued until it looks colorless. The plant digest was run through the Atomic Absorption Spectrophotometer (AAS) using the graphite furnace atomizer (Model: Shimadzu AA-7000) to determine the As concentration in rice.

Statistical analysis

The data were analyzed statistically using two-way analysis of variance (ANOVA) and the significant ($p \leq 0.05$) difference among the treatments were determined by Tukey's test in Minitab17 statistical software.

Results

Effect of OM and As treatment on growth of rice under AWD and CF condition

Plant height, panicle length and number of filled grains per panicle varied significantly depending on water management practices and treatment combinations of As and OM amendment, with the interaction being non-significant (Table 2). The results exhibited that AWD practice was associated with at least 1.1-fold increase in the yield contributing characters in comparison to CF. Nevertheless, these parameters varied insignificantly with the addition of OM in soil in absence of As. When the plants were exposed to 20 ppm As, the above mentioned yield contributing parameters decreased significantly with the increasing OM content (Table 2).

Table 2. Effect of organic matter (OM) amendment and arsenic (As) treatment combinations on growth parameters of Boro rice (cv. BRRI dhan28) under continuous flooding (CF) and alternate wetting and drying (AWD) conditions.

Treatments		Plant height (cm)	Panicle Length (cm)	Effective Tiller/Hill	Ineffective Tiller/Hill	No. of filled grains/panicle	No. of unfilled grains/panicle	100 grain weight (g)
Water (W)	CF	56.59 b	18.49 b	16	1.54	42.20 b	29.84	1.43
	AWD	60.85 a	19.73 a	17	1.83	56.00 a	31.80	1.54
	P value	*0.002*	*0.02*	*0.17 (ns)*	*0.41 (ns)*	*0.000*	*0.42 (ns)*	*0.33 (ns)*
Treatment (T)	T1: As0 OM0	67.09 a	21.60 a	24 a	1.00 b	62.00 ab	39.00 a	2.00 a
	T2: As0 OM0.25	68.43 a	21.86 a	21 ab	0.33 b	63.00 a	38.00 ab	2.00 a
	T3: As0 OM0.5	68.60 a	21.71 a	20 bc	0.50 b	74.00 a	29.00 ab	2.00 a
	T4: As0 OM5.0	68.56 a	21.21 ab	21 ab	0.17 b	73.00 a	26.00 ab	2.00 a
	T5: As20 OM0	58.60 b	19.48 ab	17 cd	0.50 b	46.00 bc	35.00 ab	2.00 a
	T6: As20 OM0.25	54.70 b	18.27 b	14 d	1.00 b	36.00 c	33.00 ab	1.44 a
	T7: As20 OM0.5	54.98 b	18.03 b	14 d	0.00 b	39.00 c	25.00 ab	2.00 a
	T8: As20 OM5.0	28.78 c	10.74 c	1 e	10.00 a	0.00 d	21.00 b	0.33 b
	P value	*0.000*	*0.000*	*0.000*	*0.000*	*0.000*	*0.010*	*0.000*
W×T	*P* value	*0.21 (ns)*	*0.69 (ns)*	*0.22 (ns)*	*0.32 (ns)*	*0.15 (ns)*	*0.09 (ns)*	*0.30 (ns)*

Here, arsenic as As@ 0 and 20 mg/kg soil while organic matter as OM@ 0, 0.25, 0.5 and 5.0 % (w/w). Water management alternate wetting and drying as AWD and continuous flooding as CF.

Number of effective and ineffective tillers per hill, number of filled grains per panicle and 100-grain weight were significantly influenced by the treatment combinations of As and OM amendment only, with the water management practices and interactions being non-significant (Table 2). When the plants were exposed to 20 ppm As, these parameters decreased significantly with the increasing OM content. Whereas, the number of ineffective tillers per hill was the lowest when the plants were exposed to T8 treatment (As20 ppm OM5 %).

Effect of OM and As treatment on grain and straw yield of rice under AWD and CF condition

Grain yield varied significantly by water management practices, treatments, and their interactions (Table 3). The grain yield of rice exhibited significant increase under AWD condition compared to the CF condition. The results showed that grain yield varied insignificantly when the plants are exposed to different levels of OM in absence of As. When the plants were exposed to 20 ppm As, the grain yield decreased with the increasing soil OM amendment, and no grain yield was obtained when the soil was amended with 5 % OM. The highest grain yield was obtained in T_4 (As_0 $OM_{5\%}$) treatment under AWD condition and the lowest grain yield was obtained in T_6 ($As_{20\ ppm}$ $OM_{0.25\%}$) treatment under CF condition and no grain yield was obtained in T_8 ($As_{20\ ppm}$ $OM_{5\%}$) treatment in interaction with both CF and AWD condition (Table 3).

Table 3. Effect of organic matter (OM) amendment and arsenic (As) treatment combinations on growth parameters of Boro rice (cv. BRRI dhan28) under continuous flooding (CF) and alternate wetting and drying (AWD) conditions.

Treatments		Grain yield (g/pot)		Straw yield (g/pot)	
Water (W)	W_1: CF	13.48	b	12.23	a
	W_2:AWD	17.12	a	13.25	a
	P value	*0.006*		*0.147*	
Treatment (T)	T_1: As_0 OM_0	20.82	a	19.90	a
	T_2: As_0 $OM_{0.25}$	21.76	a	17.35	a
	T_3: As_0 $OM_{0.5}$	24.65	a	17.44	a
	T_4: As_0 $OM_{5.0}$	25.85	a	17.23	a
	T_5: As_{20} OM_0	12.15	b	11.85	b
	T_6: As_{20} $OM_{0.25}$	9.11	b	8.74	b
	T_7: As_{20} $OM_{0.5}$	8.10	b	7.92	b
	T_8: As_{20} $OM_{5.0}$	0.00	c	1.50	c
	P value	*0.000*		*0.000*	
Water (W)× Treatment (T)	$W_1 \times T_1$(CF×As0 OM0)	24.55	ab	21.24	a
	$W_1 \times T_2$(CF×As0 OM0.25)	20.95	abcd	16.93	abc
	$W_1 \times T_3$(CF×As0 OM0.5)	19.60	abcd	15.51	abcd
	$W_1 \times T_4$(CF×As0 OM5.0)	23.25	ab	18.56	ab
	$W_1 \times T_5$(CF×As20 OM0)	9.50	defg	10.70	cde
	$W_1 \times T_6$(CF×As20 OM0.25)	4.05	fg	6.41	efg
	$W_1 \times T_7$(CF×As20 OM0.5)	5.95	efg	7.13	efg
	$W_1 \times T_8$(CF×As20 OM5.0)	0.00	g	1.36	g
	$W_2 \times T_1$(AWD×As0 OM0)	17.10	abcde	18.56	ab
	$W_2 \times T_2$(AWD×As0 OM0.25)	22.57	abc	17.76	abc
	$W_2 \times T_3$(AWD×As0 OM0.5)	29.72	a	19.38	ab
	$W_2 \times T_4$(AWD×As0 OM5.0)	28.44	a	15.89	abcd
	$W_2 \times T_5$(AWD×As20 OM0)	14.80	bcdef	13.01	bcde
	$W_2 \times T_6$(AWD×As20 OM0.25)	14.16	bcdef	11.10	cde
	$W_2 \times T_7$(AWD×As20 OM0.5)	10.20	cdefg	8.71	def
	$W_2 \times T_8$(AWD×As20 OM5.0)	0.00	g	1.64	fg
	P value (Water × Treatment)	*0.025*		*0.048*	

Here, arsenic as As@ 0 and 20 mg/kg soil while organic matter as OM@ 0, 0.25, 0.5 and 5.0 % (w/w). Water management alternate wetting and drying as AWD and continuous flooding as CF.

Straw yield varied significantly by the treatments and the interaction of water management and treatments, with the water management practices being non-significant (Table 3). There was no significant difference in straw yield when the plants are exposed to different levels of OM in absence of As. On the other hand, the straw yield decreased at 20 ppm As concentration due to the addition of OM. The highest straw yield was obtained when both OM and As were absent and the lowest straw yield was obtained when the plants were exposed to 20ppm As concentration with 5 % OM amendment. The highest straw yield was obtained in T_1 (As_0 OM_0) treatment, and the lowest straw yield was obtained in T_8 ($As_{20\ ppm}$ $OM_{5\%}$) treatment both under AWD and CF condition (Table 3).

Effect of OM and As treatment on As concentration in grains under AWD and CF condition

Arsenic concentration in rice grains varied significantly depending on water management practices and treatment combinations of As and OM amendment (Figure 1). Arsenic concentration was 8.3% higher in CF condition than AWD condition even at the lowest level of OM amendment. Arsenic concentration in rice grains was the lowest in absence As and OM amendment both under AWD and CF conditions. The As concentration in rice grains increased with the increasing OM amendment, even in absence of As under AWD and CF conditions. The highest amount (168.44 µg/kg) of As was absorbed when the soil was amended with 0.5 % OM and the application rate of As in soil was 20 ppm under CF condition (Figure 1).
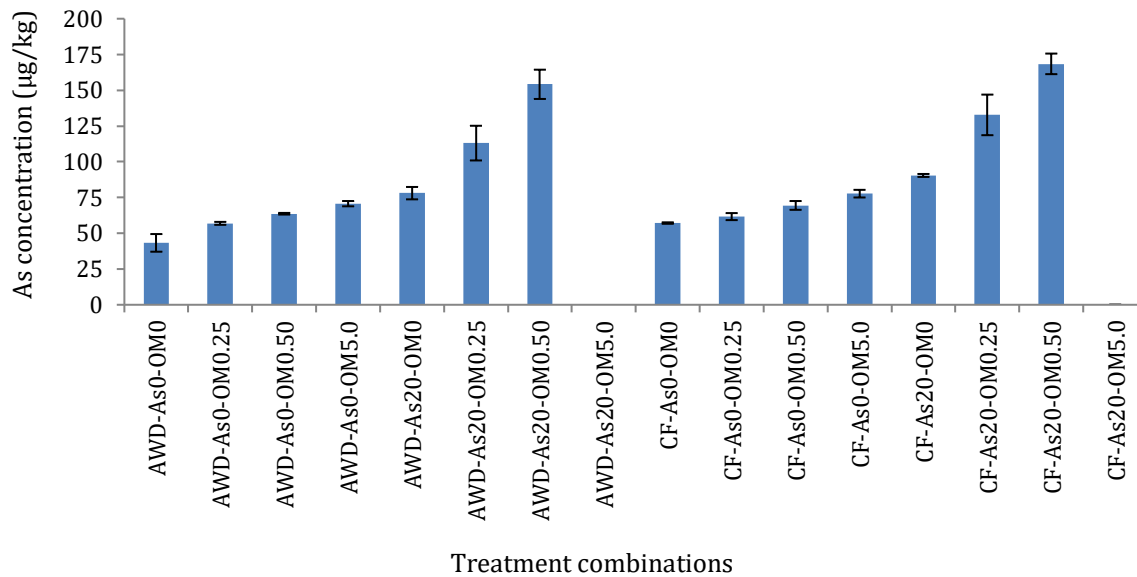
Figure 1. Effect of organic matter (OM) amendment and arsenic (As) treatment combinations on arsenic concentration in grains of Boro rice (cv. BRRI dhan28) under continuous flooding (CF) and alternate wetting and drying (AWD) conditions (p <.005). Arsenic as As@ 0 and 20 mg/kg soil while organic matter as OM@ 0, 0.25, 0.5 and 5.0 % (w/w). Water management alternate wetting and drying as AWD and continuous flooding as CF.

Discussion

It is evident that changes in As biogeochemistry in soil is dependent on the OM status of soil (Xiao et al., 2021). Here, we evaluated the changes in As mobilization in paddy soil under different OM and water management techniques. Based on the present study, As mobility in soil is likely to be increased by applying OM to soil. For examples, applying 5 % (w/w) OM to soil significantly increased As concentration in rice grains both under AWD and CF conditions. The result is also in covenant with Kumarathilaka et al. 2018, who also described that oxidation and reduction of As varies with the added dissolved organic matter (DOM) in soil because of it's potential to mobilize As in soil. Thus, it is evident that OM contributes to enhance As release in soils by accelerating the dissolution of Fe (III) minerals and enhances As concentrations in paddy soils under irrigated condition. Alternate wetting and drying practice contributes to enhanced rice growth and yield compared to CF condition in As contaminated soils. The results from previous research has also highlighted that bioavailability As in soil depends on the soil moisture and irrigation intervals (Harine et al., 2021). Anaerobic conditions promote As mobilization in soil, As severely reduced rice growth and yield under CF conditions (Honma et al., 2016). On the other hand, the soil is getting wet and dry sporadically, and the paddy soil is getting prolonged aerobic period being re-irrigated under AWD condition. This might decreased the mobilization of As in paddy soil, which ultimately lead to minimum accumulation of As in rice grain and straw samples due to the extended drying period in AWD systems (Harine et al., 2021).

We observed that the application of As to soil decreased rice growth, and the water management practice was likely to change the As concentration in rice grain. Arsenic content is more spontaneous in grain sample under CF condition than AWD condition. For example, As concentration was 1.1-fold higher under CF condition compared to AWD condition, when the soil was amended with 0.5 % OM and the application rate of As in soil was 20 ppm (Figure 1). The findings are similar with the results of Wang et al. (2019) and Li et al. (2019), who found that As uptake is much greater in CF compared to AWD condition. The accumulation of As in rice grains increases under anaerobic conditions because of the increase in As mobilization through reductive dissolution of iron oxyhydroxides and reduction of arsenate to arsenite (Jahan et al., 2021). On the other hand, As accumulation in rice grains was significantly lower under AWD water management practice compared to CF condition, which might occur due to maintaining intermittent wetting and drying condition in paddy field.

In conclusion, application of OM in soil contributed to increase As mobilization and decreased rice growth and yield. Water management practices including AWD condition and OM amendment increase the concentration of As in rice grain. However, it is necessary to validate the present findings under field condition.

References

Abbas, F., Hammad, H.M., Ishaq, W., Farooque, A.A., Bakhat, H.F., Zia, Z., Fahad, S., Farhad, W., Cerdà, A., 2020. A review of soil carbon dynamics resulting from agricultural practices. *Journal of Environmental Management* 268: 110319.

Abbas, G., Murtaza, B., Bibi, I., Shahid, M., Niazi, N.K., Khan, M.I., Amjad, M., Hussain, M., Natasha, 2018. Arsenic uptake, toxicity, detoxification, and speciation in plants: physiological, biochemical, and molecular aspects. *International Journal of Environmental Research and Public Health* 15(1): 59.

Bouyoucos, G.J., 1926. Estimation of the colloidal material in soils. *Science* 64(1658): 362.

Bremner, J.M., Mulvaney, C.S., 1982. Nitrogen-Total. In: Methods of soil analysis. Part 2. Chemical and microbiological properties, Page, A.L., Miller, R.H., Keeney, D.R., (Eds.). American Society of Agronomy, Soil Science Society of America, Madison, Wisconsin, USA. pp. 595-624.

Harine, I.J., Islam, M.R., Hossain, M., Afroz, H., Jahan, R., Siddique, A.B., Uddin, S., Hossain, M.A., Alamri, S., Siddiqui, M.H., Henry, R.J., 2021. Arsenic accumulation in rice grain as influenced by water management: Human health risk assessment. *Agronomy* 11(9):1741.

Honma, T., Ohba, H., Kaneko-Kadokura, A., Makino, T., Nakamura, K., Katou, H., 2016. Optimal soil Eh, pH, and water management for simultaneously minimizing arsenic and cadmium concentrations in rice grains. *Environmental Science & Technology* 50(8): 4178-4185.

Hossain, M., Mestrot, A., Norton, G.J., Deacon, C., Islam, M.R., Meharg, A.A., 2021. Arsenic dynamics in paddy soil under traditional manuring practices in Bangladesh. *Environmental Pollution* 268: 115821.

Jackson, M.L., 1962. Soil Chemical Analysis. Prentice Hall, Inc. Englewood Chiffs, New York, USA. 498p.

Jahan, I., Abedin, M.A., Islam, M.R., Hossain, M., Hoque, T.S., Quadir, Q.F., Hossain, M.I., Gaber, A., Althobaiti, Y.S., Rahman, M.M., 2021. Translocation of soil arsenic towards accumulation in rice: magnitude of water management to minimize health risk. *Water* 13(20): 2816.

Kumarathilaka, P., Seneweera, S., Meharg, A., Bundschuh, J., 2018. Arsenic speciation dynamics in paddy rice soil-water environment: sources, physico-chemical, and biological factors-a review. *Water Research* 140: 403-414.

Li, C., Carrijo, D.R., Nakayama, Y., Linquist, B.A., Green, P.G., Parikh, S.J., 2019. Impact of alternate wetting and drying irrigation on arsenic uptake and speciation in flooded rice systems. *Agriculture, Ecosystems & Environment* 272: 188-198.

Mondal, S., Dutta, P., Bandopadhyay, P., Maji, S., 2020. Arsenic contamination in major food crops: issues and mitigation in Indian subcontinent perspective. In: Agronomic Crops: Stress Responses and Tolerance. Hasanuzzaman, M. (Ed). Agronomic Crops. Springer, Singapore. pp.209-234.

Mubeen, K., Sarwar, N., Shehzad, M., Ghaffar, A., Aziz, M., 2022. Irrigation Management in Rice. In: Modern Techniques of Rice Crop Production. Sarwar, N., Atik-ur-Rehman, Ahmad, S., Hasanuzzaman, M., (Eds.). Springer Naure Singapore. pp. 105-114.

Murugaiyan, V., Zeibig, F., Anumalla, M., Siddiq, S.A., Frei, M., Murugaiyan, J., Ali, J., 2021. Arsenic stress responses and accumulation in rice. In: Rice Improvement: Physiological, Molecular Breeding and Genetic Perspectives. Jauhar, A., Wani, Shabir Hussain, W.S., (Eds.). Springer, Cham. pp. 281-313.

Najafi-Ghiri, M., Boostani, H.R., Hardie, A.G., 2023. Release of potassium from some heated calcareous soils to different solutions. *Archives of Agronomy and Soil Science* 69(1): 90-103.

Olsen, S.R., 1954. Estimation of available phosphorus in soils by extraction with sodium bicarbonate, Circular No. 939. US Department of Agriculture, Washington, D.C. USA. 19p.

Rhaman, M.S., Kibria, M.G., Hoque, A., 2022. Climate change and ıts adverse ımpacts on plant growth in South Asia: Current status and upcoming challenges. *Phyton* 91(4): 695-711.

Rhaman, M.S., Kibria, M.G., Hossain, M., Hoque, M.A., 2016. Effects of organic manure and bio-slurries with chemical fertilizers on growth and yield of rice (cv. BRRI dhan28). *International Journal of Experimental Agriculture* 6(3): 36-42.

Roberts, L.C., Hug, S.J., Voegelin, A., Dittmar, J., Kretzschmar, R., Wehrli, B., Saha, G.C., Badruzzaman, A.B.M., Ali, M.A., 2011. Arsenic dynamics in porewater of an intermittently irrigated paddy field in Bangladesh. *Environmental Science & Technology* 45(3): 971-976.

Sarap, P.A., Hadole, S.S., Lakhe, S.R., Dhule, D.T., Parmar, J.N., 2020. Assessment of soil chemical properties, available sulphur and micronutrients status of soils in Pune district of Maharashtra. *Journal of Soil and Water Conservation* 19(1): 100-104.

Sharma, P., Jha, A.B., Dubey, R.S., 2021. Arsenic toxicity and tolerance mechanisms in crop plants. In: Handbook of Plant and Crop Physiology. Pessarakli, M. (Ed.). CRC Press Boca Raton, pp. 813-873.

Upadhyay, M.K., Majumdar, A., Barla, A., Bose, S., Srivastava, S., 2019. An assessment of arsenic hazard in groundwater–soil–rice system in two villages of Nadia district, West Bengal, India. *Environmental Geochemistry and Health* 41: 2381-2395.

Walkley, A., Black, I.A., 1934. An examination of the digestion method for determining soil organic matter, and a proposed modification of the chromic acid titration method. *Soil Science* 37(1):29-38.

Wang, M., Tang, Z., Chen, X.P., Wang, X., Zhou, W.X., Tang, Z., Zhang, J., Zhao, F.J., 2019. Water management impacts the soil microbial communities and total arsenic and methylated arsenicals in rice grains. *Environmental Pollution* 247: 736-744.

Xiao, Z., Xie, X., Pi, K., Gong, J., Wang, Y., 2021. Impact of organic matter on arsenic mobilization induced by irrigation in the unsaturated and saturated zones. *Journal of Hydrology* 602: 126821.

Zhang, J., Hamza, A., Xie, Z., Hussain, S., Brestic, M., Tahir, M.A., Ulhassan, Z., Yu, M., Allakhverdiev, S.I., Shabala, S., 2021. Arsenic transport and interaction with plant metabolism: Clues for improving agricultural productivity and food safety. *Environmental Pollution* 290: 117987.

Zhao, F.J., McGrath, S.P., Meharg, A.A., 2010. Arsenic as a food chain contaminant: mechanisms of plant uptake and metabolism and mitigation strategies. *Annual Review of Plant Biology* 61: 535-559.

Eurasian Journal of Soil Science

Journal homepage : http://ejss.fesss.org
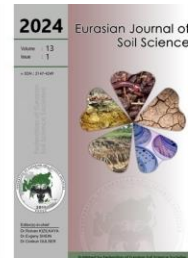
Impacts of irrigation with Cd-contaminated water from Sugovushan Reservoir, Azerbaijan on total cadmium and its fractions in soils with varied textures

Tunzala Babayeva [a,*], Alovsat Guliyev [b], Tariverdi İslamzade [b], Rahila İslamzade [b], Xayala Haciyeva [a], Nergiz Ashurova [a], Azade Aliyeva [a], Shaban Maksudov [c]

[a] Sumgayit State University, Sumgayit, Azerbaijan
[b] Institute of Soil Science and Agrochemistry, Baku, Azerbaijan
[c] Vegetable Scientific Research Institute, Baku, Azerbaijan

Abstract

Cadmium (Cd) presents a significant environmental threat due to its toxic nature and propensity to accumulate in various organs, posing serious health risks upon human exposure. This study focuses on the Sugovushan reservoir in Azerbaijan, aiming to comprehensively understand Cd behavior in soils subjected to varying water levels, shedding light on the intricate interplay between water quality and soil Cd content. Soil samples with distinct textures were collected from a agricultural area in Azerbaijan and subjected to an incubation experiment. The experiment, conducted at 20±0.5°C for 10 days, involved four water levels (%100, %75, %50, and %25 of field capacity) in a randomized complete block design. Cd-contaminated water from Sugovushan reservoir was applied, and inorganic Cd fractions were determined after incubation. The sequential extraction method, as per Shuman's procedure, was employed to assess Cd distribution in exchangeable (EX-Cd), organic (OM-Cd), Mn oxide (MnO-Cd), amorphous Fe oxide (AFeO-Cd), and crystalline Fe oxide (CFeO-Cd) fractions. The soils exhibited varying textures (Sandy Clay Loam, Silty Loam, and Clay) with alkaline reactions, differing salinity, and low organic matter content. Despite somewhat elevated total Cd levels (1.75–2.66 mg/kg), the soils remained below the 3 mg/kg contamination threshold. Water from Sugovushan reservoir, though alkaline, contained Cd concentrations exceeding agricultural use limits. Incubation with Cd-contaminated water increased total Cd content in all soils, with SaCL exhibiting the highest susceptibility. Notably, the SaCL soil showed a significant increase in the exchangeable Cd fraction, emphasizing its environmental risk. This study underscores the importance of soil texture in influencing Cd mobility, especially in low-clay-content soils. The heightened susceptibility observed in SaCL soil highlights the potential threat to food safety, emphasizing the need for sustainable agricultural practices and water management.

Keywords: Cadmium fractions, soil contamination, water quality, environmental risk.

Introduction

Cadmium (Cd) stands out as a particularly hazardous and mobile element in the environment due to its toxic nature and remarkable ability to substitute for calcium in minerals (Thornton, 1986; Alloway and Jackson, 1991; Nies, 1999, 2003). The repercussions of Cd contamination extend beyond its environmental presence, as it tends to accumulate in various organs upon entry into the human body, posing serious health risks (Pan et al., 2010; Hajeb et al., 2014). Unlike some other toxic elements, such as mercury (Hg) and arsenic (As), Cd predominantly finds its way into the human diet through terrestrial pathways, with vegetables grown in regions characterized by elevated Cd concentrations in soil and groundwater being primary contributors (Sebastian and Prasad, 2014; Liu et al., 2017; Tefera et al., 2018). The nuanced bioavailability of Cd becomes

apparent in regional variations, exemplified by the differing Cd levels in rice cultivated in the southern and northern parts of China. These variations can be attributed to factors such as soil acidity, nitrogen fertilizer use, pollution through irrigation, and crop selection (Chen et al., 2018).

Recognizing the significant threats posed by Cd to both human health and the environment, regulatory frameworks like the European Water Framework Directive and the European Groundwater Directive have implemented management plans aimed at mitigating Cd releases into the environment (EC, 2000, 2006). Various countries have responded by establishing threshold values for Cd concentrations in groundwater and drinking water, underscoring the necessity for robust monitoring and control measures (UNEP, 2010; WHO, 2011). While numerous studies have delved into the behavior of Cd in soils and groundwater, exploring its agricultural impact, bioavailability, and environmental remediation (Carrillo-González et al., 2006; Bigalke et al., 2017), many of these efforts have been compartmentalized, focusing on specific issues or localities. This has resulted in a fragmented understanding of Cd dynamics in diverse environments (Akbar et al., 2006; Karak et al., 2015).

This study aims to contribute to the comprehensive understanding of Cd behavior in the environment, specifically focusing on the Sugovushan reservoir in Azerbaijan. By investigating the changes in Cd concentrations and fractions in soils subjected to different levels of water from the Sugovushan reservoir, we aim to shed light on the intricate interplay between water quality and soil Cd content.

Material and Methods

Soil sampling, preparation and analysis

The soil samples with three distinct textures, intended for use in the incubation experiment, were collected from agricultural area in Azerbaijan, collected from a depth of 0-20 cm. The collected soil samples underwent meticulous cleaning to remove stones and plant residues from the soil surface. Subsequently, these soil samples were transported to the laboratory for further analysis. In the controlled laboratory conditions, the soil samples were subjected to a series of procedures. Initially, the samples were air-dried in a cool and shaded environment to prevent alterations in their chemical composition due to excessive heat or sunlight. Once dried, the soil samples were finely ground after eliminating any remaining moisture. This grinding process facilitated homogenization, ensuring uniformity for subsequent analyses. The soil samples were then sieved through a 2 mm mesh to achieve a consistent particle size, optimizing the analytical results. The prepared soil samples, now in a homogeneous and fine-grained state, were considered analytically ready and were utilized for subsequent investigations. Various parameters were determined in the conducted soil analyses using established scientific methods. The soil texture was determined using the hydrometer method as described by Bouyoucos (1962). pH and Electrical Conductivity (EC) were measured in a 1:1 (w/v) soil-to-distilled water suspension using a pH meter and EC meter (Peech, 1965; Bower and Wilcox, 1965). Organic matter content was assessed through wet oxidation with $K_2Cr_2O_7$, following the method proposed by Walkley and Black (1934). Calcium carbonate ($CaCO_3$) content was determined volumetrically using the Scheibler calimeter (Rowell, 2010). The water capacity (field capacity, wilting point, and available water) was determined as reported by Klute (1965) and Peters (1965). Additionally, available heavy metals (Fe, Cu, Zn, Mn, Cd, Pb, Ni) were determined using the DTPA extraction method, total heavy metals determined using the aqua regia + HF digestion method followed by analysis with Atomic Absorption Spectrophotometry (Lindsay and Norvell, 1978, EN 13656, 2002).

Water sampling, preparation and analysis

Water samples, including those from Sugovushan reservoir (40.323985 N, 46.743843 E) in Azerbaijan, were collected for analysis. The water samples were promptly transported to the laboratory and filtered using Whatman No. 41 filter paper. pH and electrical conductivity analyses were conducted using a pH meter and an EC meter, respectively. The analysis of anions (Cl^-, HCO_3^-, SO_4^{2-}, NO_2^-, NO_3^-, PO_4^{3-}.) and cations (Ca^{2+}, Mg^{2+}, $Na^+ + K^+$, NH_4^+) in the water followed the methods outlined by the US Salinity Laboratory Staff (1954). The contents of heavy metals (Fe, Cu, Zn, Mn, Cd, Pb, Ni) in the water were determined using an Atomic Absorption Spectrophotometer.

Soil incubation experiment

The experiment was conducted in a constant temperature incubator at 20±0.5°C for a duration of 10 days. The field capacity, wilting point, and available water content of the soils used in the experiment were determined according to the methodology reported by Klute (1965) and Peters (1965). The incubation experiment was established in a randomized complete block design with four different water levels (%100, %75, %50, and %25 of field capacity) and three replications. For this purpose, 50 g of each soil sample was measured and placed into a 100 mL plastic beaker. Plant-available water from Sugovushan reservoir, enriched with Cd, was

then added to the soil samples at the four different water levels mentioned above. After thorough mixing, all samples were covered with a piece of parafilm containing pores to facilitate air influx while preventing the evaporation of soil water. The samples were stored in the dark at a constant temperature of 20°C throughout the incubation period. On the 10th day of incubation, soil samples were collected, and the inorganic Cd fractions were determined.

Cadmium Fractionation

Total soil Cd was determined using aqua regia + HF digestion method (Shuman, 1979). Cadmium distribution in the exchangeable (EX-Cd), organic (OM-Cd), Mn oxide (MnO-Cd), amorphous Fe oxide (AFeO-Cd) and crystalline Fe oxide fractions (CFeO-Cd) were deter-mined according to Shuman method. The solids remaining were analyzed by complete dissolution in inorganic acids (HCl–HNO$_3$ and HF) and the fraction designed residual (Res.-Cd) (Shuman, 1979; 1983; 1988). Cd contents of the all fractions and total Cd contents in the filtered solution was determined by atomic absorption spectrophotometry. The general procedures of the sequential extractions are given in Table 1.

Table 1. Cd fractionation procedure

Fraction	Solution	Soil, g	Solution, ml	Conditions
Exchangeable (EX-Cd)	1M Mg(NO$_3$)$_2$ (pH 7)	10	40	Shake 2h
Organically complexed (OM-Cd)	0.7M NaOCl (pH 8.5)	10	20	30 min in boling water bath. Stir occasionally. Repeat extraction
Manganese oxide bound (MnO-Cd)	0.1M NH$_2$OH.HCl (pH 2)	1*	50	Shake 30 min
Amorphous iron oxide bound (AFeO-Cd)	0.2M (NH$_4$)$_2$C$_2$O$_4$ in 0.2 M H$_2$C$_2$O$_2$ (pH 3)	1	50	Shake 4h in the dark
Crystalline iron oxide bound (CFeO-Cd)	0.1M ascorbic acid in the above oxalate solution	1	50	30 min in boling water bath. Stir occasionally

*One gram from step 2 that is dried, ground and passed through a 0.5 mm screen

Results

The characteristics of the soils used in the incubation experiment are presented in Table 2. According to the obtained results, the soils selected for the experiment exhibit differences in terms of texture. Specifically, one of the experimental soils is classified as 'Sandy Clay Loam,' another as 'Silty Loam,' and the third as 'Clay.' All soils have an alkaline reaction and are calcareous. While the SaCL soil is non-saline, the others are saline. Additionally, the organic matter content in all soils is observed to be low. According to the analysis conducted by Kloke (1980), no heavy metal pollution is detected in the soils used for the experiment, and the heavy metal contents of the soils do not exceed their buffering capacity. Nevertheless, the total Cd contents of soils exhibiting different textural characteristics used in the incubation experiment were determined as 1.75, 2.12, and 2.66 mg/kg, respectively. It has been documented that soil texture, particularly the increase in clay and organic matter content, is associated with higher mean Cd concentrations in soils (Holmgren et al., 1993). The threshold value for considering soil as contaminated with Cd is generally set at concentrations above 3 mg/kg (Akbar et al., 2006). Concentration gradients are frequently observed in proximity to industrial installations, roads, and urban areas (Page et al., 1987; Joimel et al., 2016). Therefore, it can be asserted that the soils used in the experiment do not exhibit significant contamination with Cd. Since the soils for the experiment were sourced from agricultural areas in Azerbaijan, where phosphorus-containing chemical fertilizers are commonly used to enhance rice yields (Islamzade et al., 2024), the total Cd content of the soil, while somewhat elevated, remains below the threshold of 3 mg kg^{-1}, indicating an acceptable level of non-contamination.

The chemical properties of the water used in the incubation experiment are presented in Table 3. The Sugovushan Reservoir is fed by the Terter River. The River Terter is the largest river in the Karabakh region in Azerbaijan, serving the agricultural and domestic needs of over 400 thousand inhabitants in the surrounding area for many years. Unfortunately, between 1994 and 2020, the Terter River, which was occupied by Armenian forces, witnessed extensive contamination from numerous mining sites, with gold mining being the most detrimental. The lack of any legal norms for environmental protection in Karabakh during the occupation allowed mining operators to dispose of all their waste into the river. As a result, not only did the ecology suffer, but also the Terter River and the Sugovushan Reservoir on this river became polluted, primarily with Cd. This water sample demonstrates an alkaline reaction and contains some heavy metals within its composition. Among these heavy metals, the concentration of Cd exceeds the recommended upper limit for agricultural use of water, set at 0.01 mg L^{-1} (FAO, 1985), measuring at 1.64 mg L^{-1}. However, for other heavy metals, there is not a significantly increased risk similar to that posed by Cd.

Table 2. Characteristics of the soils used in the incubation experiment

		SaCL	SiL	C
	Sampling point	38.6322740 N 48.8646310 E	40.2559770 N 47.6289990 E	40.5438710 N 47.2880790 E
Texture	Sand, %	50,69	11,55	6,76
	Silt, %	15,91	78,58	7,69
	Clay, %	33,41	9,87	85,55
	Class	Sandy Clay Loam	Silty Loam	Clay
Soil water properties	Field Capacity, % Vol	32,30	30,90	44,90
	Wilting point, % Vol	21,60	10,40	35,00
	Available Water, % Vol	10,70	20,50	9,90
	Bulk density, g cm^{-3}	1,48	1,37	1,19
Chemical properties	pH	7,70	8,17	7,86
	EC, dSm^{-1}	0,51	7,62	4,77
	CaCO$_3$, %	12,93	15,06	6,69
	Organic matter, %	1,61	0,88	2,47
Available heavy metals	Fe, mg kg^{-1}	65,50	6,21	35,71
	Cu, mg kg^{-1}	7,54	1,80	7,74
	Zn, mg kg^{-1}	0,58	0,31	0,43
	Mn, mg kg^{-1}	23,01	3,76	7,34
	Cd, mg kg^{-1}	0,20	0,16	0,15
	Pb, mg kg^{-1}	2,48	3,58	3,25
	Ni, mg kg^{-1}	3,68	2,15	3,59
Total heavy metals	Fe, %	3,12	3,81	5,39
	Cu, mg kg^{-1}	84,82	75,36	95,15
	Zn, mg kg^{-1}	191,17	185,58	296,61
	Mn, mg kg^{-1}	0,18	0,13	0,25
	Cd, mg kg^{-1}	1,75	2,12	2,66
	Pb, mg kg^{-1}	86,85	93,19	95,85
	Ni, mg kg^{-1}	75,69	65,48	86,15

Cd-contaminated water from the Sugovushan reservoir was applied to soils of three different textures (SaCL, SiL, and C) in this experiment, and changes in the soil's total and Cd fractions were assessed after irrigation with 100%, 75%, 50%, and 25% of the available water content. Figure 1 illustrates these variations, including the initial Cd fractions of the soils before irrigation. According to the obtained results, all soils irrigated with Cd-contaminated water exhibited an increase in their total Cd content. This increase was found to be correlated with the amount of water applied to the soil. In effective agricultural irrigation, it is desirable for soil moisture levels to be at field capacity (Kumar et al., 2023). Initially, the Cd levels in SaCL, SiL, and C soils were 1.75, 2.12, and 2.66 mg kg^{-1}, respectively. However, when soils were irrigated with 100% of the available water content, the total Cd contents increased to 2.10, 2.79, and 2.98 mg Cd kg^{-1} for SaCL, SiL, and C soils, respectively. A significant decrease in total Cd content was observed in all soils when the amount of applied water decreased. Similarly, previous studies have reported a significant increase in Cd and other heavy metal contents in soils irrigated with Cd-contaminated water (Chaoua et al., 2019; Orosun et al., 2023; Shahriar et al., 2023).

Table 3. Chemical properties of the water used in the incubation experiment

pH	8,00	**Anions**		**Heavy metals**	
EC, dSm^{-1}	3,10	Cl$^-$, mg L^{-1}	20,40	Fe, mg L^{-1}	210,00
Cations		HCO$_3^-$, mg L^{-1}	114,60	Cu, mg L^{-1}	<0,01
Ca^{2+}, mg L^{-1}	38,1	SO$_4^{2-}$, mg L^{-1}	67,90	Zn, mg L^{-1}	<0,01
Mg^{2+}, mg L^{-1}	9,90	NO$_2^-$, mg L^{-1}	0,01	Mn, mg L^{-1}	4,17
Na$^+$+K$^+$, mg L^{-1}	64,80	NO$_3^-$, mg L^{-1}	1,43	Cd, mg L^{-1}	1,64
NH$_4^+$, mg L^{-1}	0,15	PO$_4^3$, mg L^{-1}	0,10	Pb, mg L^{-1}	9,82
Total cations	112,95	Total anions	204,44	Ni, mg L^{-1}	<0,01

In the incubation experiment, although initially the entire set of soils used exhibited the CFeO-Cd fraction as the predominant fraction within inorganic Cd fractions, it was observed that OM-Cd and Res.-Cd contained the least Cd fraction (Figure 1). Numerous studies have demonstrated the influence of various soil physicochemical properties such as soil texture, organic matter content, and pH on the distribution of inorganic Cd fractions in soils (Anju and Banerjee, 2011; Nejad et al., 2021; Lian et al., 2022). Kızılkaya and Aşkın (2002), in their investigation of the distribution of Cd fractions and the relationships between soil

properties in agricultural fields in the Bafra Plain of Turkey, determined that the total Cd content in alluvial soils ranged from 1.83 to 2.73 mg kg^{-1}. They found that 7.3-18.5% of total Cd in the soils consisted of EX-Cd, 4.1-10.8% of OM-Cd, 6.1–7.6% of MnO-Cd, 5.2–8.7% of AFeO-Cd, and 5.8–7.2% of CFeO-Cd. Additionally, in this study, significant positive correlations were identified between the distribution of Cd fractions in soils and the clay content and cation exchange capacity of the soils.
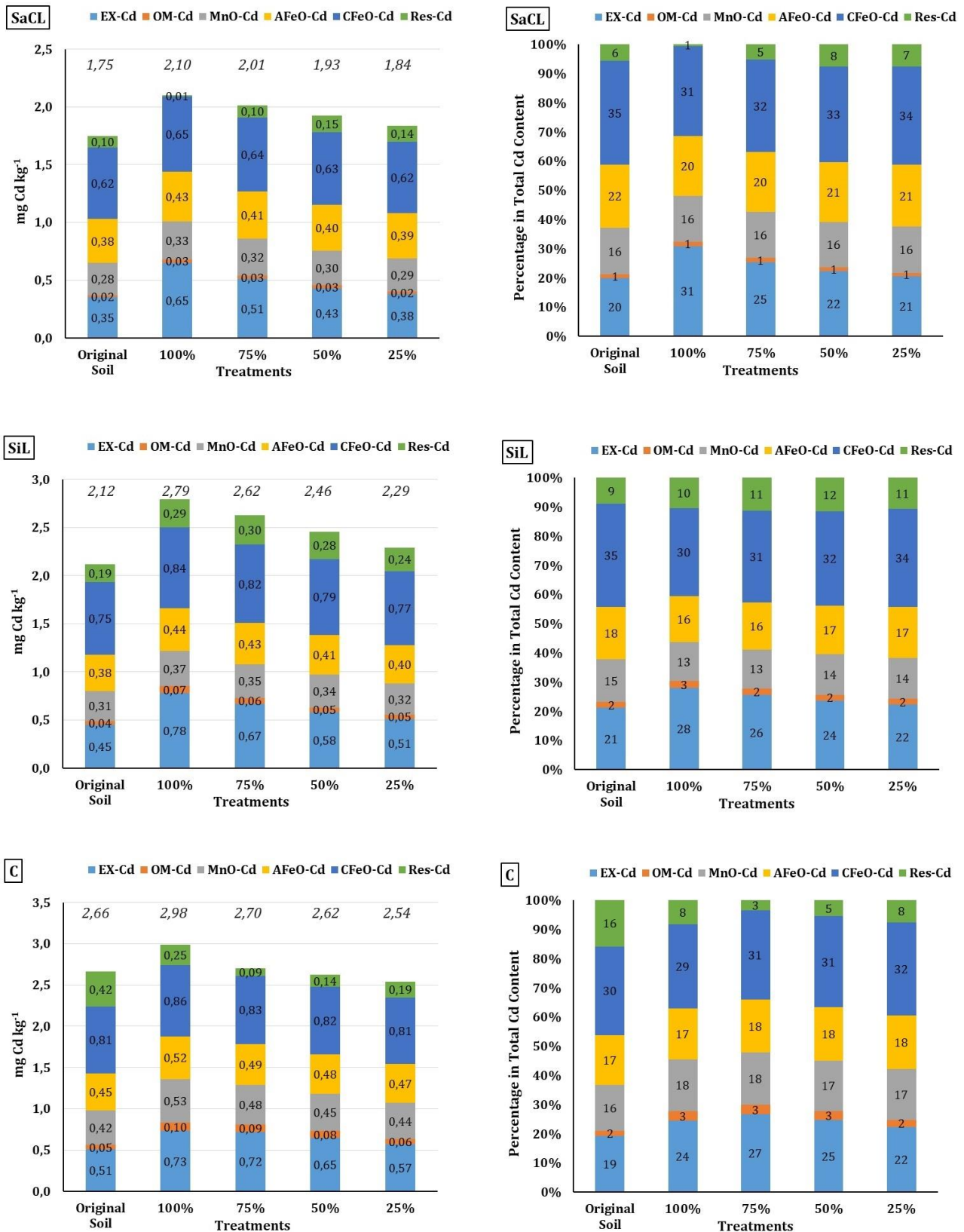

Figure 1. Changes in the different textural (SaCL, SiL and C) soil's total and Cd fractions were assessed after irrigation with 100%, 75%, 50%, and 25% of the available water content

After irrigation with Cd-enriched water in soils of different textures (SaCL, SiL, and C), increases were observed not only in the total Cd content of the soils but also in the Cd fractions. Remarkably, the increase in Cd fractions occurred in the EX-Cd fraction of the SaCL soil (Figure 1). This observation is attributed to the lower clay content of the SaCL soil compared to the other two soils (SiL and C). The exchangeable Cd fraction is particularly crucial in environmental risk assessments and soil quality management due to its susceptibility to plant uptake. This exchangeable fraction (EX-Cd) is closely monitored to assess and regulate the environmental impacts of Cd. Consequently, when low-clay-content soils are used for agricultural purposes in the presence of Cd-contaminated water, it is suggested that Cd can be more readily taken up by plants from the soil, potentially entering the food chain. This underscores the importance of monitoring and managing Cd's exchangeable fraction in mitigating the environmental implications associated with Cd-contaminated waters used for agricultural irrigation.

Conclusion

In conclusion, this study contributes valuable insights into the behavior of Cd in soils, particularly in the context of the Sugovushan reservoir in Azerbaijan. The incubation experiment revealed the nuanced response of soils with different textures to irrigation with Cd-contaminated water, emphasizing the importance of soil physicochemical properties in shaping Cd distribution. The SaCL soil, characterized by lower clay content, exhibited a heightened susceptibility to Cd mobility, particularly in the exchangeable fraction. This underscores the significance of considering soil texture in managing and mitigating the environmental risks associated with Cd-contaminated water used for agricultural purposes.

The findings highlight the potential implications for food safety as Cd may readily enter the food chain when low-clay-content soils are irrigated with contaminated water. Therefore, sustainable agricultural practices and water management strategies need to consider soil characteristics to minimize the risk of Cd exposure. As future research endeavors unfold, a more comprehensive understanding of the intricate relationships between water quality, soil properties, and Cd behavior will be crucial for developing effective strategies to safeguard environmental and human health.

References

Akbar, K.F., Hale, W.H.G., Headley, A.D., Athar, M., 2006. Heavy metal contamination of roadside soils of northern England. *Soil and Water Research* 1(4): 158-163.

Alloway, B.J., Jackson, A.P., 1991. The behaviour of heavy metals in sewage sludge-amended soils. *Science of The Total Environment* 100: 151–176.

Anju, M., Banerjee, D.K., 2011. Associations of cadmium, zinc, and lead in soils from a lead and zinc mining area as studied by single and sequential extractions. *Environmental Monitoring and Assessment* 176: 67–85.

Bigalke, M., Ulrich, A., Rehmus, A., Keller, A., 2017. Accumulation of cadmium and uranium in arable soils in Switzerland. *Environmental Pollution* 221: 85–93.

Bouyoucos, G.J., 1962. Hydrometer method improved for making particle size analyses of soils. *Agronomy Journal* 54(5): 464-465.

Bower, C.A., Wilcox L.V., 1965. Soluble Salts. In: Methods of soil analysis. Part 2. Chemical and microbiological properties. Black, C.A., Evans, D.D., White, J.L., Ensminger, L.E., Clark F.E. (Eds.). Soil Science Society of America. Madison, Wisconsin, USA. pp. 933-951.

Carrillo-González, R., Šimůnek, J., Sauvé, S., Adriano, D., 2006. Mechanisms and pathways of trace element mobility in soils. *Advances in Agronomy* 91: 111–178.

Chaoua, S., Boussaa, S., El Gharmali, A., Boumezzough, A., 2019. Impact of irrigation with wastewater on accumulation of heavy metals in soil and crops in the region of Marrakech in Morocco. *Journal of the Saudi Society of Agricultural Sciences* 18(4): 429-436.

Chen, H.P., Tang, Z., Wang, P., Zhao, F.J., 2018. Geographical variations of cadmium and arsenic concentrations and arsenic speciation in Chinese rice. *Environmental Pollution* 238: 482–490.

EC, 2000. Directive 2000/60/EC of the european parliament and of the council of 23 October 2000 establishing a framework for community action in the field of water policy. Official Journal L 327 , 22/12/2000 P. 0001 - 0073. Available at [Access date : 11.09.2023]: https://eur-lex.europa.eu/eli/dir/2000/60/oj

EC, 2006. Directive 2006/118/EC of the European Parliament and of the Council of 12 December 2006 on the protection of groundwater against pollution and deterioration. Official Journal of the European Union, L 372/19. Available at [Access date : 11.09.2023]: https://eur-lex.europa.eu/eli/dir/2006/118/oj

EN 13656, 2002. Characterization of waste: microwave-assisted digestion with hydrofluoric (HF), nitric (HNO3), and hydrochloric (HCl) acid mixture for subsequent determination of elements. EN Standards. Available at [Access date : 11.09.2023]: http://en-standards.standardsdirect.org/

FAO, 1985. Water Quality for Agriculture. Food and Agriculture Organization, Rome, Italy. Available at [Access date : 11.09.2023]: http://www.fao.org/3/T0234E/T0234E00.htm

Hajeb, P., Sloth, J.J., Shakibazadeh, S., Mahyudin, N.A., Afsah-Hejri, L., 2014. Toxic elements in food: occurrence, binding, and reduction approaches. *Comprehensive Reviews in Food Science and Food Safety* 13(4): 457–472.

Holmgren, G.G.S., Meyer, M.W., Chaney, R.L., Daniels, R.B., 1993. Cadmium, lead, zinc, copper, and nickel in agricultural soils of the United States of America. *Journal of Environmental Quality* 22(2): 335–348.

İslamzade, T., Baxishov, D., Guliyev, A., Kızılkaya, R., İslamzade, R., Ay, A., Huseynova, S., Mammadova, M., 2024. Soil fertility status, productivity challenges, and solutions in rice farming landscapes of Azerbaijan. *Eurasian Journal of Soil Science* 13(1): 70 - 78.

Joimel, S., Cortet, J., Jolivet, C.C., Saby, N.P.A., Chenot, E.D., Branchu, P., Consalès, J.N., Lefort, C., Morel, J.L., Schwartz, C., 2016. Physico-chemical characteristics of topsoil for contrasted forest, agricultural, urban and industrial land uses in France. *Science of The Total Environment* 545-564: 40–47.

Karak, T., Paul, R.K., Das, S., Das, D.K., Dutta, A.K., Boruah, R.K., 2015. Fate of cadmium at the soil-solution interface: a thermodynamic study as influenced by varying pH at South 24 Parganas, West Bengal, India. *Environmental Monitoring and Assessment* 187: 713.

Kızılkaya, R., Aşkın, T., 2002. Influence of cadmium fractions on microbiological properties in bafra plain soils. *Archives of Agronomy and Soil Science* 48(3): 263-272.

Kloke , A., 1980. Orientierungsdaten für tolerierbare Gesamtgehalte einiger Elemente in Kulturboden. Mitteilungen VDLUFA 1/III : 9 – 11 .

Klute, A., 1965. Water Capacity. In: Methods of Soil Analysis: Part 1 Physical and Mineralogical Properties, Including Statistics of Measurement and Sampling. Black, C.A., Evans, D.D., White, J.L., Ensminger, L.E., Clark F.E. (Eds.), Soil Science Society of America. Madison, Wisconsin, USA. pp. 273-278.

Kumar, H., Srivastava, P., Lamba, J., Lena, B., Diamantopoulos, E., Ortiz, B., Takhellambam, B., Morata, G., Bondesan, L., 2023. A methodology to optimize site-specific field capacity and irrigation thresholds. *Agricultural Water Management* 286: 108385.

Lian, M., Ma, Y., Li, J., Sun, J., 2022. Influence of pH on the particulate-bound Cd speciation and uptake by plants. *Polish Journal of Environmental Studies* 31(6): 5511-5517.

Lindsay, W.L., Norvell, W.A., 1978. Development of a DTPA soil test for zinc, iron, manganese, and copper. *Soil Science Society of America Journal* 42(3): 421-428.

Liu, Y.Z., Xiao, T.F., Perkins, R.B., Zhu, J.M., Zhu, Z.J., Xiong, Y., Ning, Z.P., 2017. Geogenic cadmium pollution and potential health risks, with emphasis on black shale. *Journal of Geochemical Exploration* 176: 42–49.

Nejad, Z.D., Rezania, S., Jung, M.C., Al-Ghamdi, A.A., Mustafa, A.E.M.A., Elshikh, M.S., 2021. Effects of fine fractions of soil organic, semi-organic, and inorganic amendments on the mitigation of heavy metal(loid)s leaching and bioavailability in a post-mining area. *Chemosphere* 271: 129538.

Nies, D.H., 1999. Microbial heavy-metal resistance. *Applied Microbiology and Biotechnology* 51: 730–750.

Nies, D.H., 2003. Efflux-mediated heavy metal resistance in prokaryotes. *FEMS Microbiology Reviews* 27(2-3): 313–339.

Orosun, M.M., Nwabachili, S., Alshehri, R.F., Omeje, M., Alshdoukhi, I.F., Okoro, H.K., Ogunkunle, C.O., Louis, H., Abdulhamid, F.A., Osahon, S.E., Mohammed, A.U., Ehinlafa, E.O., Yunus, S.O., Ife-Adediran O., 2023. Potentially toxic metals in irrigation water, soil, and vegetables and their health risks using Monte Carlo models. *Scientific Reports* 13: 21220.

Page, A.L., Chang, A.C., El-Amamy, M., 1987. Cadmium levels in soils and crops in the United States. In: Lead, Mercury, Cadmium and Arsenic in the Environment. Hutchinson, T.C., Meema, K.M. (Eds.). John Wiley & Sons Ltd. New York, pp. 119–146.

Pan, J.L., Plant, J.A., Voulvoulis, N., Oates, C.J., Ihlenfeld, C., 2010. Cadmium levels in Europe: implications for human health. *Environmental Geochemistry and Health* 32: 1–12.

Peech, M., 1965. Hydrogen-Ion Activity. In: Methods of soil analysis. Part 2. Chemical and microbiological properties. Black, C.A., Evans, D.D., White, J.L., Ensminger, L.E., Clark F.E. (Eds.), Soil Science Society of America. Madison, Wisconsin, USA. pp. 914-926.

Peters, D.B., 1965. Water Availability. In: Methods of Soil Analysis: Part 1 Physical and Mineralogical Properties, Including Statistics of Measurement and Sampling. Black, C.A., Evans, D.D., White, J.L., Ensminger, L.E., Clark F.E. (Eds.), Soil Science Society of America. Madison, Wisconsin, USA. pp. 279-285.

Rowell, D.L., 1996. Soil Science: methods and applications. Longman, UK. 350p.

Sebastian, A., Prasad, M.N.V., 2014. Cadmium minimization in rice. A review. *Agronomy for Sustainable Development* 34: 155–173.

Shahriar, S.M.S., Munshi, M., Zakir, H.M., Islam, M.J., Mollah, M.M.A., Salam, S.M.A., 2023. Assessment of Heavy Metal Pollution in Irrigation Water of Rajshahi City, Bangladesh. *Environmental and Earth Sciences Research Journal* 10(3): 100-110.

Shuman, L.M., 1979. Zinc, manganese and copper in soil fractions. *Soil Science* 127(1): 10–17.

Shuman, L.M., 1983. Sodium hypochlorite methods for extracting microelements associated with soil organic matter. *Soil Science Society of America Journal* 47(4): 656 – 660.

Shuman, L.M., 1988. Effect of phosphorus level on extractable micronutrients and their distribution among soil fractions. *Soil Science Society of America Journal* 52(1): 136 – 141.

Tefera, M., Gebreyohannes, F., Saraswathi, M., 2018. Heavy metal analysis in the soils of in and around Robe town, Bale zone, South Eastern, Ethiopia. *Eurasian Journal of Soil Science* 7(3): 251 - 256.

Thornton, I., 1986. Geochemistry of cadmium. In: Cadmium in the Environment. Mislin, H., Ravera, O. (Eds.). Experientia Supplementum, vol 50. Birkhäuser Basel. pp. 7–12.

UNEP, 2010. Final Review of Scientific Information on Cadmium. United Nations Environment Programme Chemicals Branch, DTIE, 201p. Available at [Access date : 11.09.2023]: https://wedocs.unep.org/bitstream/handle/20.500.11822/27636/Cadmium_Review.pdf?sequence=1&isAllowed=y

US Salinity Laboratory Staff, 1954. Diagnosis and improvement of saline and alkali soils. US Department of Agriculture Handbook 60, Washington, DC.

Walkley, A., Black, C.A., 1934. An examination of the Degtjareff method for determining soil organic matter and a proposed modification of the chromic acid titration method. *Soil Science* 37(1): 29–38.

WHO, 2011. Guidelines for Drinking Water Quality, Fourth Edition Incorporating The First Addendum. World Health Organization, Geneva. 541p. Available at [Access date : 11.09.2023]: https://iris.who.int/bitstream/handle/10665/254637/9789241549950-eng.pdf?sequence=1

Eurasian Journal of Soil Science

Journal homepage : http://ejss.fesss.org
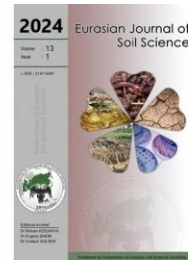
Response of *L. Scoparium* and *K. Robusta* to biosolids and dairy shed effluent application in a low fertility soil

Obed Nedjo Lense [a,*], Shamim Al Mamun [b]

[a] University of Papua (UNIPA), Faculty of Forestry, Department of Forest Regeneration, Manokwari, Papua Barat, Indonesia
[b] Department of Environmental Science and Resource Management, Mawlana Bhashani Science and Technology University, Tangail-1902, Bangladesh

Abstract

Biosolids and Dairy Shed Effluent (DSE) can contain high concentrations of plant nutrients, making them potential resources for enhancing forest tree species growth and soil fertility. This study aimed to investigate the effects of biosolids and DSE application on the growth and nutrient uptake of *Leptospermum scoparium* and *Kunzea robusta*, while also considering the potential accumulation of contaminants. The results demonstrated that amending low-fertility soil with 2600 kg N ha^{-1} of biosolids and 200 kg N ha^{-1} of DSE positively influenced the growth of both *L. scoparium* and *K. robusta*. This improvement was evident through increased biomass production and enhanced uptake of essential elements such as calcium (Ca), potassium (K), and sulfur (S). Notably, *L. scoparium* exhibited superior growth when combined with DSE, while both species showed similar positive responses when combined with biosolids. However, it should be noted that the application of biosolids resulted in elevated concentrations of certain trace elements in the plants, whereas DSE did not. These trace elements included cadmium (Cd), copper (Cu), manganese (Mn), and zinc (Zn). Despite the increase, the levels of these elements did not exceed unacceptable thresholds. Considering the potential influence of biosolids on plant rhizodeposition, it is recommended that future studies investigate the interactions between plant roots and microbes, particularly in relation to plant element uptake. This line of research would further enhance our understanding of the underlying mechanisms involved. In conclusion, the findings suggest that the application of biosolids and DSE can effectively improve forest tree growth and nutrient uptake. However, careful management is necessary to mitigate the potential accumulation of trace elements. These results provide valuable insights for optimizing the use of biosolids and DSE in forestry practices, with potential economic and environmental benefits.

Keywords: Native plants, biosolids, dairy shed effluent, macronutrients, essential trace element, nutrients uptake.

Introduction

Biosolids and Dairy Shed Effluent (DSE) can contain elevated concentrations of plant nutrients (Di et al., 1998; Zaman et al., 1999; Antolín et al., 2005; Hawke and Summers, 2006; Haynes et al., 2009; Bai et al., 2013a,b; Cogger et al., 2013 Hedley et al., 2013; Moir et al., 2013; Paramashivam et al., 2016). The low C: N ratio of biosolids and DSE makes them a net N source, where the N and other nutrients are released slowly from these biowastes as they decompose in the soil (Gilmour et al., 2003; Murphy et al., 2007; Powlson et al., 2012). Therefore, the land application of these biodegradable materials can provide short and long-term benefits to soils (Ginting et al., 2003) and crops, which can lead to a lower requirement for mineral fertilizers. Various studies have shown positive effects of DSE and biosolids application on forest tree species, which can subsequently provide economic returns through increased biomass and soil nutrients, while avoiding

accumulation of biosolids derived contaminants above threshold values (Zaman et al., 2002; Kimberley et al., 2004; Singh and Agrawal, 2008; Wang and Jia, 2010). The application of biosolids provides nutrients, increases organic matter, improves soil structure, enhances nutrient absorption by plants (Freeman and Cawthon, 1999; Morera et al., 2002; Antolín et al., 2005; Weber et al., 2007; Singh and Agrawal, 2008), as well as increase the number and activities of soil microbes (Rogers and Smith, 2007; Singh and Agrawal, 2008; Cytryn et al., 2011). Biosolids have been used as fertilizers or composts in land applications to improve and maintain soil productivity, stimulate plant growth and establish sustainable vegetation at mine sites (Fresquez et al., 1990). They enhance the activities of soil enzymes as well as the number and biomass of soil organisms due to its high organic matter content and nutrient availability (Lteif et al., 2007; Singh and Agrawal, 2008). Frequent applications of biosolids has positive ecosystem effects with relatively low extractable metal levels in soil and support greater plant biomass and tissue quality (Sullivan et al., 2006). Moderate application rates of biosolids to low organic matter and clay content soils enhances soil organic carbon and increases nutrient retention (Antoniadis, 2008), enhances the adsorption capacity of soil to immobilize heavy metals such as Cu, and effectively reduced Pb availability in a high Pb urban soil (Brown et al., 2003). The application of DSE, resulted in a greater and more diverse microbial biomass in soil (Hawke and Summers, 2006). In addition, the enzyme activities of root exudates of Lolium L. and Trifolium repens L., grown on Templeton sandy loam, significantly increased N mineralization due to the application of DSE (Zaman et al., 1999). Another study found that the application of DSE improved long-term soil fertility by increasing the concentration of total N, total P and plant available nutrients (Hawke and Summers, 2006). However, the application of biosolids and DSE to forest soil can result in decreased forest productivity because there is a strong dependence on the composition of biowastes, soil type and plant species (Cline et al., 2012).

I hypothesised that biosolids, but not DSE, will lead to elevated concentrations of Cd, Cu and Zn in the plants, as these elements occur at elevated concentrations in biosolids (Simmler et al., 2013). Further, I also hypothesize that fresh biosolids and DSE will enhance the growth of *L. scoparium* and *K. robusta* in low fertility soil because DSE and biosolids which high concentrations of these macronutrients (Zaman et al., 1999; Kimberley et al., 2004; Antolín et al., 2005; Hawke and Summers, 2006; Singh and Agrawal, 2008; Wang et al., 2009). The aim of the research was to assess the growth and elemental composition of the foliar part of *L. scoparium* and *K. robusta* after the application of fresh biosolids and fresh DSE, with the goal of obtaining accurate measurements.

Material and Methods

Experimental setup

The experiment was conducted at Lincoln University greenhouse facility (43o38'42.3"S 172o27'41.0"E). Low fertility soil with yellow-grey earths, mostly classified as Lismore stony silt-loam derived from Greywacke gravels and thin loess deposits from a former pine plantation of Eyrewell (Figure 1A - 43⁰ 25'19" S, 172⁰ 15'52"E), New Zealand, was used as planting medium. Fresh Dairy Shed Effluent (DSE) was collected from Lincoln University Dairy Farm, New Zealand (Figure 1B - 43°38'40"S, 172°26' 32" E; 17 m asl) in January 2015. Biosolids were obtained from the Kaikoura Wastewater Treatment Plant, New Zealand (Figure 1C - 42°21'37.40"S, 173°41'27.35"E) in July 2014. The initial treatment consisted of sedimentation and anaerobic digestion in settlement ponds for 6-8 months. The key properties of soil, DSE, and biosolids used in this experiment are presented in Table 1.

Table 1. Concentration of nutrients, trace elements and contaminants in soils, DSE, and biosolids used in the present study. Values in brackets represent standard error (n=15[1]; n=6[2]; n=5[3])

Properties	Soil[1]		DSE[2]		Biosolids[3]	
pH	4.5	(0.3)	7.5	(0.01)	4.5	(0.0)
C, %	4.3	(0.4)	0.11	(0.0)	27	0.7)
N, %	0.17	(0.02)	0.02	(0.0)	2.5	(0.6)
P, %	0.05	(0.00)	0.001	(0.0)	0.50	(0.0)
K, %	0.2	(0.01)	0.002	(0.0)	0.14	(0.01)
S, %	0.03	(0.00)	0.001	(0.0)	0.87	(0.01)
Ca, %	0.2	(0.01)	0.003	(0.0)	0.63	(0.01)
Mg, %	0.3	(0.00)	0.001	(0.0)	0.30	(0.00)
B, mg kg^{-1}	5.0	(0.3)	0.04	(0.0)	27	(0.1)
Cu, mg kg^{-1}	4.1	(0.2)	0.0	(0.0)	891.0	(18.9)
Zn, mg kg^{-1}	72	(1.5)	0.08	(0.0)	1073	(27)
Mn, mg kg^{-1}	265	(15)	0.04	(0.0)	185	(4.5)
Fe, mg kg^{-1}	21121	(291)	0.05	(0.0)	14534	(92)
Cd, mg kg^{-1}	0.2	(0.01)	0.04	(0.0)	4.0	(0.1)

Thirty-six 10 L pots (25 cm in diameter with a height of 29 cm) were used. The treatments contained total of 6 L Dairy Shed Effluent (DSE) which is 220 kg N ha^{-1} equiv. and 1 kg fresh biosolids per pot, which was 2600 kg N ha^{-1} equiv. The DSE and biosolids were first homogenised thoroughly using a 100 L plastic tank and black tarpaulin respectively**.** DSE then further stored in the fridge for further application in the greenhouse. The biosolids were mixing with soils at the beginning of the experiment. For each individual pot, 1 kg fresh biosolids was mixed completely with 9 kg fresh soil using a 20 L bucket. The soil was then filled into the pot in layers to give a soil bulk density of approximately 1.3 g cm^{-3}. *L. scoparium* and *K. robusta* seedlings were obtained from Waiora Nursery Ltd., Christchurch, New Zealand. All plants were transplanted directly after all pots were filled with medium (soil and plus biosolids). The pots were arranged in the glasshouse using a randomized block design.

To avoid preferential flow, DSE was applied gently on to the soil surface of the pots which contained 9 kg of fresh soil with soil bulk density of approximately 1.3 g cm^{-3}. DSE was applied weekly (500 mL week^{-1}). In the first two weeks (January 12th, 2015 and January 19th, 2015), the DSE was applied daily (from Monday to Friday) of 100 mL of each application, 3 hours after irrigating the pots. During the next three weeks (Jan 26th, 2015; Feb 2nd and 9th, 2015) the DSE was applied on Monday, Wednesday, and Friday at rates of 150 mL, and 200 mL respectively. From February 2nd, 2015 to March 3rd, 2015, it was applied twice per week (Monday and Friday) of 250 mL of each application. In the last two weeks before harvesting the experiment, 500 mL of fresh DSE was applied weekly only (Mondays). Each treatment had 4 replicates. The controls received neither biosolids nor Dairy Shed Effluent. During the experiment, the pots were irrigated with measured amount of water using an automated irrigation system. Each pot received 200 mL of water twice a day over the experimental period to ensure optimal plant growth at conditions near field capacity. The temperature in the greenhouse ranged from 9 to 20°C during the night (10 pm until 6 am) and from 14°C to 28°C during the day. After 12 weeks, the above ground biomass was carefully harvested and weighed. Plant samples was dried at 70^{0}C until constant weight was obtained and ground using a Retch ZM200 grinder.

Soil pH was determined using pH meter (MTSE). A 10 g portion of soil of soil was mixed with 25 mL deionised water and then shaken for two hours using an end-over-end shaker (at 20 rpm). The plant-available elements were determined using a 0.05 M Ca(NO$_3$)$_2$ extraction (Esperschuetz et al., 2017). Concentrations of Ca, K, S, Cd, Cu, Mn, and Zn were determined using inductively coupled plasma optical emission spectrometry (ICP-OES Varian 720 ES - USA). Reference soil and plant material from Wageningen University, the Netherlands (International Soil analytical Exchange 921 and International Plant analytical Exchange 100) was analysed with the samples. Recoverable concentrations were 81–112% of the certified values.

Data and statistical analysis

Significant differences (α=0.05) between treatments were determined by analysis of variance, followed by Duncan post-hoc tests at *P=0.05*. The analyses were done in IBM SPSS v.22.

Results

Aerial biomass production

Figure 1 shows the cumulative biomass (g per pot) of *L. scoparium*, and *K. robusta* in combination with DSE, biosolids, and control. With the exception combination of DSE and *L. scoparium*, compared to the control, the addition of 2600 kg N ha^{-1} equiv. of biosolids and 200 kg N ha^{-1} equiv. significantly (*p≤ 0.05*) increased the cumulative biomass production of *L. scoparium* and *K. robusta.* Twelve weeks after applying treatments, significant differences were detected in the growth response of *L. scoparium* and *K. robusta* as a result of different treatments, ranking in order of biosolids > DSE > control (Figures 1 and 2).

In combination with *K. robusta*, biosolids application resulted in the highest increment (100%) of biomass, from 105 g per pot, equivalent to 21 t ha^{-1} to 210 g per pot, equivalent to 43 t ha^{-1}. In combination with *L. scoparium* by comparison, biosolids application significantly increased its biomass by 44% higher than the control, from 144 g per pot to 207 g per pot, equivalent to 41 t ha^{-1}.

DSE increased the above ground biomass of *K. robusta* by 24%, up to 135g per pot, equivalent to 28 t ha^{-1}. Whereas in combination with *L scoparium*, amending soil with DSE resulted in a significant increase of the above ground dried biomass by 29%, up to 179 g per pot, equivalent to 36 t ha^{-1}. There was a significant difference in above ground biomass between *L. scoparium* and *K. robusta* in combination with DSE (Figure 3). In combination with DSE, *L. scoparium* produced 25% higher above ground dried biomass than that of in *K. robusta.*
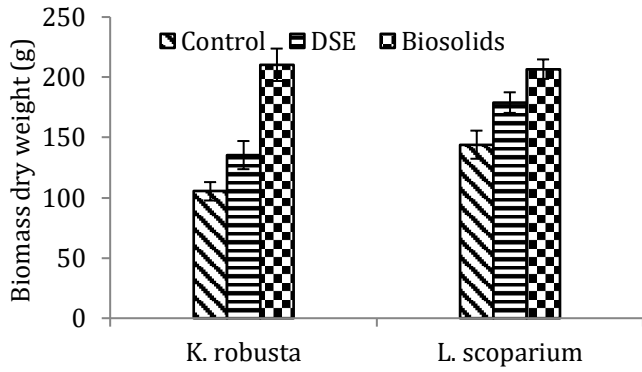
Figure 1. The cumulative biomass (g per pot) of L. scoparium, and K. robusta in combination with DSE, biosolids, and control
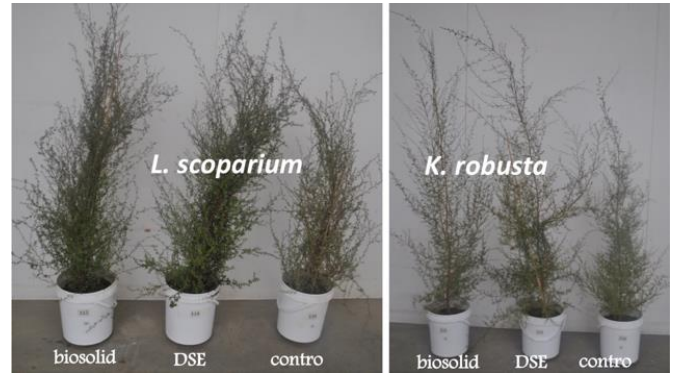

Figure 2. Plant growth responses under different treatments of 12 weeks experiment period under Eyrewell soil medium

Element uptake
Macronutrients

The foliar macronutrient concentrations and ratios of *L. scoparium* and *K. robusta* measured at the end of the experiment are presented in Figures 3 and 4. Compared to the control, in combination with *L. scoparium*, the application of both DSE and biosolids significantly ($p \leq 0.05$) increased the uptake of the concentration of foliar Ca by 21% and 29% higher than the control, respectively (Figure 5). Whereas in combination with *K. robusta,* DSE and biosolids addition resulted in 22% and 51% higher concentration of foliar Ca than control. There was no significant different of Ca uptake between DSE and biosolids treatment in combination with *L. scoparium* (Figure 3). Although in combination with *L. scoparium* and *K. robusta* there was no significant difference in N uptake between treatments, these New Zealand native species responded differently in accumulating foliar N (Figure 4). In combination with *L. scoparium*, biowastes application increased significantly increased the foliar N uptake compared to that of when combined with *K. robusta*. Amending DSE and biosolids increased the foliar N uptake of *L. scoparium* by 23% and 29%, respectively compared to *K. robusta*.
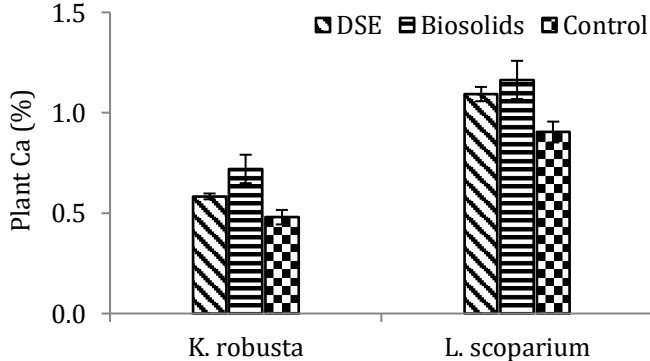

Figure 3. Total concentrations of foliar Ca (%) of *L. scoparium* and *K. robusta* measured at the end of experiment. Error bars represent the standard error of the mean. Treatment that share letters have means that do not differ significantly (p<0.05).
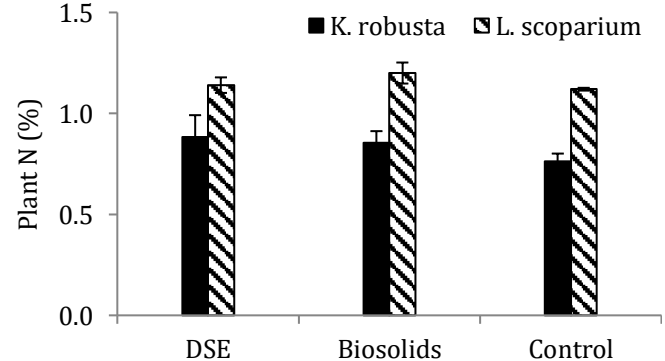

Figure 4. Total concentrations of foliar N (%) of *L. scoparium* and *K. robusta* measured at the end of experiment. Error bars represent the standard error of the mean. Asterisks (*) signify significant differences between the effluents (striped bars) and controls (solid bars) at $p \leq 0.05$.

Micronutrients

Figure 6 shows total concentrations of foliar micronutrients (mg/kg) of *L. scoparium* and *K. robusta* measured at the end of experiment. The application of biosolids and DSE to *K. robusta* increased the concentration of foliar Cu by 78% and 15%, whereas these treatments increased Cu in *L. scoparium* by Cu by 42 and 46%, respectively (Figure 6). Biosolids significantly increased the uptake of Zn by both *L. scoparium* and *K. robusta* by 569% and 298% respectively (Figure 6). In comparison, the DSE did not significantly change the Zn concentration in the leaves of *K. robusta* and only produced a 37% increase in *L. scoparium* (Figure 6).

K. robusta accumulated significantly ($p \leq 0.05$) higher Cd in the biosolids treatment**,** whereas the DSE treatment, *K. robusta* was not different to the control (Figure 7). *K. robusta* responded to the application of biowastes in related to Mn uptake. Biosolids application significantly increased ($p \leq 0.05$) the uptake of Mn (Figure 6B). The application of biosolids increased the concentration of foliar Mn in *K. robusta* by 71% compared to the control. In contrast, Figure 8B shows that in combination with *K. robusta*, there was no significant difference in total concentration of foliar Mn between DSE and the control. In addition, there were no significant differences of foliar Cd and Mn in both *L. scoparium* and *K. robusta* compared to the control (Figures 7 and 8).
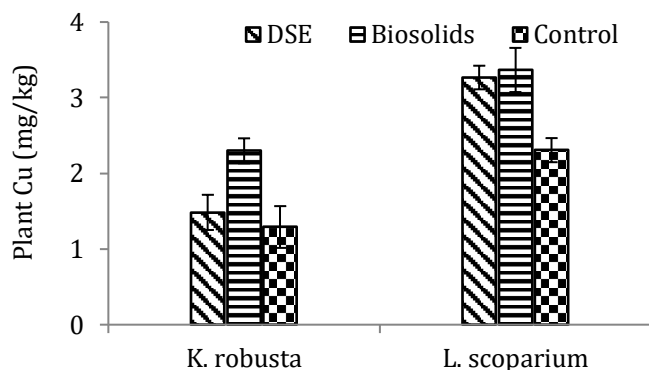
Figure 5. Total concentrations of foliar Cu (mg/kg) of *L. scoparium* and *K. robusta* measured at the end of experiment. Error bars represent the standard error of the mean. Treatment that share letters have means that do not differ significantly (p<0.05)
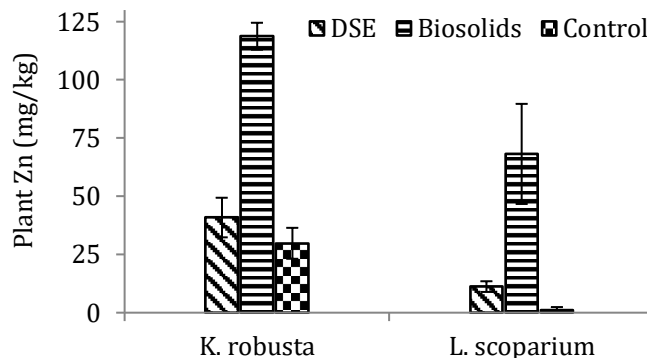
Figure 6. Total concentrations of foliar Zn (mg/kg) of *L. scoparium* and *K. robusta* measured at the end of experiment. Error bars represent the standard error of the mean. Treatment that share letters have means that do not differ significantly (p<0.05)
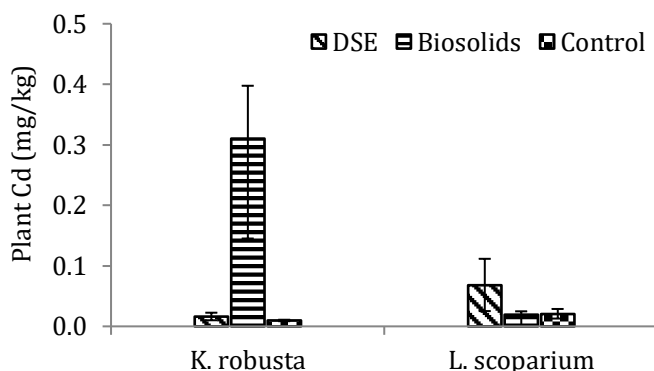
Figure 7. Total concentrations of foliar Cd (mg/kg) of *L. scoparium* and *K. robusta* measured at the end of experiment. Error bars represent the standard error of the mean. Treatment that share letters have means that do not differ significantly (p<0.05)
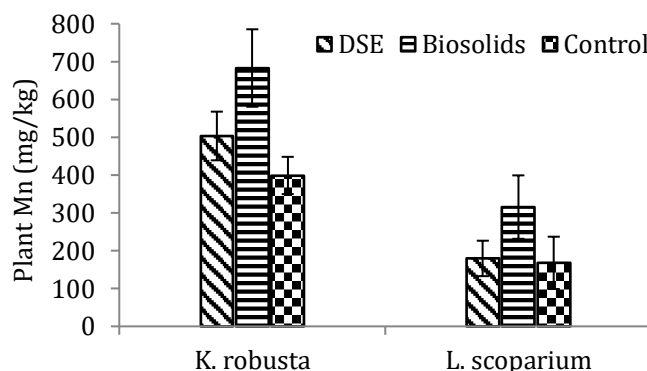

Figure 8. Total concentrations of foliar Mn (mg/kg) of *L. scoparium* and *K. robusta* measured at the end of experiment. Error bars represent the standard error of the mean. Treatment that share letters have means that do not differ significantly (p<0.05)

Discussion

Plant growth

The positive growth effects of biosolids and DSE may be due to their contribution of available nutrients, especially, N, P, K and S. As organic materials, amending these biowastes increased the concentration of organic C and, therefore, increased the Cation Exchange Capacity - CEC (Antolín et al., 2005; Weber et al., 2007; Brady and Weil, 2008), contributed in retaining nutrients and making them available to plants (Wong et al., 2001; García-Gil et al., 2004; Kaur et al., 2008; Delibacak et al., 2009). As a source of valuable nutrients, the application of DSE improved long-term soil fertility by increasing the plant available nutrients (Hawke and Summers, 2006). Esperschuetz et al. (2016) reported that adding 1250 kg N ha^{-1} equiv. of biosolids improved the growth of *Brassica napus* and *Sorghum bicolor* compared to the control. The effect of applying biosolids and DSE on plant growth could be related to role in stimulating root-microbe interactions processes (Khan, 2006), in which adding biowastes such as DSE to soil could provide a source of food for the microbes (Hawke and Summers, 2006). Mok et al. (2013) pointed out that other myrtaceae family members, *Eucalyptus polybractea* and *Eucalyptus cladocalyx* grown on biosolids produced high biomass. Moyersoen and Fitter (1999) and Weijtmans et al. (2007) reported that Ectomycorrhizal has been identified with *L. scoparium* and *K. robusta*.

Nutrients and trace elements in plant biomass

The application of biosolids and DSE to soil influenced nutrient cycling by increasing bioavailability and the uptake Ca, K, S, Cu, Zn, and Mn to plants. The biowastes may have increased nutrient cycling, making more nutrients available (Morera et al., 2002; Antolín et al., 2005; Murphy et al., 2007; Singh and Agrawal, 2008). Nutrients incorporated into organic matter can be consumed by bacteria, fungi, and other decomposers and transformed into plant-available forms. The present study found that the uptake of nutrients and contaminants associated with biowastes (NCAB) is species dependent. In combination with biosolids and DSE, both *L. scoparium* and *K. robusta* accumulated Ca, Cu, and Zn, whereas plant K, S, Mn, and Cd were only detected in biomass of *K. robusta.* These findings are in agreement with (Baldani and Döbereiner, 1980) and Mazzola

et al. (2002) who found that the role of plants in the availability and mobility of nutrients and contaminants associated with biowastes through root-microbes interaction is dependent on the species. Biosolids and DSE application could have stimulated root exudation (Koo et al., 2013), including organic acids, which have played an important role for solubilisation and mobilization of NCAB (Bertin et al., 2003), particularly elevating the availability of Zn (Keller and Römer, 2001; Hinsinger, 2001). Since exudate composition strongly varies with plant species (Walker et al., 2003), this can lead to different plant responses in terms of NCAB uptake.

Copper and Zn uptake by *L. scoparium* and *K. robusta* were higher than that of reported by Beshah et al. (2015) for other species. They found that the application of 65 t ha^{-1} dried biosolids significantly increased the accumulation of foliar Zn of oats (*Avena sativa*) by 280% (from 16 to 61 mg kg^{-1}) which are lower than our results of *L. scoparium* by 569% (increased from 1.2 to 68.2 mg kg^{-1}) and *K. robusta* by 298.3% (increased from 29.8 to 118.7 mg kg^{-1}). Mok et al. (2013) reported that two myrtaceae members, *Eucalyptus cladocalyx,* and *E. polybractea*, which were grown in a pot trial in heavy metal-contaminated biosolids reported that these species accumulated Cu (5.3 – 16.3 mg kg^{-1}) and Zn (215.4 – 2074 mg kg^{-1}), which were higher than this study. Another similar study showed that adding 65 t ha^{-1} dried biosolids significantly increased foliar Cu (Beshah et al., 2015). As reported by Beshah et al. (2015), both *Brassica napus* and *Avena sativa* increased herbage Cu by 100% (from 10 to 20 mg kg^{-1} and from 3.5 to 7.0 mg kg^{-1}), which was higher than the increases in this study. Prosser (2011) reported that the application of biosolids contained 0, 300, and 600 mg kg^{-1} Zn and 0, 100, and 200 mg kg^{-1} Cu within 6-month experimental period resulted in the accumulation of total foliar Cu and Zn in *L. scoparium* by 30-58 mg kg^{-1} and 79 – 140 mg kg^{-1} respectively, which were higher than our finding. In the present study, the DSE and biosolids contained somewhat lower concentrations of Cu and Zn the experimental period was shorted. Increasing the application rate and extending the experimental period could promote higher foliar Cu and Zn of this species. Although these elements were increased, the levels in all treatments were in the reported range of toxic thresholds (Broadley et al., 2007; Alloway, 2013). The lower concentration of foliar K found in *K. robusta* was probably influenced by either structural roles in cell walls and membranes or inter- and intracellular functions (Marschner, 2012). It is suspected that adding biosolids may have changed either chemical properties or growth environment of root. This condition is in agreement with (White and Broadley, 2003) who reported that the uptake of K mainly occurs via root tips.

Contaminants accumulation in the leaves

Concentrations of Cd in *K. robusta* were between 0.02 and 0.3 mg kg^{-1}, which has been reported as a normal range in plants (Alloway, 2013). The significant increase of Cd found in *K. robusta* biomass due to biosolids application compared to control, was not in the range that would pose a risk to human or animal health (Alloway, 2013; Esperschuetz et al., 2016). While the concentration of Cd in honey or essential oils were not measured, the low foliar concentrations indicates that transfer of excessive Cd into saleable plant products is unlikely. This indicates that biosolids can enhance uptake of essential trace elements in plant parts while not increasing toxic elements like Cd to levels dangerous for animal and human health. *L. scoparium* which did not accumulate increased contaminants from the biosolids treatment, may be safely amended with higher rates of biosolids.

Conclusion

The study demonstrated that amending low-fertility soil with 2600 kg N ha^{-1} of biosolids and 200 kg N ha^{-1} of DSE resulted in improved growth of both *L. scoparium* and *K. robusta*. This improvement was evident through increased biomass production and enhanced uptake of essential elements such as Ca, K, and S. Interestingly, *L. scoparium* exhibited better growth when combined with DSE, while both species showed similar positive responses in combination with biosolids. The application of biowastes also led to increased uptake of certain essential trace-elements and contaminants, but these levels did not exceed acceptable thresholds. Notably, the discrepancy in biomass increase between *L. scoparium* and *K. robusta* when combined with DSE compared to biosolids treatment suggests the stimulation of different types of mycorrhiza, associated with each respective species. This finding presents an intriguing area for future research. Additionally, since biosolids may have influenced plant rhizodeposition, it is recommended that future studies investigate plant root-microbe interactions concerning plant element uptake. Overall, the results indicate the potential of biosolid and DSE applications in enhancing plant growth and nutrient uptake. However, further exploration of the underlying mechanisms and long-term effects is warranted to fully understand the implications and optimize the use of these biowastes in agricultural practices.

Acknowledgment

References

Alloway, B.J., 2013. Heavy metals in soils : trace metals and metalloids in soils and their bioavailability. Springer Dordrecht. 614p.

Antolín, M.C., Pascual, I., García, C., Polo, A., Sánchez-Díaz, M., 2005. Growth, yield and solute content of barley in soils treated with sewage sludge under semiarid Mediterranean conditions. *Field Crops Research* 94(2–3): 224-237.

Antoniadis, V. 2008. Sewage sludge application and soil properties effects on short-term zinc leaching in soil columns. *Water, Air, and Soil Pollution* 190(1-4): 35-43.

Bai, Y., Gu, C., Tao, T., Wang, L., Feng, K., Shan, Y., 2013a. Growth characteristics, nutrient uptake, and metal accumulation of ryegrass (Lolium perenne L.) in sludge-amended mudflats. *Acta Agriculturae Scandinavica Section B-Soil and Plant Science* 63(4): 352-359.

Bai, Y.C., Tao, T.Y., Gu, C.H., Wang, L., Feng, K., Shan, Y.H., 2013b. Mudflat soil amendment by sewage sludge: Soil physicochemical properties, perennial ryegrass growth, and metal uptake. *Soil Science and Plant Nutrition* 59(6): 942-952.

Baldani, V.L.D., Döbereiner, J., 1980. Host-plant specificity in the infection of cereals with Azospirillum spp. *Soil Biology and Biochemistry* 12(4): 433-439.

Bertin, C., Yang, X., Weston, L.A., 2003. The role of root exudates and allelochemicals in the rhizosphere. *Plant and Soil* 256(1): 67-83.

Beshah, F.H., Porter, N.A., Wrigley, R., Meehan, B., Adams, M., 2015. Soil residuals and plant uptake of Cu and Zn from biosolids applied to a clay loam soil under field conditions in Victoria, Australia. *Soil Research* 53(7): 807-814.

Brady, N.C., Weil, R.R., 2008. The nature and properties of soil. 14th Ed.. Prentice-Hall, Upper Saddle River, New Jersey.

Broadley, M.R., White, P.J., Hammond, J.P., Zelko, I., Lux, A., 2007. Zinc in plants. *New Phytologist* 173(4): 677-702.

Brown, S., Chaney, R.L., Hallfrisch, J.G., Xue, Q., 2003. Effect of biosolids processing on lead bioavailability in an urban soil. *Journal of Environmental Quality* 32(1): 100-108.

Cline, E.T., Nguyen, Q.T., Rollins, L., Gawel, J.E., 2012. Metal stress and decreased tree growth in response to biosolids application in greenhouse seedlings and in situ Douglas-fir stands. *Environmental Pollution* 160: 139-144.

Cogger, C.G., Bary, A.I., Myhre, E.A., Fortuna, A.M., 2013. Biosolids applications to tall fescue have long-term influence on soil nitrogen, carbon, and phosphorus. *Journal of Environmental Quality* 42(2): 516-522.

Cytryn, E., Kautsky, L., Ofek, M., Mandelbaum, R.T., Minz, D., 2011. Short-term structure and functional changes in bacterial community composition following amendment with biosolids compost. *Applied Soil Ecology* 48(2): 160-167.

Delibacak, S., Okur, B., Ongun, A.R., 2009. Influence of treated sewage sludge applications on temporal variations of plant nutrients and heavy metals in a Typic Xerofluvent soil. Nutrient Cycling in Agroecosystems 83(3): 249-257.

Di, H.J., Cameron, K.C., Moore, S., Smith, N.P., 1998. Nitrate leaching from dairy shed effluent and ammonium fertiliser applied to a free-draining pasture soil under spray or flood irrigation. *New Zealand Journal of Agricultural Research* 41(2): 263-270.

Esperschuetz, J., Anderson, C., Bulman, S., Katamian, O., Horswell, J., Dickinson, N.M., Robinson, B.H., 2017. Response of Leptospermum scoparium, Kunzea robusta and Pinus radiata to contrasting biowastes. *Science of the Total Environment* 587-588: 258-265.

Esperschuetz, J., Anderson, C., Bulman, S., Lense, O., Horswell, J., Dickinson, N., Hofmann, R., Robinson, B.H., 2016. Production of Biomass crops using biowastes on low-fertility soil: 1. Influence of biowastes on plant and soil quality. *Journal of Environmental Quality* 45(6): 1960-1969.

Freeman, T., Cawthon, D., 1999. Use of composted dairy cattle solid biomass, poultry litter and municipal biosolids as greenhouse growth media. *Compost Science and Utilization* 7(3): 66-71.

Fresquez, P., Francis, R., Dennis, G., 1990. Sewage sludge effects on soil and plant quality in a degraded, semiarid grassland. *Journal of Environmental Quality* 19(2): 324-329.

Garcıa-Gil, J., Ceppi, S., Velasco, M., Polo, A., Senesi, N., 2004. Long-term effects of amendment with municipal solid waste compost on the elemental and acidic functional group composition and pH-buffer capacity of soil humic acids. *Geoderma* 121(1-2): 135-142.

Gilmour, J.T., Cogger, C.G., Jacobs, L.W., Evanylo, G.K., Sullivan, D.M., 2003. Decomposition and plant-available nitrogen in biosolids. *Journal of Environmental Quality* 32(4): 1498-1507.

Ginting, D., Kessavalou, A., Eghball, B., Doran, J.W., 2003. Greenhouse gas emissions and soil indicators four years after manure and compost applications. *Journal of Environmental Quality* 32(1): 23-32.

Hawke, R.M., Summers, S.A., 2006. Effects of land application of farm dairy effluent on soil properties: A literature review. *New Zealand Journal of Agricultural Research* 49(3): 307-320.

Haynes, R.J., Murtaza, G., Naidu, R., 2009. Inorganic and organic constituents and contaminants of biosolids: Implications for land application. *Advances in Agronomy* 104: 165-267.

Hedley, C., Lambie, S., Dando, J., 2013. Edaphic and environmental controls of soil respiration and related soil processes under two contrasting manuka and kanuka shrubland stands in North Island, New Zealand. *Soil Research* 51(5): 390-405.

Hinsinger, P., 2001. Bioavailability of soil inorganic P in the rhizosphere as affected by root-induced chemical changes: a review. *Plant and Soil* 237(2): 173-195.

Kaur, T., Brar, B., Dhillon, N., 2008. Soil organic matter dynamics as affected by long-term use of organic and inorganic fertilizers under maize–wheat cropping system. *Nutrient Cycling in Agroecosystems* 81(1): 59-69.

Keller, H., Römer, W., 2001. Cu-, Zn- und Cd-Aneignungsvermögen von zwei Spinatgenotypen in Abhängigkeit von der P-Versorgung und Wurzelexsudation. *Journal of Plant Nutrition and Soil Science* 164(3): 335-342.

Khan, A., 2006. Mycorrhizoremediation—An enhanced form of phytoremediation. *Journal of Zhejiang University SCIENCE B* 7(7): 503-514.

Kimberley, M.O., Wang, H., Wilks, P.J., Fisher, C.R., Magesan, G.N., 2004. Economic analysis of growth response from a pine plantation forest applied with biosolids. *Forest Ecology and Management* 189(1): 345-351.

Koo, B.-J., Chang, A.C., Crowley, D.E., Page, A.L., Taylor, A., 2013. Availability and plant uptake of biosolid-borne metals. *Applied and Environmental Soil Science* Article ID 892036.

Lteif, A., Whalen, J.K., Bradley, R.L., Camiré, C., 2007. Mixtures of papermill biosolids and pig slurry improve soil quality and growth of hybrid poplar. *Soil Use and Management* 23(4): 393-403.

Marschner, H., 2012. Marschner's mineral nutrition of higher plants. 3rd edition. Academic Press, Elsevier. 672p.

Mazzola, M., Granatstein, D.M., Elfving, D.C., Mullinix, K., Gu, Y.-H., 2002. Cultural management of microbial community structure to enhance growth of apple in replant soils. *Phytopathology* 92(12): 1363-1366.

Moir, J.L., Edwards, G.R., Berry, L.N., 2013. Nitrogen uptake and leaching loss of thirteen temperate grass species under high N loading. *Grass and Forage Science* 68(2): 313-325.

Mok, H.F., Majumder, R., Laidlaw, W.S., Gregory, D., Baker, A.J.M., Arndt, S.K., 2013. Native Australian species are effective in extracting multiple heavy metals from biosolids. *International Journal of Phytoremediation* 15(7): 615-632.

Morera, M., Echeverria, J., Garrido, J., 2002. Bioavailability of heavy metals in soils amended with sewage sludge. *Canadian Journal of Soil Science* 82(4): 433-438.

Moyersoen, B., Fitter, A.H., 1999. Presence of arbuscular mycorrhizas in typically ectomycorrhizal host species from Cameroon and New Zealand. *Mycorrhiza* 8(5): 247-253.

Murphy, D., Stockdale, E., Brookes, P., Goulding, K.T., 2007. Impact of microorganisms on chemical transformations in soil. In: Soil Biological Fertility. Abbott, L., Murphy, D. (Eds.). Springer, Dordrecht. pp. 37-59.

Paramashivam, D., Clough, T.J., Dickinson, N.M., Horswell, J., Lense, O., Clucas, L., Robinson, B.H., 2016. Effect of pine waste and pine biochar on nitrogen mobility in biosolids. *Journal of Environmental Quality* 45(1): 360-367.

Powlson, D., Bhogal, A., Chambers, B., Coleman, K., Macdonald, A., Goulding, K., Whitmore, A., 2012. The potential to increase soil carbon stocks through reduced tillage or organic material additions in England and Wales: a case study. *Agriculture, Ecosystems & Environment* 146(1): 23-33.

Prosser, J.A., 2011. Manuka (Leptospermum scoparium) as a remediation species for biosolids amended land. MSc Thesis, Massey University, New Zealand.

Rogers, M., Smith, S.R., 2007. Ecological impact of application of wastewater biosolids to agricultural soil. *Water and Environment Journal* 21(1) 34-40.

Simmler, M., Ciadamidaro, L., Schulin, R., Madejón, P., Reiser, R., Clucas, L., Weber, P., Robinson, B., 2013. Lignite reduces the solubility and plant uptake of cadmium in pasturelands. *Environmental Science & Technology* 47(9): 4497-4504.

Singh, R.P., Agrawal, M., 2008. Potential benefits and risks of land application of sewage sludge. *Waste Management* 28(2): 347-358.

Sullivan, T., Stromberger, M., Paschke, M., Ippolito, J., 2006. Long-term impacts of infrequent biosolids applications on chemical and microbial properties of a semi-arid rangeland soil. *Biology and Fertility of Soils* 42(3): 258-266.

Walker, T.S., Bais, H.P., Grotewold, E., Vivanco, J.M., 2003. Root exudation and rhizosphere biology. *Plant Physiology* 132(1): 44-51.

Wang, B., Liu, L., Gao, Y., Chen, J., 2009. Improved phytoremediation of oilseed rape (Brassica napus) by Trichoderma mutant constructed by restriction enzyme-mediated integration (REMI) in cadmium polluted soil. *Chemosphere* 74(10): 1400-1403.

Wang, X., Jia, Y., 2010. Study on adsorption and remediation of heavy metals by poplar and larch in contaminated soil. *Environmental Science and Pollution Research* 17(7): 1331-1338.

Weber, J., Karczewska, A., Drozd, J., Licznar, M., Licznar, S., Jamroz, E., Kocowicz, A., 2007. Agricultural and ecological aspects of a sandy soil as affected by the application of municipal solid waste composts. *Soil Biology and Biochemistry* 39(6): 1294-1302.

Weijtmans, K., Davis, M., Clinton, P., Kuyper, T.W., Greenfield, L., 2007. Occurrence of arbuscular mycorrhiza and ectomycorrhiza on Leptospermum scoparium from the Rakaia catchment, Canterbury. *New Zealand Journal of Ecology* 31(2): 255-260.

White, P.J., Broadley, M.R., 2003. Calcium in plants. *Annals of Botany* 92(4): 487-511.

Wong, J.W.C., Lai, K.M., Su, D.C., Fang, M., Zhou, L.X., 2001. Effect of applying Hong Kong biosolids and lime on nutrient availability and plant growth in an acidic loamy soil. *Environmental Technology* 22(12): 1487-1495.

Zaman, M., Cameron, K.C., Di, H.J., Inubushi, K., 2002. Changes in mineral N, microbial biomass and enzyme activities in different soil depths after surface applications of dairy shed effluent and chemical fertilizer. *Nutrient Cycling in Agroecosystems* 63(2-3): 275-290.

Zaman, M., Di, H.J., Cameron, K.C., Frampton, C.M., 1999. Gross nitrogen mineralization and nitrification rates and their relationships to enzyme activities and the soil microbial biomass in soils treated with dairy shed effluent and ammonium fertilizer at different water potentials. *Biology and Fertility of Soils* 29(2): 178-186.

Eurasian Journal of Soil Science

Journal homepage : http://ejss.fesss.org
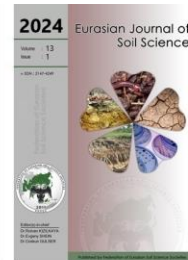
Effect of organic pest control products on Arbuscular Mycorrhizal colonization in Bulgarian rose plantations: A two-year field study

Rumyana Georgieva [a,*], Siegrid Steinkellner [b], Ivan Manolov [c], Paul John M. Pangilinan [d], Desmond Kwayela Sama [e]

[a] Agricultural University of Plovdiv, Faculty of Agronomy, Department of Crop Science, Mendeleev blvd 12, 4000 Plovdiv, Bulgaria

[b] University of Natural Resources and Life Sciences, Department of Crop Science, Institute of Plant Protection, Gregor-Mendel-Straße 33 A, 1180 Vienna, Austria

[c] Agricultural University of Plovdiv, Faculty of Agronomy, Department of Agrochemistry and Soil Science, Mendeleev blvd 12, 4000 Plovdiv, Bulgaria

[d] Central Luzon State University, Science City of Muñoz, Nueva Ecija, Philippines

[e] Ondokuz Mayıs University, Faculty of Agriculture, Department of Soil Science and Plant Nutrition, Samsun, Türkiye

Abstract

This two-year field study aims to investigate the impact of organic pesticides used in organic Damask rose (*Rosa damascena* Mill.) fields on Arbuscular Mycorrhizal Fungal (AMF) colonization. Conducted in the renowned Rose Valley of Bulgaria, specifically in the village of Kliment, the experiment employed a randomized complete block design with two rows of 21 plants each in organic certified plots. The results revealed low AMF colonization in the first year, ranging between 14.78% and 20.89%, with no significant differences between treatments. In the second year, while no significant differences were observed between treatments (ranging from 48.00% to 76.49%), there was a notable increase in AMF colonization compared to the initial sampling. The study concluded that specific organic pesticides, including Neemazal, Limocide, Phytosev, and Nano sulfur, had minimal negative effects on AMF colonization. These findings contribute to understanding the implications of organic farming practices on AMF and soil health in the context of Damask rose cultivation.

Keywords: Arbuscular mycorrhiza, oil-bearing rose, organic production.

Introduction

Mycorrhizal association is a natural symbiotic relationship between endophytic fungi and several higher plant species. It poses a number of beneficial effects that ranges from improvement of basic growth parameters (Nadeem et al., 2014) and biotic and abiotic stress mitigation (Abdel-Salam et al., 2017; Begum et al., 2019). Under the paradigm of organic farming, such natural interactions are capitalized to help attain an economical sustainable and ecologically sound system which has the potential to outperform conventional production systems (Gamage et al., 2023).

Bulgaria is among the biggest exporter and producer of rose oil with the highest quality. Roses in particular, an economic and culturally important crop, is grown in about 5.269 ha of land and contributes most of the total contribution of the cut-flower industry (Ministry of Agriculture, 2022). Various products such as essences and cut-flowers are also important commodities produced by Bulgarian farmers (Tineva and Nencheva, 2021). Both the quantity and quality of these products are affected by basic growth parameters such as primal and lateral root and shoot growth, number of floral primordia and inflorescence induction time. Bulgarian rose production continues to fluctuate as a result of unstable climatic patterns, shorting cultivation cycles and degrading soil conditions. For instance, in 2022 there has been a recorded decrease in the total rose petal and oil production due to higher amount of precipitations. Arbuscular Mycorrhizal Fungi (AMF) can improve soil health and functioning leading to a more resilient system and affect the plant's growth

parameters by enhancing root nutrient absorption capacity and serve as a natural protection against other pathogenic microorganisms (Begum et al., 2019).

Under the EU provisions and regulations, certain organically based biocontrol agents are allowed to be used. Their compounds may range from natural extracts (e.g. Neem Extract) to biosynthetic compounds and volatiles. The extent of influence of these compounds on the below-ground ecosystem is not yet fully explored and its influence on its functioning which has a significant influence of the quantity and quality of produce (Hage-Ahmed, 2019). This study evaluated the degree of mycorrhizal colonization in organically grown roses in village Kliment, Bulgaria supplemented by various pesticides permissible for organic production under EU regulations.

Material and Methods

Description of the location

The experiment was carried out with organic Damasc Rose (*Rosa damascena* Mill.) in the region of the village Kliment, Bulgaria (W: 42.59699739096776, L: 24.682717358466093) for two consecutive years, 2022 and 2023. The village of Kliment is part of the famous Rose Valley of Bulgaria, where is concentrated the oil-bearing rose production. The region is surrounded by mountains and well protected from north cold winds. The rivers Stryama and Tundzha provide good water supply for the rose plantations.

Site characterization

The soil cover in the Rose Valley is represented by deluvial noncalcareous sediments (Todorova et al., 2020). The colluvium is presented by rock fragments consisting of sand, silt, and clay, which are collected at the base of steep slopes. According to the World Reference Base for Soil Resources (WRB) the soils in the region are classified as *Fluvisols*. In these deluvial soils, the content of organic matter naturally decreases over time. The pH reaction of the soil is acid, which is characteristic for this soil type.

Soil analysis

Soil samples have been taken annually from the layer 0-30 cm, to determine the pH and content of mineral nitrogen, available phosphorus (P_2O_5) and exchanged potassium (K_2O) and analyzed in the accredited laboratory complex at the Agricultural University, Plovdiv. In the present investigation the pH values were determined by potentiometric method and the values ranged between 4.37 in 2022 to 5. 74 in 2023. Because of liming made by farmer owner of the plantation soil pH was increased in the second year. The humus content for the upper horizons by Turin varied between 3.32 to 3.87%. The mineral nitrogen content was determined by the Kjeldahl method as the values ranged between 14.47 to 15.68 mg kg^{-1} for the first and the second year respectively. Available potassium and available phosphorus content was evaluated using the Egner-Riem method. In terms of mobile phosphorus content, the values were in the range of 12.67 mg 100 g^{-1} in 2022 to 12.85 mg 100 g^{-1} in 2023. The content of available potassium ranged between 16.60 mg 100 g^{-1} and 17.27 mg 100 g^{-1}. The content of SOC was measured according to the Nikitin-modified Tyurin method using the spectrophotometric procedure at the wavelength of 590 nm (Slepetiene et al., 2023). For the study period the values of SOC varied between 14.9 mg g^{-1} and 15.7 mg g^{-1}.

Wheater conditions

The oil-bearing rose is a plant of the cool climate. The soft winter, the long and humid spring and the cool summer which are characteristic of the area, create the ideal conditions for growing the crop. The air in the closed valley fields contributes to the formation of abundant dew during rose-picking and protects rose oil from evaporation. Another important characteristic of the valley is the big temperature amplitude, which is necessary for the staking and the growth of the buttons, as well as for the storage of the formed essential oil. The climate is transitional continental and annual precipitation amount is 930 mm. The climatic conditions during the years of the experiment are presented in detail in Table 1. The evenly distributed rainfall and moderate average monthly temperatures create good conditions for the development of rose plants.

Table.1. Climate conditions

Year	Temperature (⁰C)											
	I	II	III	IV	V	VI	VII	VIII	IX	X	XI	XII
2022	3.2	7.1	9.2	12.0	16.0	22.7	26.0	26.5	20.0	12.4	10.2	4.5
2023	1.5	6.4	9.6	14.0	17.3	24.2	28.0	28.3	21.7	15.0	13.4	4.6
long-term average	0.5	2.2	5.1	10.0	16.5	20.8	24.5	24.5	17.4	14.3	8.5	2.0
	Precipitation (mm)											
2022	55.1	35.6	58.0	62.3	68.8	62.0	41.7	45.3	85.4	92.0	78.7	105.5
2023	61.0	73.3	90.2	80.0	120.2	115.4	60.3	62.2	95.8	103.9	62.3	92.0
long-term average	70.0	80.4	72.8	72.0	110.4	50.5	40.0	50.5	100.2	80.0	115.0	90.0

Experimental setup

Since the experiment is established with a five-year-old rose plantation, the purpose of the study is to determine the presence of natural mycorrhiza. No mycorrhizal fungus inoculation was applied. Oil-bearing rose is a perennial plant and the right agrotechnical approach is of great importance for the optimal development and prolonged exploitation of the plantation. In the spring, with the beginning of the growing season, the inter-rows were plowed at a depth of 18-20 cm. The soil has been cultivated twice before the period of blooming at a depth of 5-6 cm. The nutritional regime of the roses was improved through the application of 2% solution of the leaf fertilizer Acramet Ultra® (N – 12.5%, P_2O_5 - 5.7 % K_2O - 11%; S-2.9%; B-0.35%; Cu- 0.025%; Mg-0.48%; Mn-0.028%; Zn-0.125%; Fe - 0.026%; Mo-0.024%; ultratrace elements – cobalt, chromium, vanadium). The product was applied twice in 15 days before flowering. Weed control was achieved mechanically. In autumn the area was fertilized annually with 20 t ha^{-1} organic manure, which is ploughed with the last tillage. Before the last cultivation in October 2022, the soil was limed (ground limestone in a dose of 3t ha^{-1}) to adjust the pH value. Due to lack of built irrigation systems, the area was not irrigated, as the producer relied on the drought resistance of the plant and the uniform distribution of rainfall in the Rose Valley.

Four organically certified insect pest control products, Phytosev®, Limocide® , Nano sulfur (Calcium polysulfide-CaS5 (20nm)), Neemazal® and one biological agent- *Chrysoperla carnea* (Stephens) were employed as treatments. Each plot in the field had two rows of plants (21 plant in total). The plot was 6 m in length and 3 m in width. The field was set up in a randomized complete block design in four replications. Rows were spaced 3 m apart, with 0.40 m inter row space. In order to determine the percentage of Arbuscular mycorrhiza fungal colonization, root samples were taken during the picking period on 26th of May during the first year (2022) and on 5th of June during the second year (2023). The products have been applied three times in the interval of 10 days in April and May depending on the weather but not later than 10 days before the harvest of the rose flowers at the respective doses shown in Table 2. The bioagent *Chrisoperla carnea* has been released 3 times during the springtime depending on the aphid's population.

Table 2. Description of the applied biological products

Product name	Manufacturer	Active substances	Applied amount
NeemAzal® T/C	Trifolio-M GmbH	azadirachtin A -1%; azadirachtin B, C, D, D-0.5 %; Nime-substance – 2.5 %	4 g ha^{-1}
Limocid ®	Vivagro	60 g/L orange oil	2000 ml ha^{-1}
Nano sulfur ®	Bio fertilizer Ltd Bulgaria	Calcium polysulfide – CaS5 (size 20 nm) – 230 g/l.	300 ml ha^{-1}
FytoSave®	Fytofend S.A	oligosaccharides COS-OGA 12.5 g l^{-1}	200 ml ha^{-1}

Root sample collection

For the assessment of the percentage of arbuscular mycorrhizal root colonization (Betancur-Agudelo et al., 2021), rose roots have been sampled from the field experiment after harvest in 2022 and 2023. Three 500 g soil samples (0–20 cm depth) pro variant were collected from randomly selected rose plants during the intensive vegetation period. Fine roots were rinsed free from soil and 2 cm down the hypocotyl, 2 cm root segments were used for the further staining procedure for determination of the mycorrhiza.

Root clearing and staining

A modified staining procedure (Phillips and Hayman, 1970) was performed on the fine rose root samples taken from Plovdiv, Bulgaria. 5-10 mL of 10% KOH was added to falcon tubes containing the root samples. The samples were then placed into a water bath at 70°C for 20 min. This was done to remove the natural pigments and facilitate easier visualization of AMF structures; excess KOH solution was then discarded afterwards, and the samples were rinsed with distilled water. 10 mL of 3.5% H_2O_2 was added to remove any remaining pigments. The samples were then placed in a water bath at 70 °C for 5 minutes. Afterwards, the samples were rinsed with 1:1 water : vinegar solution to acidify the roots for better staining results. 5-10 mL of 5% vinegar: ink solution was used to stain the roots. Samples were placed in a water bath at 70 °C for 20 mins.

Data gathering

Gridline intersection method (Newman, 1966; Giovanetti, 1980) was used to estimate the degree of AMF colonization, an improvised counting plate was made by drawing 10 mm x 10 mm grid on its surface using a scalpel. Root samples were then placed on the counting plate and the number of positive and total intersections was assessed. Degree of root colonization was calculated using the formula;

$$\text{Root Colonization Percentage} = \frac{\text{Number of AMF Positive Intersections}}{\text{Total Number of Intersections}} \times 100\%$$

Data analysis

Statistical analysis was performed using Statistical Tool for Agricultural Research (STAR). Colonization percentage 2022 and 2023 were analyzed using one-way ANOVA, least significant differences were assessed using Tukey's HSD Test.

Results and Discussion

Site Characterization

Organic agriculture is the answer to the need for sustainable agriculture and biodiversity conservation. The main challenges which are facing Bulgarian rose growers are resistance to diseases, combined with appropriate genotype conservation and plant propagation in order to maintain the necessary traditional aroma and chemical composition of rose oil (Chalova et al., 2017). Due to the lack of resistance of R. damascena to the major diseases and pests and the prohibition on the use of chemical treatments the cultivation of healthy plants in organic farming is difficult. When developing the plant protection strategy the rose growers rely mainly on self experience. These study aims to observe if the tested products, which are effective against the main pests and deseas of roses have negative action on the mycorrhizal colonization. There is a lack of information about the presence of AMF in the rose plantations in the Rose Valley of Bulgaria. AMF are of great importance especially in organic farming systems because they are not only improving the soil nutritional properties, but also increasing the crop yields (Gosling et al., 2006).

AVM Colonization

During the initial phases of the project (2022), results reveal low AMF colonization ranging in between 14.78 ± 4.44 % to 20.89 ± 14.89 % showing no significant differences between treatments. No-significant differences between treatments was also observed (48.00 ± 11.00 % to 76.49 ± 8.21 %) during the second sampling (2023), but AMF colonization increased sigficantly as compared to initial sampling (Figure 1).
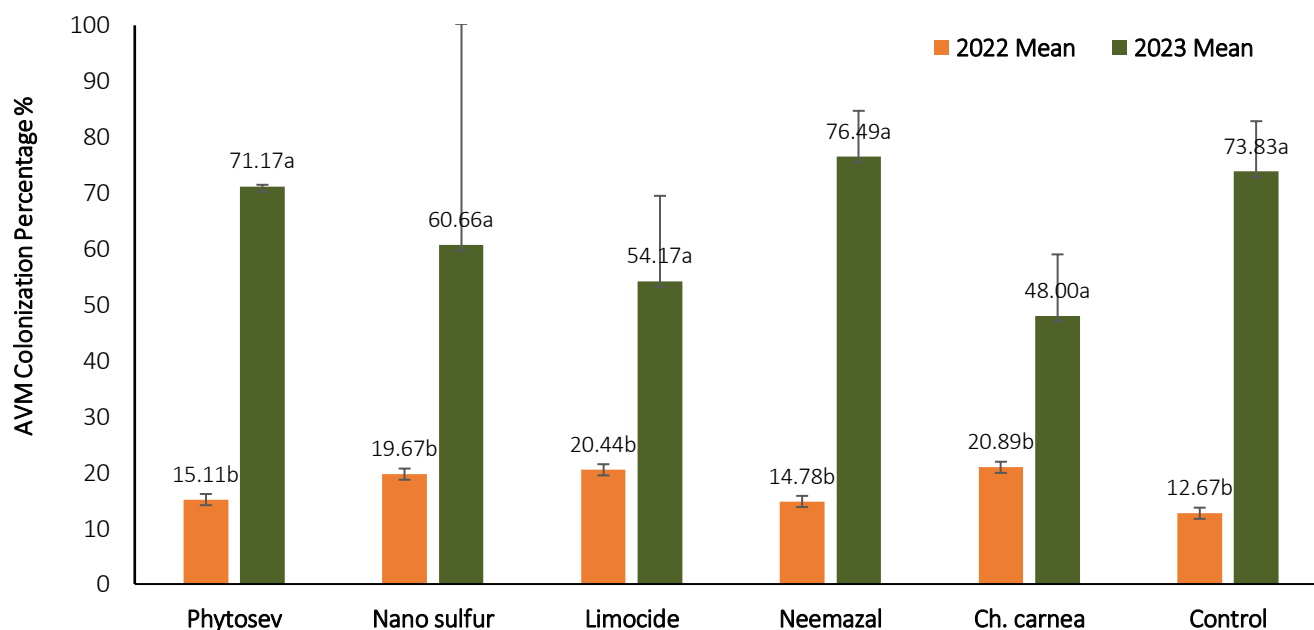
Figure 1. Rose Roots AMF Colonization Percentage

Pesticides can alter soil microbiological and chemical properties depending on several factors but the major of them are the amount of active ingredient which enters the soil system, the degradability of active substance and the mode of action of the active substance in relation to key physiological processes (Hage-Ahmed 2019; Tian et. al., 2019). Soil conditions especially hydraulic conductivity, organic matter content and texture significantly affect the amount of active ingredient in the soil (Yu et al., 2010; Mosquera-Vivas et al., 2023). There are relatively few studies related to the effect of Neemazal, Limocide, Phytosev and Nano sulfur on mycorrhizal species, but significant reduction in mycelial growth has been observed in some commonly fungal genera as these compounds affect key physiological processes such as chitin synthesis and ergosterol production (Tian et. al., 2019; Kilani-Morakchi et al., 2021; Jian et. al., 2023). Gopal et al (2006) stated, that azadirachtin applied in higher doses has negative effect on fungi and nitrifying bacteria. The field application of azadirachtin had no significant influence on mycorrhizal colonization but modified the structure of the AMF community (Ipsilantis et al., 2012). The same author observed the stimulating action of terpenes on the

mycorrhizal colonization. When applied in combination with AMF inoculation azadirachtin could increase the root colonization (Bharadwaj and Sharma, 2006). Organic plant protection products are increasingly used as they respect the principles of sustainable agriculture. Few studies have investigated the action of those products on non-target organisms, such as the soil microbiome and the AMF. Some authors reported stimulatory effect of insecticides on arbuscular mycorrhizal fungal colonization, as well as on plant growth (Schweiger and Jacobsen, 1997; Schweiger et al., 2001).

The absence of significant differences in the mycorrhizal colonization of the treated plants with respect to the control plants and the significant increase in AMF colonization from 2022-2023 presents that with the application of compounds for pest control allowed for use in organic crop production, there is minimal effect on mycorrhizal colonization (Figure 1). This result can also be explained by the relationship between pesticide interference on mycorrhizal on both pre- and post-symbiotic phases. Since treatments were applied on an already established rose plantation, it can be said that a symbiotic community has already been established prior to the study. The more acidic soil reaction and the higher amount of precipitation in 2022 could also have negative effect on the mycorrhizal fungi colonization rate, but the influence must be further investigated.

Conclusion

The present study is the first which investigated the effect of biological products for plant protection on the AMF density in organic oil-bearing rose plantation. The results prove the presence of natural AMF on the roots of *Rosa damascena* Mill. The applied products didn't negatively affect the AMF density, but their action on non-target organisms should be further investigated. Probably the more acid soil reaction and the higher amount of precipitations during the first year of the experiment had left to lower mycorrhizal fungi colonization rate, but there is a need of further investigation and observation to make a concrete conclusions, because various factors could affect the soil rhizobium. Further experiments will investigate the impact of organic products on the colonization ability and the community structure of AMF on oil-bearing roses roots.

Acknowledgment

References

Abdel-Salam, E., Alatar, A., El-Sheikh, M.A., 2018. Inoculation with arbuscular mycorrhizal fungi alleviates harmful effects of drought stress on damask rose. *Saudi Journal of Biological Sciences* 25(8): 1772-1780.

Begum, N., Qin, C., Ahanger, M. A., Raza, S., Khan, M. I., Ashraf, M., Ahmed, N., Zhang, L., 2019. Role of Arbuscular mycorrhizal fungi in plant growth regulation: Implications in abiotic stress tolerance. *Frontiers in Plant Science* 10: 466052.

Betancur-Agudelo, M., Meyer, E., Lovato, P.E., 2021. Arbuscular mycorrhizal fungus richness in the soil and root colonization in vineyards of different ages. *Rhizosphere* 17: 100307.

Bharadwaj, A., Sharma, S. 2006. Biocontrol of Meloidogyne incognita in Lycopersicon esculentum with AM fungi and oil cakes. *Plant Pathology Journal* 5: 166-172.

Chalova, V.I., Manolov, I.G., Manolova, V.S., 2017. Challenges for commercial organic production of oil-bearing rose in Bulgaria. *Biological Agriculture & Horticulture* 33: 1-12.

Gamage, A., Gangahagedara, R., Gamage, J., Jayasinghe, N., Kodikara, N., Suraweera, P., Merah, O., 2023. Role of organic farming for achieving sustainability in agriculture. *Farming System* 1(1): 100005.

Giovanetti, M., Mosse, B., 1980. An evaluation of techniques for measuring vesicular arbuscular mycorrhizal infection in roots. *New Phytologist* 84(3): 489-500.

Gopal, M., Gupta, A., Arunachalam, V., Magu, S.P., 2007. Impact of azadirachtin, an insecticidal allelochemical from neem on soil microflora, enzyme and respiratory activities. *Bioresource Technology* 98(16): 3154-3158.

Gosling, P., Hodge, A., Goodlass, G., Bending, G.D., 2006. Arbuscular mycorrhizal fungi and organic farming. *Agriculture, Ecosystems & Environment* 113(1-4): 17-35.

Hage-Ahmed, K., Rosner, K., Steinkellner, S., 2019. Arbuscular mycorrhizal fungi and their response to pesticides. *Pest Management Science* 75(3): 583-590.

Ipsilantis, I., Samourelis, C., Karpouzas, D.G., 2012. The impact of biological pesticides on arbuscular mycorrhizal fungi. *Soil Biology & Biochemistry* 45: 147-155.

Jian, Y., Chen, X., Ma, H., Zhang, C., Luo, Y., Jiang, J., Yin, Y., 2023. Limonene formulation exhibited potential application in the control of mycelial growth and deoxynivalenol production in Fusarium graminearum. *Frontiers in Microbiology* 14: 1161244.

Kilani-Morakchi, S., Morakchi-Goudjil, H., Karima, S., 2021. Azadirachtin-based insecticide: Overview, risk assessments, and future directions. *Frontiers in Agronomy* 3: 676208.

Ministry of Agriculture, 2022. Annual Report on the State and Development of Agriculture – Bulgaria Ministry of Agriculture Report 2022. Bulgaria

Mosquera-Vivas, C.S., Celis-Ossa, R.E., González-Murillo, C.A., Obregón-Neira, N., Martínez-Cordón, M.J., Guerrero-Dallos, J.A., García-Santos, G., 2023. Empirical model to assess leaching of pesticides in soil under a steady-state flow and tropical conditions. *International Journal of Environmental Science and Technology* 21: 1301–1320.

Nadeem, S.M., Ahmad, M., Zahir, Z.A., Javaid, A., Ashraf, M., 2014. The role of mycorrhizae and plant growth promoting rhizobacteria (PGPR) in improving crop productivity under stressful environments. *Biotechnology Advances* 32(2): 429-448.

Nencheva, V., Tineva, N., 2021. Bulgarian rose oil industry-challenges and motors of growth. Proceedings; Industrial Growth Conference 2020. University of National and World Economy, Sofia, Bulgaria.

Newman, E.I., 1966. A method of estimating the total length of root in a sample. *Journal of Applied Ecology* 3(1): 139-145.

Phillips, J.M., Hayman, D.S., 1970. Improved procedures for clearing roots and staining parasitic and vesicular-arbuscular mycorrhizal fungi for rapid assessment of infection. *Transactions of the British Mycological Society* 5(1): 158-161.

Schweiger, P.F., Jakobsen, I., 1997. Dose–response relationships between four pesticides and phosphorus uptake by hyphae of arbuscular mycorrhizas. *Soil Biology and Biochemistry* 30(10-11): 1415-1422.

Schweiger, P.F., Spliid, N.H., Jakobsen, I., 2001. Fungicide application and phosphorus uptake by hyphae of arbuscular mycorrhizal fungi into field-grown peas. *Soil Biology and Biochemistry* 33(9): 1231-1237.

Slepetiene, A., Ceseviciene, J., Amaleviciute-Volunge, K., Mankeviciene, A., Parasotas, I., Skersiene, A., Jurgutis, L., Volungevicius, J., Veteikis, D., Mockeviciene, I., 2023. Solid and liquid phases of anaerobic digestate for sustainable use of agricultural soil. *Sustainability* 15(2), 1345.

Tian, H., Kah, M., Kariman, K., 2019. Are nanoparticles a threat to mycorrhizal and rhizobial symbioses? A critical review. *Frontiers in Microbiology* 10: 456732.

Todorova, M., Grozeva, N., Gerdzhikova, M., Dobreva, A., Terzieva, S., 2020. Productivity of oil-bearing roses under organic and conventional systems. Scientific Papers of University of Agronomic Sciences and Veterinary Medicine of Bucharest, Romania, Series A, Agronomy, Vol. LXIII,(1): 580 – 585.

Yu, X., Pan, L., Ying, G., Kookana, R.S., 2010. Enhanced and irreversible sorption of pesticide pyrimethanil by soil amended with biochars. *Journal of Environmental Sciences* 22(4): 615–620.

Zhang, W., Yu, L., Han, B., Liu, K., Shao, X., 2022. Mycorrhizal inoculation enhances nutrient absorption and induces insect-resistant defense of Elymus nutans. *Frontiers in Plant Science* 13: 898969.

Eurasian Journal of Soil Science

Journal homepage : http://ejss.fesss.org
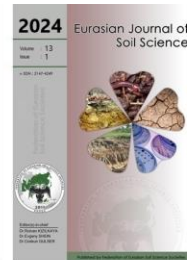
Distribution of soil minerals along the toposequence of Hyang-Argopuro Volcanic Mountain, Jember, Indonesia

Cahyoadi Bowo [a,*], Wahyu Hidayat [a], Victor B. Asio [b]

[a] Department of Soil Science, Faculty of Agriculture, University of Jember, Indonesia
[b] Department of Soil Science, College of Agriculture and Food Science, Visayas State University, Baybay City, Philippines

Abstract

Author(s)
C.Bowo *
W.Hidayat
V.B.Asio

* Corresponding author

The study was conducted in the Hyang-Argopuro volcanic mountain in Jember, Indonesia, with the aim of assessing the distribution of soil minerals along a toposequence and their relationship to soil genesis. Three soil profiles representing the upper, middle, and lower slopes of the toposequence were analyzed. The results revealed that the predominant sand minerals in the soils are opaque minerals, weatherable minerals, amphibole groups, and ferromagnesian minerals. The presence of magnetite, primarily found in the soil profile on the upper slope, suggests the effect of the well-drained topography on its formation. Clay mineral analysis showed that halloysite dominates in soil profile 1, along with traces of gibbsite and cristobalite in the surface horizon. Soil profile 2 is characterized by a combination of halloysite and illite, while kaolinite and illite dominate in soil profile 3. The presence of illite in these soils aligns with previous studies conducted in volcanic regions. The degree of soil development follows the sequence: Soil Profile 2 > Soil Profile 1 > Soil Profile 3. This corresponds to the soil classification, where soil profile 3 is classified as an Alfisol, soil profile 1 as a Mollisol, and soil profile 3 as an Inceptisol. The Andic properties, such as low bulk density and high pH in NaF, observed in soil profile 1 suggest its development from an Andisol. Overall, the study findings highlight the significant influence of basaltic andesite parent material, mountainous topography, and warm and wet climate on the mineral composition and development in the area.

Keywords: Soil development, toposequence, tuff, volcanic minerals.

Introduction

Soils are formed from the interactions of parent material, climate, topography, organism, and time. Parent material, the geologic material from which a soil develops, influences the mineral composition of young soils produced but not the old or highly weathered soils (Chesworth, 1973; Buol et al., 2011; Blume et al., 2016). Likewise, parent material composition affects soil texture. For instance, quartz-rich parent materials such as granite and sandstone produce coarse-textured young soils, while alkaline parent rocks produce fine-textured soils. It has also been shown that the amount of feldspar in the parent rock is directly related to the amount of clay in the soil that is formed (Birkeland, 1984). Moreover, Blume et al. (2016) noted that the direction and intensity of soil development depend strongly on the parent rock's compactness, mineral composition, and texture. Deeper soils form from unconsolidated sediments compared to those neighboring soils from hard rock, even if these have been disintegrated through weathering.

Soil minerals are divided into two groups, namely primary and secondary minerals. Primary minerals are minerals formed from crystallization of magma inside the earth or of lava during volcanic eruption, while secondary minerals result from the alteration of primary minerals (Blume et al., 2016). The actual mineral assemblage in soils may originate from the minerals coming from other rocks and soils transported by air, water, or gravity; from minerals inherited from the parent rock; as relictic materials from paleoenvironments; and as products of neoformation, transformation, and destruction of minerals under the current environment (Stahr, 1994).

Soil minerals distribution may vary vertically with soil depth and horizontally in the toposequence, a sequence of related soils that vary in topography or physiographic position. The vertical distribution is generally a function of the composition of the parent material, degree of weathering, pedoturbation, and anthropogenic influences. On the other hand, the horizontal distribution of soil minerals in the toposequence is generally the effect of topography and land use (Duchaufour, 1977; Buol et al., 2011). Topography controls the movement of water and materials along the slope (Duchaufour, 1977; Blume et al., 2016). Topography can change the mineralogical arrangement in the soil even though the soil comes from the same parent material. Along the slopes is one of the simplest but most elegant ways to spatially distinguish the reciprocal relationship between soil and topography (Schaetzl and Anderson, 2005).

Limited studies have been done on the distribution of soil minerals in the humid tropics, such as in the Argopuro volcanic mountains in Jember, Indonesia. Research on the distribution of soil minerals is relevant since it can provide new knowledge about the development, characteristics, and nutrient status of soils which in turn are crucial for the sustainable management of soil resources. Thus, the aim of this study was to evaluate the distribution of soil minerals in the toposequence of the Hyang-Argopuro volcanic mountain in Jember, Indonesia, and examine their relationship with soil genesis. By analyzing three soil profiles representing the upper, middle, and lower slopes of the toposequence, we aimed to determine the dominant soil minerals and their variations across the landscape. Additionally, we aimed to investigate the influence of factors such as topography, parent material (basaltic andesite), and climate (warm and wet) on the mineral composition and development of the soils. Understanding the spatial distribution of soil minerals and their associations with soil genesis can provide valuable insights into the formation processes and landscape dynamics of volcanic regions.

Material and Methods

The study was conducted in the Jelbuk Sub-district on the southeastern slope of the mountains of Argopuro. Generally, the shape of the land is undulating with a slope of <3% to hilly with a slope of 25%. The altitude of the study area ranges from 300 masl – 1,110 m asl. Physiographically, the area is part of the footslope and midslope of the Argopuro volcanic complex.

The study area comprises of Argopuro Breccia (Qvab) Formation, an andesitic volcanic breccia, and lava inclusions. This unit is the result of the last Gunung Hyang-Argopuro geological formation activity. Under the Argopuro Breccia (Qvab) unit, there is an Argopuro Tuff unit (Qvat), with tuff as the primary unit consisting of interrupted tuffs, ash tuffs, and glass tuffs. Interrupted tuffs consist of andesite pyroxene compiled rock fragments with porphyritic textures (Sapei et al., 1992). Jelbuk Subdistrict has an average annual rainfall of 2,335 mm with seven rainy months starting from October to April. The climate station used in this study was located 5 km from the furthest sample point (upper slope) location. Annual rainfall data were obtained from the average annual rainfall over the past 15 years (Figure 1).
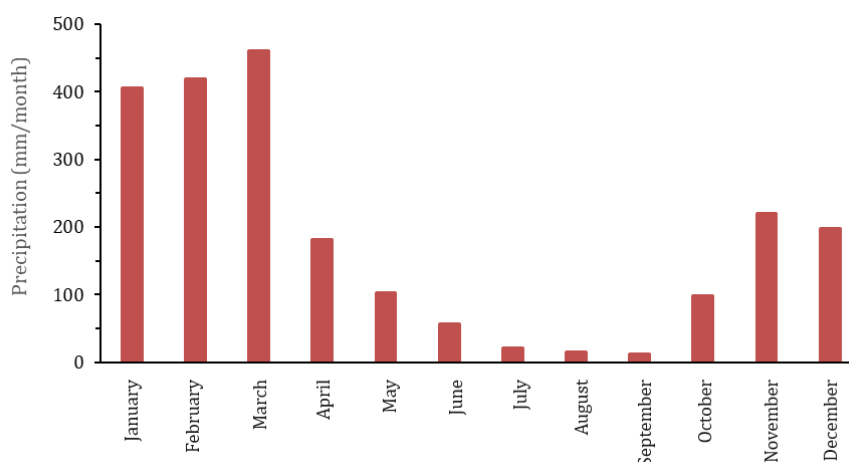
Figure 1. Rainfall distribution in the study area (2000 – 2015)

To select the three (3) soil profiles for the study, a seven (7) km transect was chosen from the upper to the lower slope of the study area (Figure 2a,b). The first soil profile 1 representing the upper slope was dug at an altitude of 1,110 masl with coordinates of 08002'06.07 "S. - 113042'05.17" E. The soil profile 2 representing the middle slope, was excavated at an altitude of 600 m.a.s.l with coordinates of 08002'09.46 "S. - 113043'05.46 E. Soil profile 3 representing the lower slope was located at an altitude of 327 masl and coordinates of 08003'08.31" S - 113045'08.77 E.
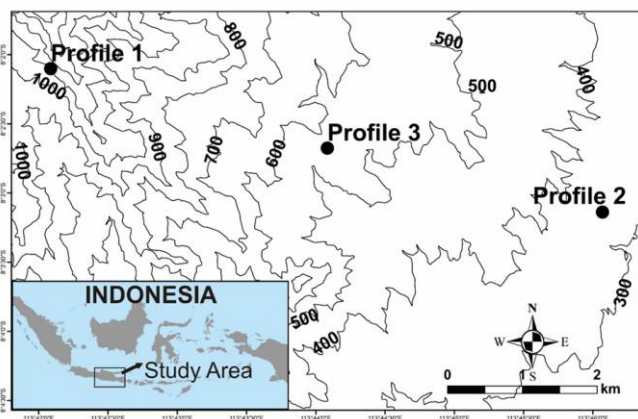
Transect map of soil profiles location in the Jelbuk Subdistrict, Jember
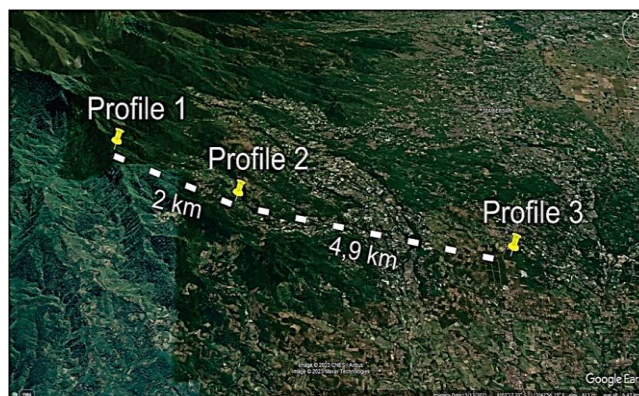
Figure 2b. Aerial map of transect location (Source: Google Earth, accessed in May 2021)

Each soil profile was described following the FAO Guidelines for Soil Description, and then about 1.0 kg of soil samples were collected from each horizon for laboratory soil analysis. The samples were transported to the laboratory, air-dried, freed of rocks and plant debris, ground using a wooden hammer, and sieved using a 2.0 mm mesh sieve. The analyses performed included the actual soil pH measured by mixing soil and aquadest with a ratio of 1: 2.5 m/v, the potential pH is measured by mixing soil with 1 M KCl by a ratio of 1: 2.5 m/v and then reading the pH values with the use of a pH meter (Balai Penelitian Tanah, 2005). Soil texture was analyzed by pipette method after organic matter destruction using a 10% H_2O_2 and clay dispersion using $Na_4P_2O_7.10$ H_2O (Balai Penelitian Tanah, 2005). Bulk density was measured using the core method, and particle density was determined based on measurements of the mass and volume of soil particles. Saturated hydraulic conductivity was measured using laboratory methods (Balai Penelitian Tanah, 2005). The mineral composition of the sand fraction was determined by the line-counting method. Crystalline soil minerals were determined on the Random Powder Specimen using XRD (X-ray diffraction) (Van Reeuwijk, 2002).

Results and Discussion

Soil morphological, physical, and chemical characteristics

Soil horizon differentiation is an essential parameter in evaluating soil development. Results revealed that the horizons arrangement on the upper slope is Ah1 – Ah2 - AB – Bw1 – Bw2, on the middle slope is Ap - AB - Bt1 - Bt2 – Bt3, and on the lower slope is Ah1 – Ah2 - Bw - BC - 2A - 2Bw1 - 2Bw2 (Table 1).

Table 1. Soil morphology in toposequence

Horizon	Soil Depth (cm)	Soil Color (wet)	Soil Texture	Structure	Rooting
Soil Profile 1. Upper slope, the elevation of 1110 m.a.s.l., the slope of <3%, use of primary forest land, bushland cover, and shrubs					
Ah1	0 – 10	7.5 YR $^{2,5}/_2$	SiCL	Gr	va
Ah2	10 – 24,5	7.5 YR $^{2,5}/_3$	SiCL	Gr	a
AB	24,5 – 42	7.5 YR $^3/_3$	SiL	Cr	c
Bw1	42 – 71	7.5 YR $^3/_4$	CL	SUB	c
Bw2	71 – 130	10 YR $^3/_4$	SiCL	AB	vf
Soil Profile 2. Middle slope, 600 m.a.s.l elevation, 25% slope, dry land with paddy - maize/soybean - tobacco planting system					
Ap	0 – 11	7.5 YR $^3/_4$	SiCL	Gr	a
AB	11 – 24	7.5 YR $^3/_5$	SiCL	SUB	c
Bt1	24 – 44	7.5 YR $^4/_6$	SiCL	SUB	c
Bt2	44 – 60	7.5 YR $^3/_4$	SiC	SUB	ni
Bt3	60 – 107	5 YR $^3/_4$	SiC	AB	ni
Soil Profile 3. Lower slope, 327mdpl elevation, 5% slope, industrial forest land, pine, and bushland cover					
Ah1	0 – 7	7.5 YR $^3/_1$	L	Gr	va
Ah2	7 – 26	7.5 YR $^{2,5}/_2$	SiCL	SUB	a
Bw	26 – 48	7.5 YR $^3/_2$	CL	SUB	c
BC	48 – 57	10 YR $^4/_1$	L	Cr	vf
2A	57 – 73	7.5 YR $^3/_2$	SiCL	SUB	vf
2Bw1	73 – 94	7.5 YR $^3/_2$	SiCL	SUB	vf
2Bw2	94 – 150	7.5 YR $^{2,5}/_3$	SiC	SUB	ni

SiCL = silty clay loam, SiL = silt loam, SiC = silty clay, CL = clay loam, L = loam, Gr = granular, Cr = crumb, SUB = sub angular blocky, AB = angular blocky, va = very abundant, a = abundant, c = common, f = few, vf = very few, ni = not identified

These results suggest that the soil on the upper slope is moderately developed, as indicated by the presence of a cambic B horizon (Bw). In contrast, on the middle slope, the soil is well developed, as reflected by the presence of an argillic horizon (Bt). Argillic horizons are horizons of illuvial accumulation of layer silicate clays and are found in well-developed or mature soils (Buol et al., 2011). Moreover, the results indicate that the soil on the lower slope is poorly developed, as shown by the lithologic discontinuity in the soil profile. The lower slope (a footslope) is a depositional surface which suggests that soil materials are periodically deposited on the existing soil, thereby retarding soil development. Figure 3 presents the depth functions of sand, silt, and clay which also show the significant increase of clay (argillic horizon) in the lower horizons of soil profile 2, and the irregular decrease with depth of sand, silt, and clay in soil profile 3.
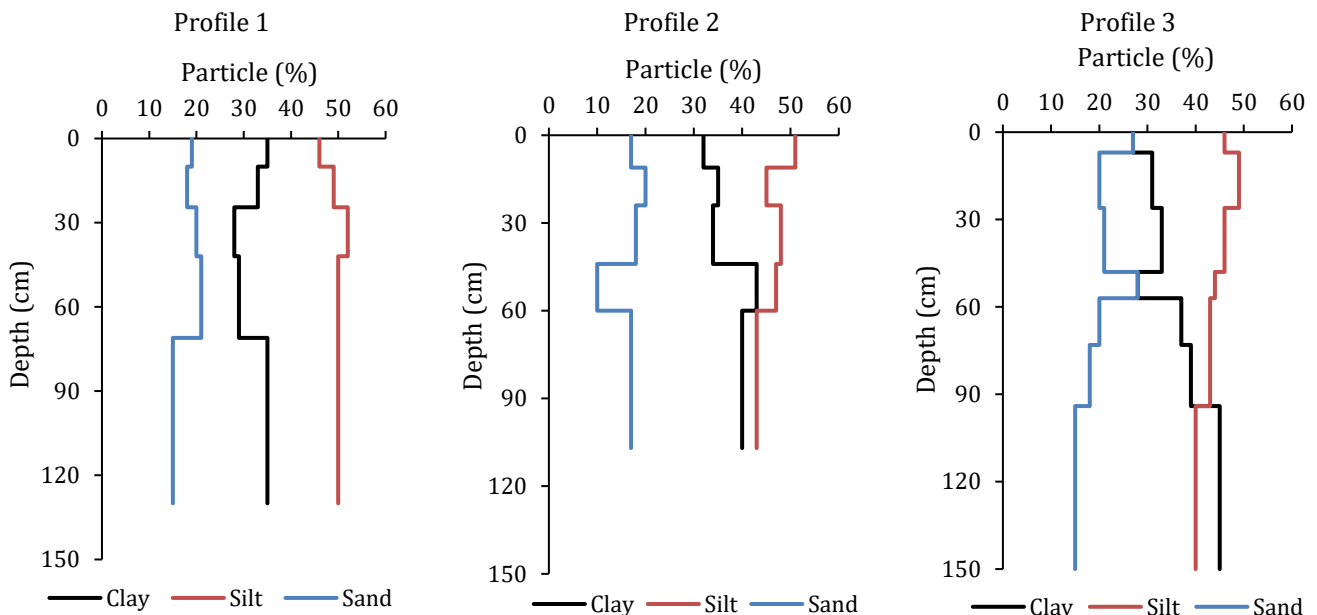

Figure 3. Depth function of sand, silt, and clay particles in the soils studied

Soil color reflects the soil composition as well as the past and present conditions of the soil (Blume et al., 2016). The dominant soil color hue of the volcanic toposequence evaluated is 7.5 YR (Table 1). Colors other than 7.5YR are only found in the Bw2 horizon (10 Y.R.) of soil profile 1, the Bt3 horizon (5YR) of soil profile 2, and BC horizons (10YR) of soil profile 3. Shoji et al. (1993) reported that volcanic soils in Japan have color hues ranging from 7.5YR to 10YR. Miehlich (1991) observed that most volcanic soils from Mexico he studied had color hues of 7.5YR and 10YR. The same trend was observed for the volcanic soils in Leyte, Philippines (Asio, 1996). Details of the morphology of the soil profiles are found in Figure 4, 5 and 6.

Table 2 presents the clay content and other physical properties of soils developed from igneous rocks. It shows that the clay content of the soils in the toposequence studied ranges from 27 to 45 percent. The textural class ranges from silty clay loam in horizon A to silty clay loam to silty clay in horizon B. The soil structure is granular in the A horizons, sub-angular blocky, and angular blocky in the B horizons. Such soil structures are common in volcanic soils (Miehlich, 1991; Shoji et al., 1993; Asio, 1996). The presence of roots in a soil horizon is a good indicator of the suitability of the soil for the development of the plant root systems and is directly related to the fertility status of the soil. As can be expected, the highest number of roots is found in the A horizons of all the soils evaluated.

The bulk density values in soil profile 1 are less than 1.0 g cm^{-3} indicating a very porous soil (average of 64 percent). Such low bulk density values of Inceptisols from volcanic rocks in Taiwan were attributed to high inter- and intraaggregate voids caused by the high organic matter content and isovolumetric weathering (Miehlich, 1991; Chen et al., 2001). It can be partly attributed to the high amounts of halloysite which in itself is highly porous (Quantin, 1990). Soil profiles 2 and 3 have average bulk density values of 1.18 g cm^{-3} and 1.21 g cm^{-3}, respectively. These values indicate a relatively porous soil favorable to root development and water movement. The results also showed that the particle density values of the soils range from 1.69 to 2.43 g cm^{-3} which are way below the widely used standard value of 2.65 g cm^{-3}. The K_S values are highest in soil profile 1 and lowest in soil profile 2 which follows the same order of the soil porosity values. This means that the more porous soil resulted in higher saturated hydraulic conductivity values.

Coordinates	:	08⁰02'06.07" S - 113⁰42'05.17" E	Epipedon	:	Mollic	

Coordinates   : 08°02'06.07" S - 113°42'05.17" E   Epipedon : Mollic
Altitude : 1110 masl   Endopedon : Cambic
Slope : 0 - 3 %   Soil Classification
Land Use : Primary Forest   Soil Taxonomy : Andic Hapludolls
Land Cover : Shrubs   FAO : Andic Chernozem (Siltic)
Surface Rocks : Not Rocky   Indonesian system : Molisol Haplik
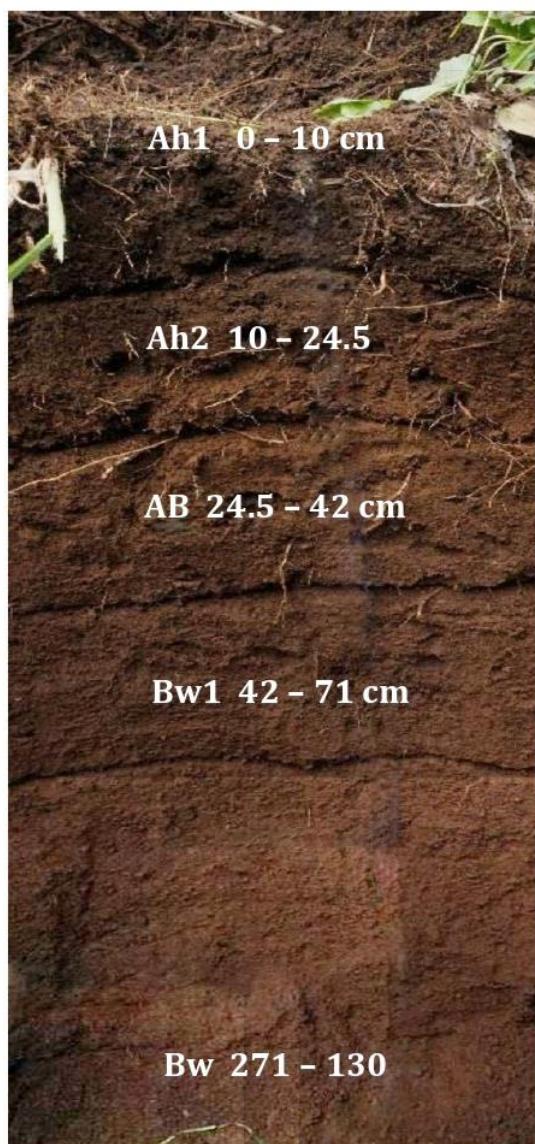
DESCRIPTION

Ah1
clear boundary layer, oblique flat shape, many root, silty clay loam, granular structure, fine size, weak, non sticky wet consistency, loose moist consistency, loose dry consistency, soil color 7.5 YR $^{2,5}/_3$, pH H_2O 4.76; KCl 4.25; NaF 10.98, no nodules.

Ah2
clear boundary layer, oblique flat shape, many root, silty clay loam, granular structure, fine size, weak, non sticky wet consistency, loose moist consistency, loose dry consistency, soil color 7.5 YR $^{2,5}/_3$, pH H_2O 4.76; KCl 4.25; NaF 10.98, no nodules.

AB
clear boundary layer, oblique flat shape, few root, silty loam, crumb structure, fine, weak, non sticky wet consistency, loose moist consistency, loose dry consistency, soil color 7.5 YR $^3/_3$, pH H_2O 4.74; KCl 4.37; NaF 11.17, tuffs found, few, no nodules.

Bw1
slightly diffuse boundary layer, oblique flat shape, few root, clay loam, sub angular blocky, fine, weak, slightly sticky wet consistency, slightly firm moist consistency, soft dry consistency, soil color 7.5 YR $^3/_4$, pH H_2O 4.79; KCl 4.32; NaF 9.24, nodules.

Bw2
diffuse boundary layer, oblique flat shape, very little root, silty clay loam, angular blocky structure, fine, weak, slightly sticky wet consistency, firm moist consistency, slightly hard dry consistency, soil color 10 YR $^3/_4$, pH H_2O 4.45; KCl 3.97; NaF 9.40, no nodules.

Ah1
clear boundary layer, oblique flat shape, many root, silty clay loam, granular structure, fine size, weak, non sticky wet consistency, loose moist consistency, loose dry consistency, soil color 7.5 YR $^{2,5}/_3$, pH H_2O 4.76; KCl 4.25; NaF 10.98, no nodules.

Figure 4. Soil morphology of soil profile 1

Coordinates	:	08002'09.46"S - 113043'05.46"E	Epipedon	: Ocric
Altitude	:	600 masl	Endopedon	: Argillic
Slope	:	25 %	Soil Classification	
Land Use	:	Upland	Soil Taxonomy	: Typic Hapludalf
Land Cover	:	Tobacco	FAO	: Hydragic, Irragric Anthrosols (Siltic)
Surface Rocks	:	A little rocky	Indonesian system	: Mediteran Haplik

Ap 0 – 11 cm

AB 11 – 24 cm

Bt1 24 – 44 cm

Bt2 44 – 60 cm

Bt3 60 – 107 cm

DESCRIPTION

Ap
clear boundary layer, Wavy, root slightly many, silty clay loam, wet consistency is slightly sticky, friable moist consistency, slightly hard dry consistency, soil color 7.5 YR $^3/_4$, pH H_2O 5.16; KCl 4.49; NaF 9.29, no nodules.

AB
slightly diffused boundary layers, wavy, root slightly many, silty clay loam, sub angular blocky structure, very fine, weak, slightly sticky wet consistency, friable moist consistency, slightly hard dry consistency, soil color 7,5 YR $^3/_5$, pH H_2O 5.41; KCl 4.52; NaF 9.47, no nodules.

Bt1
slightly diffused boundary layers, wavy, few root, silty clay loam, sub angular blocky structure, fine, weak, slightly sticky wet consistency, firm moist consistency, slightly hard dry consistency, soil color 7.5 YR $^4/_6$, pH H_2O 6.12; KCl 5.37; NaF 9.40, Fe and Mn nodules, few.

Bt2
slightly diffused boundary layers, wavy, no root, silty clay, sub angular blocky structure, fine, weak, sticky wet consistency, firm moist consistency, hard dry consistency, soil color 7.5 YR $^3/_4$, pH H_2O 5.96; KCl 5.08; NaF 9.34, Fe and Mn nodules, few.

Bt3
clear boundary layers, wavy, no root, silty clay, sub angular blocky structure, fine, weak, sticky wet consistency, firm moist consistency, hard dry consistency, soil color 5 YR $^3/_4$, pH H_2O 5.97; KCl 4.99; NaF 9.22, Fe and Mn nodules, few
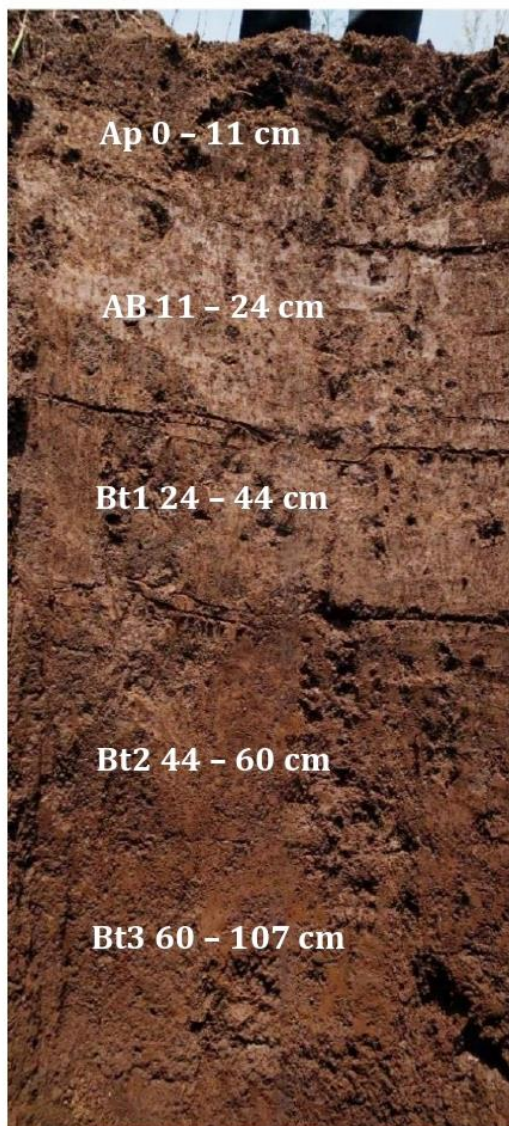
Figure 5. Soil morphology of soil profile 2

Coordinates	:	08003'08.31"S - 113045'08.77"E	Epipedon	:	Umbric
Altitude	:	325 masl	Endopedon	:	Cambic
Slope	:	5 %	Soil Classification		
Land Use	:	Industrial Plantation Forest	Soil Taxonomy	:	Typic Eutrudepts
Land Cover	:	Pine	FAO	:	Haplic Cambisols (Eutric, Humic, Siltic)
Surface Rocks	:	A little rocky	Indonesian system	:	Kambisol Eutrik

DESCRIPTION
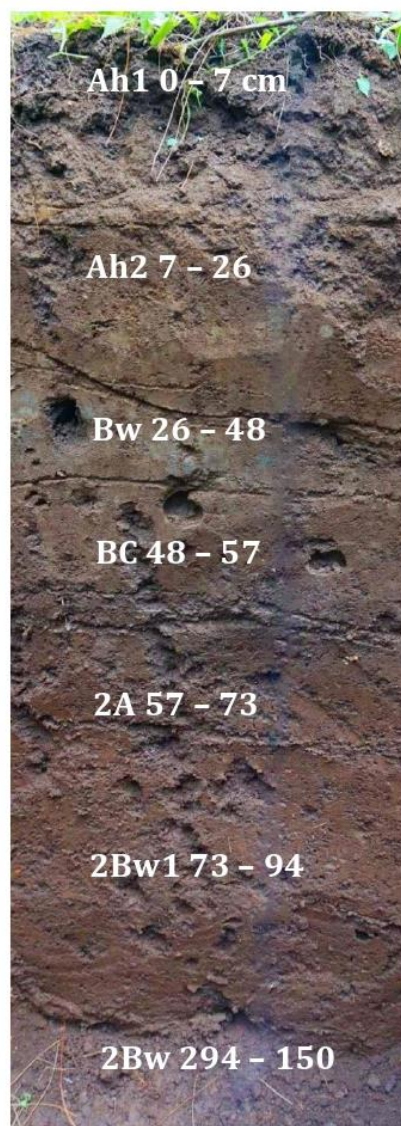
Ah1
clear boundary layer, wavy, slightly many root, silty clay loam, crumb structure, non sticky wet consistency, soft moist consistency, soft dry consistency, soil color 7,5 YR 3/1, pH H2O 5.31; KCl 4.40; NaF 9.25, no nodules

Ah2
clear boundary layer, wavy, root many, silty clay loam, sub angular blocky structure, fine, weak, slightly sticky wet consistency, soft moist consistency, soft dry consistency, soil color 7.5 YR ^{2,5}/$_2$, pH H_2O 5.62; KCl 4.71; NaF 9.51, no nodules

Bw
clear boundary layer, oblique flat shape, few root, clay loam, sub angular blocky structure, fine, weak, slightly sticky wet consistency, friable moist consistency, soft dry consistency, soil color 7.5 YR ^{3}/$_2$, pH H2O 5.83; KCl 4.74; NaF 9.40, no nodules

BC
clear boundary layer, wavy, very few root, loam, crumb structure, fine, weak, non sticky wet consistency, friable moist consistency, loose dry consistency, soil color 10 YR ^{4}/$_1$, pH H_2O 5.86; KCl 4.75; NaF 9.36, there are tuffs, few, no nodules

2A
clear boundary layer, oblique flat shape, very few root, silty clay loam, sub angular blocky structure, fine, weak, slightly sticky wet consistency, firm moist consistency, soil color 7.5 YR ^{3}/$_2$, pH H_2O 6.16; KCl 4.88; NaF 9.28, no nodules

2Bw1
clear boundary layer, oblique flat shape, silty clay loam, sub angular blocky structure, fine, weak, slightly sticky wet consistency, firm moist consistency, soft dry consistency, soil color 7.5 YR ^{3}/$_2$, pH H_2O 5.89; KCl 4.88; NaF 9.33., Fe and Mn nodules, few

2Bw2
clear boundary layer, oblique flat shape, no root, silty clay, sub angular blocky structure, fine, weak, slightly sticky wet consistency, firm moist consistency, soft dry consistency, soil color 7.5 YR ^{2,5}/$_3$, pH H_2O 6.01; KCl 4.75; NaF 9.41, Fe and Mn nodules, few

Figure 6. Soil morphology soil Profile 3

Table 2. Soil physical characteristics

	Horizon	Depth (cm)			Texture			BD (g/cm³)	PD (g/cm³)	Porosity (%)	K.S. (cm/day)
					Sand (%)	Silt (%)	Clay (%)				
Soil Profile 1	Ah1	0	-	10	19	46	35	0.72	1.87	61	267.5
	Ah2	10	-	24.5	18	49	33	0.67	2.04	67	563.7
	AB	24,5	-	42	20	52	28	0.78	2.14	64	372.3
	Bw1	42	-	71	21	50	29	0.73	2.34	69	129.4
	Bw2	71	-	130	15	50	35	0.96	2.43	60	64.3
Soil Profile 2	Ap	0	-	11	17	51	32	1.32	1.69	22	9.3
	AB	11	-	24	20	45	35	1.11	2.01	45	38.3
	Bt1	24	-	44	18	48	34	1.10	1.88	41	38.7
	Bt2	44	-	60	10	47	43	1.28	2.61	51	22.7
	Bt3	60	-	107	17	43	40	1.09	1.96	44	24.9
Soil Profile 3	Ah1	0	-	7	27	46	27	1.31	1.96	33	149.2
	Ah2	7	-	26	20	49	31	1.22	2.29	47	67.9
	Bw	26	-	48	21	46	33	1.17	2.12	45	68.8
	BC	48	-	57	28	44	28	1.15	2.31	50	24.9
	2A	57	-	73	20	43	37	1.30	2.38	45	54.4
	2Bw1	73	-	94	18	43	39	1.16	2.26	49	25.7
	2Bw2	94	-	150	15	40	45	1.19	2.26	47	83.7

BD = bulk density, PD = particle density, KS = saturated hydraulic conductivity

Table 3 presents the soil chemical characteristics in the volcanic toposequence studied. The soil pH (H_2O) values of the three soil profiles range from 4.45 to 6.16 while pH (KCl) ranges from 3.97-5.37. Soil profile 1 appears to be more acidic than the other soil profiles. The lower pH (KCl) values relative to pH(H_2O) indicate that the net charge of the soil colloids in the three soil profiles is negative (-) according to the delta pH principle introduced by Mekaru and Uehara (1972). Results also revealed that the pH(NaF) are all above 9.0. The pH(NaF) of soil profile 1 ranges from 9.24 to 11.17 with the upper half meter showing values above the 9.5 limit for andic materials (Shoji et al., 1993; Buol et al., 2011). The pH(NaF) of soil profiles 2 and 3 range from 9.22 to 9.47 and 9.28 to 9.51, respectively. The pH(NaF) is used as an indicator of the abundance of active Al and Fe compounds as well as the P sorption capacity of soils. Soil organic carbon content is higher in the surface horizons of three soil profiles with soil profile 1 showing the highest amount. This is also reflected by the darker color of the surface horizons compared to the subsurface horizons. The lithologic discontinuity indicated by the horizons of soil profile 3 is also reflected by the irregular decrease of organic carbon content with soil depth.

Table 3. Soil chemical characteristics

	Horizon	Soil Depth (cm)			pH			Org C (%)
					H_2O	KCl	NaF	
Soil Profile 1	Ah1	0	-	10	4.91	4.21	9.62	4.55
	Ah2	10	-	24.5	4.76	4.25	10.98	2.70
	AB	24,5	-	42	4.74	4.37	11.17	1.96
	Bw1	42	-	71	4.79	4.32	9.24	1.10
	Bw2	71	-	130	4.45	3.97	9.40	0.66
Soil Profile 2	Ap	0	-	11	5.16	4.49	9.29	1.41
	AB	11	-	24	5.41	4.52	9.47	1.34
	Bt1	24	-	44	6.12	5.37	9.40	1.21
	Bt2	44	-	60	5.96	5.08	9.34	0.96
	Bt3	60	-	107	5.97	4.99	9.22	0.96
Soil Profile 3	Ah1	0	-	7	5.31	4.40	9.25	2.92
	Ah2	7	-	26	5.62	4.71	9.51	1.34
	Bw	26	-	48	5.83	4.74	9.40	1.20
	BC	48	-	57	5.86	4.75	9.36	0.60
	2A	57	-	73	6.16	4.88	9.28	0.92
	2Bw1	73	-	94	5.89	4.88	9.33	0.97
	2Bw2	94	-	150	6.01	4.75	9.41	076

Sand Mineralogy

Sand is a soil particle measuring 2 mm - 0.02 mm in diameter. Blume et al. (2016) stated that the sand fraction consists mainly of stable igneous and metamorphic minerals such as quartz, potash feldspars, micas, and numerous heavy minerals that remain after weathering. Thus, the mineralogy of the sand fraction generally reflects the mineral composition of the parent rock. In the present study, microscopic examination of sand samples from the three soil profiles revealed that the opaque minerals are the most abundant, followed by the rock fragments, then by pyroxene (augite and hyperstene), Ca - Na plagioclase (andesine and labradorite), weathered mineral, amphibole (brown and green hornblende), and mineral series from ferrous magnesia (olivine, tourmaline, and epidote) (Table 4). Moreover, the sporadic presence of iron concretions, bytownite, and tourmaline can be observed in all soil profiles. Sporadic occurrence of olivine, epidote, and brown hornblende is observable in soil profile 3.

Table 4. Sand mineral analysis

Depth (cm)	Horizon	Opaque	Zirkon	Clear Quartz	Turbid Quartz	Iron Concretion	Zeolite	Weathered Mineral	Rock Fragments	Volcanic Glass	Oligoclase	Andesine	Labradorites	Bytownite	Green Hornblende	Brown Hornblende	Augite	Hypersthene	Olivine	Epidotes	Tourmaline	Total (100%)
Soil Profile 1																						
0-10	Ah	47	-	-	-	sp	-	8	15	2	sp	sp	9	sp	3	-	7	9	-	-	sp	100
24-42	A2	52	-	-	-	-	-	6	19	3	-	-	7	sp	3	-	4	6	-	-	sp	100
71-130	Bw2	46	-	-	-	sp	-	5	21	3	sp	sp	10	sp	4	sp	6	5	-	-	sp	100
Soil Profile 2																						
0-11	Ap	32	sp	sp	sp	sp	sp	15	22	4	-	-	11	1	2	sp	7	6	-	-	sp	100
24-44	Bt2	47	-	-	-	sp	-	11	20	2	-	-	8	sp	2	-	3	5	-	-	sp	100
60-107	B	38	sp	-	-	sp	-	13	18	4	-	sp	10	sp	4	-	5	8	-	-	sp	100
Soil Profile 3																						
7-26	A1	30	-	-	-	sp	-	2	27	2	-	1	16	sp	7	sp	6	8	sp	sp	1	100
48-57	BC	34	-	-	-	sp	-	1	32	1	-	sp	12	sp	5	sp	7	8	sp	sp	sp	100
94-150	2Bw2	42	-	sp	sp	sp	-	sp	28	sp	-	sp	15	sp	4	sp	4	7	sp	sp	sp	100

SP: Sporadic on orientation found, but not offending line counting; - : Not found on orientation

Opaque minerals are minerals that do not transmit light in thin sections and they have high density. Common members of this mineral are magnetite and ilmenite. Based on the geological map of East Java, several studies indicate that the rock composition of the Hyang mountain range (Argopuro, Raung, and Ijen) is basaltic andesite (Sapei et al., 2009; Indarto et al., 2011; Abdullah, 2016). Abdullah (2016) revealed that the opaque mineral in soils developed from the Raung volcanic material is magnetite. From the mineral composition found in this present study, it can be assumed that the opaque mineral detected is also magnetite which according to Haldar and Tisljar (2014) is common in igneous rocks.

The highest number of opaque minerals is found in soil profile 1, followed by soil profile 2, and the lowest is in soil profile 3. The trend shows a decrease from the upper slope to the foot slope, which can be explained by the fact that opaque minerals have a high density, such that their amount will increase towards the caldera upslope. In addition, the opaque mineral content is higher, the higher is the sand content. This pattern also occurs in rock fragments. The abundance of magnetite in the upper slope (soil profile 1) can also be explained by the well-drained condition of the site. Ahmed and Maher (2018) reported that the dominance of magnetite shows that its formation occurs in well-drained and oxidizing soils.

Rock fragments are an aggregate of several minerals with a specific composition, so rock fragments are put into a separate group in the examination of the mineral composition of sand. The amount of rock fragments in the soil profile is directly proportional to the sand content. This is because rock fragments will contribute to the sand content in the soil.

Clay Mineralogy

Clay minerals are secondary minerals derived from the alteration of primary minerals and have a size of <0.002 mm. The XRD analysis showed that the clay in soil profile 1 is dominated by halloysite with a few accompanying gibbsite and cristobalite (Table 5, Figure 7). Soil profile 2 is dominated by halloysite and illite, whereas soil profile 3 is dominated by kaolinite and illite. Illite is a non-expanding clay mineral belonging to

the 2:1 type, whereas halloysite and kaolinite belong to the 1:1 type of clay mineral. Studies on the volcanic soils of Mexico (Miehlich, 1991), Taiwan (Chen et al., 2001), and the Philippines (Asio, 1996; Navarrete et al., 2009) revealed the common occurrence of halloysite and kaolinite.

Table 5. Clay mineralogy of the soils

Horizon	Depth (cm)	Halloysite (10Å)	Halloysite (7.2Å)	Kaolinite	Gibbsite	Cristobalite	Illite
Soil Profile 1							
Ah1	0 – 10	-	+++	-	+	+	-
AB	24.5 – 42	-	+++	-	-	-	
Bw2	71 – 130	+++					++
Soil Profile 2							
Ap	0 – 11	-	+++	-	-	-	++
Bt1	24 – 44	-	++	-	-	-	++
Bt3	60 – 107	-	++	-	-	-	+++
Soil Profile 3							
Ah1	7 – 26	-	-	++++	-	-	(+)
BC	48 – 57	-	-	++	-	-	++
2Bw2	94 – 150	-	-	++	-	-	+++

Note: ++++ Predominant; +++ Dominant; ++ Moderate; + Few; (+) Very few; - Nothing
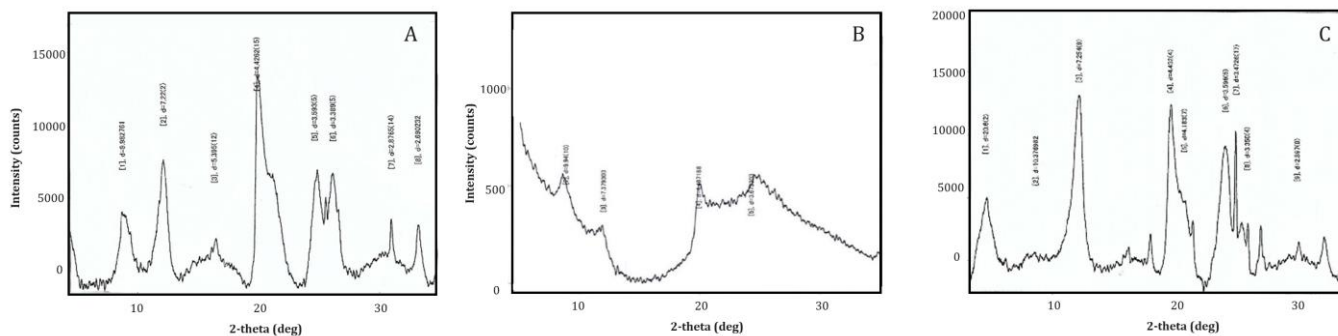
Figure 7. XRD analysis of top layer clay minerals from soil profile 1 (A), soil profile 2 (B), and soil profile 3 (C).

Results also revealed that halloysite mineral is dominant in the upper layers of soil profiles 1 (upper slope) and 2 (middle slope) but is not present in soil profile 3 on the footslope. Halloysite is a form of kaolinite in which water is held between structural units in the basal plane. In a completely hydrated state, halloysite exhibits an intense peak at 10 Å. This corresponds to a single sheet of water molecules ~2.8 Å thick between the 7.2 Å layers. The interlayer water is, however, very labile so that halloysite is most commonly observed in a more dehydrated form which displays a diffraction peak of 7.2 Å (Hillier and Ryan, 2002; Bohn et al., 2001). Halloysite can come from the transformation of amorphous minerals such as allophane and imogolite. The abundance of halloysite minerals in soil profile 1 suggests that the soil developed from amorphous minerals that characterize Andisols. The high NaF-pH and low H_2O-pH also point to the Andisol origin of this soil. Prasetyo et al. (2009) argued that the low allophane in soils was due to the development of the soil and the desilification process so that the allophane content was reduced and formed halloysite hydrate crystalline minerals.

The halloysite of 10 Å is found only on the Bw2 horizon in soil profile 1, while the halloysite with 7 Å diffraction peak is the one found in the Ah horizons of soil profiles 1 and 2. Soil profile 3 is dominated by kaolinite (7 Å) particularly on the surface horizon. The greater abundance of kaolinite in tropical soils lies in the stage of weathering of the soils. The mineral feldspar can progressively weather to mica, kaolinite, and gibbsite. Warm and humid conditions in the tropics facilitate a rapid removal of potassium and dissolved silica so that feldspar and mica quickly turn into kaolinite and gibbsite (Uehara and Gillman, 1981). Kaolinite is generally formed by the weathering of 2:1 mineral, but some researchers report that kaolinite can also be formed through other processes. Jahn (1988) showed that kaolinite can be formed through halloysite kaolinization. Hydration and carbonation can cause the alteration of Ca-Na feldspar to become clay (Hunt, 1976).

$$CaAl_2Si_2O_8 \cdot 2NaAlSi_3O_8 + 4H_2CO_3 + 2(nH_2O) \longrightarrow 2Al_2(OH)Si_4O_{10}nH_2O \text{ (clay)} + Ca(HCO_3)_2 + 2NaHCO_3$$
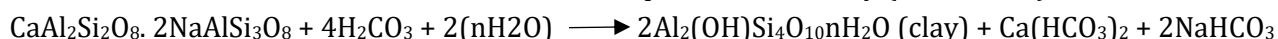
Furthermore, some studies cited by Buol et al. (2011) showed that kaolinite can be formed by altering albite minerals.

$$2NaAlSi_3O_8 \text{(albite)} + 2H_2CO_3 + 9H_2O \longrightarrow Na^+ + 2HCO^-_3 + 4H_4SiO_4 + Al_2Si_2O_5(OH)_4 \text{ (kaolinite)}.$$
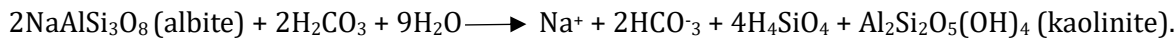
Cristobalite is a silica $(SiO2)$ mineral member, while gibbsite is an aluminum hydroxide mineral $(Al(OH_3))$. Gibbsite can be formed directly through the weathering of primary minerals (Wada and Aomine, 1966; Prasetyo et al., 2009). Cristobalite can be known through XRD analysis with diffraction peaks of 4.26 and 3.34 Å. Gibbsite displays a diffraction peak of 4.82 Å.

Interestingly, illite (10 Å) is present in few to moderate amounts in all soil profiles and tends to increase with soil depth. Several hypotheses have been proposed to explain the occurrence of illite in volcanic soils (Shoji et al., 1993). One is that it is an alteration product from mafic minerals such as pyroxene, amphiboles, and micas in parent material. Second, it is formed from amorphous materials as product of an advanced stage of weathering. Third, hydrothermal alteration products. Fourth is the solid-state transformation of volcanic glass by K retention (Shoji et al., 1993).

Soil Genesis

Soil formation is influenced by climate, parent material, organism, topography, and time. Results of the study clearly indicate the major influence of climate, parent material, and topography on the formation of the soils. The hot and wet humid tropical climate favored fast weathering and soil formation resulting in the formation of kaolinite, halloysite, and gibbsite from the primary minerals present in the basaltic andesite parent rock. The high rainfall not only enhanced weathering but also leaching of ions released during chemical weathering and transport of soil materials from the upper slopes to the lower slopes. The relatively fast weatherability of the parent rock also contributed to the fast weathering and soil development. The mountainous topography not only enhanced drainage and leaching process but also the transport of soil materials, which led to the lithologic discontinuity observed on soil profile 3.

The degree of soil development can be evaluated based on soil profile morphology, particularly horizonation, degree of weathering, loss and gain of elements, and clay mineralogy (Duchaufour, 1977; Birkeland, 1984; Buol et al., 2011). It is also possible to use the presence of resistant and weathered minerals, as Alam et al. (2011) recently used on the soil development from weathered ultramafic rocks in two toposequences in Southeast Sulawesi. Jackson et al. (1948) published a pioneering work on the weathering sequence of soils based on clay mineralogy. They reported that illite indicates stage 7 while kaolinite and halloysite indicate stage 10 out of 11 stages of weathering they have observed.

Based on the above indicators, the degree of soil development of the soils evaluated is: Soil Profile 2>Soil Profile 1>Soil Profile 3. This also agrees with the soil classification of the soils in that Soil Profile 3 is an Alfisol, Soil Profile 1 is a Mollisol, and Soil Profile 3 is an Inceptisol. Finally, the presence of Andic properties such as low bulk density and high pH in NaF of soil profile 1 tends to indicate that this soil developed from an Andisol similar to what was reported in Taiwan by Chen et al. (2001).

Conclusion

The soils in the volcanic toposequence are dominated in their sand fraction by opaque minerals, weatherable minerals, amphibole groups, and ferromagnesian. The abundance of the opaque mineral (mainly magnetite) in the soil profile on the upper slope suggests the effect of a well-drained topography on its formation. In terms of clay minerals, soil profile 1 is dominated by halloysite with a few gibbsite and cristobalite on the surface horizon, soil profile 2 by halloysite and illite, and soil profile 3 by kaolinite and illite. The presence of illite in the two of the soils studied agrees with the findings of previous studies in other volcanic regions. The degree of soil development of the soils evaluated is: Soil Profile 2>Soil Profile 1>Soil Profile 3. This appears to confirm with the soil classification of the soils in that Soil Profile 3 is an Alfisol, Soil Profile 1 is a Mollisol, and Soil Profile 3 is an Inceptisol. The presence of Andic properties such as low bulk density and high pH in NaF of soil profile 1 tends to indicate that this soil developed from an Andisol. Lastly, the results obtained can be valuable for land management practices, such as soil conservation, agricultural planning, and land-use decision-making in volcanic landscapes. Understanding the mineralogical characteristics and soil development patterns can support optimizing soil fertility, water management, and sustainable land-use practices in similar volcanic regions.

Acknowledgment

References

Abdullah, 2016. Minerals in volcanic ash soil of Mount Raung in Jember Regency as Soil Nutrient Reserves. Undergraduate Thesis. Digital Repository Universitas Jember. 54p. [in Indonesian].

Ahmed, I.A.M., Maher, B.A., 2018. Identification and paleoclimatic significance of magnetite nanoparticles in soils. *PNAS* 115(8): 1736-1741.

Alam, S., Sunarminto, B.H., Siradz, S.A., 2011. Soil genesis of ultramafic rocks weathered on two toposequence in Southeast Sulawesi. *Agroteknos* 1 (3): 119-126.

Asio, V. B., 1996. Characteristics, weathering, formation and degradation of soils from volcanic rocks in Leyte, Philippines. Hohenheimer Bodenkundliche Hefte, vol. 33, Stuttgart, Germany. 209p.

Balai Penelitian Tanah, 2005. Technical guidelines for the chemical analysis of soil, plants, water, and fertilizers. Agricultural Research and Development Agency, Ministry of Agriculture, Indonesia. 136 pp [in Indonesian].

Birkeland, P.W., 1984. Soils and Geomorphology. Oxford University Press, New York. 372p.

Bohn, H. L., McNeal, B. L., O'Connor, G. A., 2001. Soil Chemistry (3rd Ed.). John Wiley & Sons, Inc, New York. 307p.

Blume, H.-P., Brümmer, G.W., Horn, R., Kandeler, E., Kögel-Knabner, I., Kretzschmar, R., Schad, P., Stahr, K., Wilke, B.-M., 2016. Scheffer/Schachtschabel Soil Science. Springer-Verlag Berlin Heidelberg. 630p.

Buol, S.W., Hole, F.D., McCracken, R.J., 2011. Soil Genesis and Classification. The Iowa State University Press, Ames Iowa. 527p.

Chen, Z.S., Tsou, T.C., Asio, V.B., Tsai, C.C., 2001. Genesis of Inceptisols on a volcanic landscape in Taiwan. *Soil Science* 166(4): 255-266.

Chesworth, W., 1973. The parent rock effect in the genesis of soil. *Geoderma* 10(3): 215-225.

Duchaufour, P., 1977. Pedology: Pedogenesis and Classification. Masson, Paris. 476p.

Haldar, S.K., Tisljar, J., 2014. Introduction to Mineralogy and Petrology. Elsevier, Amsterdam. 341p.

Hillier, S., Ryan, P.C., 2002. Identification of halloysite (7 Å) by ethylene glycol solvation: the 'MacEwan effect'. *Clay Minerals* 37(3): 487–496.

Hunt, C.B., 1972. Geology of Soils. W.H.Freeman & Co Ltd, USA. 344p.

Indarto, S., Sudarsono, Fauzi, A., Eddy, Z., Gaffar., Andrie, K., Abdullah., Jakah, Sunardi., 2011. Manifestasi Permukaan Panas Bumi Daerah Rabunan, Gunung Argopuro, Jawa Timur Berdasarkan Mineralogi dan Kimia Unsur Utama. Prosiding Pemaparan Hasil Penelitian Puslit Geoteknologi LIPI 2011, pp. 53-61 [in Indonesian].

Jackson, M.L., Tyler, S.A., Willis, A.L., Bourbeau, G.A., Pennington, R.P., 1948. Weathering sequence of clay-size minerals in soils and sediments I. Fundamental Generalizations. *Journal of Physical and Colloidal Chemistry* 52(7): 1237-1259.

Jahn, R., 1988. Böden Lanzarotes. Vorkommen, Genese und Eigenschaften von Böden aus Vulkaniten im semiariden Klima Lanzarotes (Kanarische Inseln). PhD Thesis, Univ. Stuttgart-Hohenheim, Hohenheimer Arbeiten (Ulmer) Stuttgart, Germany. 257p.

Mekaru, T., Uehara, G., 1972. Anion adsorption in ferruginous tropical soils. *Soil Science Society of America Journal* 36(2): 296-300.

Miehlich, G., 1991. Chronosequences of volcanic ash soils. Hamburger Bodenkundliche Arbeiten, Vol.15. Hamburg, Germany. 207p.

Navarrete I.A., Tsutsuki, K., Asio, V.B., Renzo, K., 2009. Characteristics and formation of rainforest soils derived from Late Quaternary basaltic rocks in Leyte, Philippines. *Environmental Geology* 58: 1257-1268.

Prasetyo, B.H., Suharta, N., Yatno, A., 2009. The characteristic of soils with andic properties derived from acid pyroclastic materials in Toba High Land. *Indonesian Soil and Climate Journal* 9: 1-14 [in Indonesian].

Quantin, P., 1990. Specificity of the halloysite-rich tropical or subtropical soils. Proceedings of the 14th International Congress of Soil Science, 12-18 August 1990, Kyoto, Japan. Vol. VII, pp. 16-21.

Sapei, T., Suganda, A.H., Astadiredja, K.A.S., Suharsono, 1992. Geological Map of Jember, East Java. Geological Research and Development Centre, Bandung.

Schaetzl, R., Anderson, S., 2005. Soils: Genesis and Geomorphology. Cambridge University Press, New York. 817p.

Shoji, S., Nanzyo, M., Dahlgren, R.A., 1993. Volcanic Ash Soils: Genesis, properties and utilization. Developments in Soil Science No. 21. Elsevier, Amsterdam. 288p.

Stahr, K., 1994. Soil minerals in space and time. Transactions 15th World Congress of Soil Science, 10-16 July 1994, Acapulco, Mexico. Vol. I, pp.111-121.

Uehara, G., Gillman, G., 1981. The mineralogy, chemistry, and physics of tropical soils with variable-charge clays. West-View Press, Boulder. 170p.

Van Reeuwijk, L.P., 2002. Procedures for soil analysis. Technical Paper 9. 6th Edition. International Soil Reference and Information Centre (ISRIC) & Food and Agricultural Organization of the United Nations (FAO). Wageningen, The Netherlands.

Wada, K., Aomine, S., 1966. Occurrence of gibbsite in weathering of volcanic materials at Kuroishibaru, Kumamoto. *Soil Science and Plant Nutrition* 12(4): 151-157.